NASA CR-
144557

APPENDIX II

(NASA-CR-144557) ENGINEERING STUDIES OF VECTORCARDIOGRAPHS IN BLOOD PRESSURE MEASURING SYSTEMS, APPENDIX 2 Final Report (Trustees of Health and Hospitals of the City) 299 p HC $9.25 CSCL 06E G3/52

N76-12697

Unclas
01915

APPENDIX II

A. Pulse Wave Velocity as a Measure of Arterial Blood Pressure by Kenneth A. Labresh

B. Diastolic Blood Pressure and Pulse Wave Velocity in Humans by Harvey Goldberg

C. Transducer Development for Blood Pressure Measuring Device by Donald E. Gorelick

D. Cardiovascular Monitoring System - User's Manual, Volume 1

PULSE WAVE VELOCITY AS A MEASURE OF ARTERIAL BLOOD PRESSURE

by

KENNETH ALBERT LABRESH

Submitted in Partial Fulfillment
of the Requirements for the
Degree of Bachelor of Science
at the
MASSACHUSETTS INSTITUTE OF TECHNOLOGY
June, 1970

Signature of Author....Kenneth A. LaBresh....
Department of Electrical Engineering, June 4, 1970

Certified by....Roger G. Mark, M.D. / S.C. Burns....
Thesis Supervisor

Accepted by....Robert L. Kyhl....
Chairman, Departmental Committee on Theses

PULSE WAVE VELOCITY AS A

MEASURE OF ARTERIAL BLOOD PRESSURE

by

KENNETH ALBERT LABRESH

Submitted to the Department of Electrical Engineering on June 4, 1970 in partial fulfillment of the requirements for the degree of Bachelor of Science

ABSTRACT

Experiments are described in which the pulse wave velocity is found to be linearly related to diastolic blood pressure. The ultimate objective of this study is to provide data on the feasibility of utilizing this relationship to develop an instrument which will monitor diastolic blood pressure in ambulatory patients. It was found, in experiments on dogs, that this relationship holds over a wide range of blood pressure and in the presence of such physiological perturbations as vasoconstriction, vasodilation, sympathetic stimulation, and changes in cardiac contractility, cardiac output, heart rate, and blood volume.

Thesis Supervisor: Roger G. Mark
Title: Assistant Professor in Electrical Engineering

ACKNOWLEDGEMENT

I am deeply grateful to Dr. Roger G. Mark for supervision and experimental assistance. His conscientious teaching and example has contributed much to my thinking. I would also like to thank the Boston City Hospital for the use of facilities at the Sears Surgical Laboratory. I would like especially to acknowledge the guidance and encouragement given by Dr. Henry Brown during the surgical procedures. I am indebted to the Heart Station at Boston City Hospital for the use of instrumentation, and to Dr. Richard Wagner for instruction in blood pressure measurement techniques and assistance with the instrumentation. I appreciate the help of Professor Stephen Burns and the stimulating atmosphere created by him and Dr. Mark. Finally, I gratefully acknowledge the assistance of Miss Andrea Sanders, Miss Elaine Kant, Miss Emily Bass, and Miss Joan Fleischnick in the preparation of the manuscript.

TABLE OF CONTENTS

LIST OF FIGURES

I. INTRODUCTION

The clinical assessment of the blood pressure in ambulatory patients as usually carried out may not give a complete picture of the patient's usual cardiovascular status. Although the traditional auscultatory method [Gilford (1954)] gives accurate results at the time it is performed, the physician is provided with only a single data point under test conditions which may significantly alter the variable being measured. Stress, both physical and emotional, is known to alter blood pressure. [Friedberg (1956)] For some individuals the visit to the doctor's office is traumatic in itself. Moreover, the physician cannot assess the degree of lability of blood pressure due to stressful situations which may occur during the day. Ideally he wants to measure blood pressure throughout a usual day's activities. The physician is concerned about cardiovascular complications due to blood pressure which are related to 1.) average pressure in the system over long periods, and 2.) maximum and minimum excursions. The average pressure in the system is related to the amount of work performed by the heart. An increased average pressure will cause an increased cardiac workload, and hence, hypertrophy of the heart. [Friedberg (1956)] Excessive maximum excursions of blood pressure are related to cerebral hemorrhage and dissecting aneurisms. On the other hand, excessive minimum excursions may cause dizziness, fainting spells, or even strokes. [Friedberg (1956)] A record of the blood variations during normal daily activities would also be of key importance in assessing the effectiveness of drugs used in the treatment of hypertension. Therefore, long-term monitoring of blood pressure in ambulatory patients would be an important clinical tool.

The need for long-term blood pressure monitoring has been recognized for some time, and there have been numerous attempts to devise systems to do this. [Doupe (1939), Gilson (1942), Lange (1943)] Arterial blood pressure may be meas either directly or indirectly. The direct method a needle or cannula inserted into the artery. [Moulopo os (1963)] This method provides continuous, accurate information, but has a number of disadvantages. The introduction of any foreign body into the artery is traumatic and may cause ischaemia, thrombosis, infection, hemorrhage, etc. It is certainly not a suitable method for ambulatory patients.

The only widespread method of indirectly measuring blood pressure is the auscultatory (sphygmomanometric) method mentioned earlier. The auscultatory method makes use of a cuff, attached to a manometer, which is placed around the arm. The cuff pressure is increased above the systolic pressure in the artery so that the vessel is completely occluded. The cuff pressure is then slowly decreased. When the cuff pressure drops to systolic pressure, there exists a time at which the level of pressure inside the artery equals that of the pressure outside. This creates an unstable mechanical situation, and the vibrations produced by the sudden reexpansion of the compressed artery with each pulse generates audible sounds (Korotkoff sounds) which may be heard by placing a stethoscope over the artery. As the cuff pressure is decreased, the point is reached at which the intra-arterial pressure always exceeds cuff pressure. Thus, no Korotkoff sounds are heard. The cuff pressure at the disappearance of the sound is the diastolic pressure. [Gilford (1954)]

Nearly all indirect methods for continuously monitoring blood pressure have made use of the auscultatory method. [Corell (1959)] Instruments which automate the sphygmomanometric method are of two types. The first type provides the physician with a recording of the cuff pressure and the corresponding arterial event (sound, radial pulsations, or volumetric changes) and leaves the interpretation of the data to the physician. The second type makes the interpretations electronically or mechanically and displays the corresponding pressures directly. [Gilford (1954)]

The principle objection to all of these systems is their use of a cuff to occlude an artery intermittently over a long period of time. This may cause damage to the extremity, and is certainly not comfortable. Furthermore, automated cuff devices require a source of compressed air to inflate the cuff. They tend to be bulky and inconvenient for ambulatory patients.

The various problems with these methods have prevented their widespread use. Because of the extensive work done on these approaches with less than optimal results, a new approach is suggested. Previous work has suggested that a systematic relationship exists between pulse wave velocity in the arterial system and arterial pressure. In this project we have 1.) reviewed the literature for both mathematical models and experimental results, and 2.) performed experiments on dogs to verify this relationship.

II. REVIEW OF THE LITERATURE

A. Mathematical Model

The pulse wave may be thought of as a ripple on moving water with the arterial wall exerting an elastic constraint on the fluid. Thus the pulse wave velocity is the sum of the velocity of the pulse relative to the blood and the velocity of blood in the artery. [Bramwell and Hill (1922)] Although a complete theory of pulse wave transmission is very complex, Bramwell and Hill have simplified it by assuming 1.) the wave is propagated over relatively short distances; and 2.) because of the elasticity of the arteries, there are no sharp discontinuities in the waveform, so only the lower frequencies must be considered. More complete treatments have been carried out, but will not be reviewed here. [Morgan and Kiely (1954), Womersley (1957), Atabek and Lew (1966)] With the above simplifications, the formula of Moens (1878) (see Appendix A) may be used to relate velocity to properties of the artery:

$$v = (Ea/2\rho r)^{1/2} \qquad (1)$$

Where:
- v = velocity of the onset of the pulse wave
- E = modulus of elasticity for lateral expansion of the artery
- a = thickness of the arterial wall
- ρ = density of blood
- r = radius of the artery

A transformation of this formula was done by Bramwell and Hill (1922) to relate pulse wave velocity to more easily measured properties <u>in vivo</u>.

Consider a segment of elastic tube of thickness a, radius r, and length dz, with an applied tension per unit length T, as shown in Figure 1a. The same segment, rolled out into a thin sheet, is shown in Figure 1b.

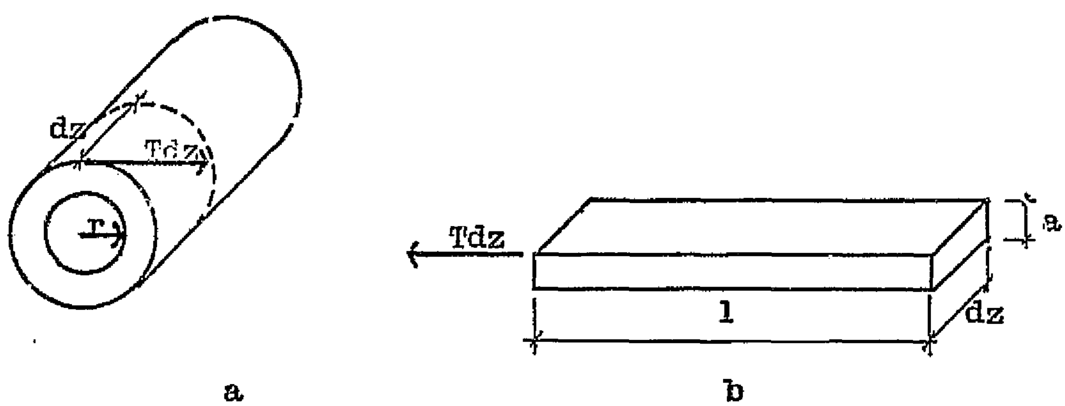

Figure 1

From Hooke's Law applied to the sheet:

$$dl/l = (1/EA)\ dTdz \qquad (2)$$

Substituting $A = adz$ and $l = 2\pi r$ into equation (2) gives:

$$dr/r = (1/Eadz)\ dTdz = dt/Ea \qquad (2a)$$

From Laplace's Law for a cylinder, $Pr = T$ where P = pressure, equation (2a) becomes:

$$dr/r = (1/Ea)\ d(Pr) = (1/Ea)(rdP+Pdr) \qquad (2b)$$

Since Pdr is small compared to rdP, equation (2b) becomes:

$$dP = (Ea/r^2)dr \qquad (2c)$$

Introducing the volume per unit length:

$$V = \pi r^2 \qquad (3)$$
$$\partial V/\partial r = 2\pi r \qquad (3a)$$

$$dV/dP = (\partial V/\partial r)(\partial r/\partial P) \qquad (4)$$

Combining equations (2c), (3a), and (4) gives:

$$dV/dP = 2\pi r(r^2/Ea) = 2\pi r^3/Ea \qquad (5)$$

From equations (3) and (5):

$$dV/dP = 2rV/Ea \qquad (6)$$

From equations (1) and (6):

$$v = (V/(\rho dV/dP))^{1/2} \qquad (7)$$

Equation (7) is the Bramwell-Hill Equation Bramwell and Hill (1922) which, if v is in meters per second, P is in millimeters of mercury, dV/V is a percentage increase in volume, and $\rho = 1.055$, may also be expressed as:

$$v = 3.57\ (dP/(dV/V))^{1/2} \qquad (7a)$$

The Bramwell-Hill Equation may be used to calculate pulse wave velocities from pressure-volume curves measured experimentally, and hence, to derive a relationship between pulse wave velocity and arterial pressure. Figure 2a is a pressure-volume curve from the excised thoracic aorta of a dog. [Hallock and Benson (1937)] The vessel was first filled with saline solution, the radius was measured, and the volume was calculated for zero arterial pressure. The pressure in the artery was then increased step-wise, with a two minute pause between steps to allow equilibration, and a pressure-volume curve obtained. Data taken from Hallock and Benson (1937) is plotted as the percentage increase in volume versus the pressure in the vessel (Figure 2a). Figure 2b is the derivitive of the pressure-volume curve in Figure 1a with respect to percentage volume, and is plotted against pressure. The equation of the curve is the equation of a parabola:

$$dP/(dV/V) = 2.9x10^{-4}P^2 - .68x10^{-2}P + \overset{.044}{\cancel{.44}} \tag{8}$$

$$dP/(dV/V) = (1.7x10^{-2}P - .21)^2 \tag{8a}$$

Equation (8a) combined with equation (7a) gives:

$$v = 6.08x10^{-2}P - .75 \tag{9}$$

For a diastolic pressure of 100 mm of Hg, equation (9) gives a pulse wave velocity of 5.23 m/sec, which compares favorably to values found in other studies. [Bramwell and Hill (1922), Hallock and Benson (1937), Haynes, Ellis, and Weiss (1936), Nye (1964), Schimmler (1966), and Steele (1937)]

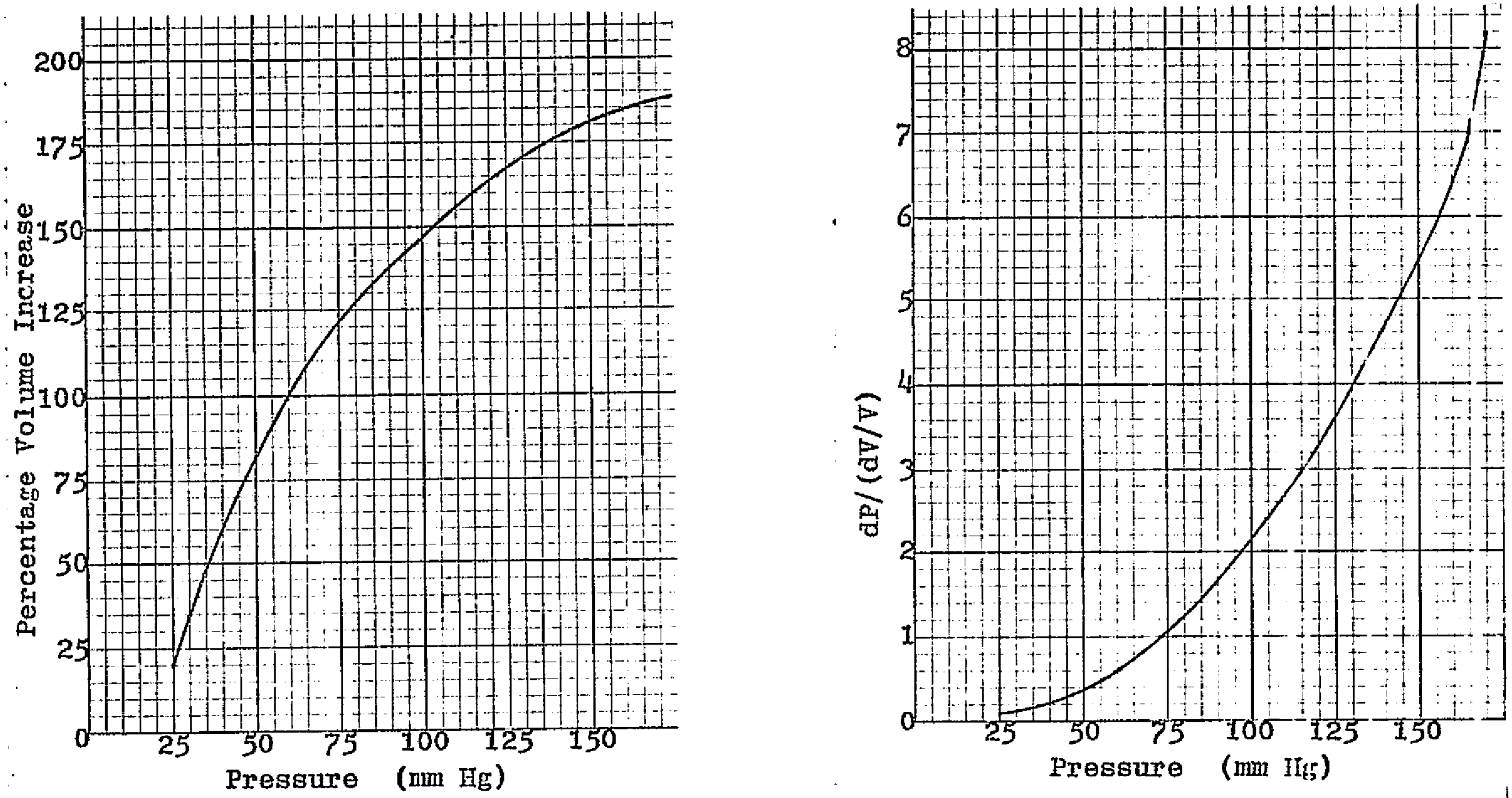

a

b

FIGURE 2. a. Pressure-volume curve from an excised aorta.
b. Derivative of pressure-volume curve with respect to percent volume increase plotted against pressure.

B. Previous Experiments

Several papers have dealt with the pressure-velocity relationship empirically. One of the most complete early studies was done by Steele (1937). Other workers [Nye (1964), Haynes, Ellis, and Weiss (1936)] have found that data taken from a number of individuals gives no significant correlation between pulse wave velocity and diastolic pressure. Steele illustrates that individual differences are large, but that for a given individual the relationship is linear. From curves taken from the brachioradial arteries of four individuals it can be seen that each of the curves is approximately linear, but there is a significant difference in their slopes, with larger slopes for curves taken from older individuals. In a set of four curves taken from the same individual over a six month period, Steele shows that the relationship for a given individual remains relatively constant.

Schimmler (1966), however, found that it was possible to generalize data across large numbers of patients if age is used as the parameter. First, plotting pulse wave velocity against the age of patients for a given mean arterial pressure gave a curve of positive slope. A family of curves were plotted in this manner, each curve for a different pressure, with curves of steeper slopes taken at higher pressures. From this family of curves, Schimmler plotted the values of pulse wave velocity against mean pressure for a given age and generated a straight line relating velocity to pressure. Having done this for a number of ages, Schimmler obtained a family of straight lines with age as the parameter, and lines for greater age had steeper slopes. Since age is regarded as a rough index of elasticity, this observation, also noted by Steele, is explained by Moens' formula. As can be seen from equation (1), pulse wave velocity is proportional to the square root of the elastic modulus; stiffer arteries, which are associated with older people, have higher velocities for the same pressure.

Schimmler (1966), in contrast to Steele (1937), related pulse wave velocity to mean arterial pressure rather than diastolic pressure; there has been ambiguity in the literature as to which is the significant variable. Steele (1937) resolves this problem by a series of experiments on dogs in which a.) the systolic pressure is altered without changing the diastolic pressure, b.) the systolic pressure is increased while the diastolic pressure is decreased, and c.) the systolic pressure is not changed while the diastolic pressure is altered. In all cases the pulse wave velocity followed changes in the diastolic level. These results led Steele to conclude: "The pressure upon which the speed is dependent is not systolic, mean, or pulse pressure but unequivocably diastolic pressure." [Steele (1937)]

III. EXPERIMENTAL WORK

A. Objectives

The ultimate objective of our research is to develop a device which will utilize the pulse wave velocity as a measure of diastolic blood pressure in ambulatory patients. Experimental data was necessary to answer several questions relating to the feasibility of such an instrument. First, could we verify the earlier experimental data and mathematical model which predicted a linear relation between diastolic pressure and pulse wave velocity? Would this relation hold even in the presence of such physiological perturbations as vasoconstriction, vasodilation, sympathetic stimulation, changes in cardiac contractility, cardiac output, heart rate, and blood volume?

In measuring pulse wave velocity, one needs to measure the time interval between pulse wave arrival at two separate points in the elastic portion of the arterial system. An ideal reference time, t_o, would be the onset of the pressure wave in the proximal aorta which corresponds to the onset of ventricular emptying. Clearly it is difficult to measure this time directly in a non-invasive manner. However, if the onset of ventricular emptying (opening of aortic valve) were related in a predictable way to the electrical depolarization of the ventricles, the QRS complex of the EKG could serve as a reference time in computing pulse wave velocity. The critical question to be answered is what is the variability in the latency, $\mathcal{T}$, between ventricular depolarization and aortic valve opening. It is known that $\mathcal{T}$ is on the order of 100msec. [Braunwald (1955)] which is comparable to the pulse wave transmission time from the aorta to the femoral artery. The variability in τ must therefore be very small to permit the use of the EKG as a timing reference. The literature indicates, however, that τ may vary substantially, even for consecutive cardiac cycles. In a study done by Agress (1964), the standard deviation in τ for ten consecutive cycles was 4.6 msec. For values taken two weeks apart, the average standard deviation was 7.3 msec.

One might therefore expect considerable variability in the latency τ, particularly under conditions of blood volume changes, changes in sympathetic tone, and wide variations in blood pressure. One of the objectives of our experiments therefore was to examine the variability of τ with various hemodynamic manipulations.

B. Methods

Three dogs weighing approximately 45 pounds each were used in the experiments. Each was anesthetized with nembutal injected intravenously at a dosage of 1 mg per 5 pounds of body weight. The chest, neck, and groin were shaved and prepped. The right common carotid artery and the left femoral artery were surgically exposed. The chest was opened by a transverse intercostal incision extending across the sternum. The left common carotid artery was exposed just distal to its point of origin at the arch of the aorta. (see Figure 3)

Pressures were recorded from the right carotid, the

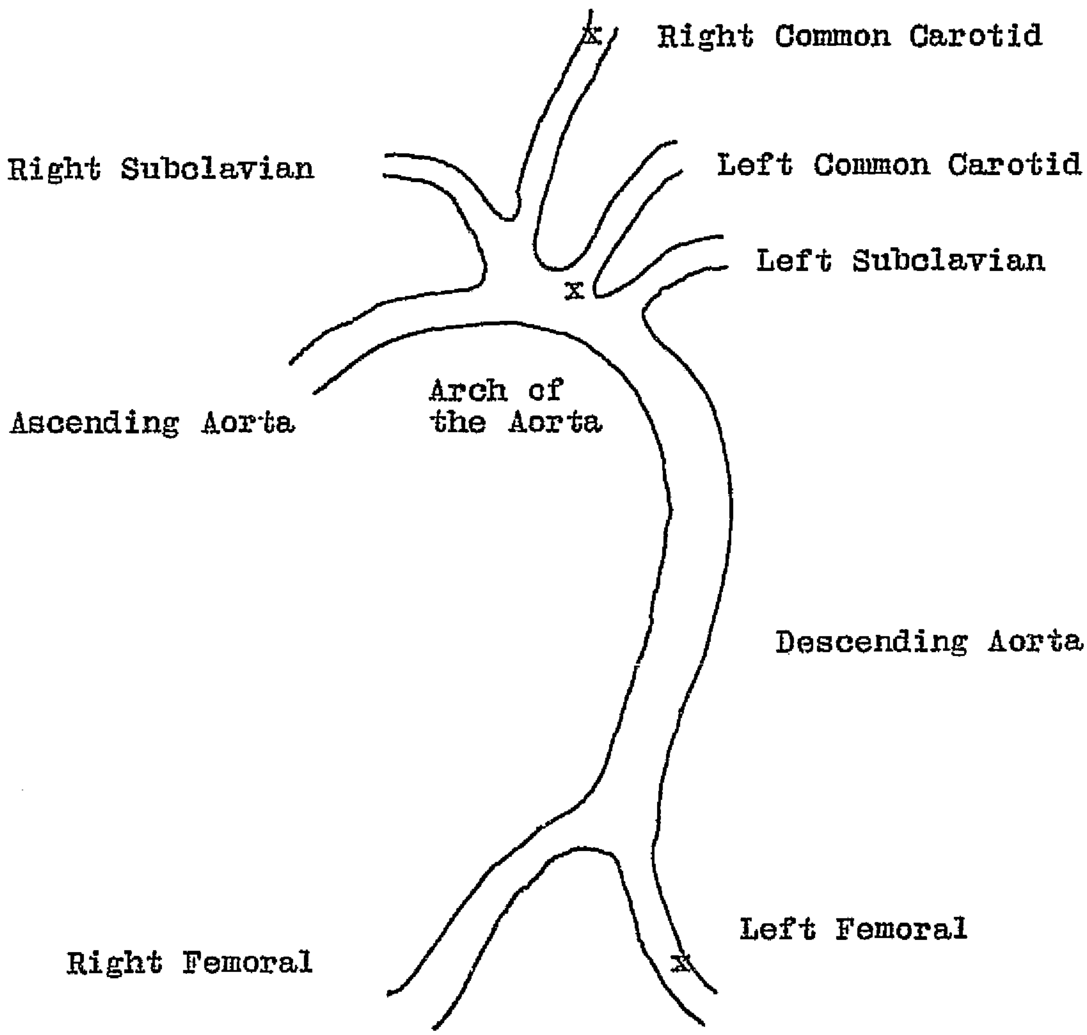

FIGURE 3. The aorta and its major branches. (x indicates locations where pressures were measured)

arch of the aorta, and the left femoral artery. Statham model P23Gb strain gage pressure transducers were used (P23Db for aorta), and were coupled to the arterial lumens by uniform 18.5 cm lengths of no. 220 polyethylene tubing. Aortic cannulation was accomplished via the left common carotid. In Experiment III the femoral pressure was recorded from the right femoral artery.

Sanborn carrier amplifiers (model 350-1100B) were used to amplify the pressure signals. The amplifiers were calibrated against a mercury manometer. Pressure wave forms were recorded on FM tape, and a multichannel chart recorder. Frequency responses of the components of the system are given in Table 1. The frequency response of the over-all system was limited by the pressure transducer and catheter, and was flat from 0 to 50 Hz.

In the third animal, mechanical movements of the left femoral and right carotid arteries were measured by means of transducers made from ceramic phonograph cartridges. (Figure 4) In order to obtain low frequency sensitivity, a very high input impedance voltage follower stage was used as a buffer between the cartridge and the recording system amplifiers. The LM302 was used, with an input impedance of 10^9 ohms.

Outputs from pressure transducers, mechanical transducers, and the EKG were recorded on both a chart recorder and FM tape recorder. Both a Sanborn hot stylus recorder and a Brush model 260 ink recorder were used in

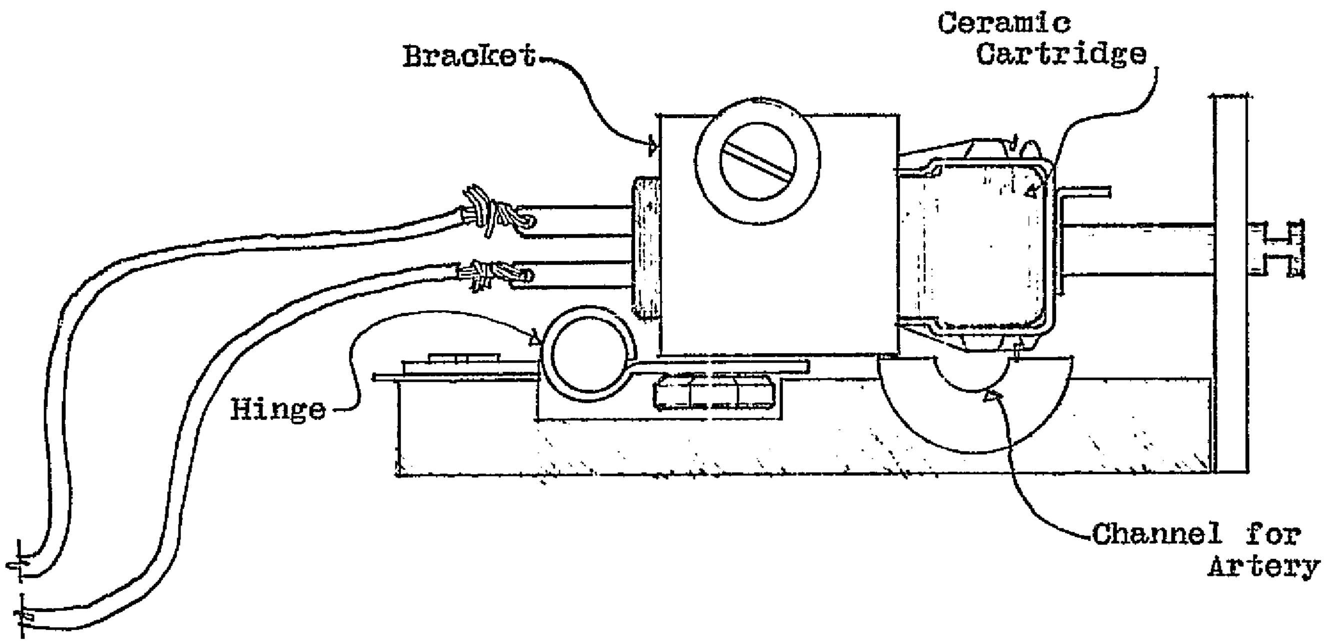

FIGURE 4. Mechanical transducer used to detect mechanical movements of the left femoral and right carotid arteries in Experiment III.

Table 1

Frequency Response of
Pressure Recording Components

1.	Statham model P23Db and P23Gb pressure transducers and catheters	0–50 Hz (estimated)
2.	Sanborn carrier amplifiers model 350-110B	3dB down at 480 Hz
3.	Sanborn FM tape recorder model 3907A	0–625 Hz
4.	Sanborn hot stylus chart recorder	1dB down at 70 Hz (full scale)
5.	Brush chart recorder model 260	0–50 Hz (full scale)

these experiments. Typical experimental data are illustrated in Figures 5 and 6.

Blood pressure was manipulated using a variety of drugs and also through inducing hypovolumia. Vasoconstriction was produced by Levophed, increased cardiac output by epinephrine, vasodilation by Isuprel, or Isuprel in combination with Regitine. Hypotension due to hypovolumia was produced after removing 600 cc of blood from the femoral artery (Experiment I) or vein (Experiments II and III). Table 2 is a list of the drugs given to each animal, their dosage, and their cardiovascular effects. Merck (1968)

C. Results

As can be seen in Figure 5, the shape of the pulse changes as it is propagated down the system; the rising portion of the wave, from onset to peak, sharpens, while the falling portion broadens. Therefore, the onsets of pressure waves, and of mechanical displacements, were used to determine transmission times. The first sharp rise after the QRS complex of the EKG was taken to be the onset.

Transmission time, Δt, was determined from the chart recordings to an accuracy of 5 msec with the aid of a straightedge. In some cases, particularly during hypovolumia, the accuracy of the transmission time was less than this because of ambiguities in the determination of onsets, resulting in errors of up to 10 msec. Pressures were also measured with the aid of a straightedge with an

Table 2

Drugs Administered During Experiments

Name	Effect	Dosage	Experiment
Epinephrine	Sympathetic stimulation, Increased heart rate, Increased cardiac output, Vasoconstriction	1cc, Injected intravenously	I
Levophed (1-norepinephrine)	Vasoconstriction	4cc/250ml, Intravenous drip in 5% dextrose solution (drip rate adjusted to produce desired effect)	I II III
Isuprel (Isoproterenol)	Cardiac stimulation, Vasodilation	1mg/250ml, Intravenous drip in 5% dextrose solution (drip rate adjusted to produce desired effect)	II III
Regitine (Phentoamine)	Vasodilation, Increased heart rate	5mg, Injected intravenously	II III

accuracy of 2.5 mm of Hg.

"Best-fit" lines were calculated for the plots of $1/\Delta t$ versus pressure (Figures 8-18) using the method of least squares. [Davies (1961)] (Data from which these plots were constructed are given in Appendix B.) The standard deviation in measured minus calculated pressures for each plot was calculated from the following formula: [Davies (1961)]

$$\sigma = (\sum(P_i - P_{cal})^2/(N-2))^{1/2}$$

Where:
P_i = measured pressure
P_{cal} = calculated pressure
N = number of data points

Figure 7 is a plot of the transmission time from the arch of the aorta to the femoral artery versus carotid diastolic pressure, and is from Experiment I. The graph is both qualitatively and quantitatively similar to one published by Hamilton, Remington, and Dow (1945) from a nearly identical experiment in which diastolic pressure was manipulated with epinephrine and transmission times were measured from pulse wave onsets at the ascending aorta and the bifurcation of the iliacs.

If the inverse of the transmission time, which is velocity in arbitrary units, is plotted against carotid diastolic pressure (Figure 8), the straight-line relationship observed by Steele (1937) becomes apparent. Even

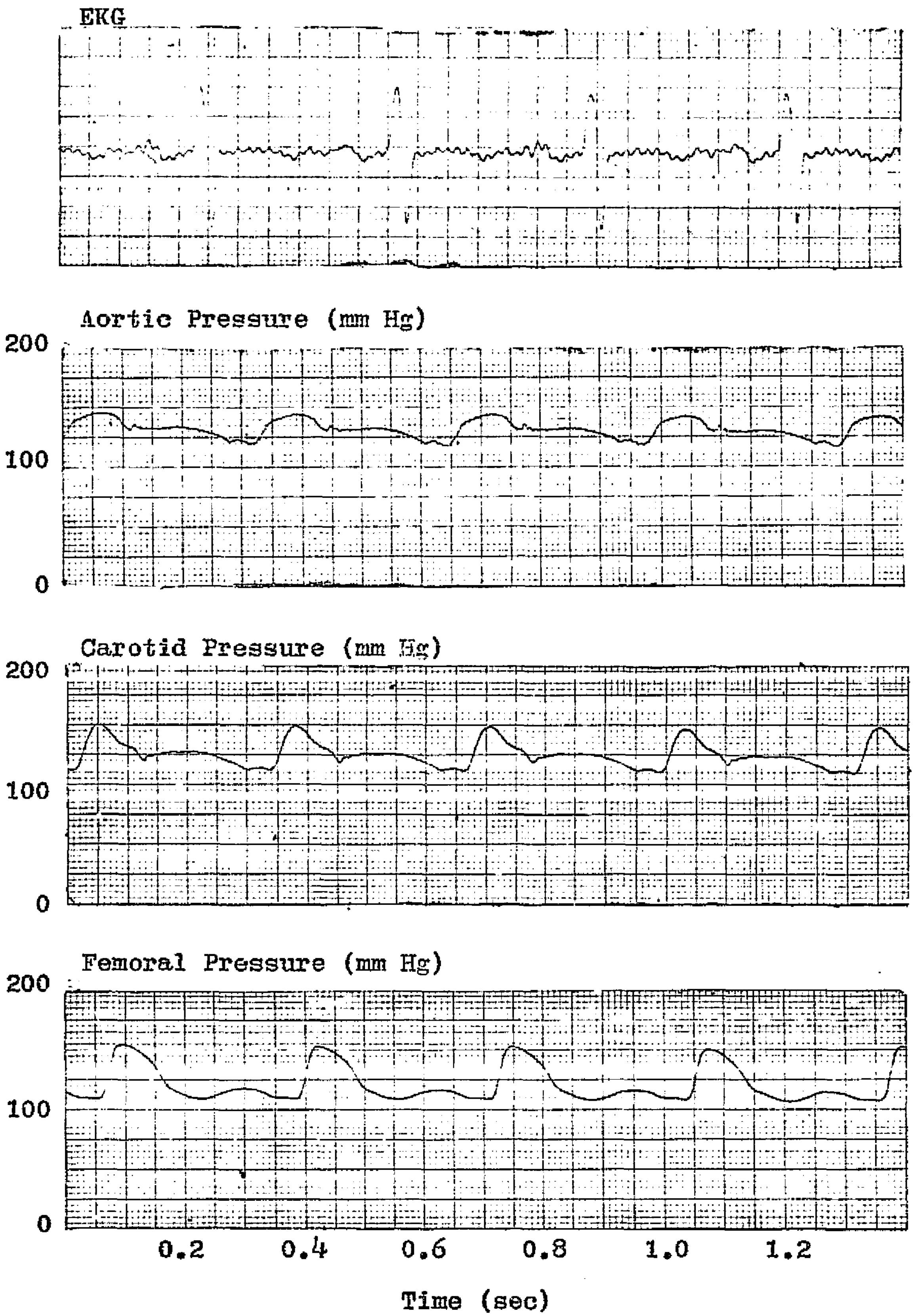

FIGURE 5. Wave forms from Experiment II. (Sanborn recorded)

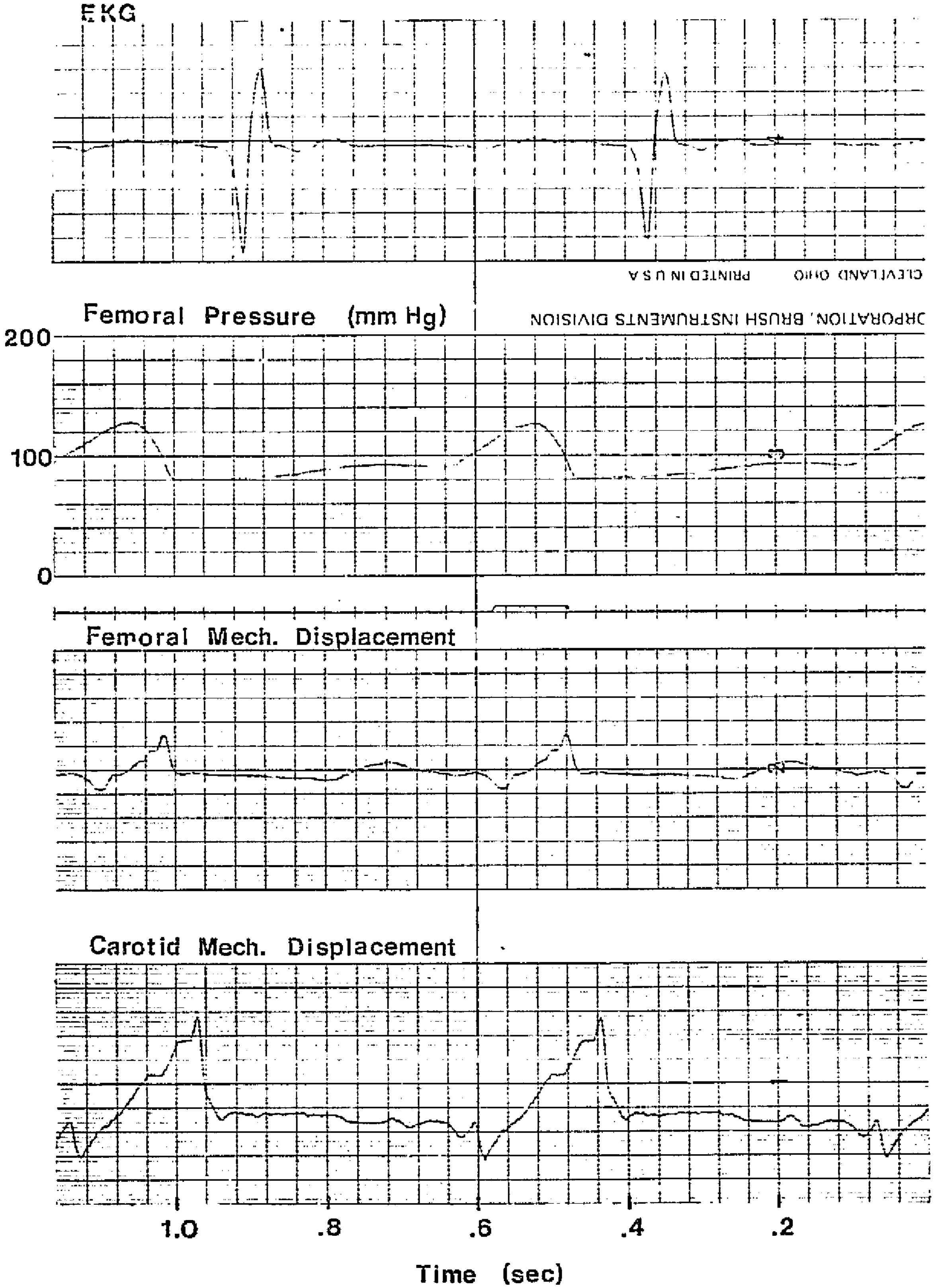

FIGURE 6. Wave forms from Experiment III. (Brush recorder)

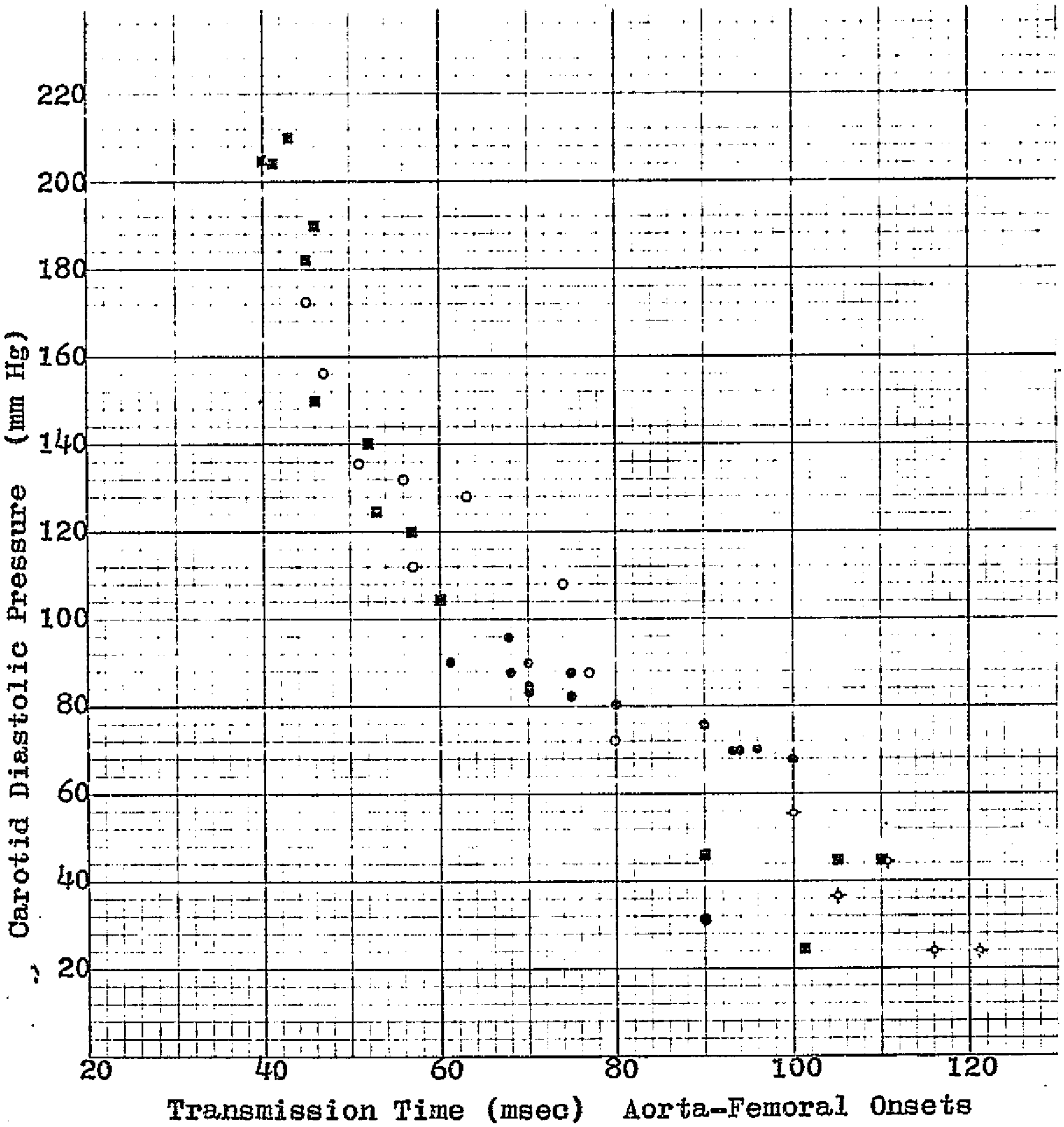

FIGURE 7. Plot of carotid diastolic pressure versus the time interval between the onset of the pulse wave in the aorta and the onset in the femoral artery. Data taken under various conditions in Experiment I (✧ = hypovolumia, • = normal, ▪ = epinephrine, ∘ = Levophed).

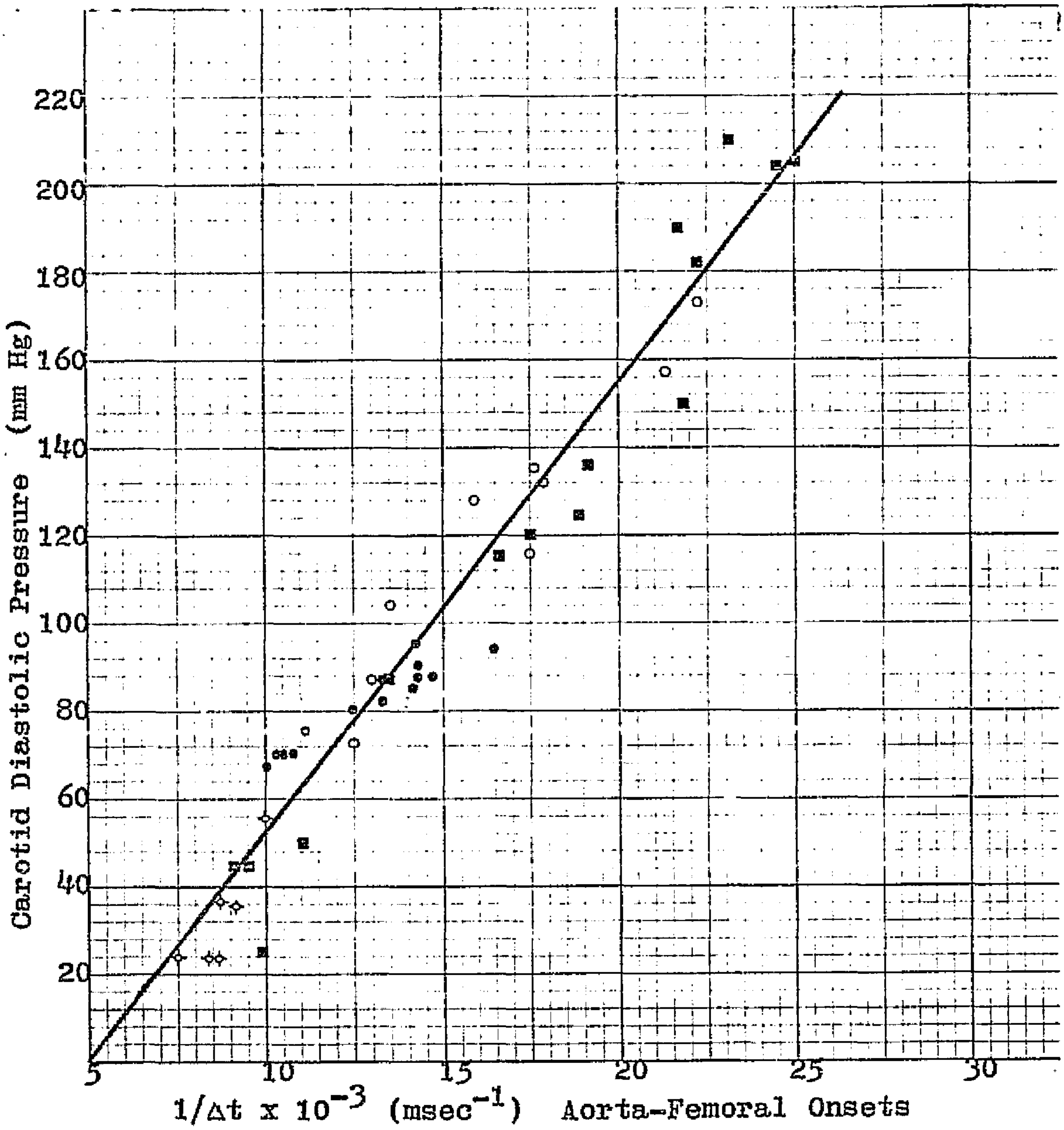

FIGURE 8. Plot of carotid diastolic pressure versus the inverse of the time interval between the onset of the pulse wave in the aorta and the onset in the femoral artery. Data taken under various conditions from Experiment I (◇ = hypovolumia, • = normal, ▪ = epinephrine, ∘ = Levophed). Best-fit line: $P = 1.02 \times 10^{4}(1/\Delta t) - 51.07$, $\sigma = 11.75$.

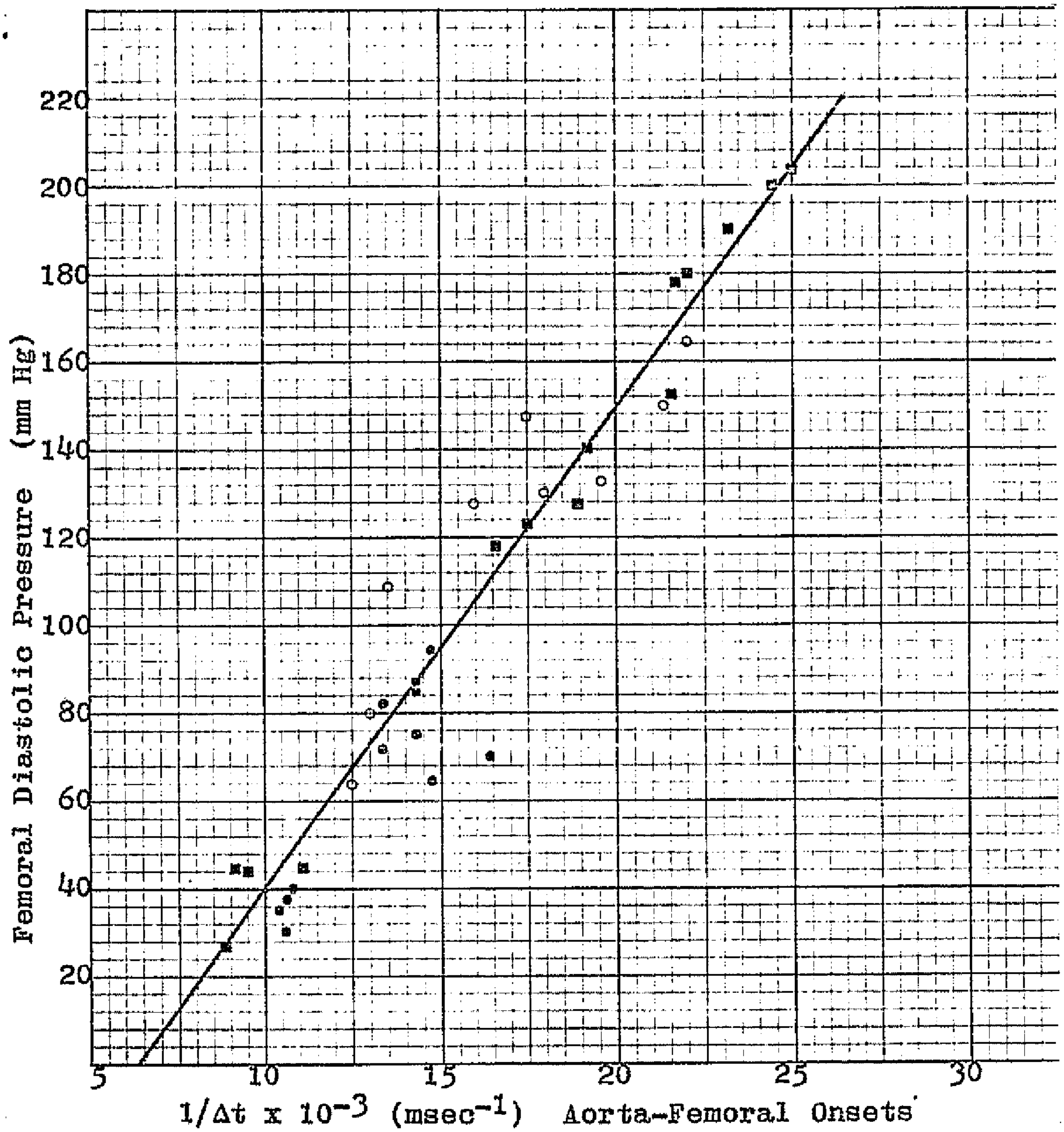

FIGURE 9. Plot of femoral diastolic pressure versus the inverse of the time interval between the onset of the pulse wave in the aorta and the onset in the femoral artery. Data taken under various conditions from Experiment I (◇ = hypovolumia, • = normal, ▪ = epinephrine, ○ = Levophed). Best-fit line: $P = 1.104 \times 10^4 (1/\Delta t) - 71.65$, $\sigma = 15.060$.

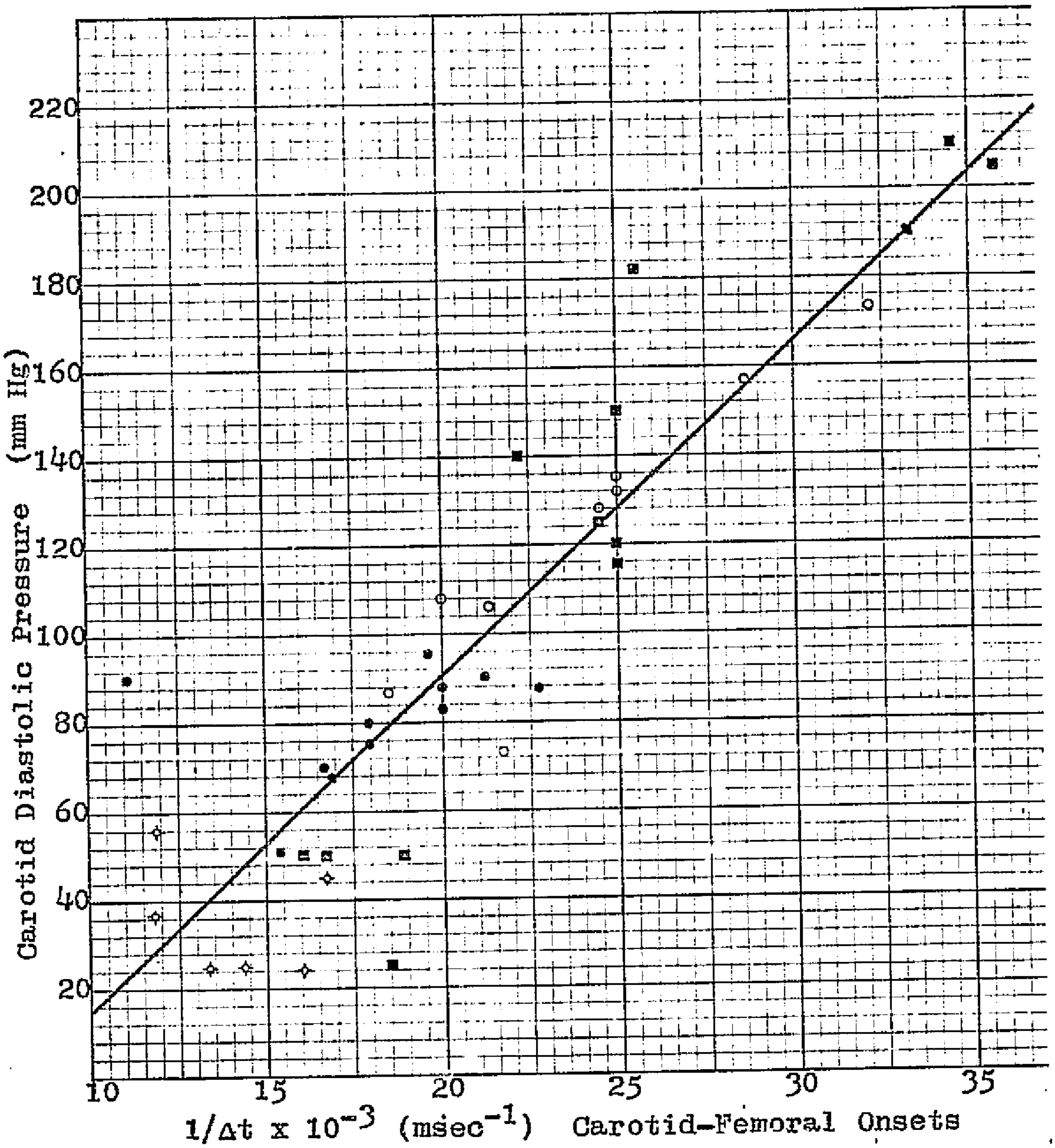

FIGURE 10. Plot of carotid diastolic pressure versus the inverse of the time interval between the onset of the pulse wave in the carotid artery and the onset in the femoral artery. Data taken under various conditions from Experiment I (✧ = hypovolumia, • = normal, ■ = epinephrine, ○ = Levophed). Best-fit line: $P = 7.38 \times 10^{3}(1/\Delta t) - 57.75, \quad \sigma = 21.976.$

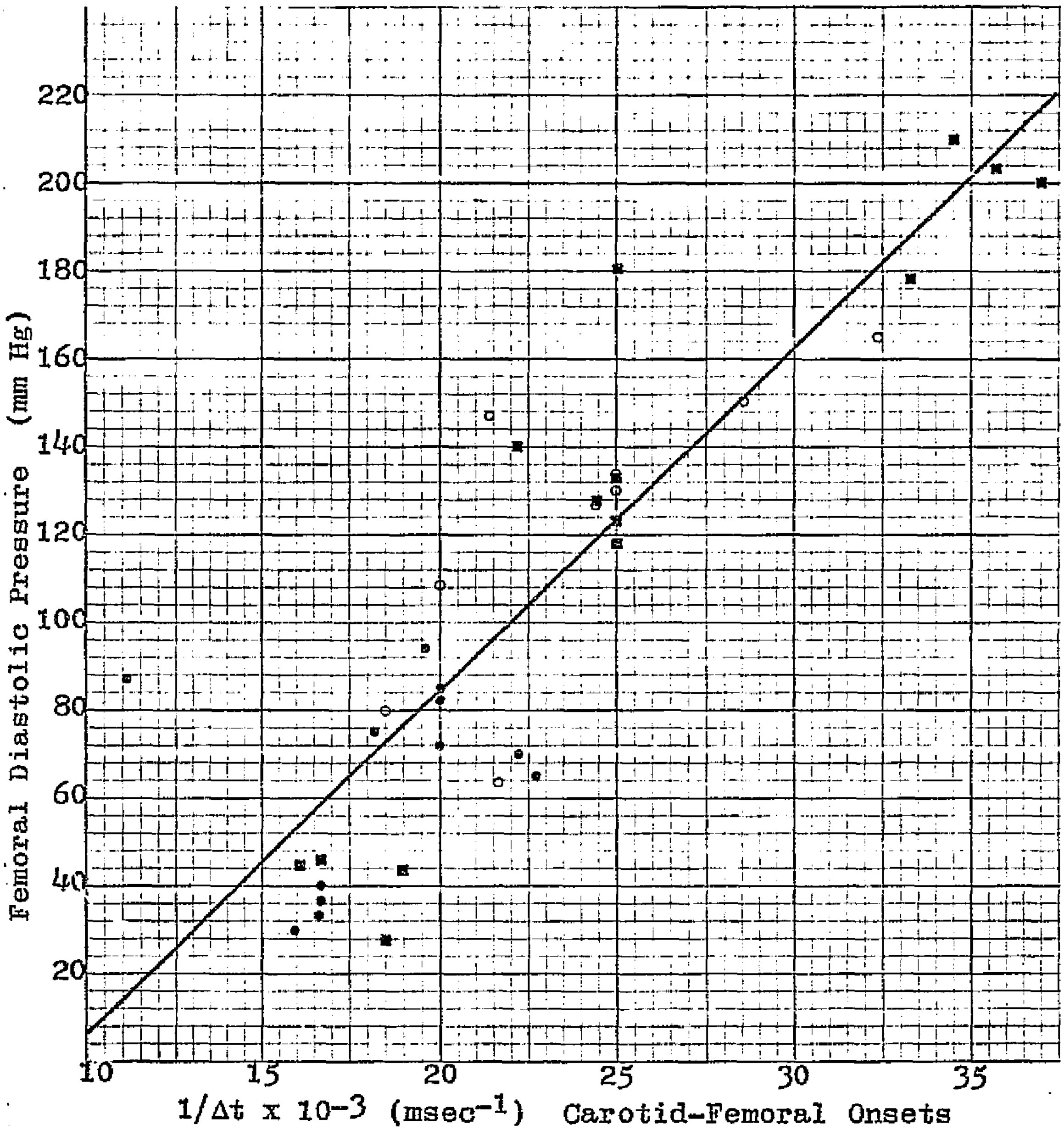

FIGURE 11. Plot of femoral diastolic pressure versus the inverse of the time interval between the onset of the pulse wave in the carotid artery and the onset in the femoral artery. Data taken under various conditions from Experiment I (✧ = hypovolumia, • = normal, ▪ = epinephrine, ∘ = Levophed). Best-fit line: $P = 7.73\times10^{3}(1/\Delta t)-70.83$, $\sigma = 26.662$.

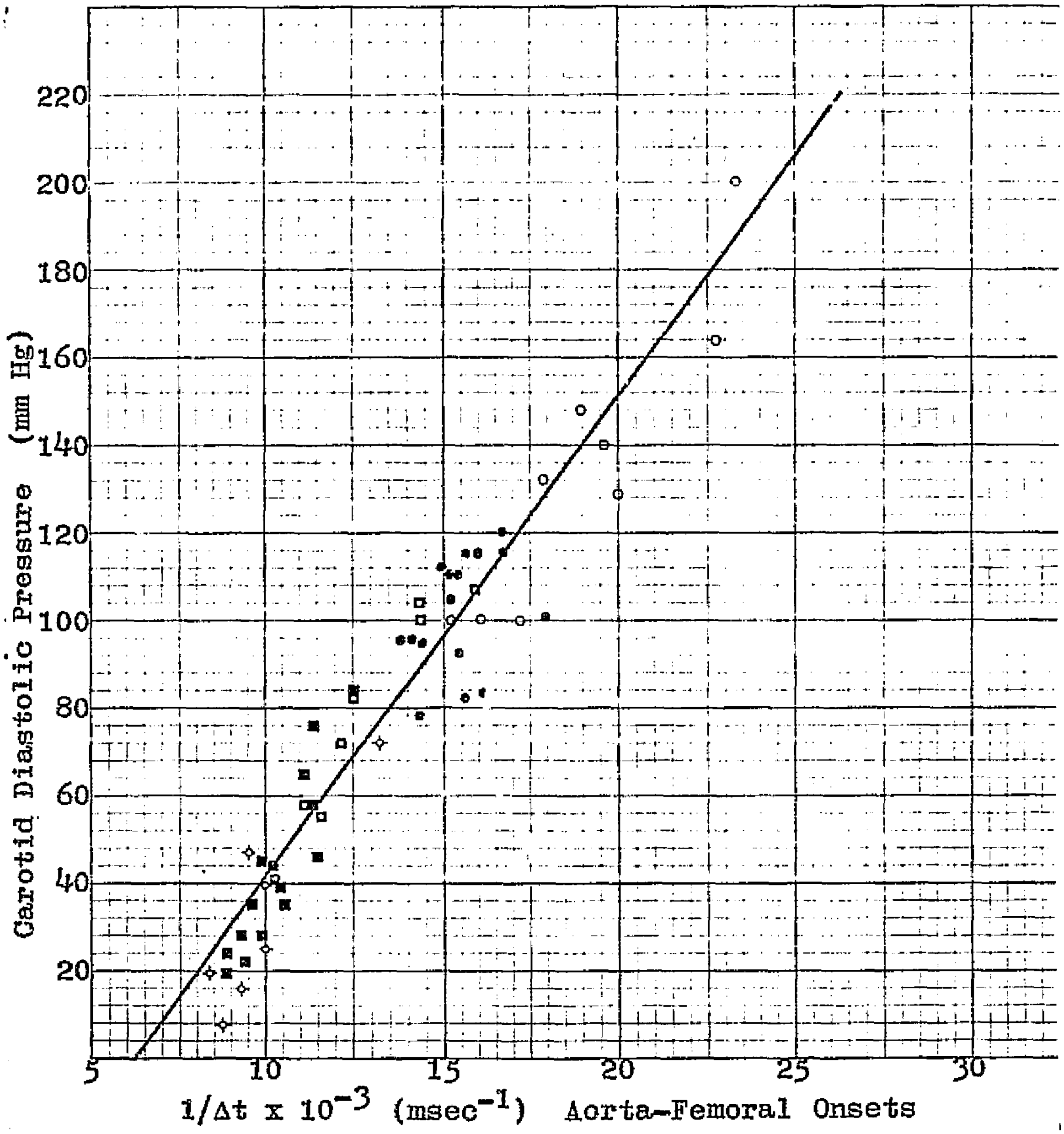

FIGURE 12. Plot of carotid diastolic pressure versus the inverse of the time interval between the onset of the pulse wave in the aorta and the onset in the femoral artery. Data taken under various conditions from Experiment II (✧ = hypovolumia, ■ = Isuprel and Regitine, □ = Isuprel, • = normal, ○ = Levophed). Best-fit line: $P = 1.107\times10^{4}(1/\Delta t)-70.31$, $\sigma = 11.85$.

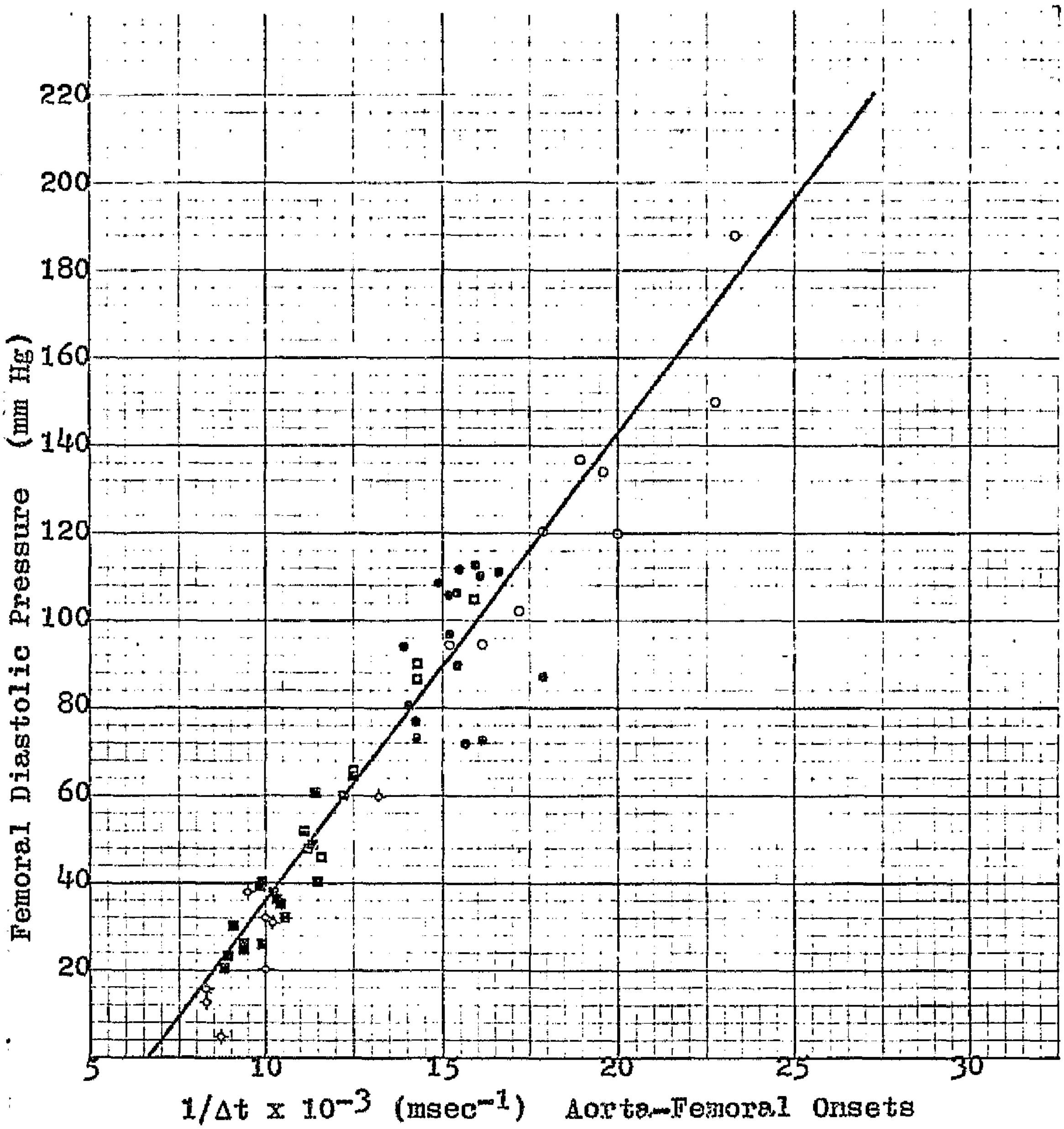

FIGURE 13. Plot of femoral diastolic pressure versus the inverse of the time interval between the onset of the pulse wave in the aorta and the onset in the femoral artery. Data taken under various conditions from Experiment II (◇ = hypovolumia, ■ = Isuprel and Regitine, □ = Isuprel, • = normal, ○ = Levophed). Best-fit line: $P = 1.06 \times 10^4 (1/\Delta t) - 70.96$, $\sigma = 11.04$.

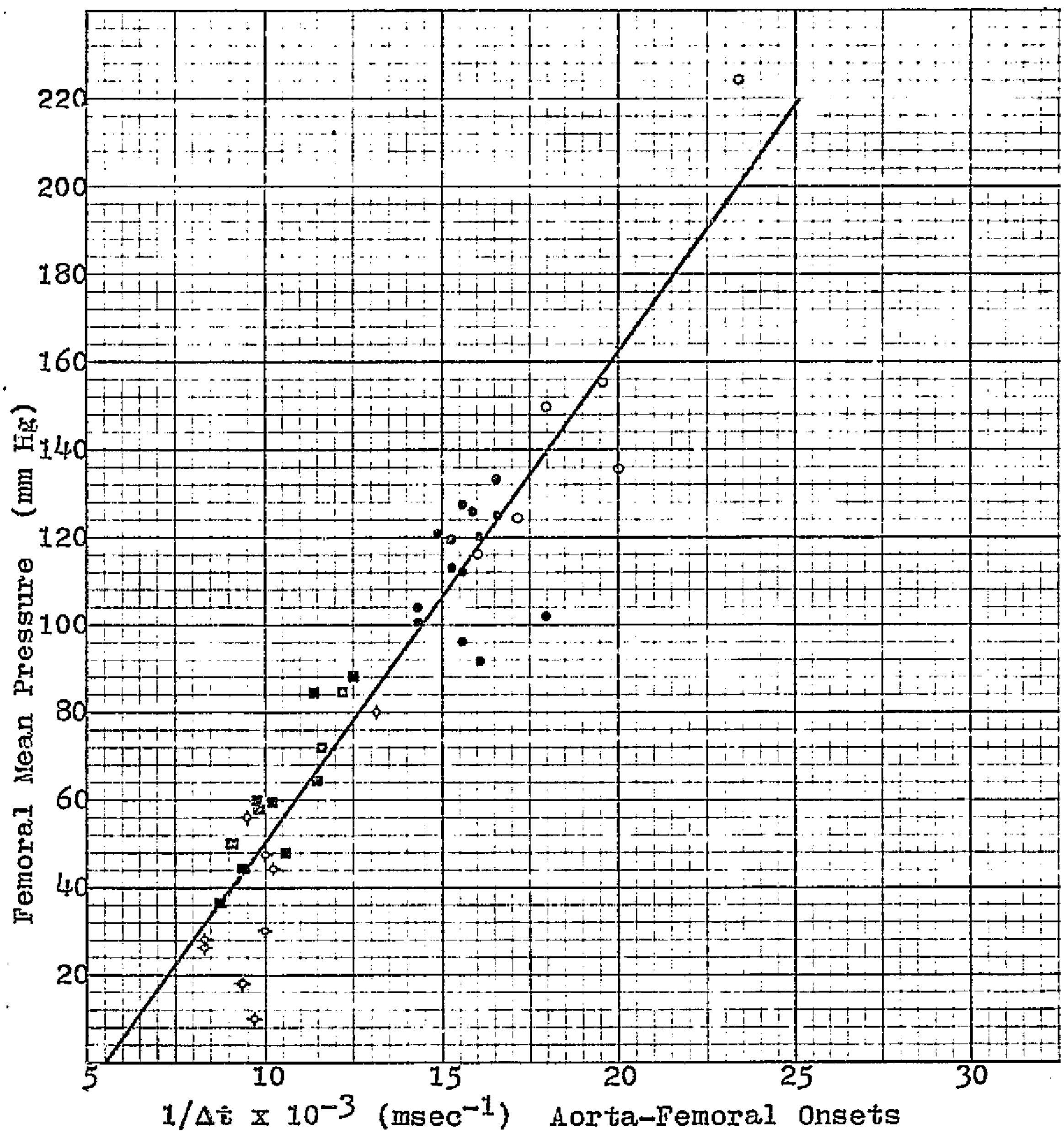

FIGURE 14. Plot of femoral mean pressure versus the inverse of the time interval between the onset of the pulse wave in the aorta and the onset in the femoral artery. Data taken under various conditions from Experiment II (✧ = hypovolumia, ▪ = Isuprel and Regitine, ▫ = Isuprel, • = normal, ∘ = Levophed). Best-fit line: $P = 1.16 \times 10^4 (1/\Delta t) - 62.65$, $\sigma = 15.265$.

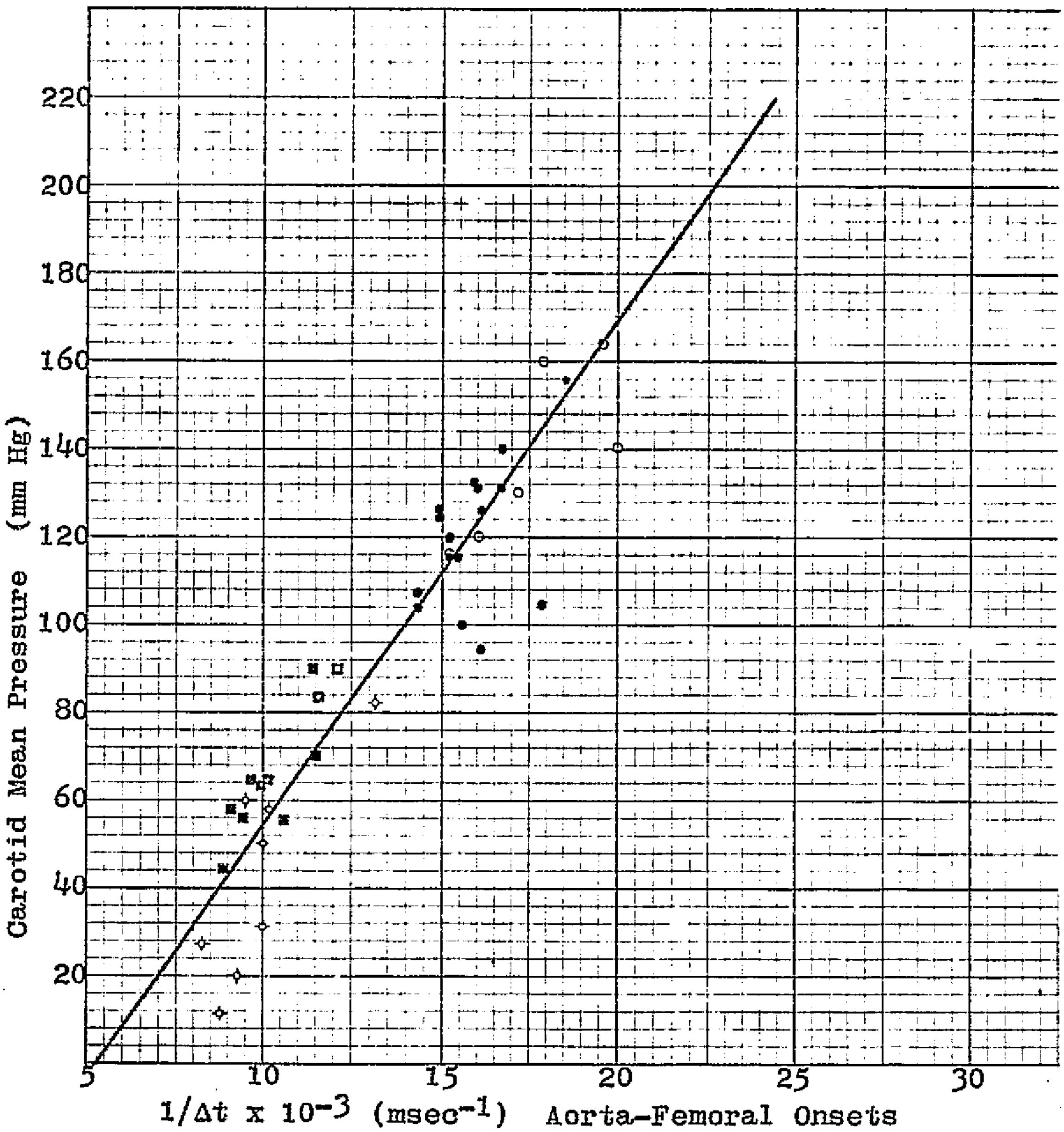

FIGURE 15. Plot of carotid mean pressure versus the inverse of the time interval between the onset of the pulse wave in the aorta and the onset in the femoral artery. Data taken under various conditions from Experiment II (◇ = hypovolumia, ▪ = Isuprel and Regitine, ▫ = Isuprel, • = normal, ○ = Levophed). Best-fit line: $P = 1.14 \times 10^4 (1/\Delta t) - 64.96$, $\sigma = 13.81$.

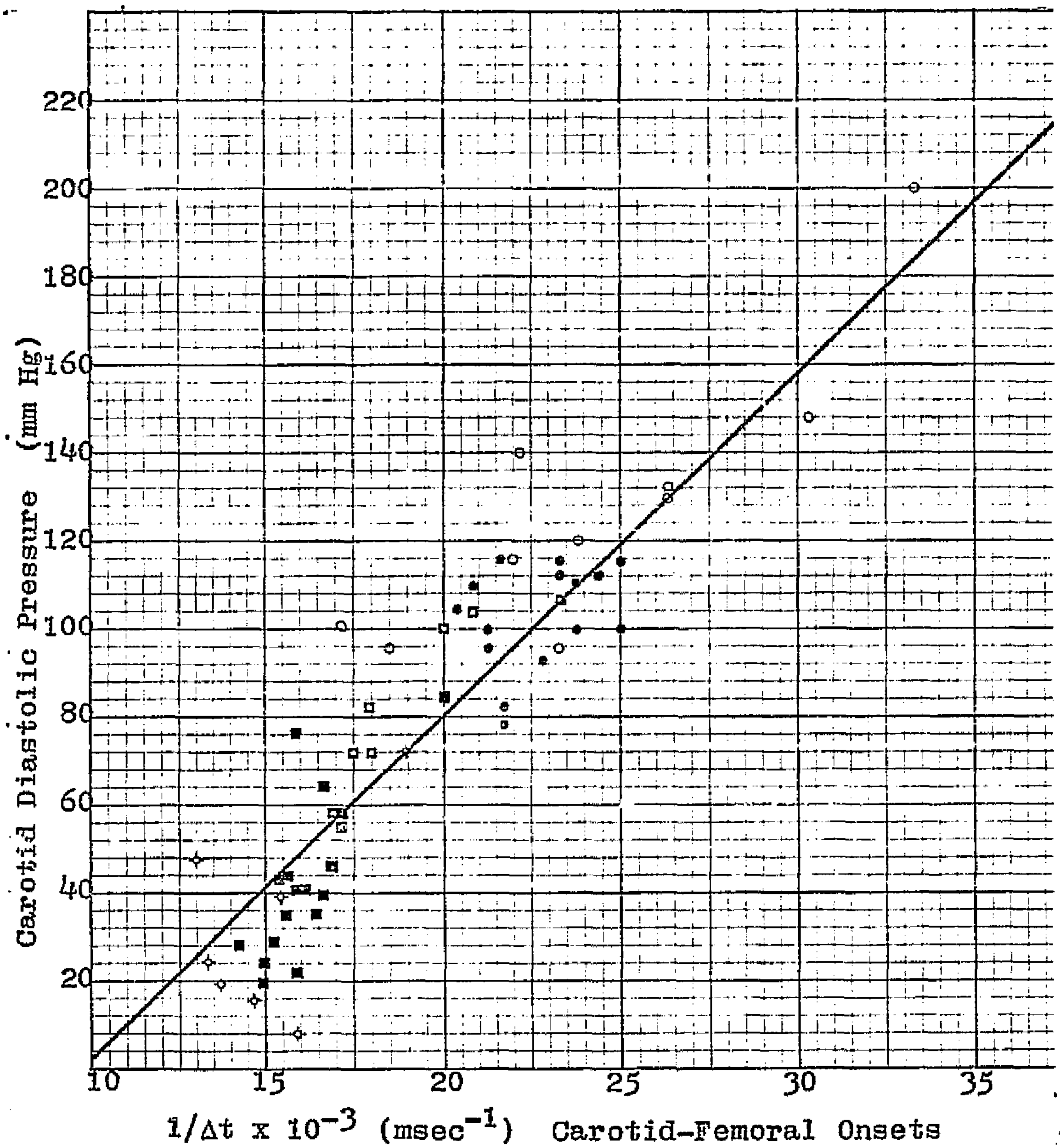

FIGURE 16. Plot of carotid diastolic pressure versus the inverse of the time interval between the onset of the pulse wave in the carotid artery and the onset in the femoral artery. Data taken under various conditions from Experiment II (⟡ = hypovolumia, ▪ = Isuprel and Regitine, ▫ = Isuprel, • = normal, ◦ = Levophed). Best-fit line: $P = 7.58x10^{3}(1/\Delta t) - 71.86$, $\sigma = 17.83$.

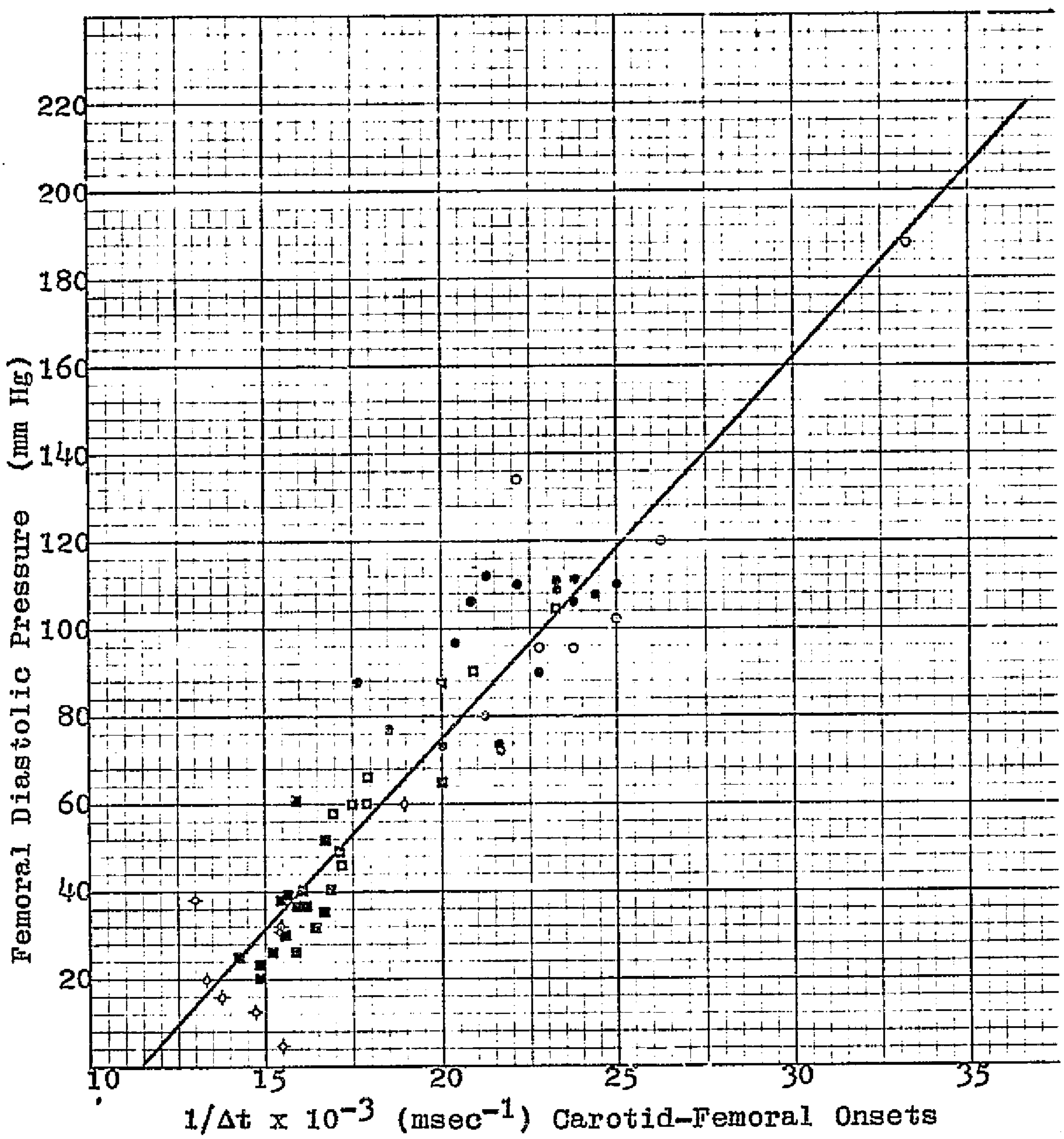

FIGURE 17. Plot of femoral diastolic pressure versus the inverse of the time interval between the onset of the pulse wave in the carotid artery and the onset in the femoral artery. Data taken under various conditions from Experiment II (✧ = hypovolumia, ▪ = Isuprel and Regitine, ▫ = Isuprel, • = normal, ◦ = Levophed). Best-fit line: $P = 8.64 \times 10^{3}(1/\Delta t) - 97.95$, $\sigma = 16.00$.

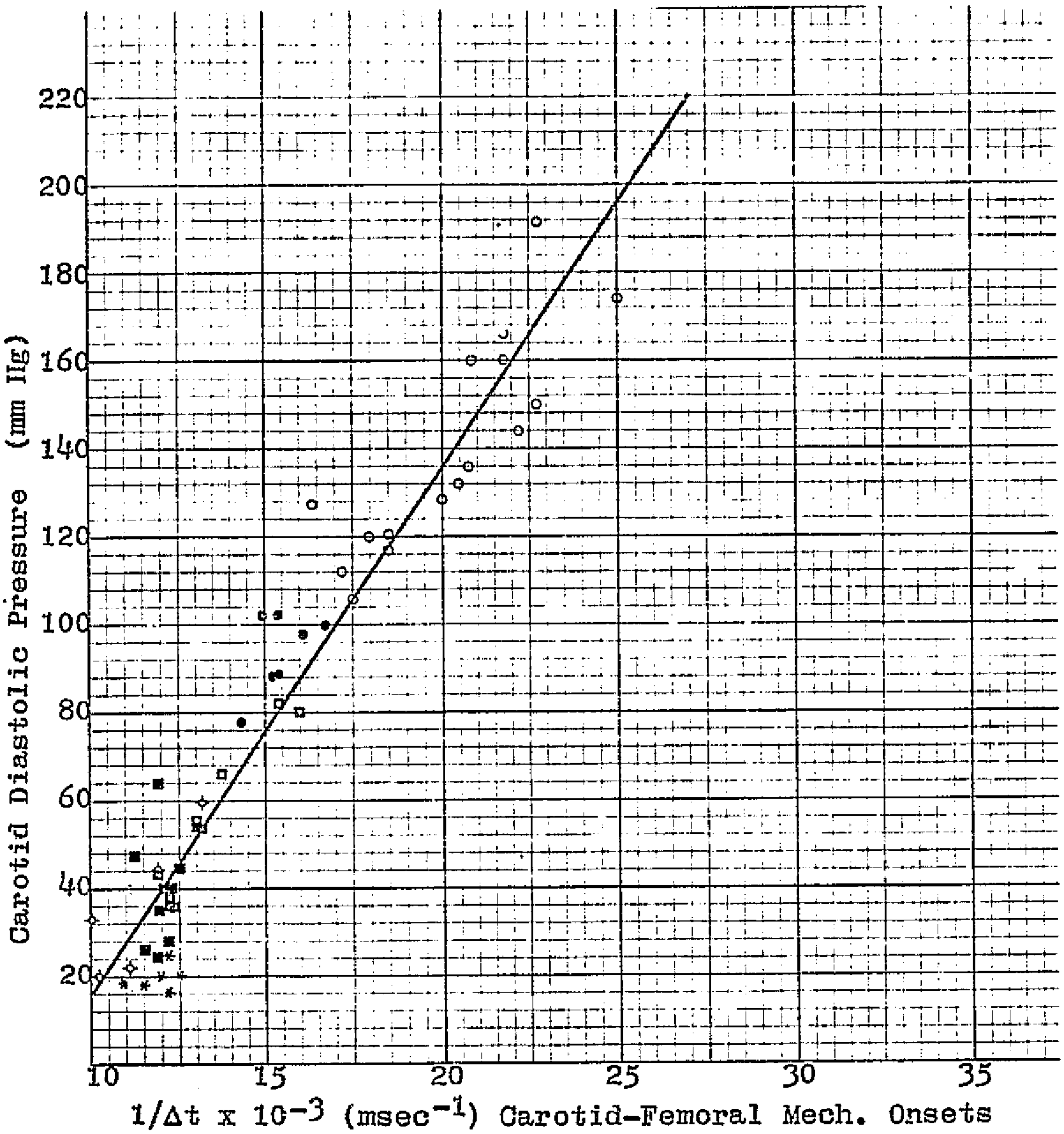

FIGURE 18. Plot of femoral diastolic pressure versus the inverse of the time interval between the onset of the mechanical displacement in the carotid artery and the onset of the displacement in the femoral artery. Data taken under various conditions in Experiment III (✧ = hypovolumia, * = hypovolumia and Isuprel, ▪ = Re[illegible]itine and Isuprel, ▫ = Isuprel, • = normal, ○ = Levophed). Best-fit line: $P = 1.20 \times 10^{4}(1/\Delta t) - 104.83$, $\sigma = 13.96$.

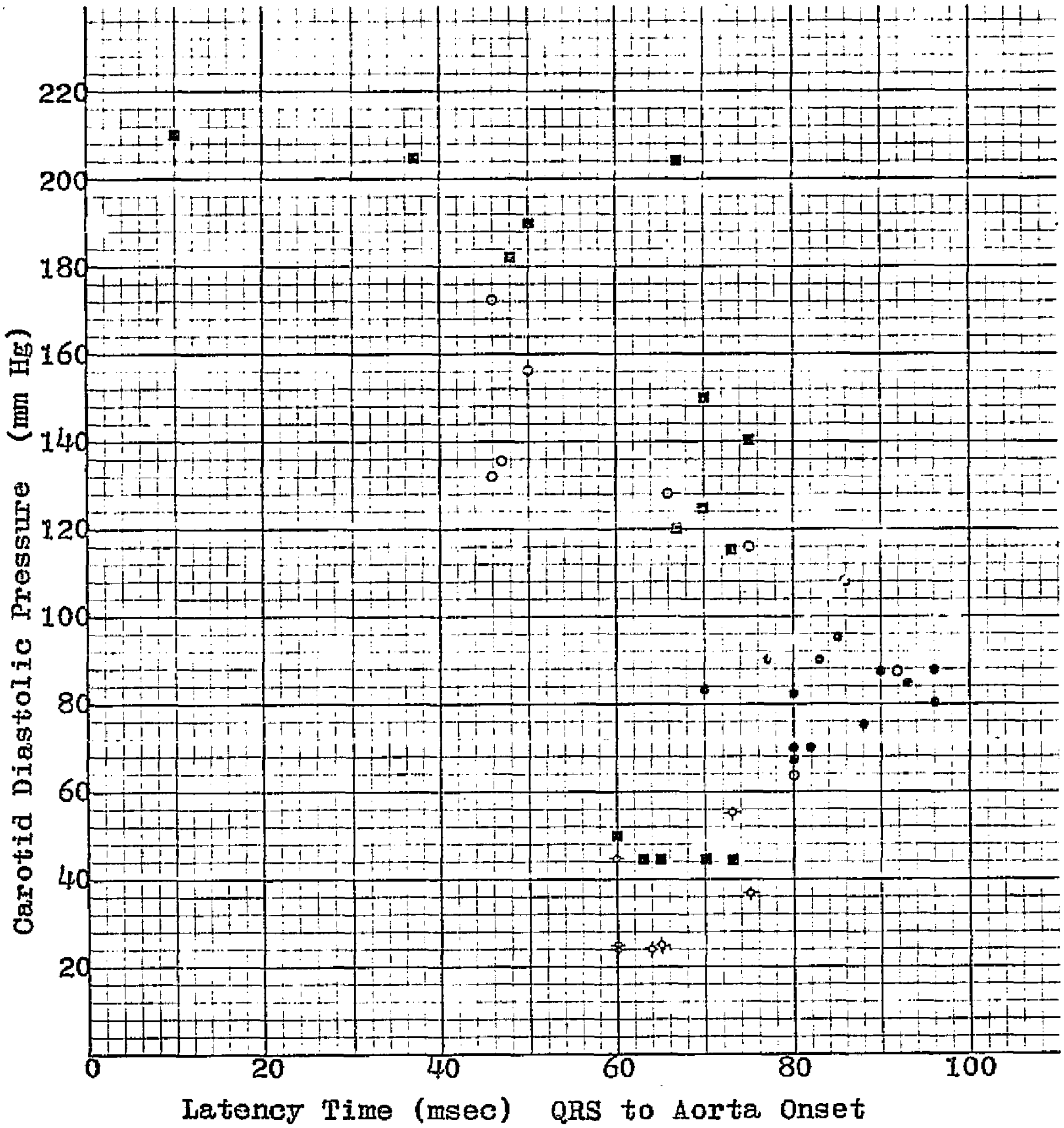

FIGURE 19. Plot of carotid diastolic pressure versus the time interval from the QRS complex to the onset of the pulse wave in the aorta. Data taken under various conditions in Experiment I (⟡ = hypovolumia, • = normal, ▪ = epinephrine, ◦ = Levophed).

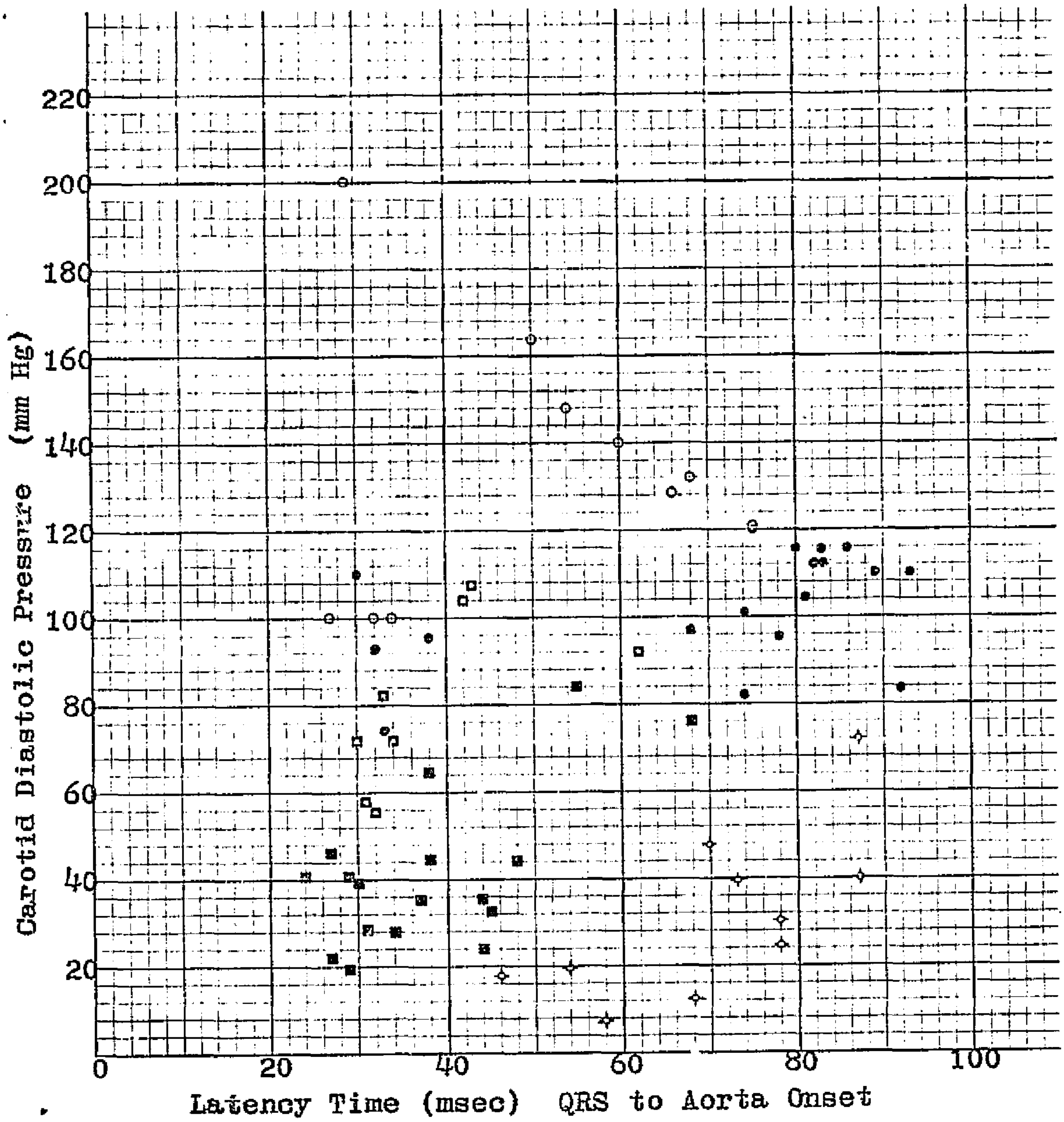

FIGURE 20. Plot of carotid diastolic pressure versus the time interval from the QRS complex to the onset of the pulse wave in the aorta. Data taken under various conditions in Experiment II (✧ = hypovolumia, ▪ = Isuprel and Regitine, ▫ = Isuprel, • = normal, ∘ = Levophed).

though the pressure was manipulated over a larger range under various conditions, there is no systematic departure from linearity with any of the drugs or hypovolumia. This was observed to be true for data from all experiments, as can be seen in Figures 8-18.

A minor exception to this observation was found in the plots of carotid and femoral mean pressures versus aorta-femoral velocity from Experiment II. (Figures 14 and 15) As mentioned earlier, Steele (1937) carried out a series of experiments illustrating that pulse wave velocity is related to diastolic pressure rather than mean pressure, even though Schimmler (1966) had found a linear relationship between velocity and mean pressure. This was explained by observing that mean pressure is usually linearly related to diastolic pressure, so velocity would vary in the same way with both. When Isuprel was given in Experiment II, the contractility of the heart, and hence the pulse pressure, increased, resulting in a larger difference than normal between the diastolic and mean pressures. Conversely, during hypovolumia, the pulse pressure was decreased, hence the difference between mean and diastolic pressures was smaller. As can be seen from Figures 14 and 15, the points taken under Isuprel tend to lie above the line, while the points taken during hypovolumia lie below the line. Although this effect was small, it agrees with Steele's conclusion that pulse wave velocity follows diastolic pressure.

The velocities measured in Experiments I and II were plotted against both carotid and femoral pressures. (Figures 8 and 9, 10 and 11, 12 and 13, 14 and 15, and 16 and 17) As can be seen from these pairs of graphs, the relationships shown do not depend on where the pressure was measured. The best example is from Experiment II with aortic-femoral diastolic pressures. (Figures 12 and 13) The slopes of the lines are 1.107×10^4 and 1.06×10^4, the intercepts are -70.31 and -70.96 and the standard deviations are 11.85 and 11.04.

Note that the slopes of the curves of Figures 9 and 13 are very similar across animals. This finding implies great similarity in the properties of the dog's vascular systems.

As noted above, it would be desirable to find a way to detect the onset of pressure in the aorta. This would provide a maximum distance over which to measure velocity in the large vessels, and therefore give more accurate results. This can be seen by comparing Figure 13, which is a plot of femoral diastolic pressure versus aorta-femoral velocity, and Figure 17, which is a plot of femoral diastolic pressure versus carotid-femoral velocity. The graph in Figure 13 has a standard deviation of 11.04, as compared to 16.00 for the graph in Figure 17.

The standard deviation for femoral diastolic pressure as a function of carotid-femoral velocity was improved by the use of mechanical transducers in Experiment III (Figure 18), giving a standard deviation of 13.96. This can be attributed to the sharper initial rise of the mechanical transducer wave form as can be seen in Figure 6, giving a more difinitive onset, and hence more consistent results. These results, however, are still not as good as those measured over a longer effective distance.

A possible method already mentioned would be use of the QRS complex of the EKG as a timing reference for the onset of pressure in the aorta. This could only be used if the variability in the time interval (τ) between the EKG and the aortic pressure onset were small. Figures 19 and 20 are plots of τ versus carotid diastolic pressure from Experiments I and II. If there were not variability, one would expect the plots to be vertical lines. As can readily be seen from the graphs, the variability in τ is large, comparable to τ itself observed under normal conditions.

The effects of the drugs and reduction of blood volume in these experiments can readily explain the effects observed on τ. Under normal conditions, τ varies from 80 to 90 msecs, which is consistent with the previous studies discussed earlier. During hypovolumia, the ventricles are not allowed to fill completely, resulting in a decreased cardiac output and lower blood pressure. Since the ventricles are not completely filled, they contract more rapidly against less resistance, resulting in the smaller values of τ observed, with τ decreasing as the effect becomes more pronounced, and blood pressure drops. Isuprel stimulates heart muscle, causing more vigorous contraction and therefore reduced values of Υ. The combination of Regitine, which is a vasodilator, and Isuprel produced a marked further decrease in blood pressure and a slight decrease in Υ. Epinephrine also stimulates the heart, increasing both cardiac output and heart rate, also resulting in more vigorous contraction and reduced values of Υ. Levophed, which is mainly a vasoconstrictor, had a smaller effect on Υ than epinephrine, but also reduced Υ as the pressure increased. This reduction was most probably a function of the observed increase in heart rate.

IV. DISCUSSION

1. There is a linear relationship between pulse wave velocity and diastolic pressure under the following conditions:
   a. Vasoconstriction, increased heart rate (Levophed)
   b. Vasoconstriction, increased heart rate, increased cardiac output (epinephrine)
   c. Normal
   d. Increased contractility of the heart and vasodilation (Isuprel)
   e. Increased contractility, increased heart rate, vasodilation (Isuprel and Regitine)
   f. Hypovolumia
2. Pressures measured in the femoral or in the carotid arteries give similar curve parameters, indicating the

pressure-velocity relationship does not depend substantially on where the pressure is measured.

3. Velocities measured between the arch of the aorta and the femoral artery give smaller standard deviations in pressure than do velocities measured between the carotid and femoral arteries.
4. Plots of mean pressures versus velocity show small systematic departures from linearity under conditions where the difference between mean and diastolic pressure is higher or lower than normal. These departures are in the direction expected if velocity follows diastolic pressure.
5. Data from mechanical transducers in Experiment III give pressure-velocity curves similar to those from pressure transducer data with a smaller standard deviation for similar variables. This is explained by a smaller onset ambiguity due to the sharper initial rise of mechanical transducer wave forms.
6. The variability in the EKG to aorta pressure onset delay time is too large to make it useful as an indication of the aortic pressure rise.

It has been seen that there is a linear relationship between diastolic pressure and pulse wave velocity over a wide variety of conditions. The parameters of the relationship are functions of the properties of the artery and vary between individuals. Therefore, they must be determined empirically for each individual. This could most easily be accomplished by measuring transmission times between two points and measuring pressure with the traditional auscultatory method. If this is done for at least two different pressures, the physician could obtain the slope and intercept of the curve relating the inverse of transmission time (velocity) to diastolic pressure for that patient and those transducer locations. With just a record of transmission times, the physician would have enough information to determine the patient's diastolic pressure throughout a day's activities.

With this scheme in mind, there are a number of areas for futute investigation:

1. The possibility of using the second heart sound as an indication of pressure onset in the aorta,
2. The development of a transducer to detect the arrival of a pulse wave without artifacts which does not interfere with an ambulatory patient's usual activities,
3. The design of a portable electronic system to process transducer input and store transmission times or their inverses.

APPENDIX A

Derivation of the Moens Formula [Hardung (1962)]

Consider a visco-elastic tube of radius r and cross-sectional area Q. When a pulse passes through the tube the radius changes, therefore:

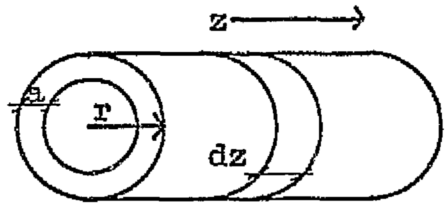

Figure 1

$$r = r(z,t)$$

$$Q = Q(z,t)$$

Consider as an element of volume a small disc of thickness dz. If P is the pressure in the tube, the force on it is given by:

$$dF_z = -(Q\cdot P)_{z+dz} + (Q\cdot P)_z = -(\partial(Q\cdot P)/\partial z)dz \qquad (1)$$

$$dF_z = -Q\cdot(\partial P/\partial z)\cdot dz - P\cdot(\partial Q/\partial z)\cdot dz \qquad (1a)$$

Since dQ/Q is small, dQ/dz is also small and:

$$dF_z \cong -Q\cdot(\partial P/\partial z)\cdot dz \qquad (1b)$$

The mass of the disc $dm = \rho Qdz$ where ρ is density. From Newton: $F = ma$, therefore:

$$\rho\cdot(\partial^2 z/\partial t^2) = -(\partial P/\partial z) \qquad (2)$$

Introducing flow volume $i_z = Q(dz/dt)$,

$$\partial i_z/\partial t = -(Q/\rho)(\partial P/\partial z) \qquad (3)$$

From the continuity equation, the intake of volume minus the outflow equals the increase of volume of the disc or:

$$di_z(z,t) = (\partial i_z/\partial z)dz = -i_r \quad (4)$$

Where:
i_r = radial current

$$i_r = (dr/dt)2\pi rdz \quad (5)$$

From Hooke's Law:

$$2\pi dr/2\pi r = (1/E\cdot a\cdot dz)\ d(P\cdot r)dz$$

Where:
a = wall thickness
P·r = T, tension on the wall, from Laplace's Law

$$dr/r = (1/E\cdot a)(Pdr + rdP) \quad (6a)$$

Since Pdr is small compared to rdP,

$$dP \cong Ea/r^2 \cdot dr \quad (6b)$$

Differentiating equation (6b) by t and combining with equations (4) and (5):

$$-(\partial P/\partial t) = 1/2\pi\ (\partial i_z/\partial z)(Ea/r^3) \quad (7)$$

Differentiating equation (7) by z:

$$-\partial^2 P/\partial z\ t = 1/2\pi\ (\partial^2 i_z/\partial z^2\ Ea/r^3 + \partial i_z/\partial z\ Ea\ \partial r^3/\partial z) \quad (7a)$$

Since $\partial r/\partial z$ is small:

$$-(\partial^2 P/\partial t\partial z) \cong (E\cdot a/2\pi r^3)(\partial^2 i_z/\partial z^2) \quad (7b)$$

Differentiating equation (3) by z twice gives:

$$\partial^3 i_z/\partial t\partial z^2 = -(Q/\rho)(\partial^3 P/\partial z^3) \quad (8)$$

Differentiating equation (7b) by z:

$$-(\partial^3 P/\partial t\partial z^2) = (Ea/2\pi r^3)(\partial^3 i_z/\partial i_z) \quad (9)$$

Combining equations (8) and (9):

$$(Q/\rho)(\partial^2 P/\partial z^2) = (2\pi r^3/E\cdot a)(\partial^2 P/\partial t^2) \quad (10)$$

or finally:

$$\partial^2P/\partial t^2 = (E\cdot a/2r\rho)(\partial^2P/\partial z^2) \tag{10a}$$

Equation (10a) is the wave equation from which comes the characteristic velocity:

$$v = (Ea/2r\rho)^{1/2} \tag{11}$$

Equation (11) is the Moens formula.

APPENDIX B

Tables of Experimental Data

The following data were used to construct the pressure-velocity curves in Figures 8-18. This data includes: 1.) the experimentally determined velocities ($1/\Delta t$, where Δt is the transmission time, and 2.) the observed pressures (either P_d, the diastolic pressure, or P_m, the mean pressure). P(calc) is the pressure calculated for a given value of the velocity using the equation of a "best-fit" line determined by the method of least squares. P_d(or P_m) - P(calc) is the vertical distance between the observed pressure and the "best-fit" line.

Drug-induced changes in cardiovascular status are denoted in the table by the drug name. (Regitine was always used in combination with Isuprel, but is listed in the table as Regitine.) Normal and hypovolumic conditions are listed as such.

Table I

Carotid Diastolic Pressures and
Aorta-Femoral Onset Velocities from Experiment I

$1/\Delta t$ ($msec^{-1}$)	P_d (mm Hg)	P(calc) (mm Hg)	P_d-P(calc) (mm Hg)	Conditions
0.0143	83	94.6	-11.6	Normal
0.0143	90	94.6	- 4.6	Normal
0.0232	210	185.3	24.7	Epinephrine
0.0217	190	170.0	20.0	Epinephrine
0.0099	25	49.8	-24.8	Epinephrine
0.0111	50	62.0	-12.0	Epinephrine
0.0091	45	41.6	3.6	Epinephrine
0.0091	45	41.6	3.6	Epinephrine
0.0095	45	45.7	- 0.7	Epinephrine
0.0133	82	84.4	- 2.4	Normal
0.0143	85	94.6	- 9.6	Normal
0.0133	87	84.4	2.6	Normal
0.0166	115	118.1	- 3.1	Epinephrine
0.0175	120	127.2	- 7.2	Epinephrine
0.0189	125	141.5	-16.5	Epinephrine
0.0217	150	170.0	-20.0	Epinephrine
0.0192	140	144.5	- 4.5	Epinephrine
0.0147	95	98.7	- 3.7	Normal
0.0175	116	127.2	-11.2	Levophed
0.0135	108	86.5	21.5	Levophed
0.0130	87	81.4	5.6	Levophed
0.0125	73	76.3	- 3.3	Levophed
0.0179	132	131.3	0.7	Levophed
0.0176	135	128.2	6.8	Levophed
0.0213	157	165.9	- 8.9	Levophed
0.0222	173	175.1	- 2.1	Levophed
0.0159	128	110.9	17.1	Levophed
0.0164	90	116.0	-26.0	Normal
0.0147	87	98.7	-11.7	Normal
0.0108	70	59.0	11.0	Normal
0.0106	70	56.9	13.1	Normal
0.0104	70	54.9	15.1	Normal
0.0100	67	50.8	16.2	Normal
0.0111	75	62.0	13.0	Normal
0.0100	55	50.8	4.2	Hypovolumia
0.0087	37	37.6	-.0.6	Hypovolumia
0.0075	25	25.3	- 0.3	Hypovolumia
0.0083	24	33.5	- 9.5	Hypovolumia
0.0086	24	36.5	-12.5	Hypovolumia
0.0091	45	41.6	3.6	Hypovolumia
0.0125	80	76.3	3.7	Normal
0.0250	205	203.6	1.4	Epinephrine
0.0244	204	197.5	6.5	Epinephrine
0.0222	182	175.1	6.9	Epinephrine

Table II

Femoral Diastolic Pressures and
Aorta-Femoral Onset Velocities from Experiment I

$1/\Delta t$ (msec^{-1})	P_d (mm Hg)	P(calc) (mm Hg)	P_d-P(calc) (mm Hg)	Conditions
0.0143	85	86.2	- 1.2	Normal
0.0143	87	86.2	0.8	Normal
0.0232	210	184.4	25.6	Epinephrine
0.0217	178	167.8	10.2	Epinephrine
0.0099	27	37.6	-10.6	Epinephrine
0.0111	45	50.9	- 5.9	Epinephrine
0.0091	46	28.8	17.2	Epinephrine
0.0091	46	28.8	17.2	Epinephrine
0.0095	45	33.2	11.8	Epinephrine
0.0133	72	75.1	- 3.1	Normal
0.0143	77	86.2	- 9.2	Normal
0.0133	82	75.1	6.9	Normal
0.0166	118	111.6	6.4	Epinephrine
0.0175	123	121.5	1.5	Epinephrine
0.0189	127	136.9	- 9.9	Epinephrine
0.0217	153	167.8	-14.8	Epinephrine
0.0192	140	140.2	0.2	Epinephrine
0.0147	94	90.6	3.4	Normal
0.0175	147	121.5	25.5	Levophed
0.0135	109	77.3	31.7	Levophed
0.0130	80	71.8	8.2	Levophed
0.0125	63	66.3	- 3.3	Levophed
0.0179	130	125.9	4.1	Levophed
0.0196	133	144.7	-11.7	Levophed
0.0213	150	163.4	-13.4	Levophed
0.0222	165	173.4	- 8.4	Levophed
0.0159	127	103.8	23.2	Levophed
0.0164	70	109.3	-39.3	Normal
0.0147	65	90.6	-25.6	Normal
0.0108	40	47.5	- 7.5	Normal
0.0106	37	45.3	- 8.3	Normal
0.0104	35	43.1	- 8.1	Normal
0.0111	30	50.9	-20.9	Normal
0.0250	203	204.3	- 1.3	Epinephrine
0.0244	200	197.6	2.4	Epinephrine
0.0220	180	173.4	6.6	Epinephrine

Table III

Carotid Diastolic Pressures and
Carotid-Femoral Onset Velocities from Experiment I

$1/\Delta t$ ($msec^{-1}$)	P_d (mm Hg)	P(calc) (mm Hg)	P_d-P(calc) (mm Hg)	Conditions
0.0200	83	89.8	- 6.8	Normal
0.0111	90	24.1	65.9	Normal
0.0345	210	196.7	13.3	Epinephrine
0.0333	190	187.9	2.1	Epinephrine
0.0185	25	78.7	-53.7	Epinephrine
0.0189	50	81.7	-31.7	Epinephrine
0.0167	45	65.4	-20.4	Epinephrine
0.0167	45	65.4	-20.4	Epinephrine
0.0161	45	61.0	-16.0	Epinephrine
0.0200	82	89.8	- 7.8	Normal
0.0182	85	76.5	8.5	Normal
0.0200	87	89.8	- 2.8	Normal
0.0250	115	126.7	-11.7	Epinephrine
0.0250	120	126.7	- 6.7	Epinephrine
0.0244	125	122.2	2.8	Epinephrine
0.0250	150	126.7	23.3	Epinephrine
0.0222	140	106.0	34.0	Epinephrine
0.0196	95	86.8	8.2	Normal
0.0213	116	99.4	16.6	Levophed
0.0200	108	89.8	18.2	Levophed
0.0185	87	79.7	8.3	Levophed
0.0217	73	102.3	-29.3	Levophed
0.0250	132	126.7	5.3	Levophed
0.0250	135	126.7	8.3	Levophed
0.0286	157	153.2	3.8	Levophed
0.0323	173	180.5	- 7.5	Levophed
0.0244	128	122.2	5.8	Levophed
0.0222	90	106.0	-16.0	Normal
0.0227	87	109.7	-22.7	Normal
0.0167	70	65.2	4.8	Normal
0.0167	70	65.2	4.8	Normal
0.0167	70	65.2	4.8	Normal
0.0159	67	59.5	7.5	Normal
0.0179	75	74.3	0.7	Normal
0.0119	55	30.0	25.0	Hypovolumia
0.0118	37	29.3	7.7	Hypovolumia
0.0133	25	40.4	-15.4	Hypovolumia
0.0143	25	47.4	-22.7	Hypovolumia
0.0161	24	61.0	-37.0	Hypovolumia
0.0167	45	65.4	-20.4	Hypovolumia
0.0179	80	74.3	5.7	Normal
0.0357	205	205.6	- 0.6	Epinephrine
0.0370	204	215.2	-11.2	Epinephrine
0.0256	182	131.1	50.9	Epinephrine

Table IV

Femoral Diastolic Pressures and
Carotid-Femoral Onset Velocities from Experiment I

$1/\Delta t$ ($msec^{-1}$)	P_d (mm Hg)	P(calc) (mm Hg)	P_d-P(calc) (mm Hg)	Conditions
0.0200	85	83.7	1.3	Normal
0.0111	87	15.0	72.0	Normal
0.0345	210	195.8	14.2	Epinephrine
0.0333	178	186.5	- 8.5	Epinephrine
0.0185	27	72.2	-45.2	Epinephrine
0.0189	45	75.3	-30.3	Epinephrine
0.0167	46	58.2	-12.2	Epinephrine
0.0167	46	58.2	-12.2	Epinephrine
0.0161	45	53.6	- 8.6	Epinephrine
0.0200	72	83.7	-11.7	Normal
0.0182	77	69.8	7.2	Normal
0.0200	82	83.7	- 1.7	Normal
0.0250	118	122.4	- 4.4	Epinephrine
0.0250	123	122.4	0.6	Epinephrine
0.0244	127	117.8	9.2	Epinephrine
0.0250	153	122.4	30.6	Epinephrine
0.0222	140	100.8	39.2	Epinephrine
0.0196	94	80.7	13.3	Normal
0.0213	147	93.8	53.2	Levophed
0.0200	109	83.7	25.3	Levophed
0.0185	80	72.2	7.8	Levophed
0.0217	63	96.9	-33.9	Levophed
0.0250	130	122.4	7.6	Levophed
0.0250	133	122.4	10.6	Levophed
0.0285	150	150.0	0.0	Levophed
0.0323	165	178.8	-13.8	Levophed
0.0244	127	117.8	9.2	Levophed
0.0222	70	100.8	-30.8	Normal
0.0227	65	104.6	-39.6	Normal
0.0167	40	58.0	-18.0	Normal
0.0167	37	58.0	-21.0	Normal
0.0166	35	57.8	-22.8	Normal
0.0159	30	52.1	-22.1	Normal
0.0357	203	205.1	-20.9	Epinephrine
0.0370	200	215.1	-15.1	Epinephrine
0.0256	180	127.3	52.7	Epinephrine

Table V

Carotid Diastolic Pressures and
Aorta-Femoral Onset Velocities from Experiment II

$1/\Delta t$ ($msec^{-1}$)	P_d (mm Hg)	P(calc) (mm Hg)	P_d-P(calc) (mm Hg)	Conditions
0.0152	110	97.9	12.1	Normal
0.0149	112	94.6	17.4	Normal
0.0156	115	102.3	12.7	Normal
0.0159	115	105.6	9.4	Normal
0.0200	129	151.0	-22.0	Levophed
0.0196	140	146.6	- 6.6	Levophed
0.0189	148	138.8	9.2	Levophed
0.0179	132	127.8	4.2	Levophed
0.0233	200	187.5	12.5	Levophed
0.0227	163	180.9	-17.9	Levophed
0.0167	120	114.2	5.8	Normal
0.0167	115	114.2	0.8	Normal
0.0159	107	105.6	1.4	Isuprel
0.0143	104	87.9	16.1	Isuprel
0.0125	82	68.0	14.0	Isuprel
0.0122	72	64.7	7.3	Isuprel
0.0122	72	64.7	7.3	Isuprel
0.0112	58	53.6	4.4	Isuprel
0.0116	55	58.0	- 3.0	Isuprel
0.0143	100	87.9	12.1	Isuprel
0.0152	105	97.3	7.7	Normal
0.0154	110	100.1	9.9	Normal
0.0149	112	94.6	17.4	Normal
0.0161	115	107.8	7.2	Normal
0.0141	97	85.7	11.3	Normal
0.0125	84	68.0	16.0	Regitine
0.0111	65	52.5	12.5	Regitine
0.0113	58	54.7	3.3	Regitine
0.0103	41	43.7	- 2.7	Regitine
0.0104	39	44.8	- 5.8	Regitine
0.0098	29	38.1	- 9.1	Regitine
0.0106	35	47.0	-12.0	Regitine
0.0089	24	28.2	- 4.2	Regitine
0.0093	28	32.6	- 4.6	Regitine
0.0091	35	30.4	4.6	Regitine
0.0102	44	42.6	1.4	Regitine
0.0098	45	38.1	6.9	Regitine
0.0088	19	27.1	- 8.1	Regitine
0.0094	22	33.7	-11.7	Regitine
0.0114	76	55.8	20.2	Regitine
0.0099	45	39.2	5.8	Regitine
0.0115	46	56.9	-10.1	Regitine
0.0103	41	43.7	- 2.7	Regitine

Table V
(continued)

$1/\Delta t$ ($msec^{-1}$)	P_d (mm Hg)	P(calc) (mm Hg)	P_d-P(calc) (mm Hg)	Conditions
0.0143	95	87.9	7.1	Normal
0.0179	101	127.8	-26.8	Normal
0.0139	95	83.5	11.5	Normal
0.0154	93	100.1	- 7.1	Normal
0.0152	100	97.9	2.1	Levophed
0.0161	100	107.8	- 7.8	Levophed
0.0172	100	120.0	-20.0	Levophed
0.0143	78	87.9	- 9.9	Normal
0.0156	82	102.3	-20.3	Normal
0.0161	83	107.8	-24.8	Normal
0.0132	72	75.8	- 3.8	Hypovolumia
0.0095	47	34.8	1.2	Hypovolumia
0.0100	39	40.3	- 1.3	Hypovolumia
0.0102	40	42.6	- 2.6	Hypovolumia
0.0100	25	40.3	-15.3	Hypovolumia
0.0083	19	21.5	- 2.5	Hypovolumia
0.0083	18	21.5	- 3.5	Hypovolumia
0.0093	15	32.6	-17.6	Hypovolumia
0.0087	7	26.0	-19.0	Hypovolumia

Table VI

Femoral Diastolic Pressure and
Aorta-Femoral Onset Velocities from Experiment II

$1/\Delta t$ ($msec^{-1}$)	P_d (mm Hg)	P(calc) (mm Hg)	P_d-P(calc) (mm Hg)	Conditions
0.0152	106	90.1	15.9	Normal
0.0149	109	86.9	22.1	Normal
0.0156	111	94.4	16.6	Normal
0.0159	112	97.5	14.5	Normal
0.0200	120	141.0	-21.0	Levophed
0.0196	134	136.7	- 2.7	Levophed
0.0189	137	129.3	7.7	Levophed
0.0179	120	118.7	1.3	Levophed
0.0233	188	175.9	12.1	Levophed
0.0227	150	169.6	-19.6	Levophed
0.0167	111	105.7	5.3	Normal
0.0167	110	105.7	4.3	Normal
0.0159	105	97.5	7.5	Isuprel
0.0143	90	80.6	9.4	Isuprel
0.0125	66	61.5	4.5	Isuprel
0.0122	60	58.3	1.7	Isuprel
0.0122	60	58.3	1.7	Isuprel
0.0112	48	47.7	0.3	Isuprel
0.0116	46	52.0	- 6.0	Isuprel
0.0143	87	80.6	6.4	Isuprel
0.0152	97	90.1	6.9	Normal
0.0154	106	92.2	13.8	Normal
0.0149	108	86.9	21.1	Normal
0.0161	110	99.7	10.3	Normal
0.0141	80	78.5	1.5	Normal
0.0125	65	61.5	3.5	Regitine
0.0111	52	46.7	5.3	Regitine
0.0113	49	48.8	2.1	Regitine
0.0103	37	38.2	- 1.2	Regitine
0.0115	41	50.9	- 9.9	Regitine
0.0103	37	38.2	- 1.2	Regitine
0.0104	35	39.2	- 4.2	Regitine
0.0098	26	32.9	- 6.9	Regitine
0.0106	32	41.4	- 9.4	Regitine
0.0089	23	23.4	- 3.5	Regitine
0.0093	25	27.6	- 2.6	Regitine
0.0091	30	25.5	4.5	Regitine
0.0102	38	37.1	0.9	Regitine
0.0098	39	32.9	6.1	Regitine
0.0099	40	34.0	6.0	Regitine
0.0088	21	22.3	- 1.3	Regitine
0.0094	26	28.7	- 2.7	Regitine
0.0114	61	49.8	11.2	Regitine

Table VI
(continued)

$1/\Delta t$ ($msec^{-1}$)	P_d (mm Hg)	P(calc) (mm Hg)	P_d-P(calc) (mm Hg)	Conditions
0.0143	77	80.6	- 3.6	Normal
0.0179	87	118.7	-31.7	Normal
0.0139	94	76.3	17.7	Normal
0.0154	90	92.2	- 2.2	Normal
0.0152	95	90.1	4.9	Levophed
0.0161	95	99.7	- 4.7	Levophed
0.0172	102	111.3	- 9.3	Levophed
0.0143	73	80.6	- 7.6	Normal
0.0156	72	94.4	-22.4	Normal
0.0161	73	94.7	-26.7	Normal
0.0132	60	68.9	- 8.9	Hypovolumia
0.0095	38	29.7	8.3	Hypovolumia
0.0100	32	35.0	- 3.0	Hypovolumia
0.0102	31	37.1	- 6.1	Hypovolumia
0.0100	20	35.0	-15.0	Hypovolumia
0.0033	16	17.0	- 1.0	Hypovolumia
0.0083	15	17.0	- 2.0	Hypovolumia
0.0083	13	17.0	- 4.0	Hypovolumia
0.0087	5	21.2	-16.2	Hypovolumia

Table VII

Carotid Mean Pressures and Aorta-Femoral Onset Velocities for Experiment II

$1/\Delta t$ ($msec^{-1}$)	P_d (mm Hg)	P(calc) (mm Hg).	P_d-P(calc) (mm Hg)	Conditions
0.0152	117	114.2	2.8	Normal
0.0149	125	110.7	14.3	Normal
0.0160	131	123.5	7.5	Normal
0.0159	132	122.4	9.6	Normal
0.0200	141	170.1	-29.1	Levophed
0.0196	164	165.4	- 1.4	Levophed
0.0179	160	145.7	14.3	Levophed
0.0233	240	208.5	31.5	Levophed
0.0167	140	131.7	8.3	Normal
0.0167	131	131.7	- 0.7	Normal
0.0122	90	79.3	10.7	Isuprel
0.0116	83	72.3	10.7	Isuprel
0.0152	120	114.2	5.8	Normal
0.0149	126	110.7	15.3	Normal
0.0161	126	124.7	1.3	Normal
0.0125	93	82.8	10.2	Regitine
0.0115	70	71.2	- 1.2	Regitine
0.0106	55	60.7	- 5.7	Regitine
0.0091	58	43.2	14.8	Regitine
0.0102	65	56.0	9.0	Regitine
0.0098	65	51.4	13.6	Regitine
0.0099	64	52.6	11.4	Regitine
0.0088	45	39.8	5.2	Regitine
0.0094	56	46.7	9.3	Regitine
0.0114	90	70.0	20.0	Regitine
0.0143	107	103.8	3.2	Normal
0.0179	105	145.7	-40.7	Normal
0.0154	115	116.6	- 1.6	Normal
0.0152	116	114.2	1.8	Levophed
0.0161	120	124.7	- 4.7	Levophed
0.0172	130	137.5	- 7.5	Levophed
0.0143	104	103.8	0.2	Normal
0.0156	100	118.9	-18.9	Normal
0.0161	94	124.7	-30.7	Normal
0.0132	82	91.0	- 9.0	Hypovolumia
0.0095	60	47.9	12.1	Hypovolumia
0.0100	50	53.7	- 3.7	Hypovolumia
0.0102	58	56.0	2.0	Hypovolumia
0.0100	31	53.7	-22.7	Hypovolumia
0.0083	27	33.9	- 6.9	Hypovolumia
0.0083	27	33.9	- 6.9	Hypovolumia
0.0093	20	45.6	-25.6	Hypovolumia
0.0087	11	38.6	-27.6	Hypovolumia

Table VIII

Femoral Mean Pressure and
Aorta-Femoral Onset Velocities from Experiment II

$1/\Delta t$ ($msec^{-1}$)	P_d (mm Hg)	P(calc) (mm Hg)	P_d-P(calc) (mm Hg)	Conditions
0.0152	119	108.6	10.4	Normal
0.0149	121	105.1	15.9	Normal
0.0160	127	117.7	9.3	Normal
0.0159	126	116.6	9.4	Normal
0.0200	135	163.4	-28.4	Levophed
0.0196	155	158.8	- 3.8	Levophed
0.0179	150	139.4	10.6	Levophed
0.0233	225	201.1	23.9	Levophed
0.0167	133	125.7	7.3	Normal
0.0167	125	125.7	- 0.7	Normal
0.0122	85	74.3	10.7	Isuprel
0.0116	71	67.5	3.5	Isuprel
0.0152	113	108.6	4.4	Normal
0.0149	121	105.1	15.9	Normal
0.0161	120	118.8	1.2	Normal
0.0125	88	77.7	10.3	Regitine
0.0115	65	66.3	- 1.3	Regitine
0.0106	48	56.1	- 8.1	Regitine
0.0091	50	38.9	11.1	Regitine
0.0102	59	51.5	7.5	Regitine
0.0098	60	46.9	13.1	Regitine
0.0099	58	48.1	9.9	Regitine
0.0088	37	35.5	1.5	Regitine
0.0094	45	42.4	2.6	Regitine
0.0114	85	65.2	19.8	Regitine
0.0143	101	98.3	2.7	Normal
0.0179	102	139.4	-37.4	Normal
0.0154	112	110.9	1.1	Normal
0.0152	113	108.6	4.4	Levophed
0.0161	117	118.8	- 1.8	Levophed
0.0172	125	131.4	- 6.4	Levophed
0.0143	100	98.3	1.7	Normal
0.0156	96	113.1	-17.1	Normal
0.0161	91	118.8	-27.8	Normal
0.0132	80	85.7	- 5.7	Hypovolumia
0.0095	56	43.5	12.5	Hypovolumia
0.0100	47	49.2	- 2.2	Hypovolumia
0.0102	45	51.5	- 6.5	Hypovolumia
0.0100	30	49.2	-19.2	Hypovolumia
0.0083	27	29.8	- 2.8	Hypovolumia
0.0083	26	29.8	- 3.8	Hypovolumia
0.0093	18	41.2	-23.2	Hypovolumia
0.0087	10	34.4	-24.4	Hypovolumia

Table IX

Carotid Diastolic Pressures and
Carotid-Femoral Onset Velocities from Experiment II

$1/\Delta t$ ($msec^{-1}$)	P_d (mm Hg)	P(calc) (mm Hg)	P_d-P(calc) (mm Hg)	Conditions
0.0238	110	108.4	1.6	Normal
0.0233	112	104.6	7.4	Normal
0.0233	115	104.6	10.4	Normal
0.0217	115	92.5	22.5	Normal
0.0263	129	127.4	1.6	Levophed
0.0222	140	96.3	43.6	Levophed
0.0303	148	157.7	- 9.7	Levophed
0.0263	132	127.4	4.6	Levophed
0.0333	200	180.4	19.6	Levophed
0.0238	120	108.4	11.6	Normal
0.0222	115	96.3	18.7	Normal
0.0233	107	104.6	2.4	Isuprel
0.0208	104	85.7	18.3	Isuprel
0.0179	82	63.7	18.3	Isuprel
0.0175	72	60.7	11.3	Isuprel
0.0179	72	63.7	8.3	Isuprel
0.0169	58	56.2	1.8	Isuprel
0.0172	55	58.4	- 3.4	Isuprel
0.0200	100	79.6	20.4	Isuprel
0.0204	105	82.7	22.3	Normal
0.0204	110	85.7	24.3	Normal
0.0244	112	113.0	- 1.0	Normal
0.0250	115	117.5	- 2.5	Normal
0.0213	97	89.5	7.5	Normal
0.0200	84	79.6	4.4	Regitine
0.0167	65	54.6	10.4	Regitine
0.0172	58	58.4	- 0.4	Regitine
0.0159	41	48.6	- 7.6	Regitine
0.0169	46	56.2	-10.2	Regitine
0.0161	41	50.1	- 9.1	Regitine
0.0167	39	54.6	-15.6	Regitine
0.0152	29	43.3	-14.3	Regitine
0.0164	35	52.4	-17.4	Regitine
0.0149	24	41.0	-17.0	Regitine
0.0143	28	36.5	- 8.5	Regitine
0.0156	35	46.3	-11.3	Regitine
0.0154	44	44.8	- 0.8	Regitine
0.0156	45	46.3	- 1.3	Regitine
0.0161	45	50.1	- 5.1	Regitine
0.0149	19	41.0	-22.0	Regitine
0.0159	22	48.6	-26.6	Regitine
0.0159	76	48.6	27.4	Regitine

Table IX
(continued)

$1/\Delta t$ ($msec^{-1}$)	P_d (mm Hg)	P(calc) (mm Hg)	P_d-P(calc) (mm Hg)	Conditions
0.0185	95	68.3	26.7	Levophed
0.0172	101	58.4	42.6	Levophed
0.0233	95	104.6	- 9.6	Levophed
0.0227	93	100.1	- 7.1	Normal
0.0227	100	100.1	- 0.1	Normal
0.0238	100	108.4	- 8.4	Normal
0.0250	100	117.5	-17.5	Normal
0.0217	78	92.5	-14.5	Normal
0.0217	82	92.5	-10.5	Normal
0.0200	83	79.6	3.4	Normal
0.0189	72	71.3	0.7	Hypovolumia
0.0130	47	26.6	20.4	Hypovolumia
0.0154	39	44.8	- 5.8	Hypovolumia
0.0154	40	44.8	- 4.8	Hypovolumia
0.0133	25	28.9	- 3.9	Hypovolumia
0.0137	19	31.9	-12.9	Hypovolumia
0.0137	18	31.9	-13.9	Hypovolumia
0.0147	15	39.5	-24.5	Hypovolumia
0.0154	7	44.8	-37.8	Hypovolumia

Table X

Femoral Diastolic Pressures and
Carotid-Femoral Onset Velocities from Experiment II

$1/\Delta t$ ($msec^{-1}$)	P_d (mm Hg)	P(calc) (mm Hg)	P_d-P(calc) (mm Hg)	Conditions
0.0238	106	107.6	- 1.6	Normal
0.0232	109	102.4	6.6	Normal
0.0233	111	103.3	7.7	Normal
0.0217	112	89.5	22.5	Normal
0.0263	120	129.2	- 9.2	Levophed
0.0222	134	93.8	40.2	Levophed
0.0263	120	129.2	- 9.2	Levophed
0.0333	188	189.7	- 1.7	Levophed
0.0238	111	107.6	3.4	Normal
0.0222	110	93.8	16.2	Normal
0.0233	105	103.3	1.7	Isuprel
0.0208	90	81.7	8.3	Isuprel
0.0179	66	56.6	9.4	Isuprel
0.0175	60	53.2	6.8	Isuprel
0.0179	60	56.6	3.4	Isuprel
0.0169	48	48.0	0.0	Isuprel
0.0172	46	50.6	- 4.6	Isuprel
0.0200	87	74.8	12.2	Isuprel
0.0204	97	78.2	18.7	Normal
0.0208	106	81.7	24.3	Normal
0.0244	108	112.8	- 4.8	Normal
0.0250	110	118.0	- 8.0	Normal
0.0213	80	86.0	- 6.0	Normal
0.0200	65	74.8	- 9.8	Regitine
0.0167	52	46.3	5.7	Regitine
0.0172	49	50.6	- 1.6	Regitine
0.0159	37	39.4	- 2.4	Regitine
0.0169	41	48.0	- 7.0	Regitine
0.0161	37	41.1	- 4.1	Regitine
0.0167	35	46.3	-11.3	Regitine
0.0152	26	33.3	- 7.3	Regitine
0.0164	32	43.7	-11.7	Regitine
0.0149	23	30.7	- 7.7	Regitine
0.0143	25	25.6	- 0.6	Regitine
0.0156	30	36.8	- 6.8	Regitine
0.0154	38	35.1	2.9	Regitine
0.0156	39	36.8	2.2	Regitine
0.0161	40	41.1	- 1.1	Regitine
0.0149	21	30.7	- 9.7	Regitine
0.0159	26	39.4	-13.4	Regitine
0.0159	61	39.4	21.6	Regitine

Table X
(continued)

$1/\Delta t$ ($msec^{-1}$)	P_d (mm Hg)	P(calc) (mm Hg)	P_d-P(calc) (mm Hg)	Conditions
0.0185	77	61.8	15.2	Normal
0.0172	87	50.6	36.4	Normal
0.0233	94	103.3	- 9.2	Normal
0.0227	90	98.1	- 8.1	Normal
0.0227	95	98.1	- 3.1	Levophed
0.0238	95	107.6	-12.6	Levophed
0.0250	102	118.0	-16.0	Levophed
0.0217	73	89.5	-16.5	Normal
0.0217	72	89.5	-17.5	Normal
0.0200	73	74.8	- 1.8	Normal
0.0189	60	65.3	- 5.3	Hypovolumia
0.0130	38	14.2	23.7	Hypovolumia
0.0154	32	35.1	3.1	Hypovolumia
0.0154	31	35.1	4.1	Hypovolumia
0.0133	20	16.9	3.9	Hypovolumia
0.0137	16	20.4	- 4.4	Hypovolumia
0.0137	15	20.4	- 5.4	Hypovolumia
0.0147	13	29.0	-16.0	Hypovolumia
0.0154	5	35.1	-30.1	Hypovolumia

Table XI

Femoral Diastolic Pressures and
Carotid-Femoral Onset Velocities from Experiment III

$1/\Delta t$ ($msec^{-1}$)	P_d (mm Hg)	P(calc) (mm Hg)	P_d-P(calc) (mm Hg)	Conditions
0.0161	98	87.8	10.2	Normal
0.0167	100	95.0	5.0	Normal
0.0200	129	134.5	- 5.5	Levophed
0.0204	132	139.3	- 7.3	Levophed
0.0217	136	154.8	-18.8	Levophed
0.0179	120	109.3	10.7	Levophed
0.0250	174	194.3	-20.3	Levophed
0.0250	174	194.3	-20.3	Levophed
0.0227	150	166.8	-16.8	Levophed
0.0208	160	144.0	16.0	Levophed
0.0222	144	160.8	-16.8	Levophed
0.0172	112	101.0	11.0	Levophed
0.0185	117	116.5	0.5	Levophed
0.0175	106	104.6	1.4	Levophed
0.0164	127	91.4	35.6	Levophed
0.0185	121	116.5	4.5	Levophed
0.0217	166	154.8	11.2	Levophed
0.0217	160	154.8	5.2	Levophed
0.0227	191	166.8	24.2	Levophed
0.0154	82	79.4	2.6	Isuprel
0.0160	80	86.6	- 6.6	Isuprel
0.0137	66	59.1	6.9	Isuprel
0.0130	55	50.7	4.3	Isuprel
0.0132	54	53.1	- 0.9	Isuprel
0.0118	43	36.4	6.6	Isuprel
0.0118	43	36.4	6.6	Isuprel
0.0121	40	39.9	0.1	Isuprel
0.0122	40	41.1	- 1.1	Isuprel
0.0122	38	41.1	- 3.1	Isuprel
0.0122	36	41.1	- 5.1	Isuprel
0.0123	36	42.3	- 6.3	Isuprel
0.0154	89	79.4	9.6	Normal
0.0149	102	73.4	28.6	Normal
0.0154	102	79.4	22.6	Normal
0.0119	64	37.6	26.4	Regitine
0.0123	47	42.3	4.7	Regitine
0.0125	45	44.7	0.3	Regitine
0.0123	40	42.3	- 2.3	Regitine
0.0119	35	37.6	- 2.6	Regitine
0.0122	28	41.1	-13.1	Regitine
0.0115	26	32.8	- 6.8	Regitine
0.0118	25	36.4	-11.4	Regitine
0.0130	55	50.7	4.3	Regitine

Table XI
(continued)

$1/\Delta t$ ($msec^{-1}$)	P_d (mm Hg)	P(calc) (mm Hg)	P_d-P(calc) (mm Hg)	Conditions
0.0143	78	66.3	11.7	Normal
0.0152	88	77.0	11.0	Normal
0.0132	59	53.1	5.9	Hypovolumia
0.0119	44	37.6	6.4	Hypovolumia
0.0100	33	14.8	18.2	Hypovolumia
0.0111	22	28.0	- 6.0	Hypovolumia
0.0102	20	17.2	2.8	Hypovolumia
0.0122	25	41.1	-16.1	Hypovolumia*
0.0125	19	44.7	-25.7	Hypovolumia*
0.0119	20	37.6	-17.6	Hypovolumia*
0.0121	15	39.9	-24.9	Hypovolumia*
0.0115	18	32.8	-14.8	Hypovolumia*
0.0109	18	25.6	- 7.6	Hypovolumia*
0.0122	17	41.1	-24.1	Hypovolumia*
0.0115	18	32.8	-14.8	Hypovolumia*

* Isuprel given during hypovolumia

BIBLIOGRAPHY

1. Agress, C. M., Wegner, S., Bleifer, Estrin, H. M., Schroyer, K., and Labins, G. (1964) Measurement of Isometric Contraction and Ejection Time by the Vibrocardiogram. Am. J. Card. 13:340.

2. Atabek, H. B. and Lew, H. S. (1966) Wave Propatation through a Viscous Incompressible Fluid Contained in an Initially Stressed Elastic Tube. Biophysical Journal 6:481.

3. Bramwell, J. C. and Hill, A. V. (1922) The Velocity of the Pulse Wave in Man. Proc. Roy. Soc., Sec. B 93:298.

4. Braunwald, E., Moscovitz, H. L., Amram, S. S., Lasser, R. P., Sapin, S. O., Himmelstein, A., Ravitch, M. M. (1955) Timing of Electrical and Mechanical Events of the Left Side of the Human Heart. J. Appl. Physiol. 8:309.

5. Corell, R. W. (1959) Theoretical Analysis and Preliminary Development of an Indirect Blood Pressure Recording Systeim. S. M. Thesis, MIT.

6. Davies, O. L. (1961) Statistical Methods in Research and Production. (Hafner:New York).

7. Doupe, I., Newman, H. W., and Wilkins, R. W. (1939) Method for Continuous Recording of Systolic Arterial Pressure in Man. J. Physiol. 95:239.

8. Friedberg, C. K. (1956) Diseases of the Heart. (Saunders:Philadelphia).

9. Gilford, S. R. and Broida, H. P. (1954) Physiological Monitoring Equipment for Anethesia and Other Uses. (National Bureau of Standards, No. 3301:Washington, D. C.).

10. Gilson, W. E. (1942) Automated Blood Pressure Recorder. Electronics.

11. Hallock, P. and Benson, I. (1937) Studies on the Elastic Properties of Human Isolated Aorta. J. Clin. Invest. 16:595.

12. Hamilton, W. F., Remington, J. W., and Dow, P. (1945) The Determination of the Propagated Velocity of the Arterial Pulse Wave. Am. J. of Physiol. 144:521.

13. Hardung, V. (1962) The Propagation of Pulse Waves in Visco-elastic Tubings. Handbook of Physiology-Circulation Vol. 1, W. F. Hamilton ed. (American Physiological Society:Washington, D. C.) 107.

14. Haynes, F. W., Ellis, L. B., and Weiss, S. (1936) Pulse Wave Velocity and Arterial Elasticity in Arterial Hypertension, Arteriosclerosis, and Related Conditions. Am. Heart Journal 16:595.

15. Lange, K. (1943) The Recording Sphymotonograph. Ann. Intern. Med. 18:367.

16. Merck Index, The (1968) (Merck and Co:Rahway, N. J.).

17. Morgan, G. W. and Kiely, P. P. (1954) Wave Propagation in a Viscous Liquid Contained in a Flexible Tube. J. Acous. Soc. Am. 25(3):323.

18. Moulopoulos, S. D. (1963) Cardiomechanics. (Thomas: Springfield).

19. Nye, E. R. (1964) The Effect of Blood Pressure Alteration on the Pulse Wave Velocity. Brit. Heart J. 26:261.

20. Schimmler, W. (1966) Correlation between the Pulse Wave Velocity in the Aortic Iliac Vessel, and Age, Sex, and Blood Pressure. Angiology 17:314.

21. Steele, J. M. (1937) Interpretation of Arterial Elasticity from Measurements of Pulse Wave Velocities. Am. Heart Journal 14:452.

22. Womersley, J. R. (1957) An Elastic Tube Theory of Pulse Transmission and Oscillatory Flow in Mammalian Arteries. Wright Air Development Center Technical Report WADC-TR56_614.

DIASTOLIC BLOOD PRESSURE
AND PULSE WAVE VELOCITY IN HUMANS

by

HARVEY LEE GOLDBERG

Submitted in Partial Fulfillment
of the Requirements for the
Degree of Bachelor of Science
at the
MASSACHUSETTS INSTITUTE OF TECHNOLOGY
January, 1972

Signature of Author. Harvey Lee Goldberg ....
Department of Electrical Engineering, January 26, 1972

Certified by.... Roger G. Mark, MD ....
Thesis Supervisor

Accepted by..
Chairman, Departmental Committee on Theses

PRECEDING PAGE BLANK NOT FILMED

DIASTOLIC BLOOD PRESSURE

AND PULSE WAVE VELOCITY IN HUMANS

by

HARVEY LEE GOLDBERG

Submitted to the Department of Electrical Engineering on January 26, 1972 in partial fulfillment of the requirements for the degree of Bachelor of Science

ABSTRACT

Experiments are described in which diastolic blood pressure is found to be linearly related to arterial pulse wave velocity. The final goal of this study is to provide data on the feasibilty of utilizing the relationship in a device to measure blood pressure non-invasively in mbulatory patients. It was found, by experiments on humans, that this relationship holds over a moderate range of pressures in normal, young, males. The feasibility of using the second heart sound as a timing reference was explored, and discarded.

Thesis Supervisor: Roger G. Mark
Title: Assistant Professor in Electrical Engineering

ACKNOWLEDGEMENT

I would like to express profound appreciation to Dr. Roger G. Mark for his supervision, teaching, and experimental assistance. My association with him has been personally most rewarding. I would also like to thank the Boston City Hospital for the use of facilities at the Heart Station. I am deeply indebted a trio of the Heart Station's personnel; Mr. Richard Wagner, for his most helpful assistance with the instrumentation; Mrs. Carol Scott, for her experimental assistance, expert advice, and sympathy; and finally, Mrs. Mary Wagner, who unselfishly gave of her time whenever it was asked. This experiment would have been impossible without Mrs. Wagner's assistance. I am grateful to Douglas Belli, Jerry Kleinbaum, J. Mike Lemeill, and Don Zimmerman for their willingness in being subjects in the experiment. Finally, I am grateful to Miss. Robin Steier for her assistance in the preparation of the manuscript.

Table of Contents

List of Figures

I. Introduction

There are presently two common methods for measuring blood pressure: the common indirect or ausculatory method, and the direct method via arterial puncture. The direct method involves directly coupling an external pressure transducer to the arterial system via a fluid-filled cannula. The output of the pressure transducer is an electrical signal which, when appropriately calibrated, indicates instantaneous arterial pressure.

The ausculatory method entails placing an inflatable cuff around a limb. The air bladder inside the cuff is attached to a pressure transducer. The cuff is first inflated to a pressure well above systolic pressure, thus completely occluding the artery throughout the cardiac cycle. As the cuff is slowly deflated, blood flows through the artery whenever arterial pressure exceeds cuff pressure. As long as the blood flow is discontinuous, it is accompanied by Korotkoff sounds; a characteristic snapping of the artery. These Korotkoff sounds are used to signal systolic pressure (evidenced by the first appearence of the sounds); and diastolic pressure (evidenced by a muffling of the sounds).

Neither of these methods is suitable for long term use in ambulatory patients. The direct method, while providing beat to beat pressure, introduces the dangers inherent in placing a foreign object into the high pressure arterial system; ie. infection, hemorrhage, and thrombosis.

The ausculatory method requires at least periodic occlusion of an artery, which is at best uncomfortable, and may cause damage to the limb used. It requires either a source of compressed air or requires the patient to periodically pump the cuff. The cyclical inflation and deflation of the cuff is obvious to the patient, and may introduce pyscholgical factors which may not be eliminated. It would not indicate blood pressure on a beat to beat basis, and would tend to be bulky.

The desire to develop a useful method for measuring blood pressure in ambulatory patients has led to a new approach. It is suggested that blood pressure is proportional to pulse wave velocity (Steele (1937), Bayett & Dreyer (1922), Hafkesbring & Ashman (1943), Sands (1924), Beyerholm (1925), Nye (1964), Haynes et al (1936)). In this project we have reviewed both the theoretical and experimental basis for this theory, and tried to verify this relationship in humans.

II. Review of the Literature

The flow of blood through an elastic artery may be thought of as the superposition of two seperate flows; the flow of a pulse wave, and the mean of the steady state flow. The velocity of the pulse wave is between four and ten meters per second, while the mean flow is about .75 m/s in the aorta to about .25 m/s in the carotid artery. As there is great fluctuation about this mean, the mean flow, which is small, but not negligible, may be ignored (Bramwell and Hill (1922)). Blood flow through the arteries is modeled then as a pulsatile flow through an elastic tube.

The first work relating pulse velocity through an elastic tube was done simultaneously and independently by Moens (1878) and Kortweig (1878). Moens, relying on experimental data, found that pulsatile blood flow could be related to properties of the artery in the following manner:

$$v = K(Ea/2wd)^{\frac{1}{2}} \tag{1a}$$

Where:

v=velocity of the onset of the pulse wave

E= Young's modulous (modulous of lateral expansion of the artery)

w=density of the fluid

d=diameter of the tube

(For derivation, see appendix A)

a=thickness of the wall

K≐.9 to .95

Kortweig performed a theoretical study and found:

$$v = (Ea/2wd)^{\frac{1}{2}} \tag{1b}$$

which, except for Moens' constant K, is identical to 1a.

The Moens - Kortweig equation is based on many assumption; 1) the vessel is culindrical and has radial symmetry; 2) there is no longitudinal extension of the tube; 3) the elastic wall is homogeneous; 4) the amount the wall is extended laterally is small; 5) Hooke's law applies to the vessel; 6) the thickness of the wall is small compared to the diameter of the tube; 7) the fluid is non - viscous (Horeman and Noordegraff, (1958)). Are these assumptions valid?

The first, while not strictly true, is a valid assumption (Horeman and Noordegraff (1958)); although advanced cases of arteriolsclerosis do introduce large amounts of tortuosity which cast coubt on this (Sands (1929)).

The second assumption causes a paradox in the initial equations; they have been solved assuming longitudinal extensions. Taking longitudinal extensions into account yields a correction term that is not larger than 5% of the total (Horeman and Noordgraff (1959).

The third has been found to be wrong, but also found to contribute negligible error (Hallock and Benson (1937)); as has the fourth (Remington, et al (1948)).

Hooke's Law definitely does not apply to an artery.(Hallock and Bnson (1937), Steele (1937), Bramwell and Hill (1922)). The deviation from Hooke's Law has been reported variously as a "hysteresis", 'elastic "after action"'. Basically, arteries, if stretched quickly, tend to continue expanding slightly after all force has been removed. However, Hooke's Law does hold if the stretching is thought of as going from diastolic pressure to systolic pressure; rather than zero pressure to systolic pressure (ie. if the amount stretched is small) (Horeman and Noordgraff (1958)).

Although not negligible in the small arteries, the thickness of the wall can be ignored in the larger arteries. (McDonald (1960)).

Blood is definitely a viscous fluid, although the effect is larger in the smaller arteries. McDonald has found that the viscous property of blood tends to reduce its speed by 5 to 10%; and attributes this fact to Moens constant of .9 to .95.(McDonald (1960)). This is in qualitative agreement with Wormsley, who also took into account the viscous nature of blood (Bargainer, J. D. (1958)).

The Moens - Kortweig equation relates blood pulse velocity to several variables which are difficult, if not impossible to measure in vivo. A transformation of this formula was done (Bramwell and Hill (1922))in order to relate pulse wave velocity to more easily measured properties. This transformation makes two simplifying assumptions: 1)the distance traveled by the wave is short and 2) the waveform has no sharp discontinuities, therefore, only the longer wavelengths must be considered. Both of these assumptions are reasonable, and the result:

$$v = 3.57\left[dP/(dV/V)\right]^{\frac{1}{2}} \qquad (2)$$

Where:

v =velocity of the blood pulse

P =pressure in the artery

(For derivation, see appendix B). V = volume in a section of artery

is accepted by most workers. It allows one to use pressure volume curves derived experimentally to obtain pulse wave velocity as a function of pressure. Bramwell and Hill did this work for several discrete points using work done previously by Roy (1880), and found that above 80 mm Hg. pulse wave velocity was proportional to pressure.

It is also possible to verify the Kortweig - Moens equation for the continuous case if one has a function relating the radicand in the Bramwell - Hill equation to pressure. Such a function can be derived in the following manner: obtain a pressure / volume curve of an artery. (There are several such curves in the literature. Perphaps the most useful set can be found in Hallock and Benson (1937)). In this study, an excised artery was filled with the minimum amount of saline solution needed to keep the artery normally distended. This initial volume, Vo, required a pressure of 7.3 mm Hg. The pressure was then slowly increased, and the percentage change in volume, (as compared to Vo) (V-Vo)/Vo, is plotted against pressure. An example of a pressure - volume curve is shown in Fig. 1a. One then finds the derivative of the line with respect to pressure to obtain (dV/Vo)/dP vs. P. This is done by finding the tangent to the line. If this is done for several points, and the inverse of the tangents are plotted versus pressure, one obtains a new curve (shown in figure 1b). This new curve, which is the best fit of a quadratic equation, represents dP/(dV/Vo)as a function of pressure. This parabola has the equation;

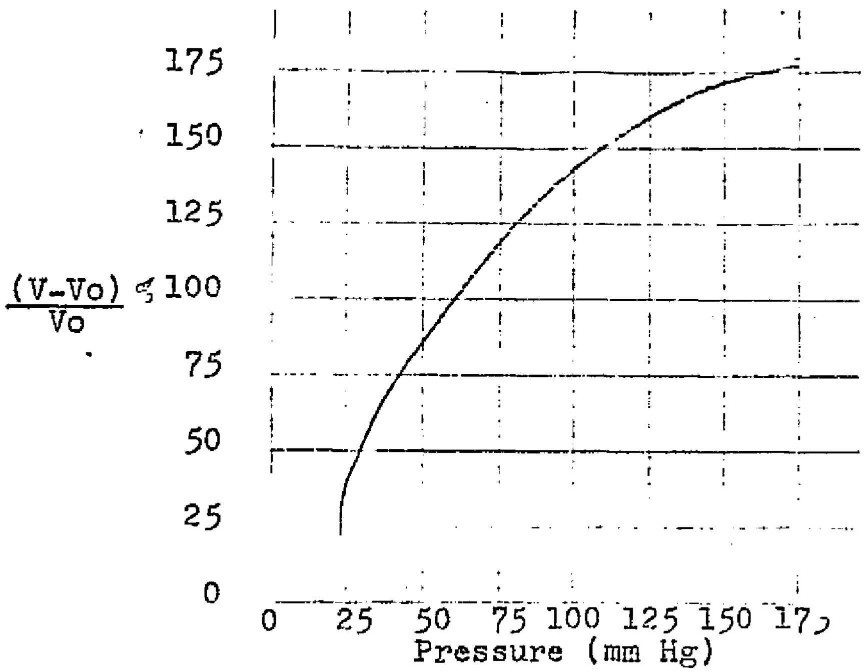

Fig. 1a Pressure-Volume Curve

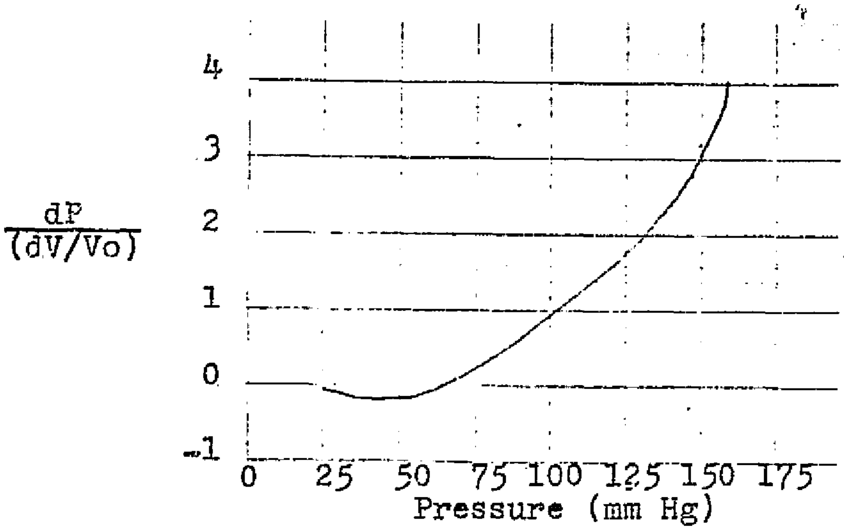

Fig. 1b Derivative of Pressure-Volume Curve with respect to Pressure plotted against Pressure

$$dP/(dV/Vo) = (2.53\text{x}10^{-4})P^{2} - (1.34\text{x}10^{-2})P - .11 \qquad (3a)$$

which is approximately

$$dP/(dV/Vo) = (1.59\text{x}10^{-2}\,P - .3)^{2} \qquad (3b)$$

By substituting Equation 3b into Equation 2, one obtains:

$$v = 5.67\text{x}10^{-2}\,P.- 1.17 \qquad (4)$$

which suggests a linear relationship between blood pressure and pulse wave velocity.

There are several different blood pressures which are in common useage; diastolic, systolic, mean, and pulse. There is some question in the literature as to which one of these corresponds to the pressure in the Bramwell-Hill equation (eq. 2). Pulse wave velocity has been variously reported as being proportional to: 1) diastolic blood pressure (Steele (1937)); 2) either diastolic or mean pressure (Bayett & Dreyer (1922)); 3) both diastolic and systolic blood pressure in women; neither diastolic nor systolic pressure in men (Hafkesbring & Ashman (1943)); 4) diastolic blood pressure in healthy subjects, nothing in patients with heart or circulation difficulties (Sands (1924)); 5) systolic blood pressure (Beyerholm (1925)); 6) mean blood pressure (Nye (1964)); and 7) pulse pressure (Haynes, Ellis, & Weiss (1936)). The fact that mean pressure and pulse pressure are proportional to both diastolic and systolic pressures, and a rise in one is usually accompanied by a rise in the other three, makes it difficult to decide on which pressure, if any, is the best determinant of pulse wave velocity: this is probably a major reason for the inconclusiveness of the literature.

III. Experimental Work

A. Objectives

The final goal of our group is the development of a device to measure diastolic blood pressure. The device should be both non-invasive, and easily adaptable for use on ambulatory patients. It will utilize the supposed fact that diastolic blood pressure is monotonically related to pulse wave velocity. Although there has been much work done on the relationship between blood pressure and pulse wave velocity, it has been inconclusive. Previous work done in our group has verified a linear relationship in dogs (La Bresh (1970)); the question now becomes: does it hold for humans?

To measure pulse wave velocity, one needs to measure the time difference between the arrival of a single pulse at two separate points in the elastic arterial system. One can also determine pulse velocity by measuring the time between onset of ejection of blood from the heart and the arrival of a pulse at a single point. It has been shown that the ECG is useless for predicting the time of ejection of blood into the aorta, due to the large variability in τ, the time interval between Q wave and pressure onset in the aorta (LaBresh (1970)). It has been suggested that the second heart sound (signaling closure of the semilunar valve (Lewis (1962))might correlate better with onset of ejection. So in addition to verifying the relationship of pulse wave velocity to diastolic blood pressure, we wished to ascertain whether there was a correlation between blood pressure and the time between the onset of the second heart sound and the arrival of a pulse at a particular point.

B. Methods

The following apparatus, designed to detect and record several pysiological signals, was assembled. The entire system is shown in Fig. 2.

A pair of piezo-electric transducers (see Figs. 3a & 3b) were used to detect arterial pulses in the carotid and femoral arteries. A change of pressure is applied to the device by means of a pliable plastic membrane stretched across a hollow disc. This disk, termed a Marey's capsule (Elema-Schnonder model EMT 521) is connected to a length of tygon tubing. The tubing serves to transmit the changes of pressure to the crystal transducer (EMT 510C). The transducer consists of a hollow cylinder, the inner wall of which is a metal membrane. The signal from the Marey's capsule enters the cylinder through a small orifice. The change in pressure causes movement of the metal membrane, which imparts movement to a piezo-electric crystal which is coupled to the membrane. Thus the electrical output is proportional to the change in pressure on the Marey's capsule. The manufacturer specifies the frequency response of these transducers as flat to 30 Hz.

(Two other methods for detecting blood pulses were looked into and discarded. It was originally proposed to use transcutaneous Doppler flowmeters in this experiment. They conform to many of the requirements of the ultimate blood pressure device sought by our group, and have been used in many applications requireing detection of blood flow. Unfortunately, the two instruments available to us were not sophisticated enough for our

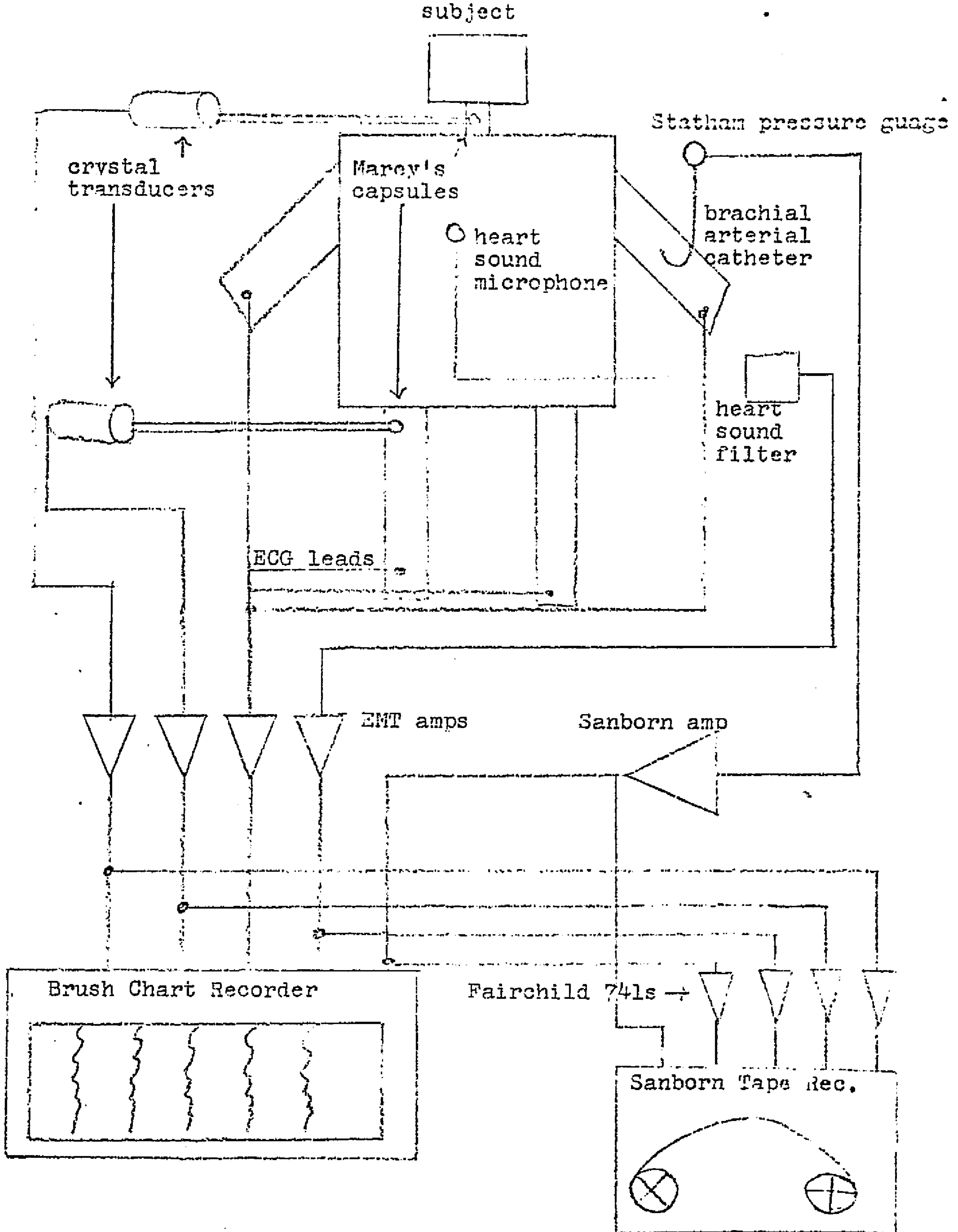

Fig. 2 Experimental System

ORIGINAL PAGE IS OF POOR QUALITY

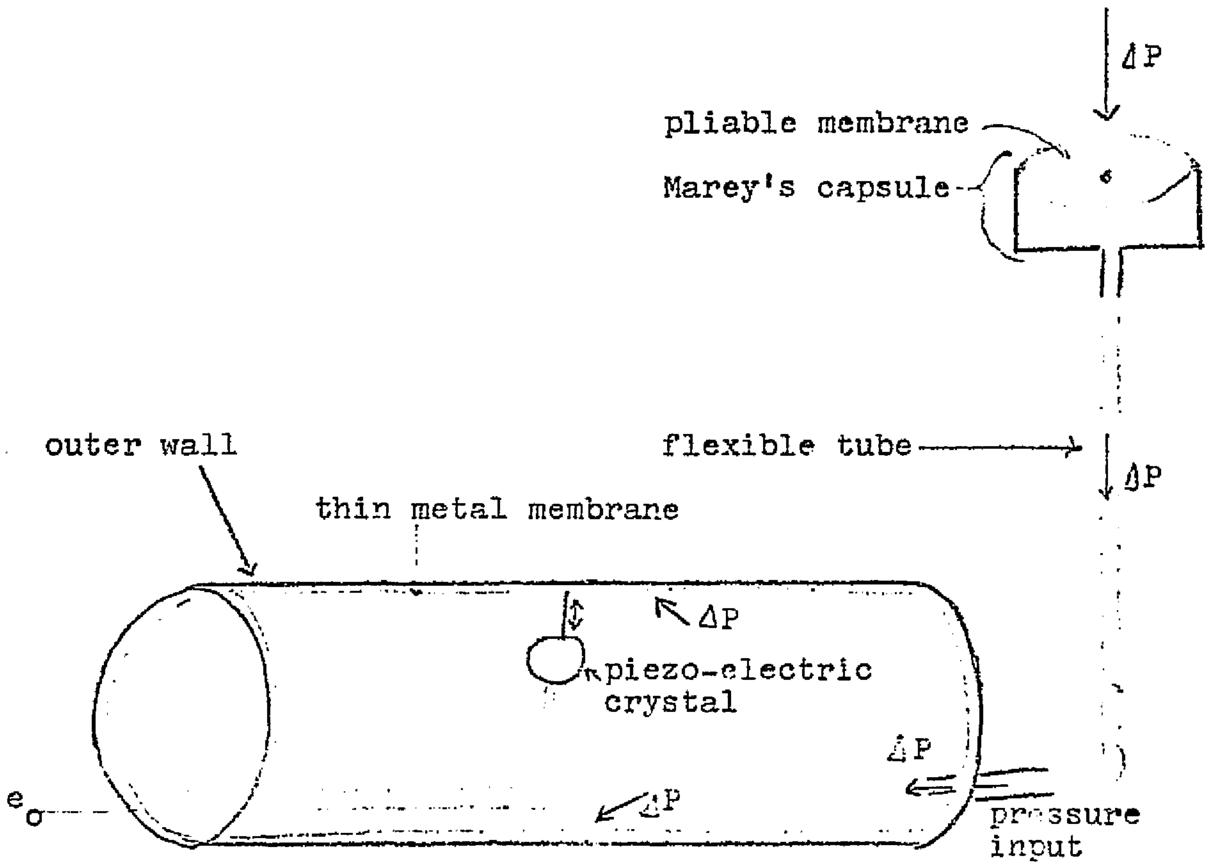

Fig. 3a Elema-Schnonder crystal transducer and Marey's capsule

ELEMA-SCHÖNANDER
INDUSTRIVAGEN 23 · STOCKHOLM-SOLNA · SWEDEN

D01
DATA
Nov. 1967
19

CRYSTAL TRANSDUCER EMT 510

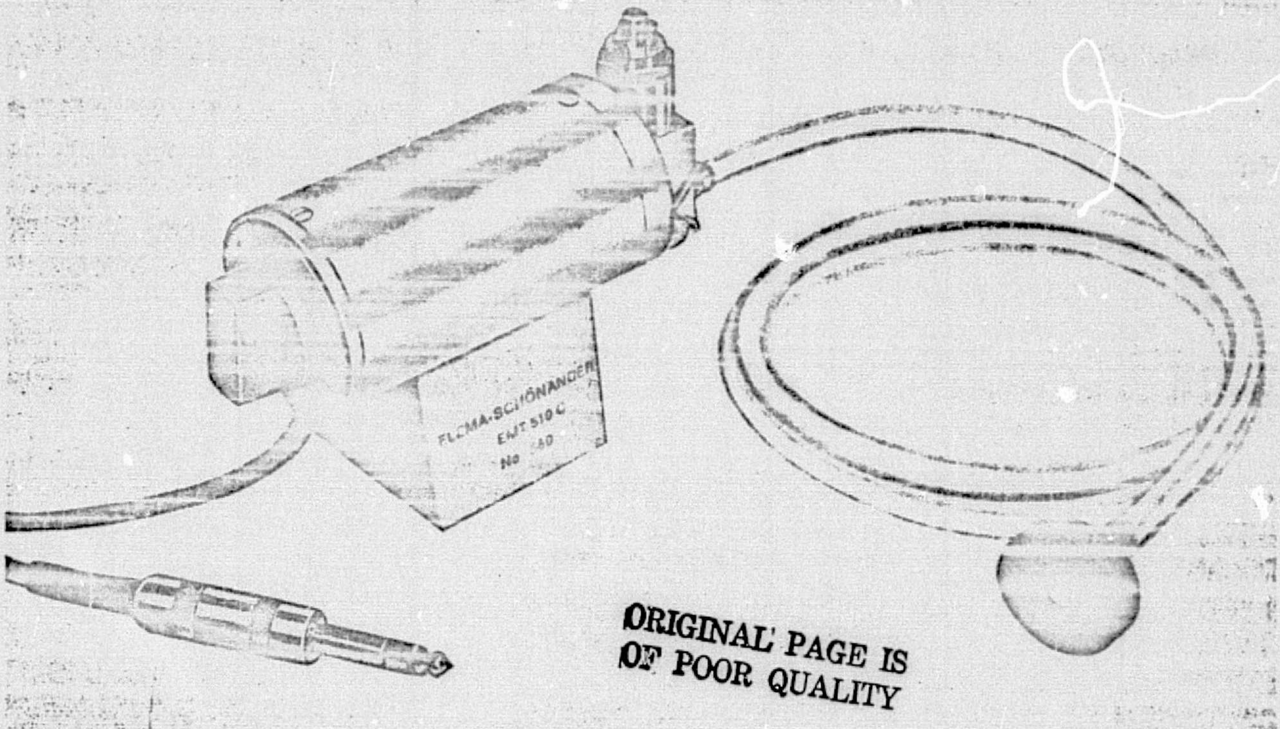

Figure 1

The crystal transducer EMT 510 is for measurement of small pressure variations. The transducer may be connected to a Mingograf recorder or any other electrocardiograph.

DESIGN

The crystal transducer contains a closed cylindrical chamber, the inner wall of which is a metal membrane. The centre of the membrane is mechanically coupled to a piezo-electric crystal. The chamber has a nipple for connection of a flexible hose, inner diameter 5 mm. Pressure variations in the chamber generates a signal voltage. By means of a voltage divider a suitable fraction of the voltage is fed to the recorder by a shielded single lead cable with a connector. For sensitivity standardization a volume calibrator is provided.

PULSE WAVE RECORDING

Combined with a Marey's capsule (see fig. 2) the crystal transducer can be used for recording of [illegible] venous pulse waves as well as apex cardiograms. If the capsule is connected to the transducer with a polyethylene tubing (length approx. 30 cm) the upper frequency limit is approx. 30 Hz.

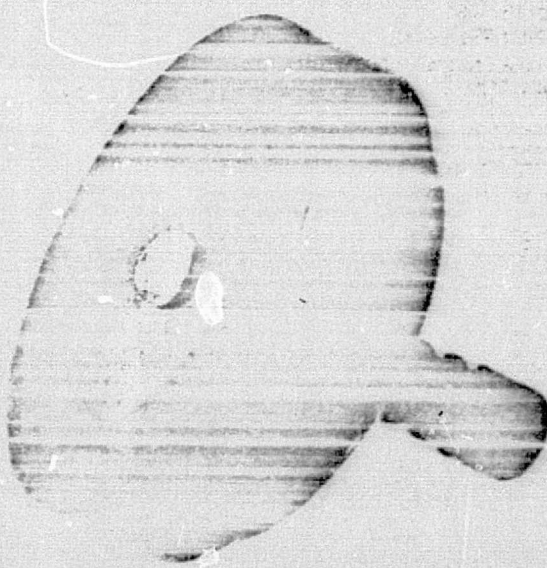

Figure 2

Fig. 3b Crystal Transducer and Marey's Capsule purposes, and were discarded.

It was also found to be possible to detect pulses by placing an inflated air bladder over an artery, and applying slight downward pressure. The bladder is compressed as a blood pulse applies pressure upward through the skin. A pressure transducer can detect the pulse wave if attached to the bladder via a tube. However, this method was not as simple to use as the EMT equipment previously described.)

Heart sounds were detected by a sensitive microphone designed for this purpose (EMT 25B). It was secured by a rubber strap over the apex. The frequency response of the microphone is governed by a filter network that must be used with the microphone.(EMT 22). As the second heart sound is primarily high frequency sound, the filter network was set to a center frequency of 400 hz, with 6 db points at 200 and 800 Hz. This setting served to accentuate the second heart sound.

One channel of scalar ECG was obtained by placing electrodes on all four limbs. Amplification for the ECG signals, heart sounds, and pulse pickups was supplied by EMT 13 amplifiers. The output of all four channels was at a nominal level of 100 mv.

Arterial blood pressure was measured by a catheter inserted into the brachial artery. Its inner diameter was .045" and outer diameter was .062". The tubing was partially filled with sterile saline solution to act as a buffer, and was coupled to a Statham model P23Gb strain guage pressure transducer. A Sanborn 350-1100B carrier amplifier was used to amplify the signal to its maximum level of 2V, which was set to correspond to a pressure of 200 mm Hg. As the Sanborn amplifier had its 3db point at 480 Hz, the frequency response of the pressure measuring sub-system was limited by the transducer, which is flat to 50 Hz.

All five channels of data were recorded simultaneously on both a Brush model 260 chart recorder, and a Sanborn model 3907A 7 channel analog magnetic F.M. tape recorder. All channels except arterial pressure required approximately 25 db of additional amplification prior to being recorded on the tape recorder. This was supplied by 4 Fairchild 741 operational amplifiers. The Brush recorder has a full scale frequency response of 50 Hz, and the tape recorder was flat ± 1db 625 Hz.

Five subjects were connected to the above system. They were all males between the ages of 18 and 23, and were not known to have any cardiovascular disease. Their blood pressure was varied by several means. Their blood pressure was raised by isometric contraction of one arm. This was accomplished by having the subjects squeeze a hand grip dynamometer; a device which measures the force applied by gripping its handle. The literature implied that this might raise pressure by about 15 mm Hg (Hurwitz, et al (1971)). It was lowered by both the inhalation of amyl nitrite, a vaso-dilator; and by performing a valsalva manouver (a straining of the thoracic muscles coupled with closing the glottis).

The Marey's capsules were placed over the femoral and carotid arteries in order to obtain pulse transit times in the aorta. The two pulse transducers were connected to their respective Marey's capsules via identical lengths of tubing. It was verified that the crystal transducers do not introduce a time difference by themselves by tapping the two Marey's capsules together, and observing simultaneous outputs.

C. Results

As shown in Fig. 4a, a signal proportional to brachial arterial blood pressure was obtainable via the catheter. Blood pressure was readable to an accuracy of 2 mm Hg.

After the second experiment, it was decided to use lead III (left arm-left leg) of ECG to minimize muscle noise during isometric contraction of the right arm. For timing purposes, it was decided to use the minimum in the QRS complex, identified in the figure with an (a).

As shown in Fig. 4c, a good heart sound signal was obtained. The first heart sound is defined as the first complex occuring after the QRS complex in the ECG; and the second heart sound is the second complex after the QRS. The beginnings of the various heart sounds were defined as being the first large negative going pulse in the complex. In Fig. 4c, the beginning of the first heart sound is identified with a (b); and the second heart sound has its beginning marked with a (c).

As shown in Figs 4d and 4e, good pulse waveforms were obtained at both the femoral and carotid locations. It was found, as was expected, that the pulse tends to be distorted as it travels further away from the heart, due to different parts of the wave traveling with different velocities. This is assumed to be due to the different pressures that the different parts of the wave "see". In addition, the foot of the wave 'sees' a harder wall, due to the viscous resistance to expansion seen in arteries; as the tail sees a softer wall, due to a viscous interference

Fig. 4b - a represents the point in the QRS complex used for timing purposes

Fig. 4c - b represents the beginning of the first heart sound

c represents the beginning of the second heart sound

Fig. 4d - d represents femoral pulse onset

Fig. 4e - e represents carotid pulse onset

f represents dicrotic notch

Fig. 4f - 1 represents time difference Δt_1

2 represents time difference Δt_2

3 represents time difference Δt_3

4 represents time difference Δt_4

5 represents time difference Δt_5

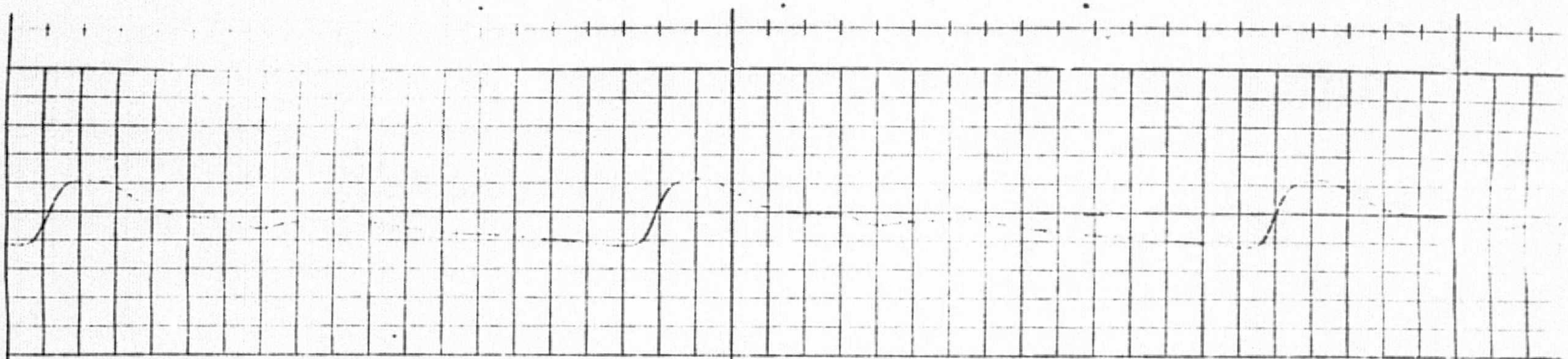

Fig. 4a Brachial Arterial Pressure

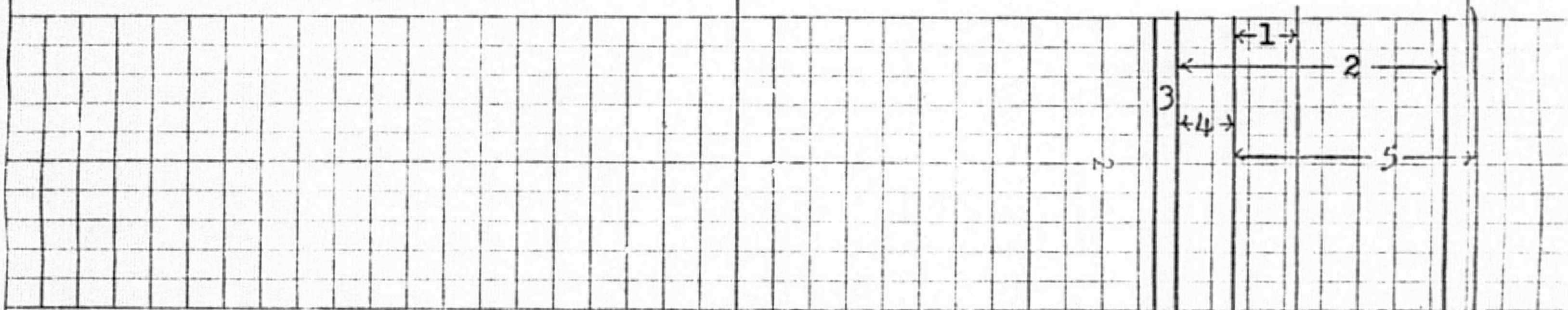

Fig. 4f Various Transmission Times

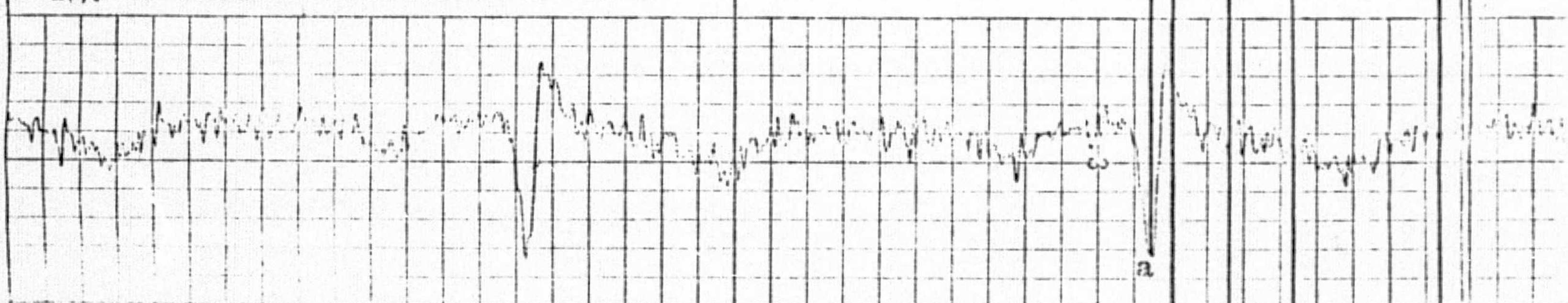

Fig. 4b ECG Lead

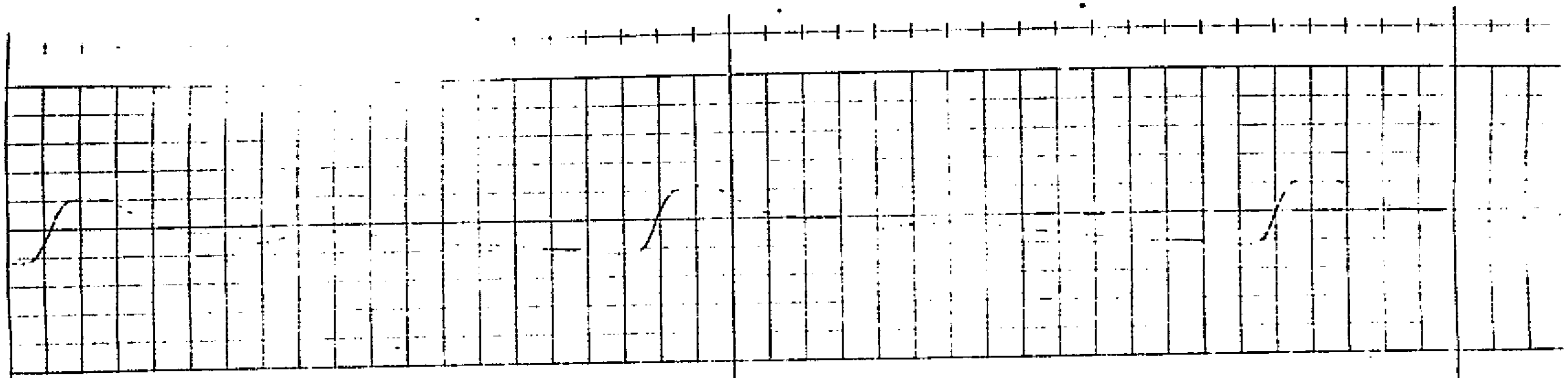

Fig. 4a Brachial Arterial Pressure

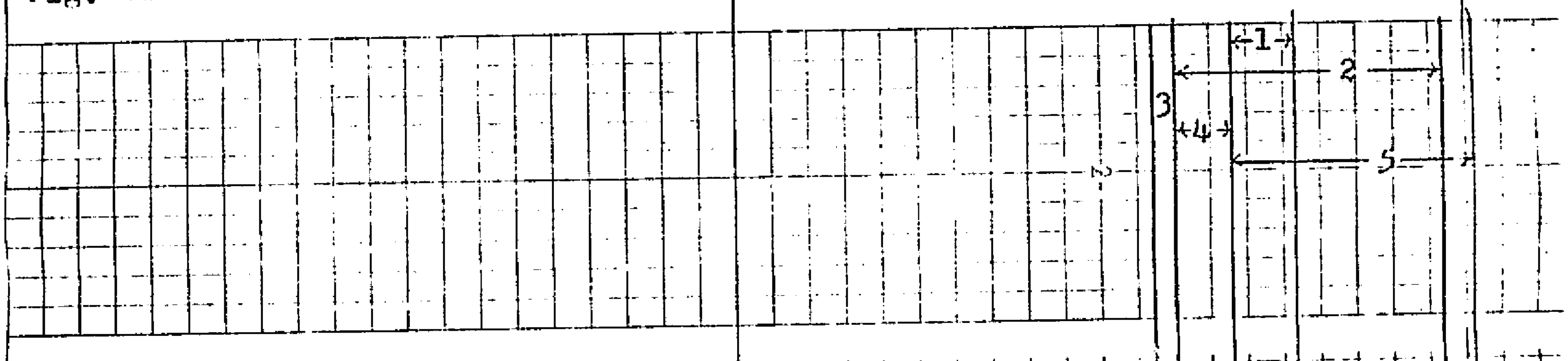

Fig. 4f Various Transmission Times

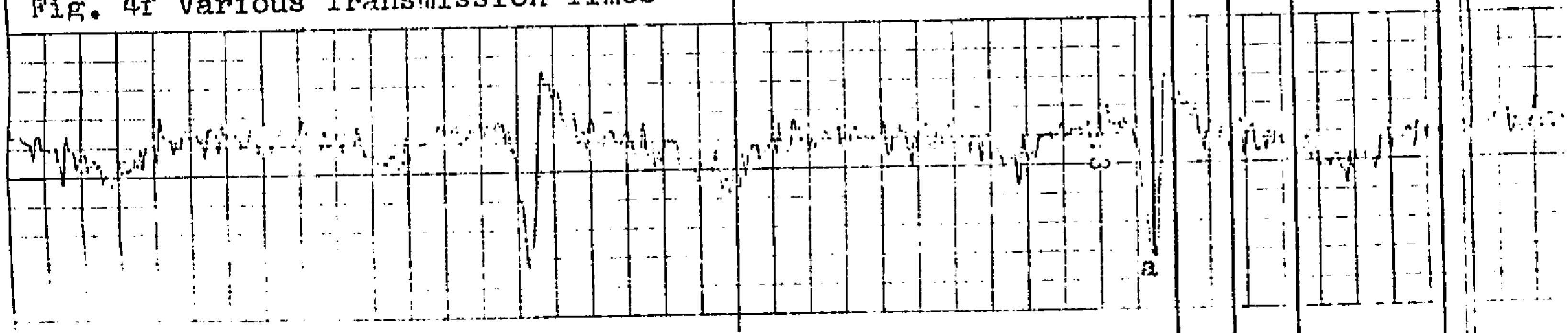

Fig. 4b ECG Lead

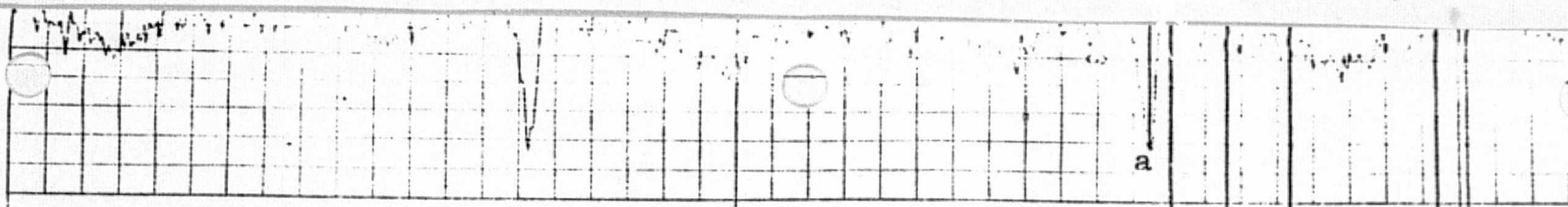

Fig. 4b ECG Lead

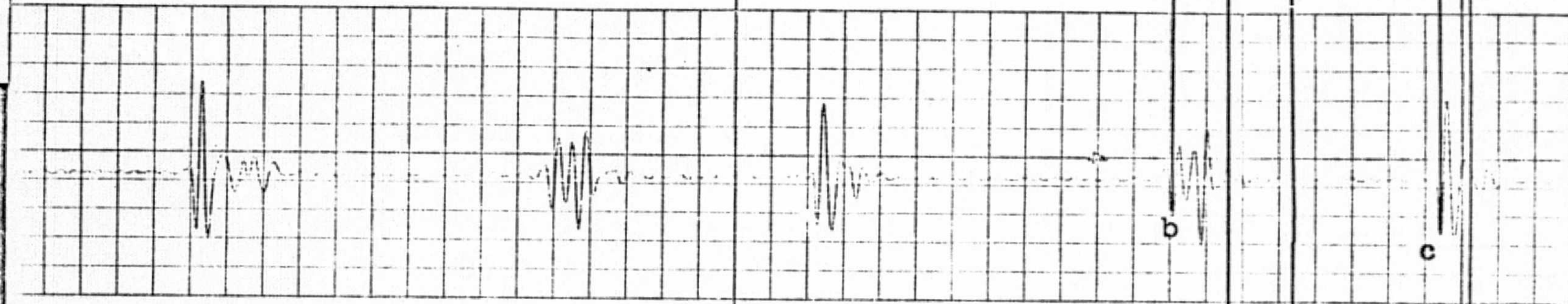

Fig. 4c Heart Sounds

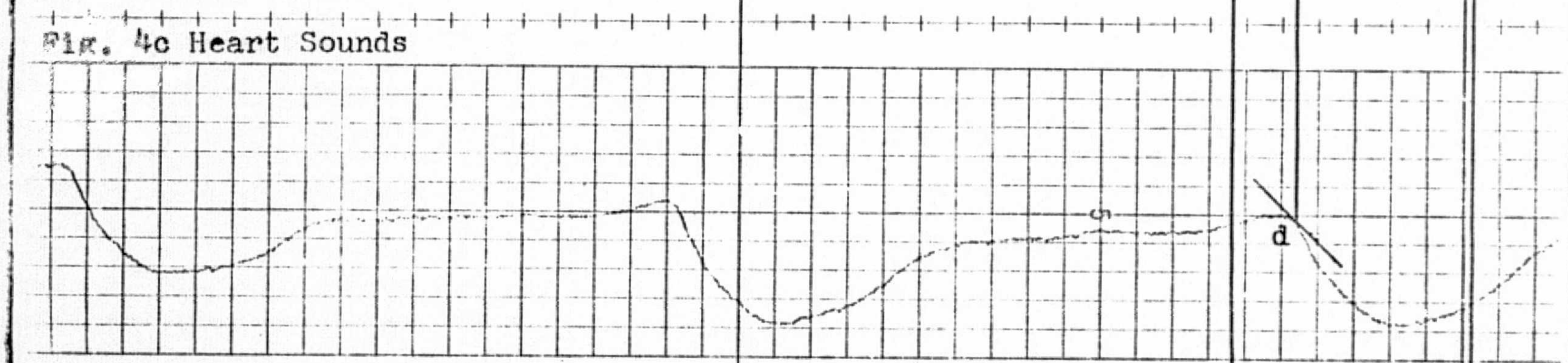

Fig. 4d Femoral Artery Pulses

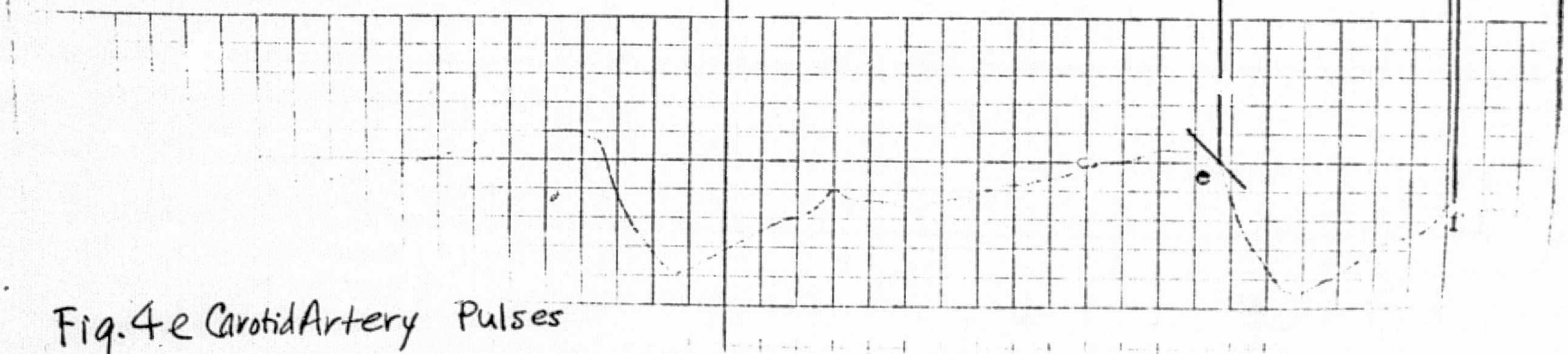

Fig. 4e Carotid Artery Pulses

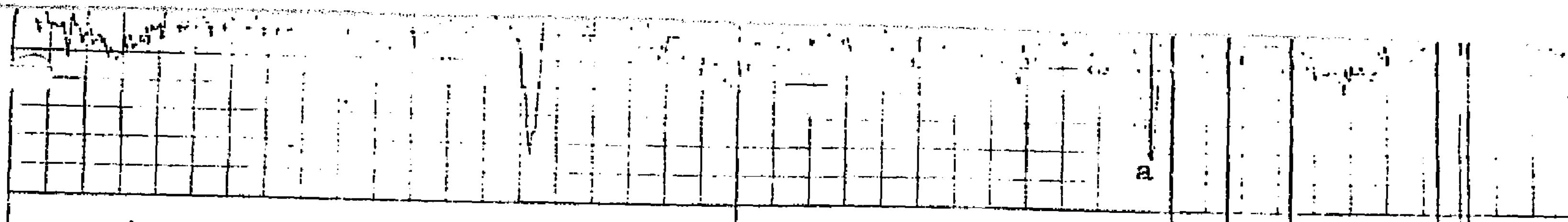

Fig. 4b ECG Lead

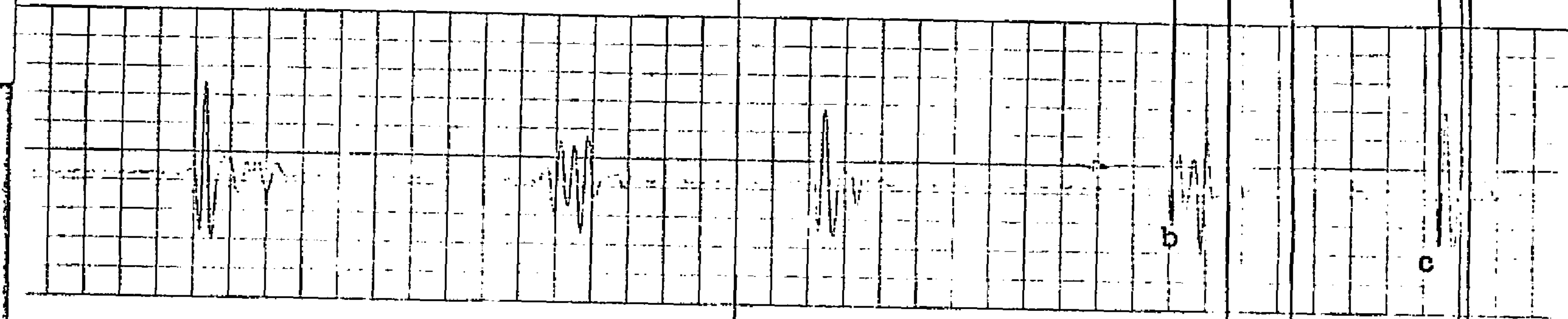

Fig. 4c Heart Sounds

Fig. 4d Femoral Artery Pulses

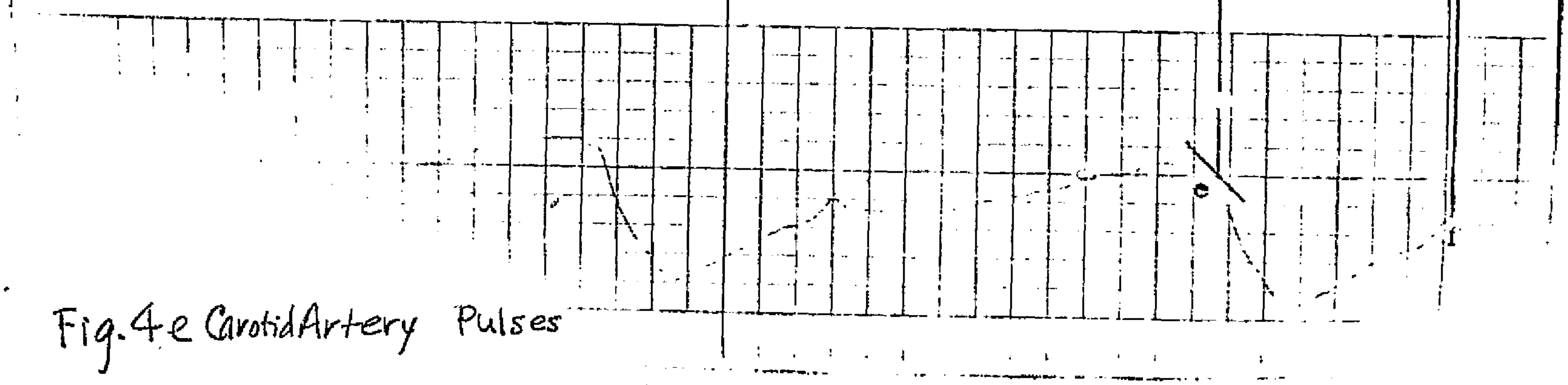

Fig. 4e Carotid Artery Pulses

with recoil (Hamilton, Remington, & Dow (1945)). It seems logical that the portion of the wave most related to diastolic blood pressure would be the onset, for this is the part of the wave that "sees" the diastolic pressure as it propagates down the artery. Thus, the onsets of the pulse pressure waves were used in determining transmission times.

It was important that consistancy be maintained when defining where on the wave the onset was. To this end, it was decided arbitrarily that the onset be defined as that point at which the tangent to the curve forms an angle of 45° with the horizontal. If a length of the curve possesed a slope of -1 (such that it would make an angle of 45° with the horizontal), the midpoint of that section was defined as the onset. Once onsets were defined (as identified with (d) in Figs. 4d and 4e), transmission times were measured to an accuracy of 4 msec. It is impossible to determine the magnitude of the errors introduced by definition or determination of onset.

It was found possible to raise diastolic blood pressure by as much as 40 mm Hg by means of isometric contraction of one arm. Examples of arterial blood pressure during contraction are shown in Figs. 5a and 5b. The discrepancy between this result and published reports that isometric contraction can raise blood pressure in healthy subjects by an average of 12 mm Hg (Hurwithz, et al (1971)) is explained by the fact that our subjects exerted maximal effort for as long as possible, while Hurwitz prescribed 1/3 maximal effort for 3 minutes. The one problem with maximum effort is that it produced bodily movement in some subjects, jarring the crystal transducers.

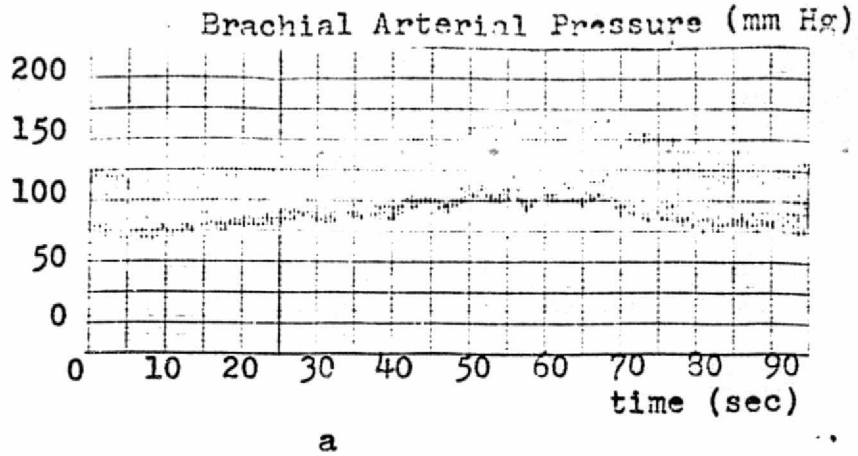

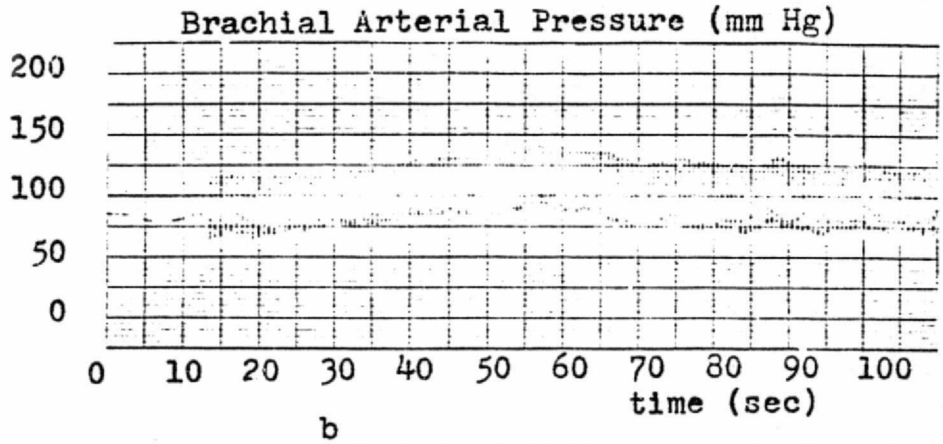

Figs. 5a & 5b Brachial Arterial Pressure during Isometric Contraction of one arm. Onset and Offset of Contraction noted by arrow

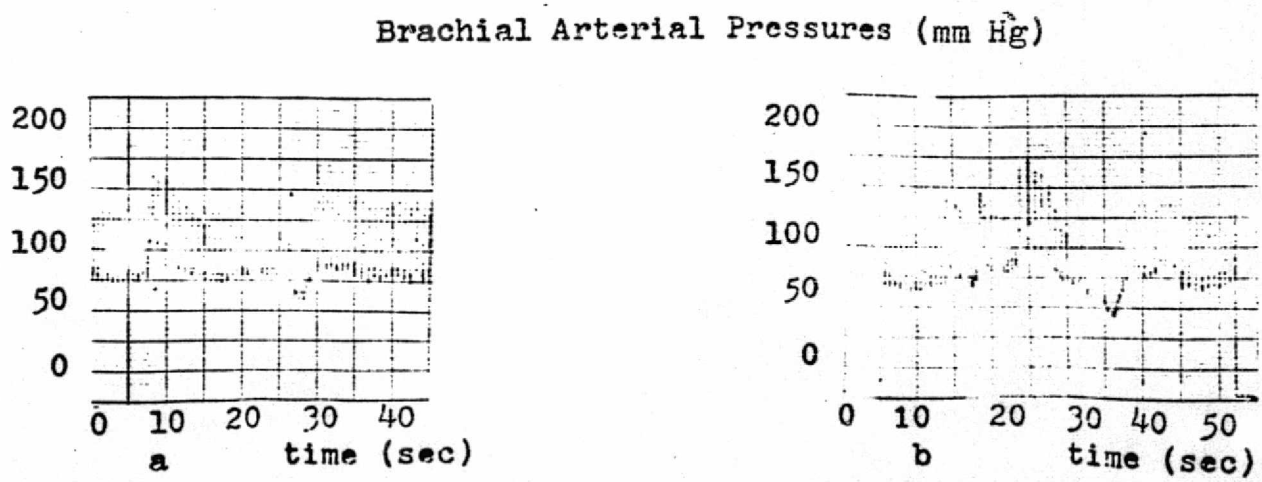

Figs. 6a & 6b Brachial Arterial Pressure during Valsalva Manouver. Onset and Offset of Straining noted by arrow.

c, 2

Valsalva manouvers were effective in lowering blood pressure by as much as 30 mm Hg. However, the drop in pressure is short lived, and the bodily movement needed to carry out a manouver was invariably accompanied by tissue movements of sufficient magnitude to cause the transducers to lose their signal; particularly in the femoral area. Thus, the valsalva manouver was unsucessful as a method to lower blood pressure in the experiment. Examples of blood pressure during valsalva manouver are shown in Figs. 6a and 6b.

Amyl Nitrite (whose effect on blood pressure is shown in Figs 7a and 7b) is a vaso dilator which was found useful in lowering diastolic blood pressure as much as 35 mm Hg due to one inhalation.

The time delay between the onset of the carotid pulse and the onset of the corresponding femoral pulse is defined as Δt_1 (see Fig. 4f). The inverse of this transmission time is proportional to velocity, thus Δt_1 provides one with the means of determining if pulse wave velocity is proportional to diastolic blood pressure. Graphs were made of the inverse of Δt_1 versus diastolic blood pressure for all five subjects.(Figs. 8,10,14, 18,22). Using the method of least squares, lines were drawn representing the 'best-fit' line of the data. The sample deviation was also calculated, and is shown along with the equation of each graph on the figures. The almost linear relationship, as predicted by several authors (Steele (1937), Bayett & Dreyer (1922)) is apparent.

From an engineering standpoint, it would be desirable to eliminate one of the crystal transducers, and measure velocity

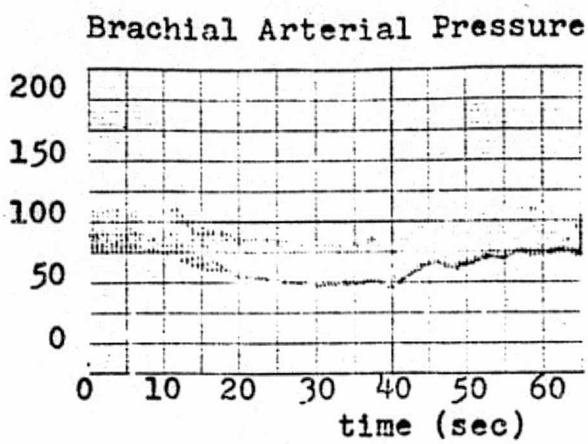

a

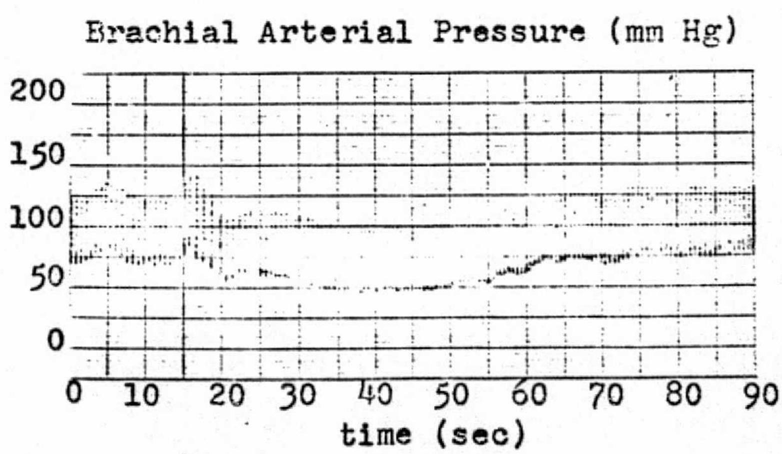

b

Figs 7a & 7b Brachial Arterial Pressure during Inhalation of Amyl Nitrite. Moment of inhalation is noted by arrow

Figs. 8 through 27

Δt_1 is the time interval between carotid pulse onset and the corresponding femoral pulse onset.

Δt_2 is the time interval between the beginning of the first heart sound and the beginning of the second heart sound

Δt_3 is the time interval between the most negative point of the QRS complex, and the beginning of the first heart sound

Δt_4 is the time interval between the beginning of the first heart sound and the onset of the corresponding carotid pulse

Δt_5 is the time interval between carotid onset and dicrotic notch

$\times$ = points taken under normal conditions

$\odot$ = points taken while the subject was isometrically contracting one arm

$\bullet$ = points taken while the subject was under the influence of Amyl Nitrite

Pressure represents brachial arterial blood pressure

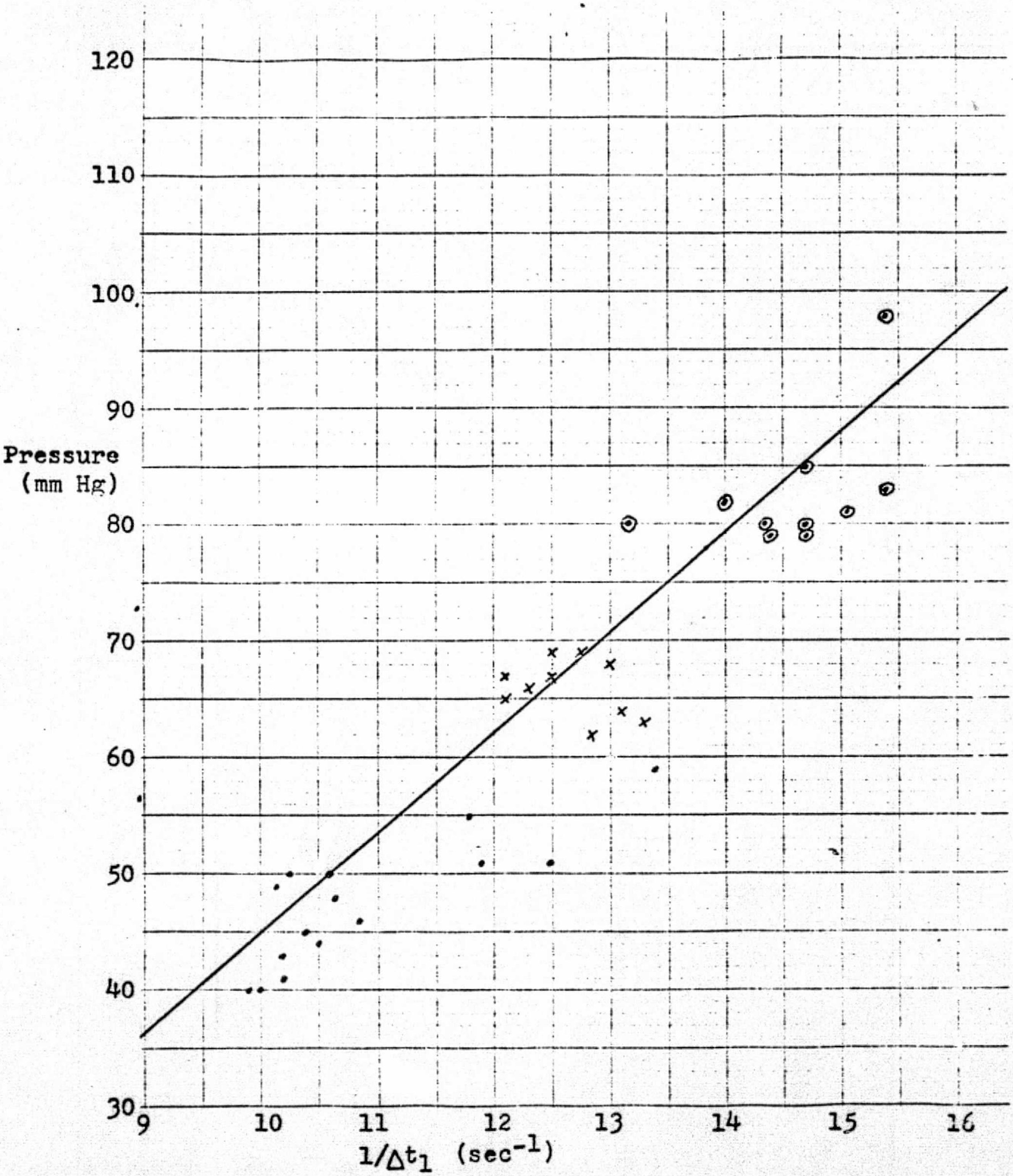

Fig. 8 $1/\Delta t_1$ plotted against pressure
Data taken from Experiment 1
Best-fit line: $P = 8.32(1/\Delta t_1) - 38.0$; $s = 7.67$

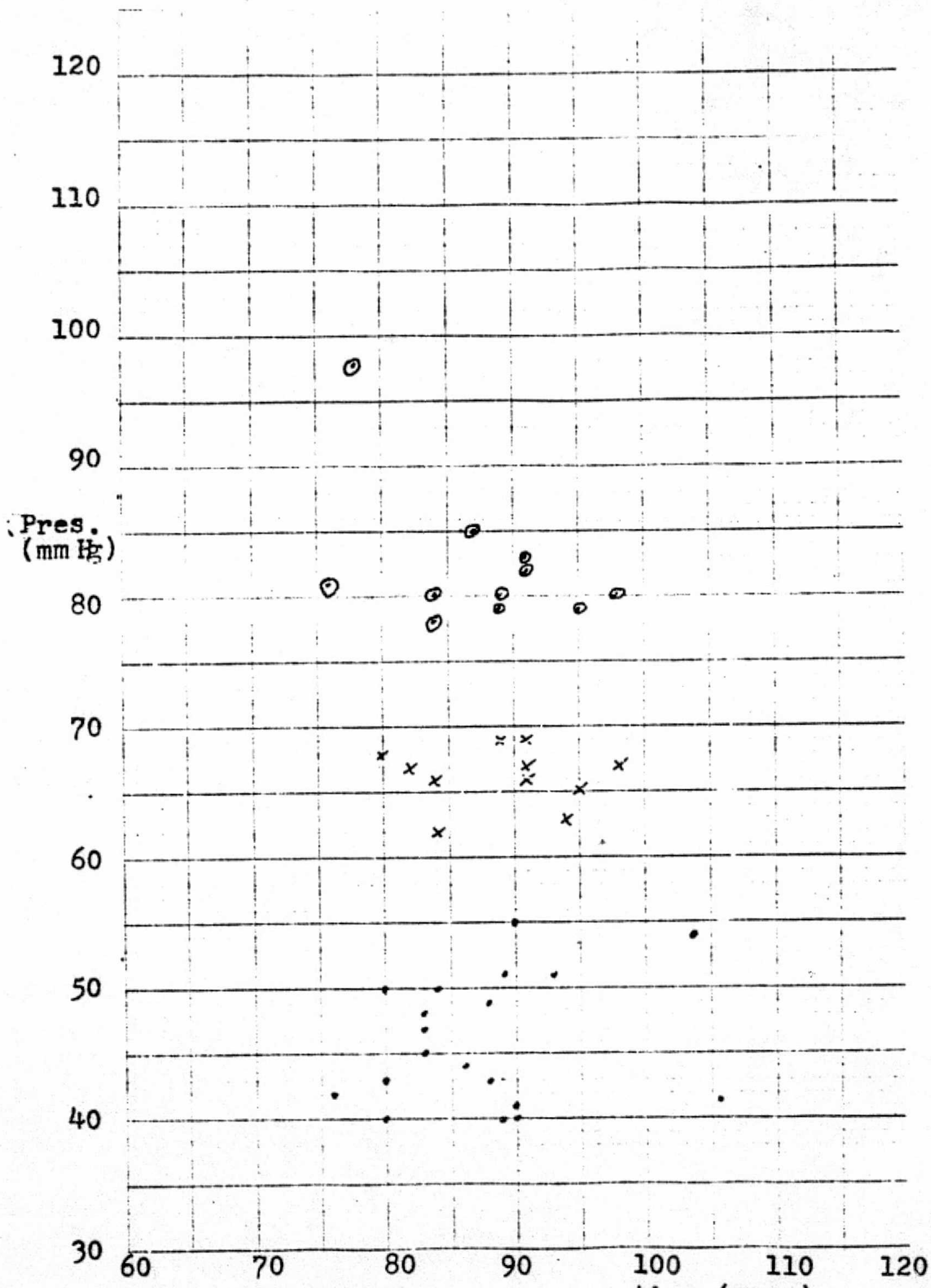

Fig. 9 Δt_3 plotted against pressure

Data taken from Experiment 1

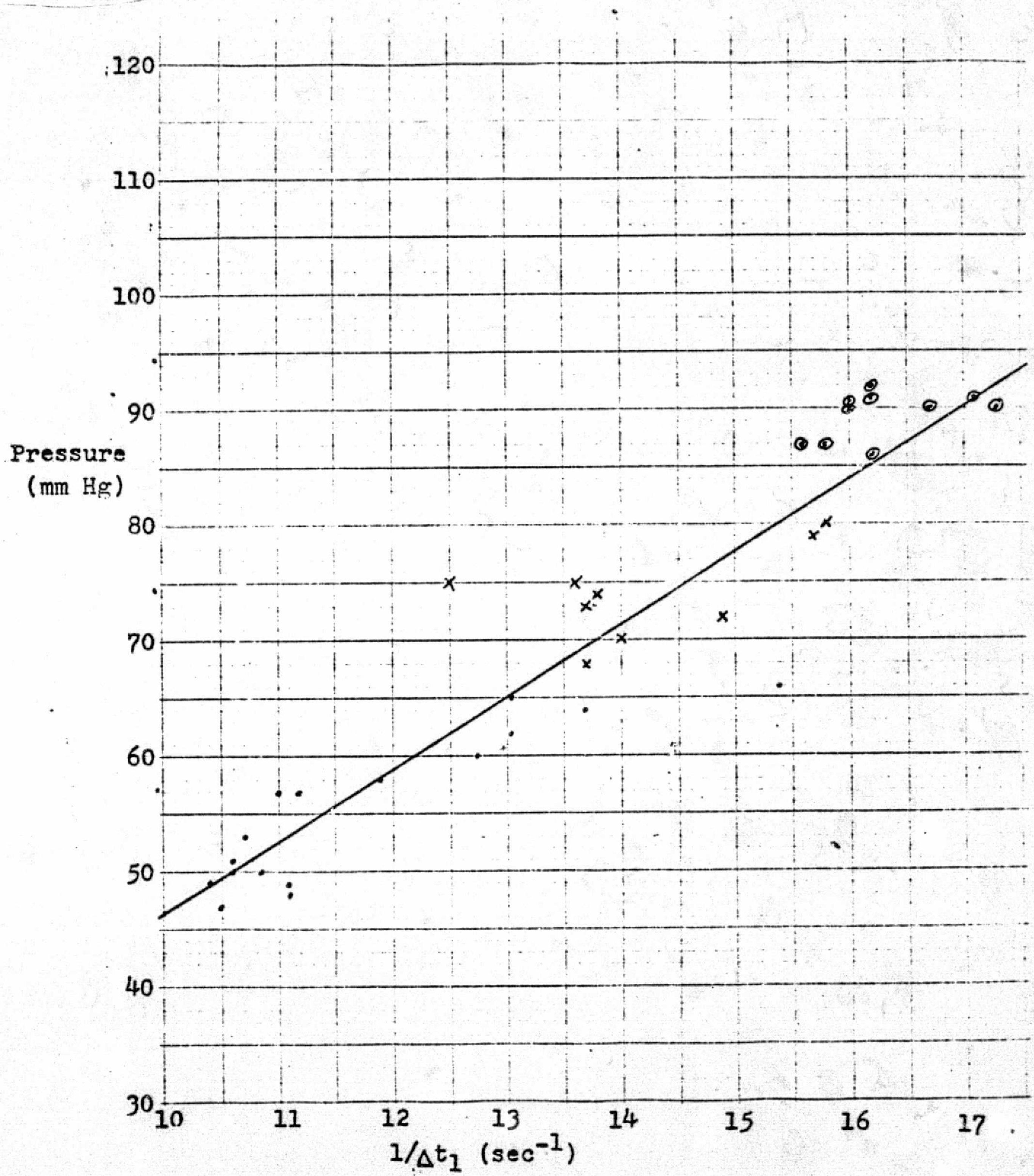

Fig. 10 $1/\Delta t_1$ plotted against pressure
Data taken from Experiment 2
Best-fit line: $P = 5.78(1/\Delta t_1) - 11.4$; $s = 4.91$

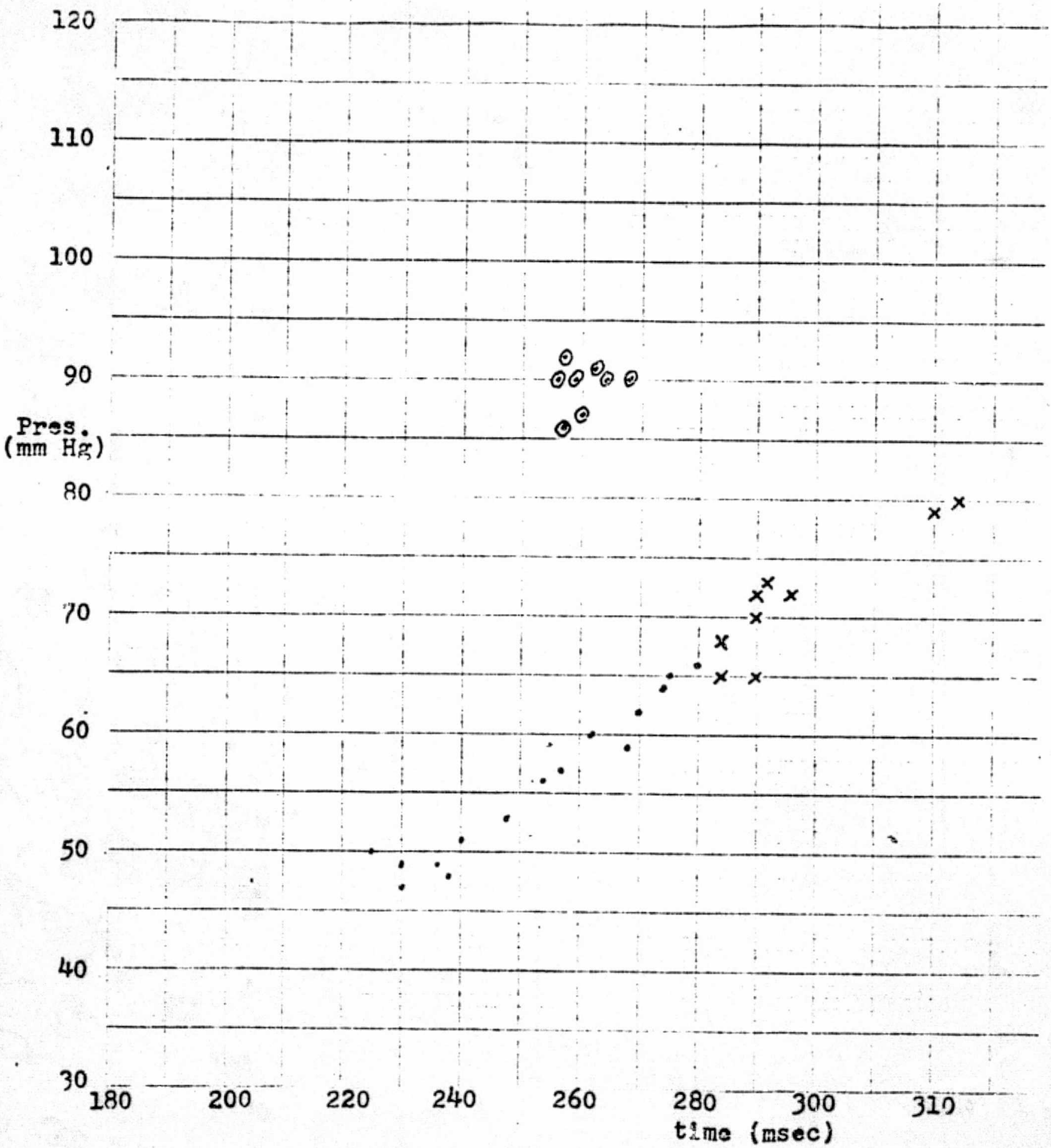

Fig. 11 Δt_2 plotted against pressure
Data taken from Experiment 2

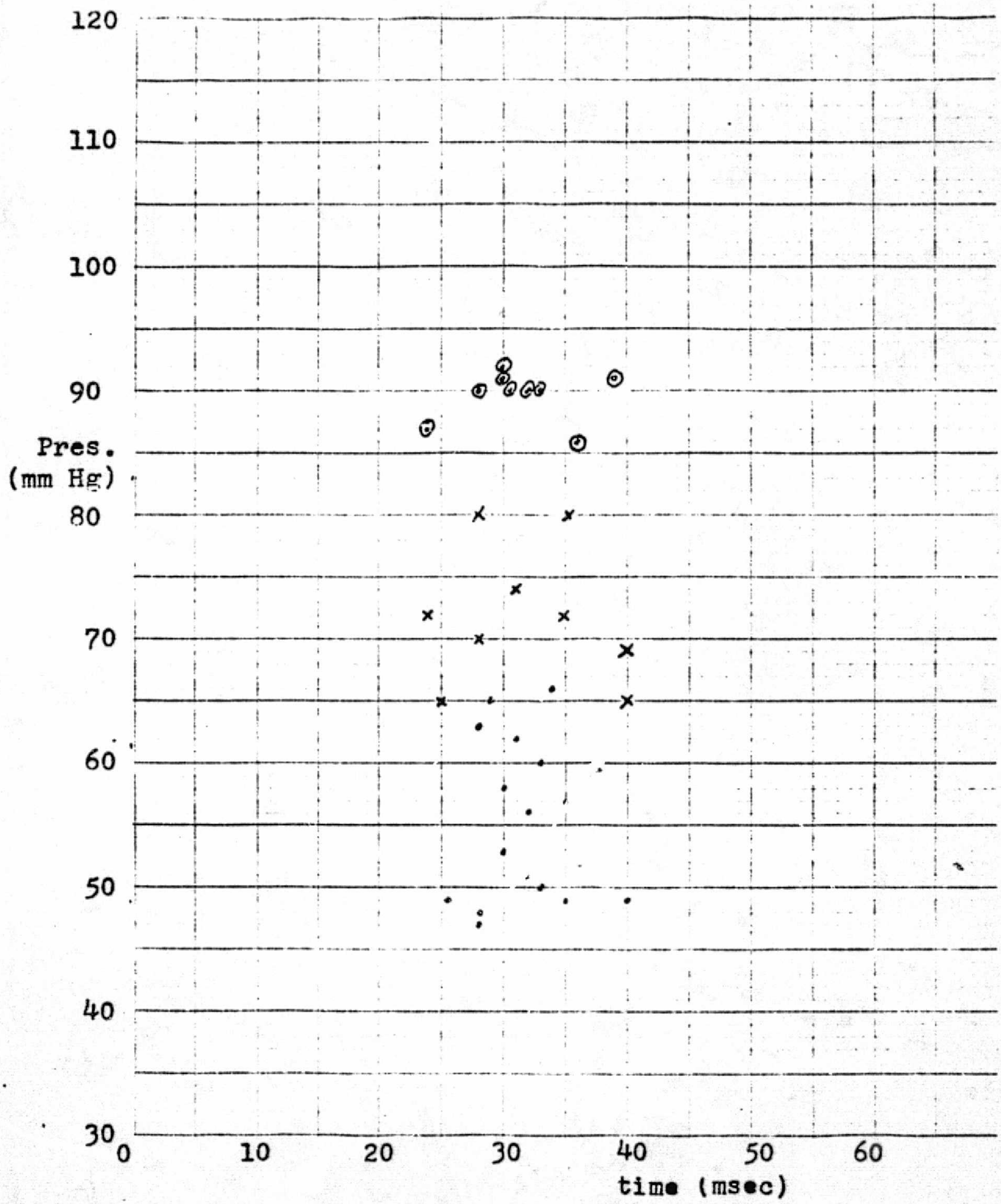

Fig. 12 Δt_3 plotted against pressure
Data taken from Experiment 2

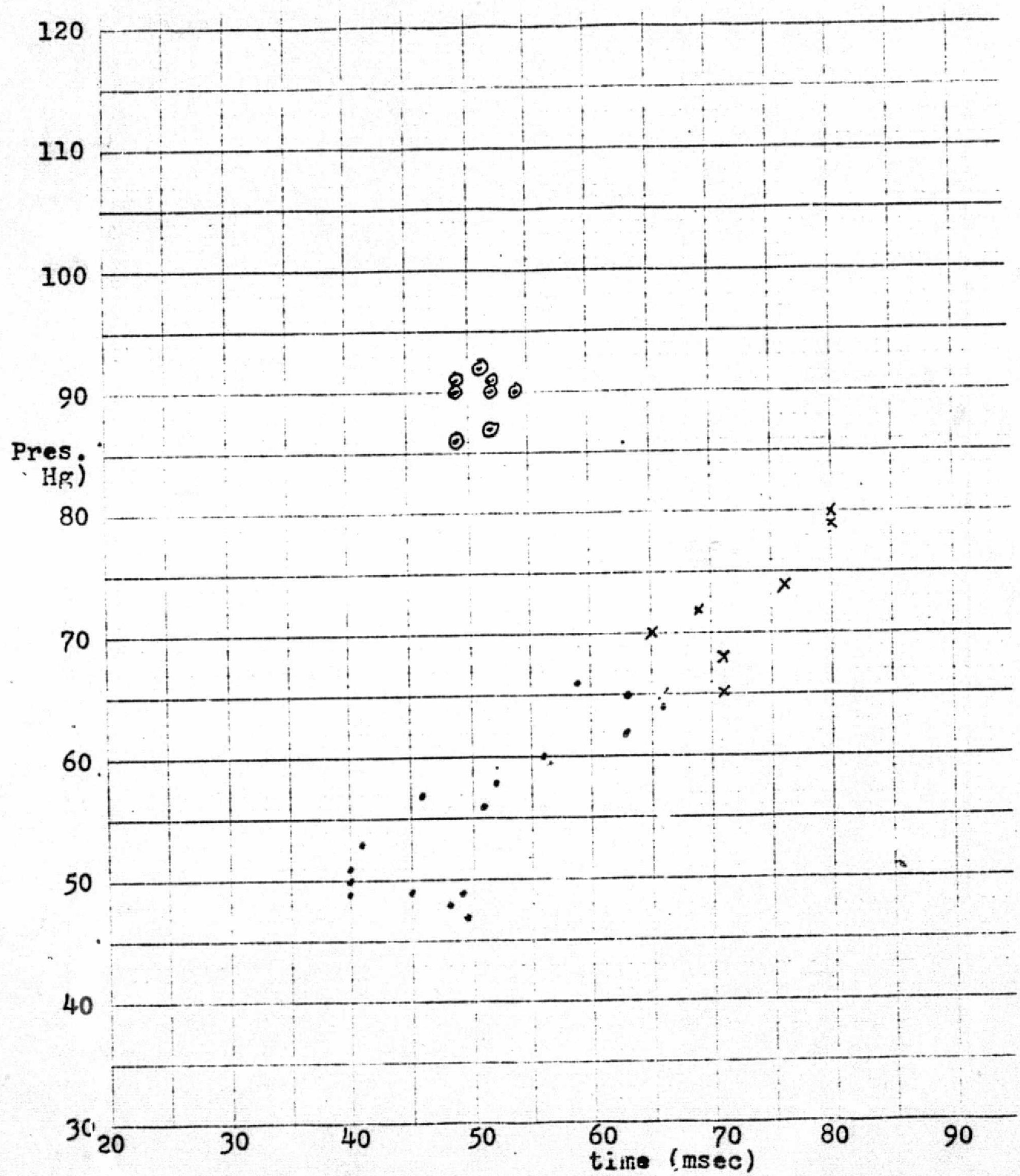

Fig. 13 Δt_4 plotted against pressure
Data taken from Experiment 2

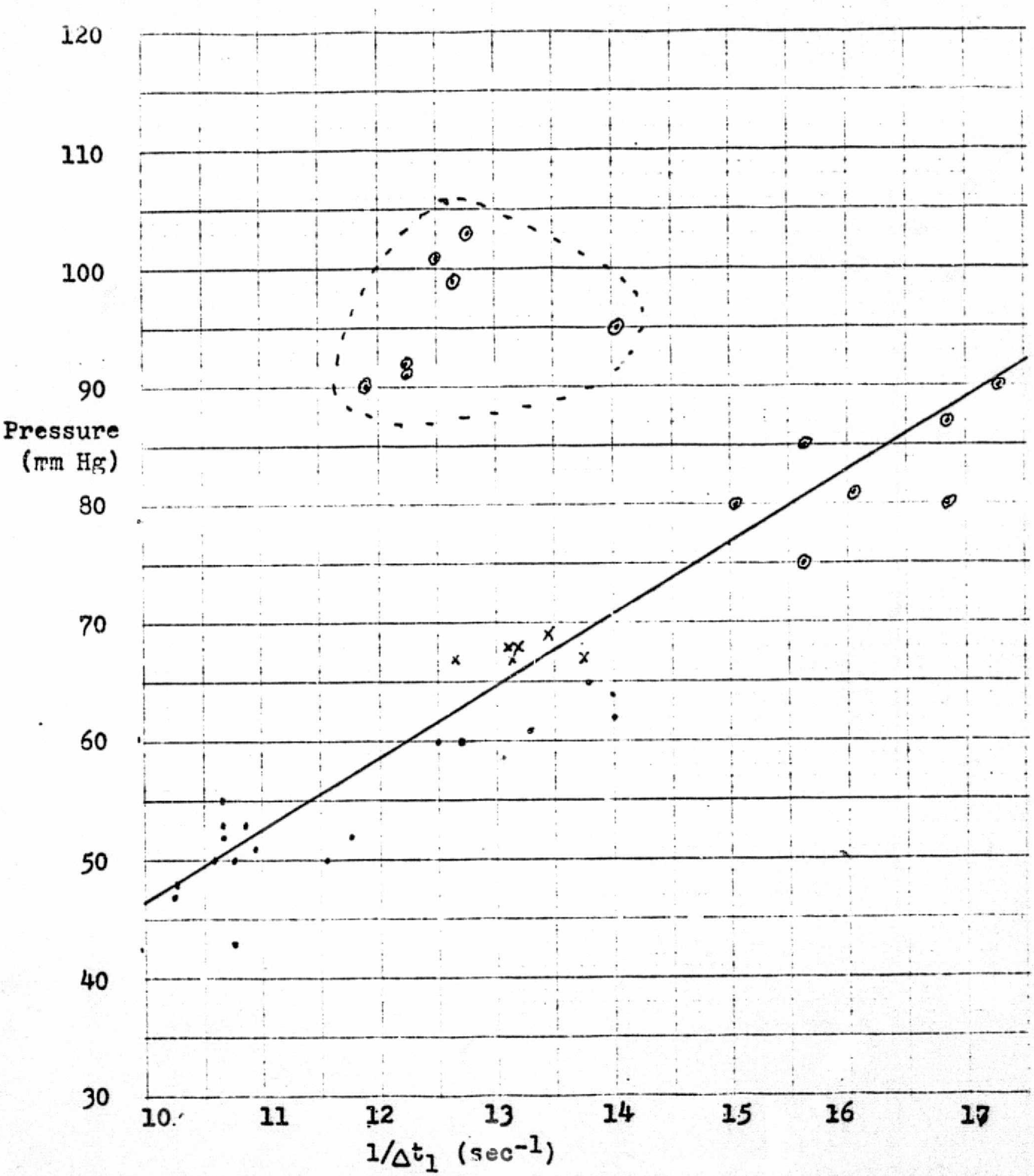

Fig. 14 $1/\Delta t_1$ plotted against pressure
Data taken from Experiment 3
Best-fit line: $P = 5.90(1/\Delta t_1) - 12.29$; $s = 3.45$
(Best-fit line does not include circled points)

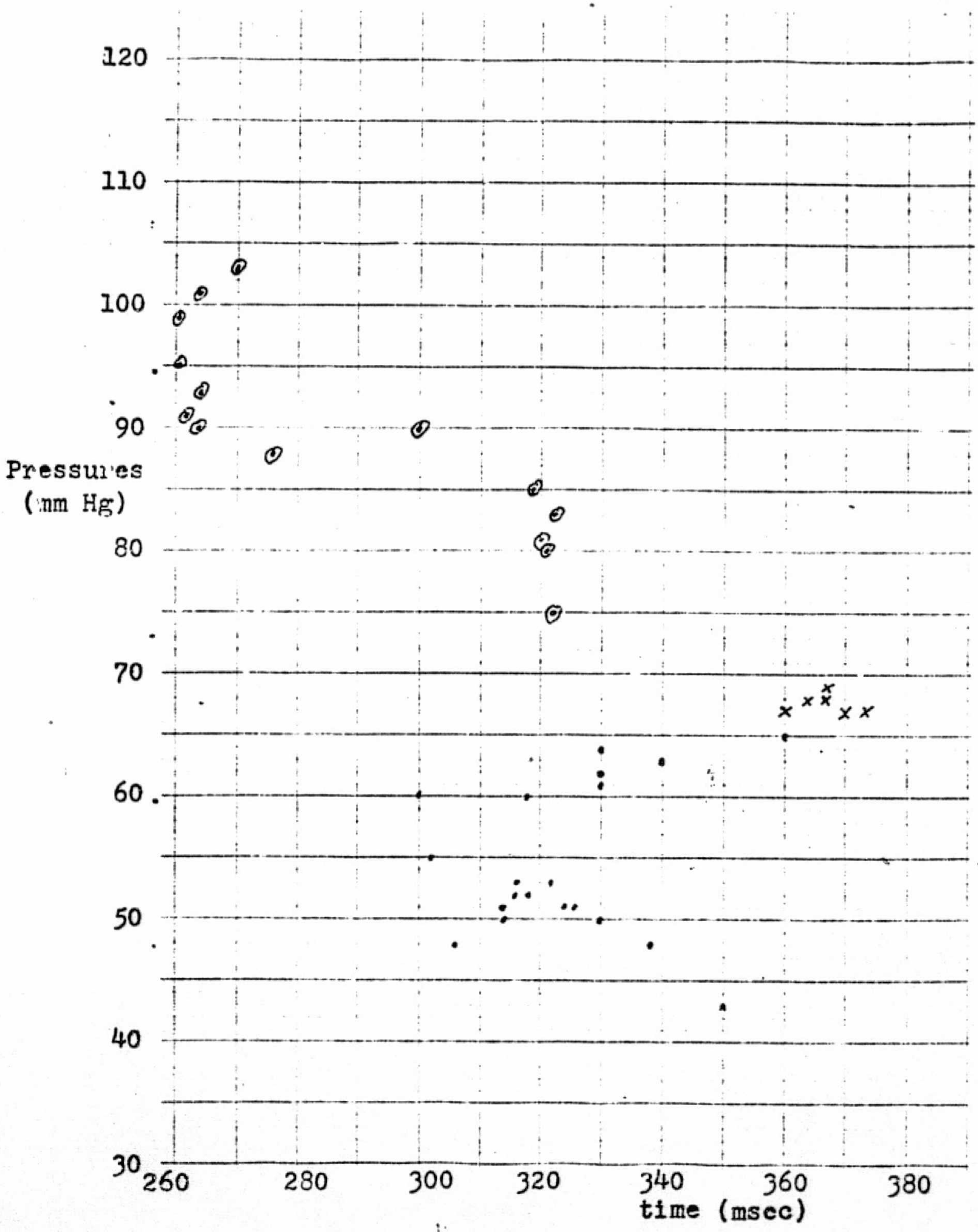

Fig. 15 Δt_2 plotted against pressure
Data taken from Experiment 3

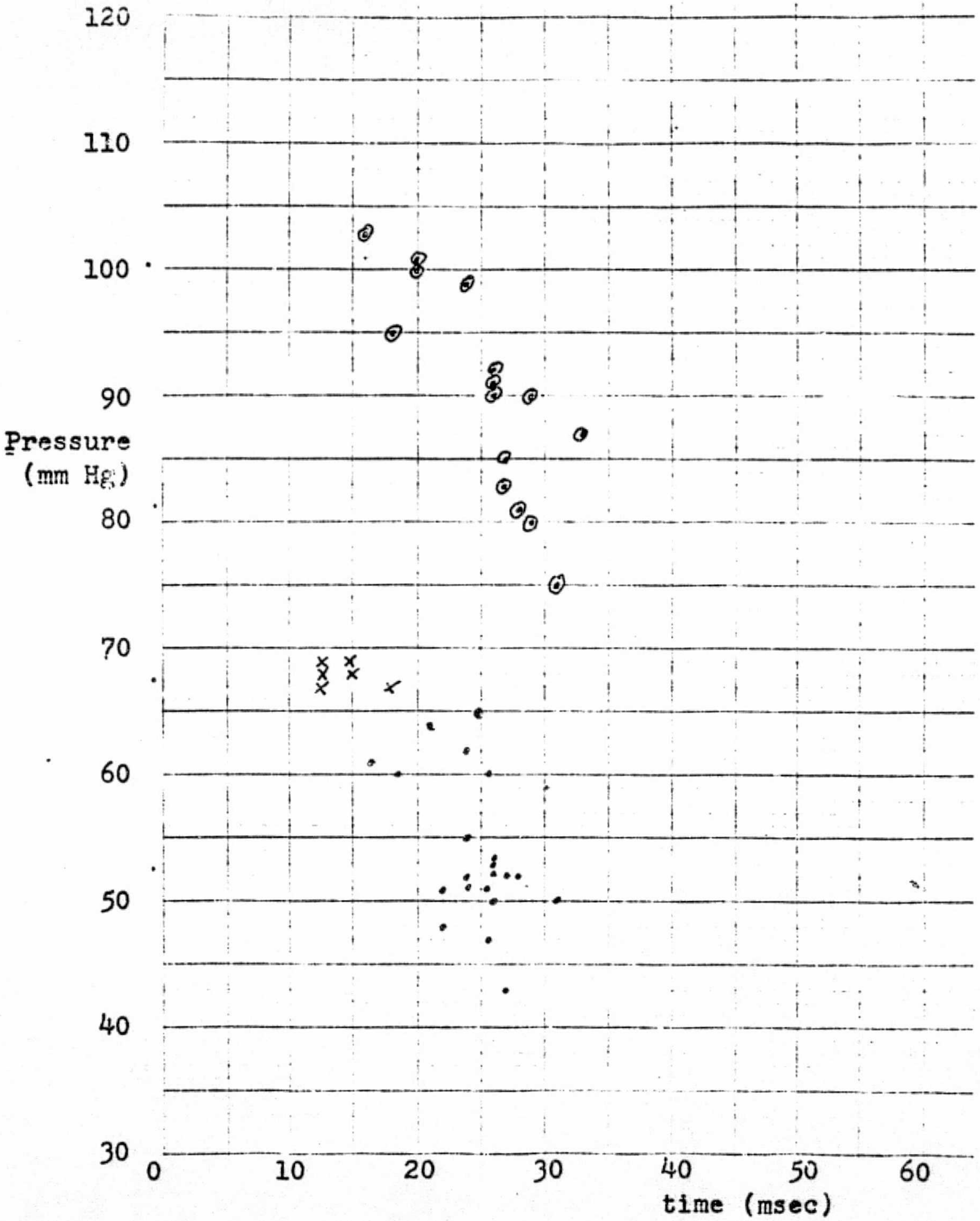

Fig. 16 Δt_3 plotted against pressure
Data taken from Experiment 3

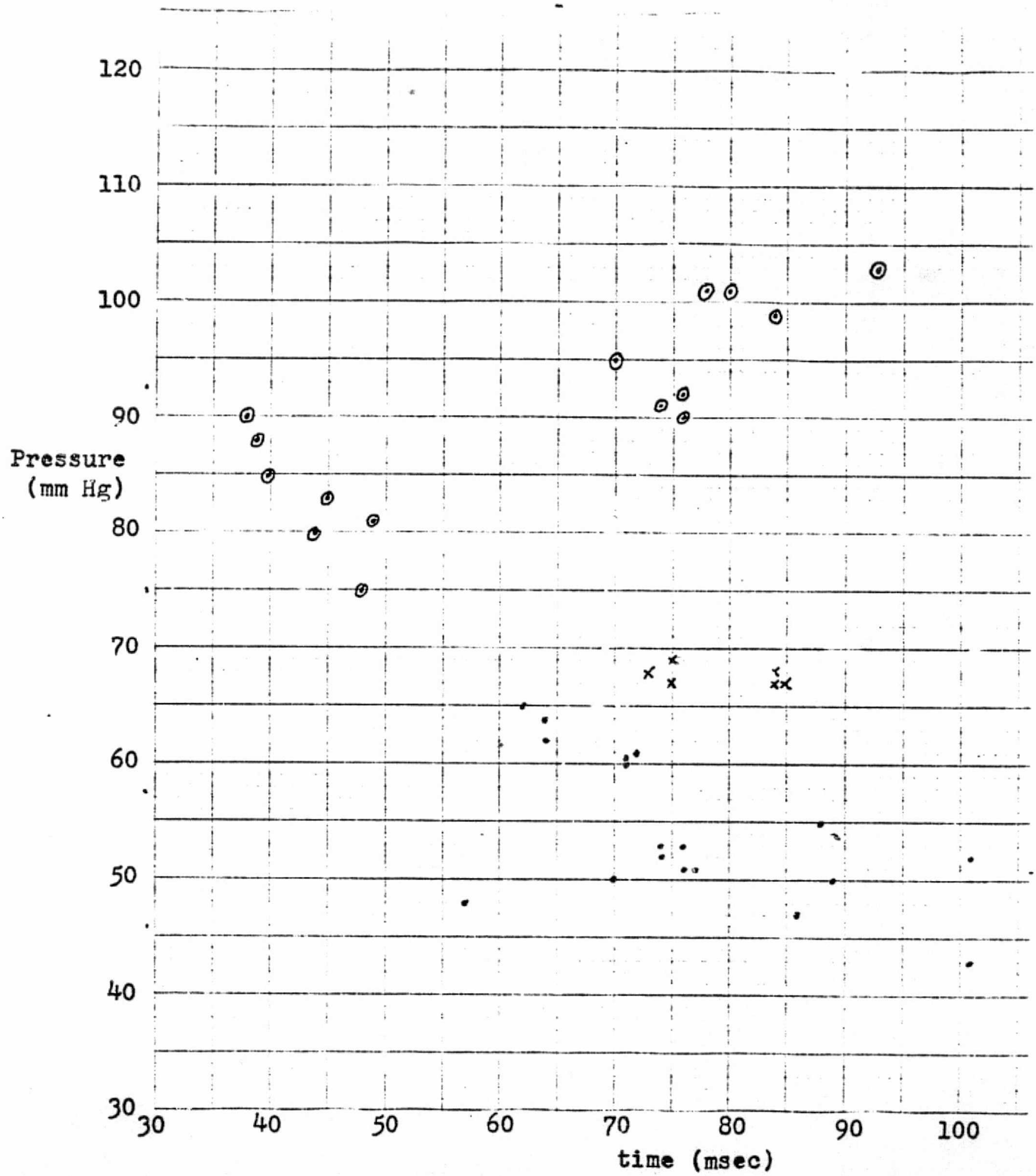

Fig. 17 Δt_4 plotted against pressure
Data taken from Experiment 3

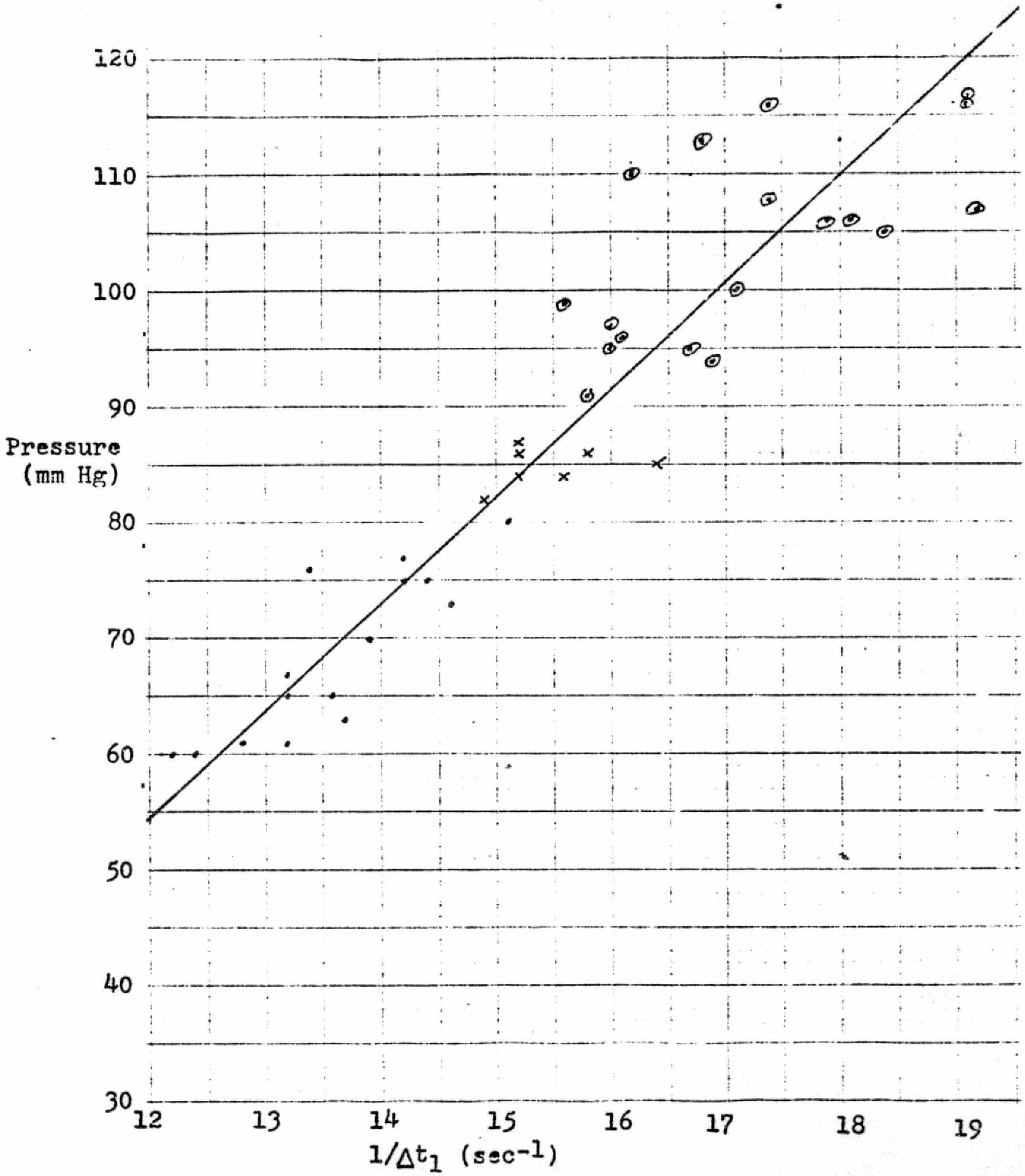

Fig. 18 $1/\Delta t_1$ plotted against pressure
Data taken from Experiment 4
Best-fit line : $P = 9.81(1/\Delta t_1) - 63.5$; $s = 6.62$

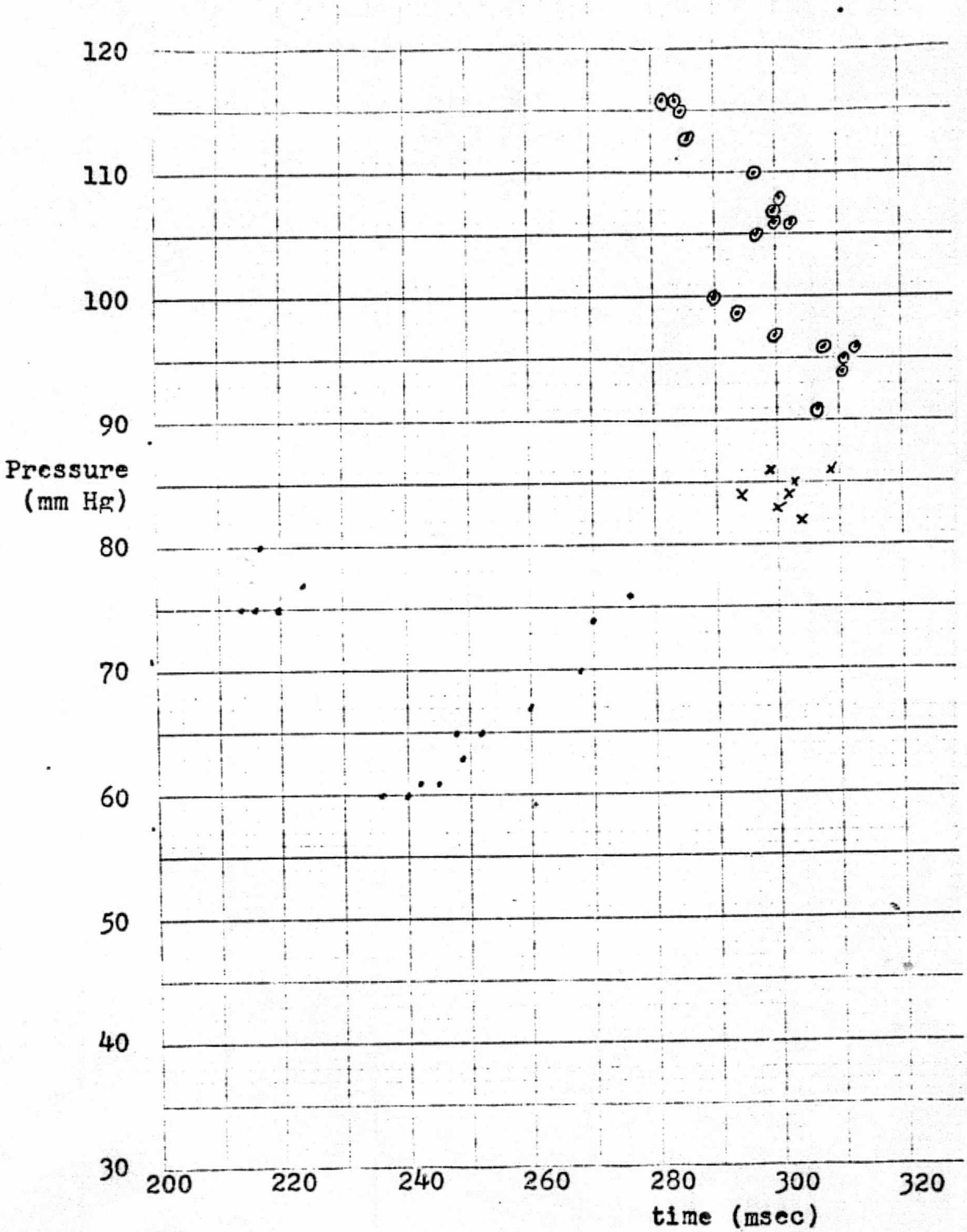

Fig. 19 Δt_2 plotted against pressure
Data taken from Experiment 4

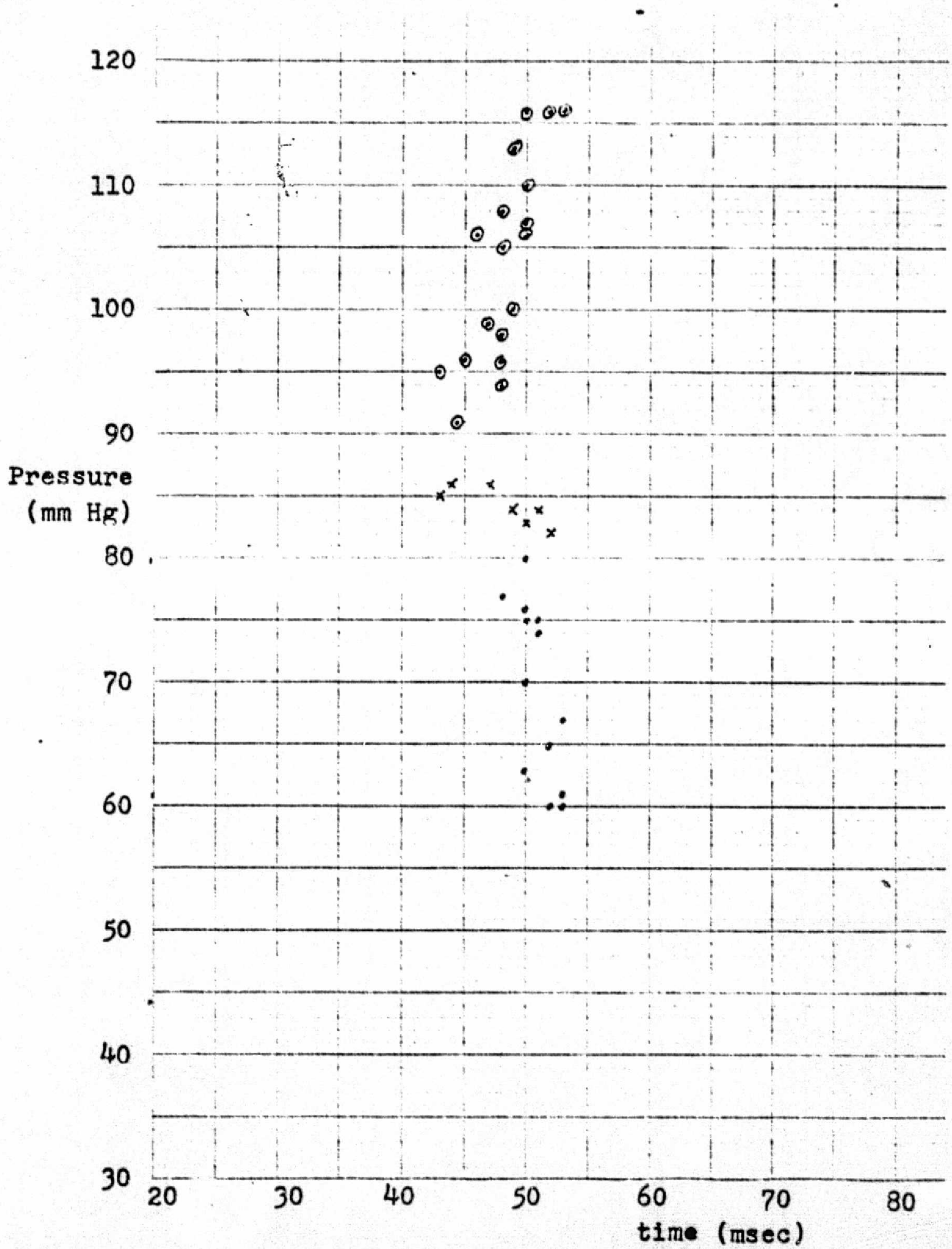

Fig. 20 Δt_3 plotted against pressure
Data taken from Experiment 4

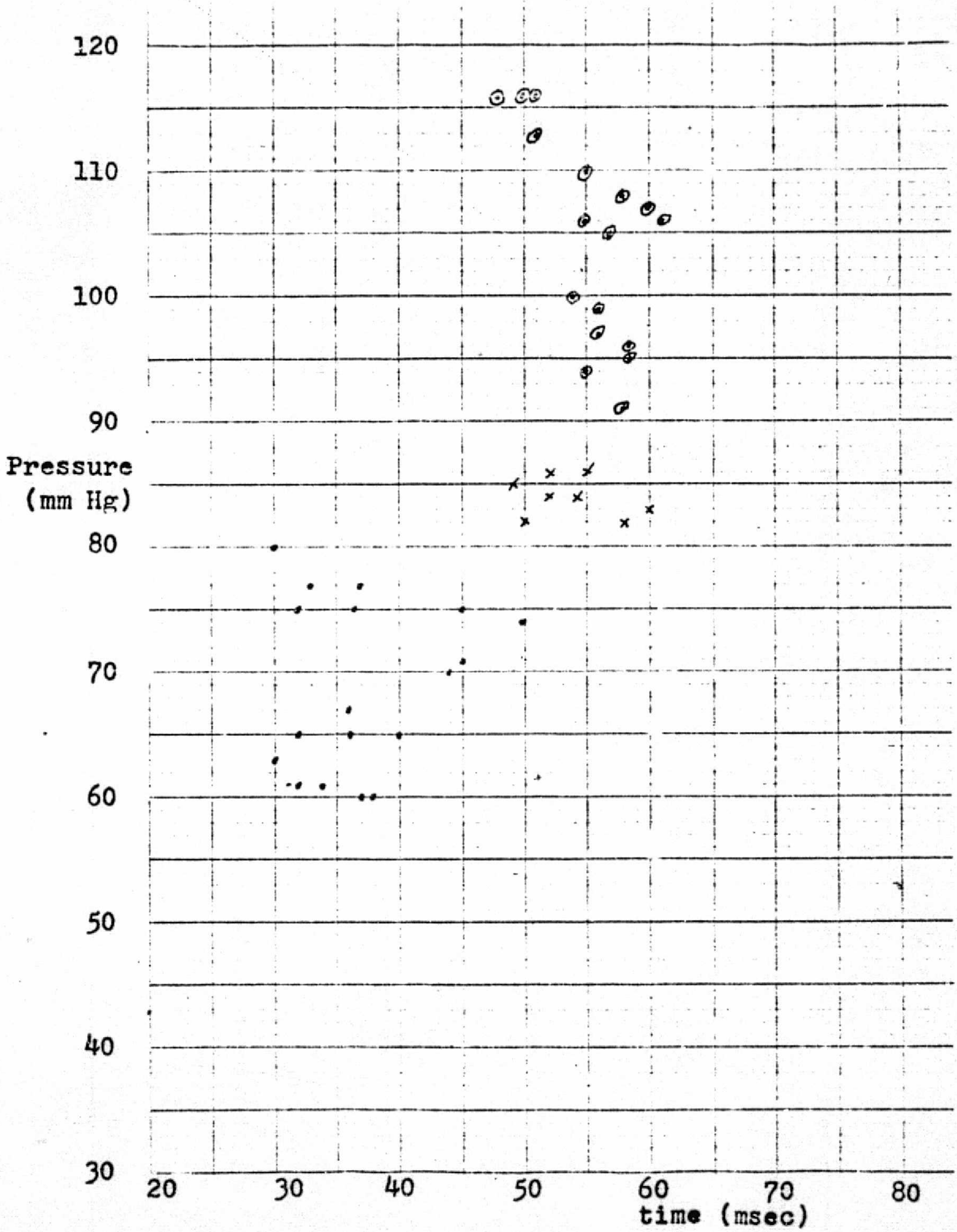

Fig. 21 Δt_4 plotted against pressure
Data taken from Experiment 4

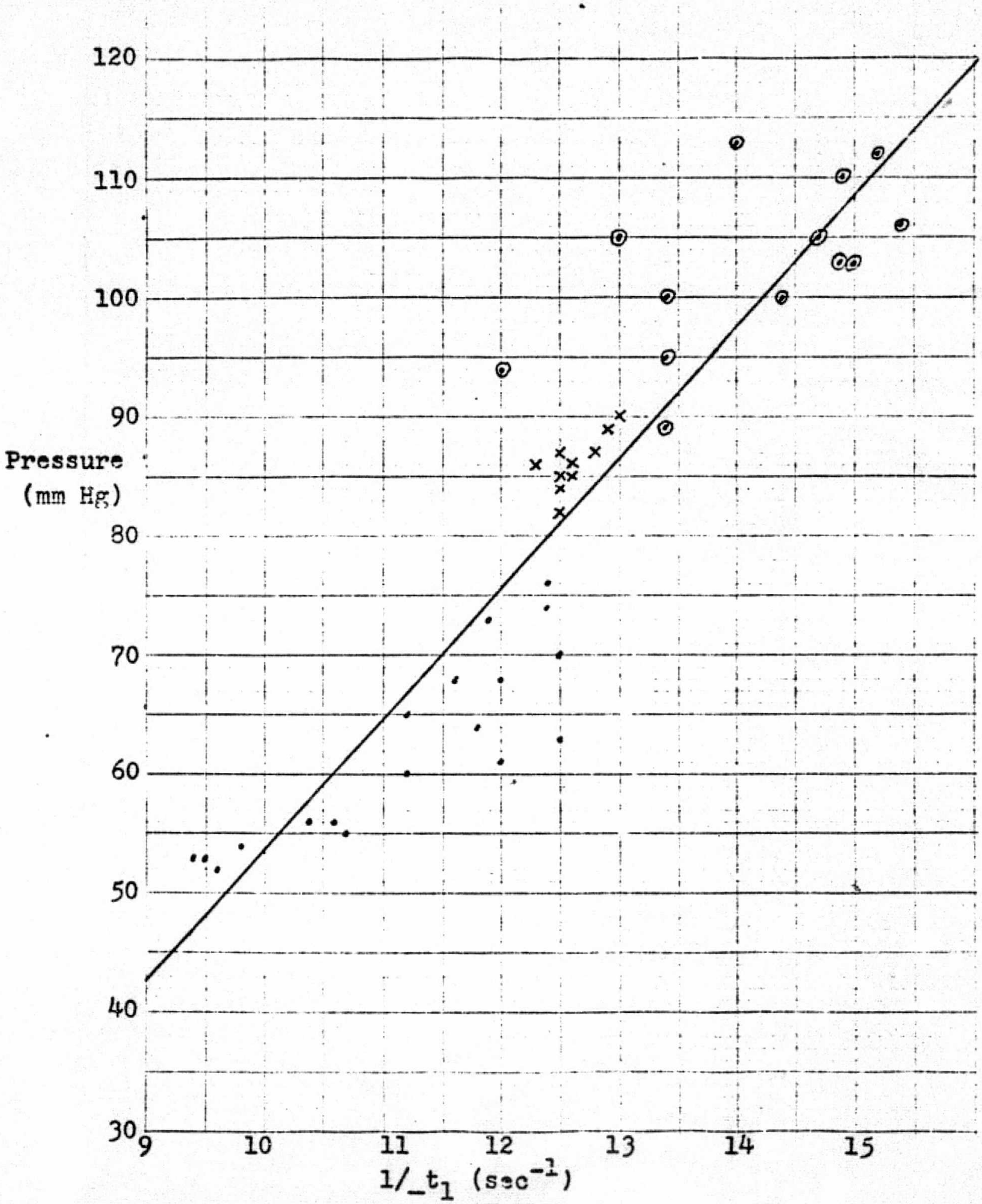

Fig. 22 $1/\Delta t_1$ plotted against pressure
Data taken from Experiment 5
Best-fit line: $P = 10.94(1/\_t_1) - 56.1$; $s = 7.20$

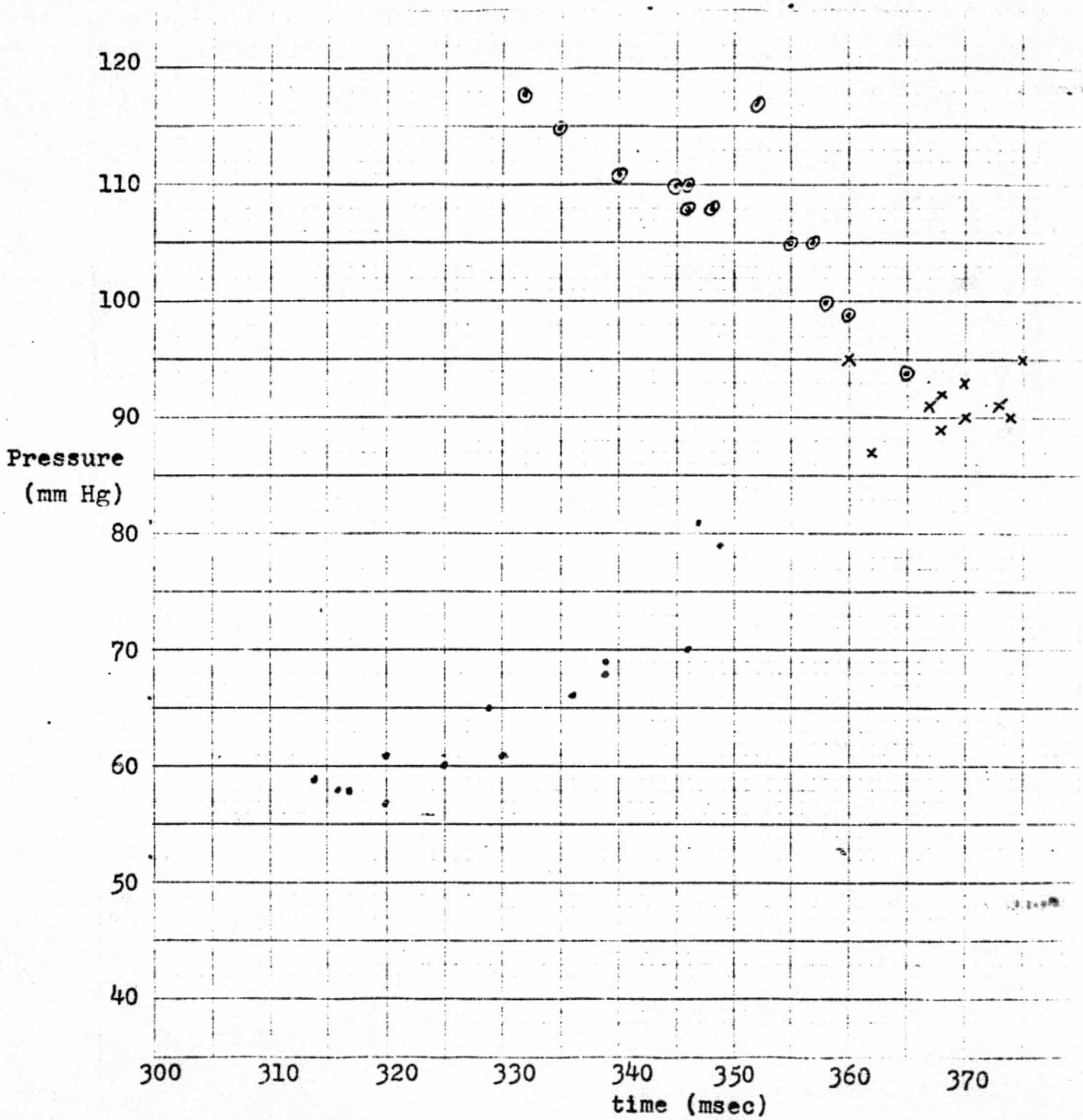

Fig. 23 Δt_2 plotted against pressure
Data taken from Experiment 5

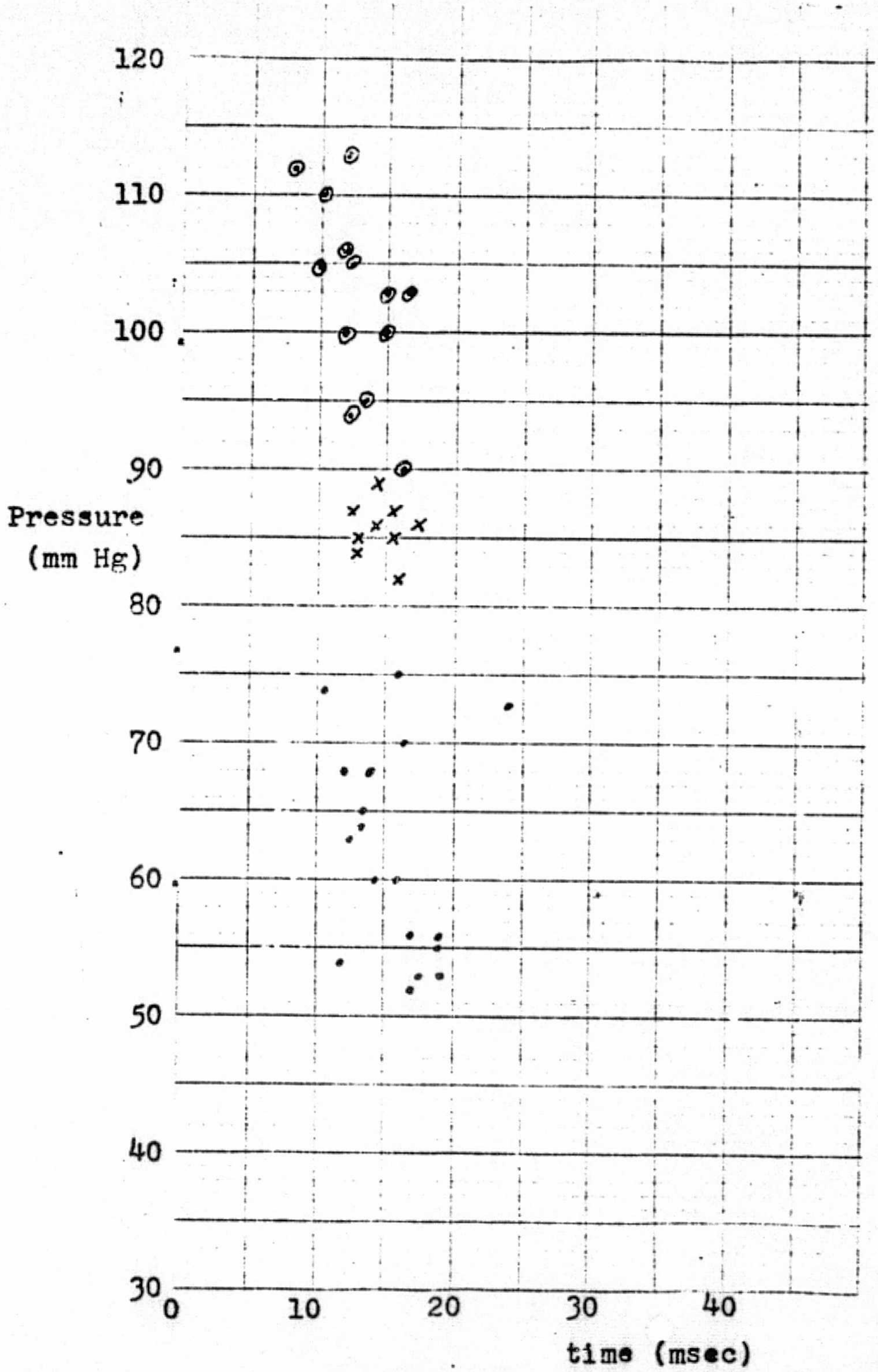

Fig. 24 Δt_3 plotted against pressure
Data taken from Experiment 5

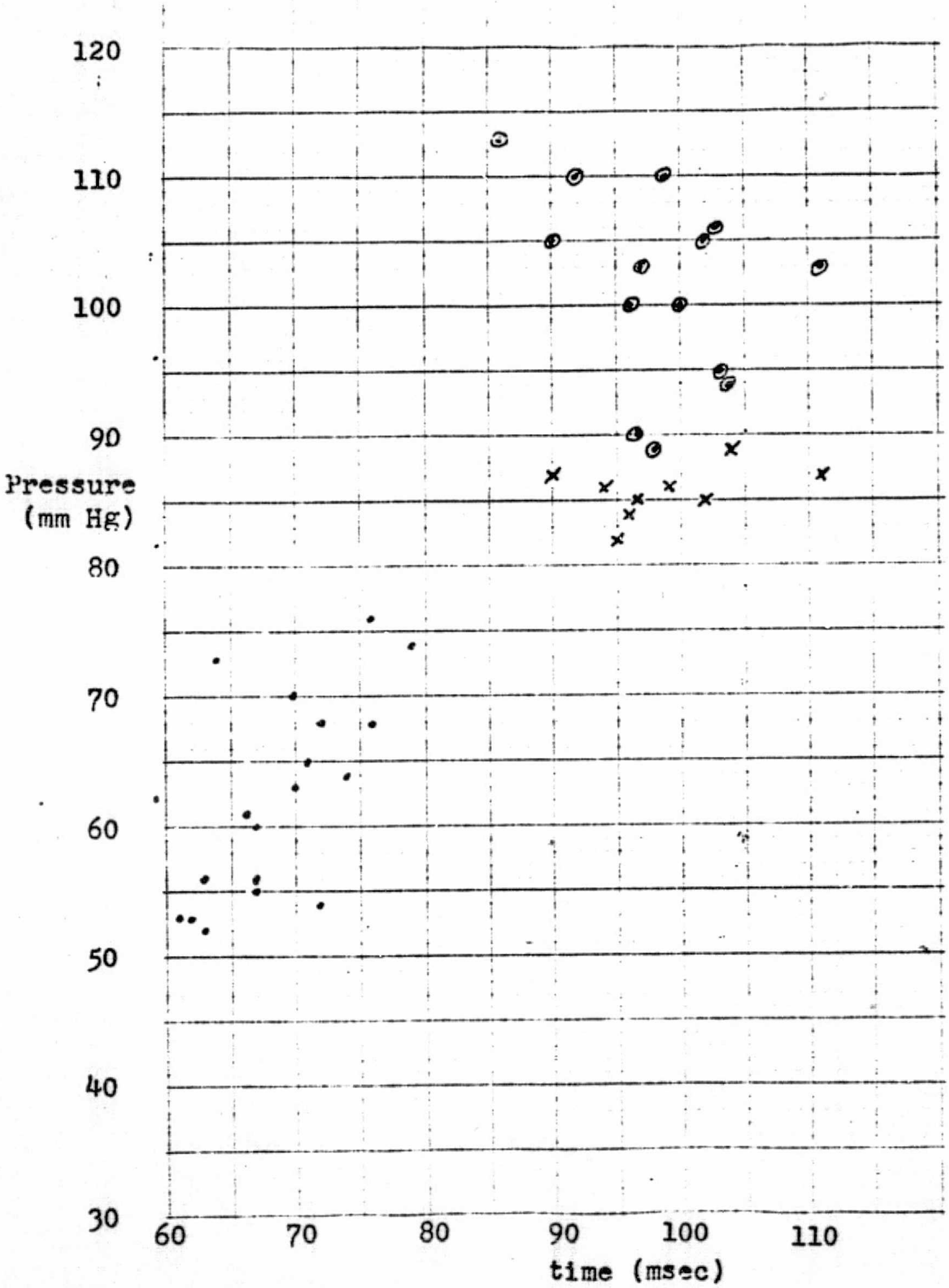

Fig. 25 Δt_4 plotted against pressure
Data taken from Experiment 5

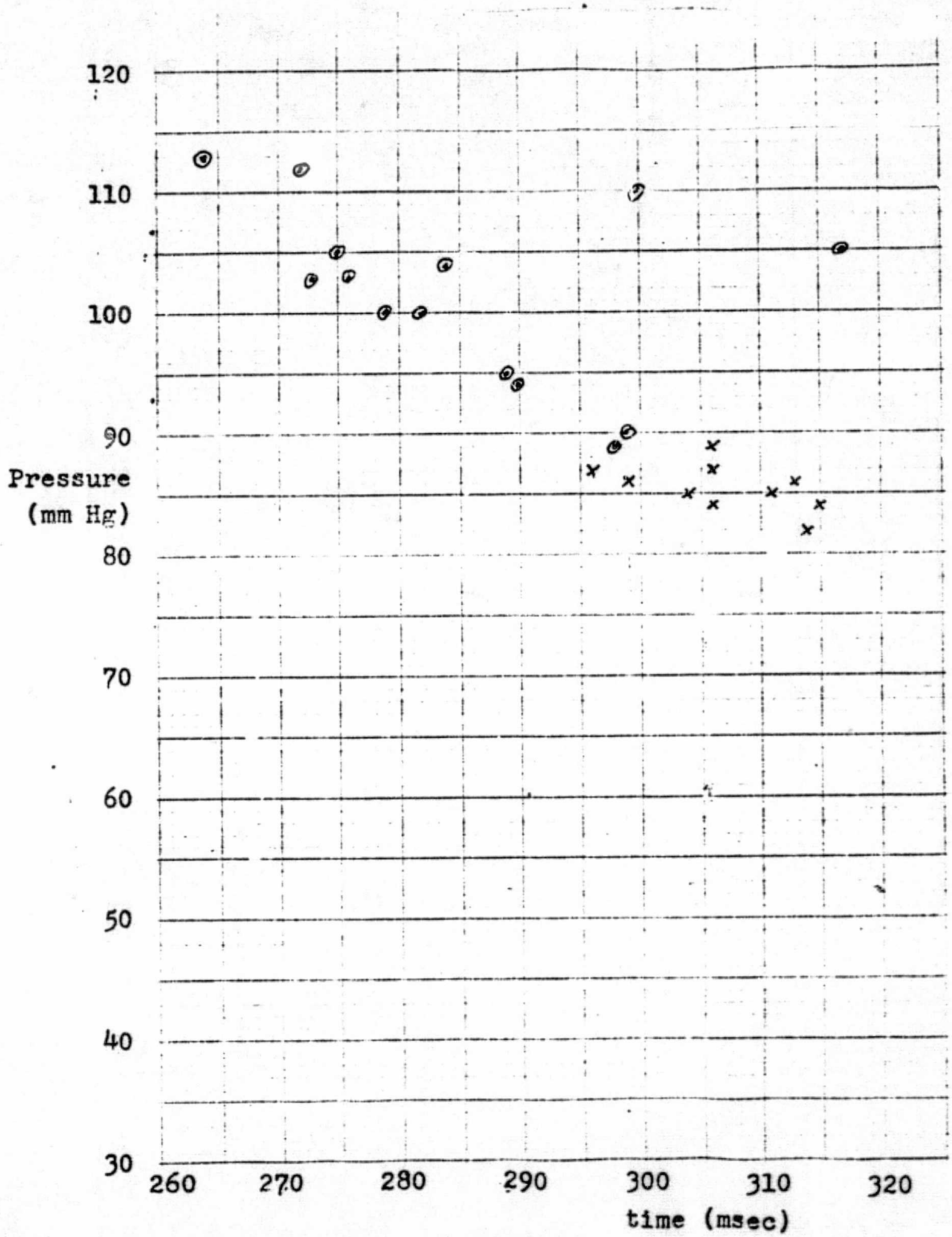

Fig. 26 Δt_5 plotted against pressure
Data taken from Experiment 5

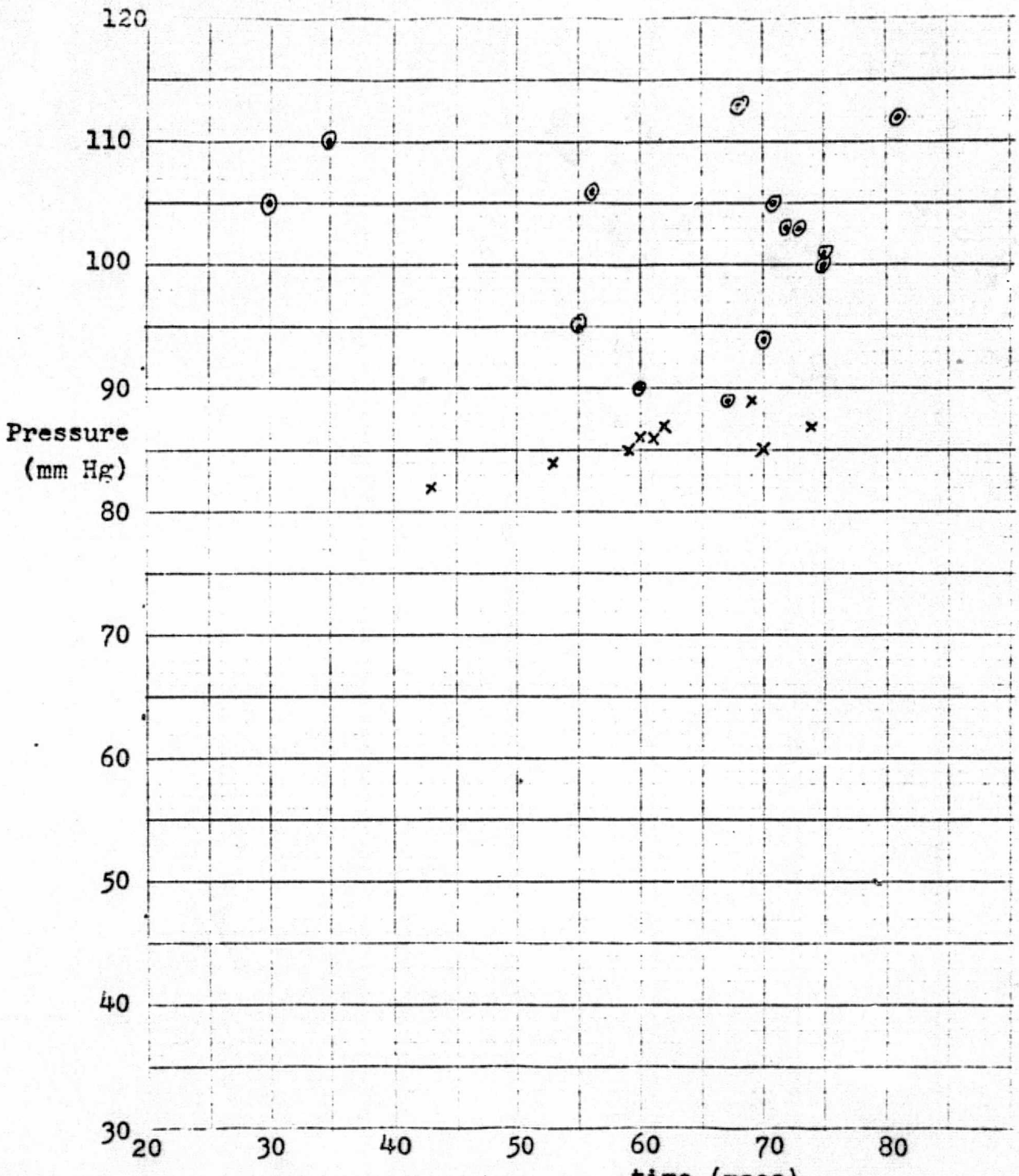

Fig. 27 $(t_2 - t_5)$ plotted against pressu:e
Data taken from Experiment 5

as the inverse of the time delay between one arterial pulse and the ejection of blood from the heart, as signaled by an easily obtained physiological signal. To this end, the femoral pulse-second heart sound time delay was measured, as it was thought that the second heart sound would predict ejection. The inverse of this time was plotted against pressure. By comparison with Δt_1, no comparable linear relationship was observed.

To understand why the second heart sound - femoral arterial pulse delay did not work, a knowledge of the sequence of events prior to and during ejection of blood from the left ventricle is required. Briefly, the first event is the electrical depolarization of the ventricle. This is marked by the QRS complex in the ECG. After this, the ventricle starts to contract. When pressure in the ventricle rises above the pressure in the atrium, the AV valve closes. This is signaled by the first heart sound. The ventricle continues to contract; no blood is ejected, as the aortic valve is closed. When ventricular pressure rises above aortic pressure, the aortic valve opens, and blood is ejected. Ejection continues until ventricular pressure falls below aortic pressure (due to the halt of contraction), at which point the aortic valve closes, causing the second heart sound. Closure of the aortic valve is also marked by the dicrotic notch in the blood pulse wave.

The event that would be of use in measuring blood pressure via the inverse of transmission time method is the beginning of ejection of blood from the ventricle. The time difference between ejection of blood and the onset of a blood pulse would clearly be the inverse of velocity. Unfortunately, there is no physiological signal marking the opening of the aortic valve. However, if there is a constant time interval between aortic valve opening and some other event, then that second event can signal ejection of blood from the heart.

In order to explore the various time relationships between the several events, a group of time differences was defined, as shown in Fig. 4f.

Δt_2 is the time difference between first and second heart sounds. This represents the time between the closing of the AV valve, and the closing of the aortic valve. As such, it consists of two components; isovolumetric contraction, and ejection of blood from the heart.

Δt_3 is the difference between a fixed point in the QRS complex, and the first heart sound. It denotes the electromechanical delay between electrical depolarization of the heart and onset of ventricular pressure.

Δt_4 is defined as the time difference between the first heart sound and the onset of the carotid pulse. As such, it gives a rough indication of isometric contraction time. (Exactly, it represents isometric contraction time and transmission time between the heart and the carotid artery. However, the entire aortic transmission time, as defined by _t_1, is on the order of 80 msec, with a total range of $\pm$ 20 msec. The distance between the heart and the carotid artery is about 1/5 the carotid - femoral distance, thus the delay due to the carotid is about 15-20 msec, with a total variance of only $\pm$ 5 msec. Thus the error introduced by transmission through the carotid artery is small.)

Δt_5 is defined as the time between carotid onset and occurence of the dicrotic notch (for location of dicrotic notch, see Fig. 4e.). This represents the total time of ejection of blood from the heart. Unfortunatoly, the dicrotic notch was not visible when the subjects were under the influence of Amyl Nitrite. If one subtracts Δt_5 from Δt_2, the difference is equal to isometric contraction time.

Graphs of Δt_3 versus pressure were made for all subjects, and are whown in Figs. 9, 12, 16, 20, 24. Graphs of both Δt_2 and Δt_4 were made for all experiments except the first, where poor quality of the heart sounds prevented accurate analysis. These are shown in Figs. 11, 15, 19, 23, and Figs 13, 17, 21, 25. Δt_5 for the last experiment is shown in Fig. 26, and $\_t_2$-$\_t_5$ is shown in Fig. 27.

As seen in the graphs of Δt_3, the electromechanical delay was relatively constant, with a range of usually no more than 20 msec.

The graphs of Δt_2 show a wide range of time differences. The span of delays is on the order of 80 msec, which is comparable to the total transmission time in the aorta.

As seen in the graphs of Δt_4, the isometric contraction period also posesses a wide variability in measured times; on the order of 40 msec.

(Both Δt_2 and Δt_4 show a similar elbow shape. This is thought to be due to an interaction of two factors. Increased pressure is accompanied by an increase in volume, therefore, contraction takes longer. In opposition to this, increased pressure leads to increased contractility, which causes quicker contraction time. This increase in contractility is non linear, and increases most rapidly in a middle range of pressures. Thus at low pressures, the first effect is dominant, and the time delays increase with increasing pressure. At higher pressures, the contractility increases, and the time delays decrease with an increase in pressure.

The one graph of Δt_5 (Fig. 26), shows a clear decrease of time delay with an increase of pressure. The graph of $\Delta t_2 - \Delta t_5$ shows an increase of delay with increasing pressure. However, the rise is not too clear cut.

Analysis of the above shows why the second heart sound cannot be used. The time difference between opening of the aortic valve and its closing is not constant. This is shown both by the single graph of Δt_5, and by noting that the spread of values in Δt_2 is only partly accounted for by the spread of values in Δt_4. Thus there is a clear variability in ejection time.

Although there is a fairly constant delay between ECG and closing of the AV valve, the spread of values in isometric contraction period make the QRS complex useless as a predictor of ejection of blood from the heart. This finding agrees with the findings of LaBresh (1970).

IV. Discussion

It has been shown that diastolic blood pressure is closely related to arterial pulse wave velocity in normal male subjects. The relationship holds over a range of pressure of about 50 mm Hg. It has also been shown that neither QRS, first heart sound, nor second heart sound is a useful estimator for ejection of blood into the aorta.

The sample deviations for the lines drawn showing the almost linear relationship between pulse wave velocity and diastolic blood pressure are 7.67, 7.2, 6.62, 4.9, and 3.45. This implies that a pressure measuring device utilizing this relationship would, in the worst case, read within ± 15.3 mm Hg 99% of the time, and within ± 7.67 mm Hg 67% of the time. In the best case, the device would read within ± 6.9 mm Hg 99% of the time, and read within ± 3.45 mm Hg 67% of the time.

It is possible that the best fit for the data is a curved line of some sort; perhaps an "s" shape. If true, then much better accuracy could be obtained.

The inaccuracies inherent in processing the data should be mentioned. It is unclear as to whether the criteria of defining onsets as being the first point posessing a slope of -1 is justified. While this criteria supplies consistant onsets for identical waveforms, it is probably not totally accurate for differing waveforms. It is possible that a large per cent of the error is due to inaccurate definition of onsets. It has been suggested that onsets be defined as the first point before the pulse that has a slope of 0. However, some waveforms show a large length of gently sloping points prior to the pulse. I doubt if the second criteria would be accurate in these cases.

As it has been shown that velocity is a good predictor of diastolic blood pressure, the groundwork for a device to measure blood pressure non-invasively in ambulatory patients is partly done. The device would consist of two transducers to detect the arrival of pulses, and suitable electronics to detect the onsets and compute the inverse of transmission time.

Every person should have a unique linear relationship between diastolic blood pressure and pulse wave velocity. The slope and intercept of this relationship would probably stay constant over a long span of time, as it is a function of arterial length and condition.

With the above fact, the use of the device would be simple. After determination of a person's unique relationship(This could most easily be done by measuring transmission times at two different pressures. These two points would define the equation of the line relating the inverse of transmission time (velocity) to diastolic blood pressure for that patient.) the device would be attached to the patient. The record of transmission times would specify diastolic blood pressure.

With this scheme in mind, there are two channels still open for investigation.

1. The development of a suitable ambulatory transducer to easily detect arterial blood pulses.

2. A continuation of my study to see if the pressure/velocity relationship holds over a wider range of both pressure and patient condition. Specifically, people with diseases of the arteries,

those most likely to use such a device, may not exhibit the usual relationship. This may be due to a tortuosity of the vessels (Sands (1924)).

Appendix A

Derivation of the Kortweig Equation (Hardung (1962))

Consider a visco - elastic tube, radius r, cross - sectional area Q, width a (fig. 1) When a pulse passes through the tube, the radius changes, as does the area:

$$r = r(z,t)$$
$$Q = Q(z,t)$$

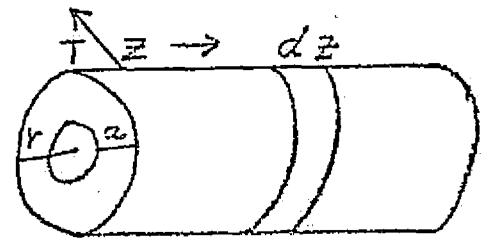

Consider a small element of volume, a small disk of thickness dz. If P is the pressure in the tube, the force on the disk is:

$$dF_z = -(QP)_{z+dz} + (QP)_z = -(\partial(QP)/\partial z)dz \qquad 1$$

$$dF_z = -Q(\partial P/\partial z)dz - P(\partial Q/\partial z)dz \qquad 1a$$

Since lateral extension is assumed to be small compared to r, dQ/Q and dQ/dz are small:

$$dF_z = -Q(\partial P/\partial z)dz \qquad 1b$$

The mass of the disk dm = wQdz (w= density). As F= ma:

$$w(\partial^2 z/\partial t^2) = -(\partial P/\partial z) \qquad 2$$

Flow volume is defined as $i_z = q(dz/dt)$:

$$i_z/t = -(Q/w)(\partial P/\partial z) \qquad 3$$

From continuity, the intake volume minus the output volume equals the increase of volume of the disk:

Define radial current i_r

$$di_z(z,t) = (\partial i_z/\partial z)dz = -i_r \qquad 4$$

$$i_r = (dr/dt)2\pi rdz \qquad 5$$

From Hooke's Law:

$$2\pi dr/2\pi r = (1/Eadz)d(T)dz \qquad 6$$

From Laplace's Law for a cylinder T = Pr, where P = pressure

$$2\pi dr/2\pi r = (1/Eadz)d(Pr)dz \qquad 6a$$

$$dr/r = (1/Ea)(Pdr + rdP)$$

As lateral extension is assumed to be small compared to r,

$Pdr \ll rdP$

$$dP = (Ea/r^2)dr \qquad 6c$$

Differentiate equation 6c, with respect to t, and combing equations 4 and 5

$$-(\partial P/\partial t) = (Ea/2\pi r^3)(\partial i_z/\partial z) \qquad 7$$

Differentiate equation 7 with respect to z

$$-\partial^2 P/\partial z\partial t = \frac{1}{2\pi}\left(\frac{\partial^2 i_z}{\partial z^2} \cdot \frac{Ea}{r^3} + \frac{\partial i_z}{\partial z} \cdot Ea\frac{\partial r^3}{\partial z}\right) \qquad 7a$$

Since r/z is small:

$$-(\partial^2 P/\partial t\partial z) = \left(\frac{Ea}{2\pi r^3}\right)(\partial^2 i_z/\partial z^2)$$

Differentiate equation 3 with respect to z twice:

$$\partial^3 i_z/\partial t\partial z^2 = -(Q/w)(\partial^3 P/\partial z^3) \qquad 8$$

Differentiate equation 7b with respect to z:

$$-(\partial^3 P/\partial t\partial z^2) = (Ea/2\pi r3)(\partial^3 i_z/\partial^3 z) \qquad 9$$

Combine equations 8 and 9

$$(Q/w)(\partial^2 P/\partial z^2) = (2\pi r/Ea)(\partial^2 P/\partial t^2) \qquad 10$$

$$\partial^2 P/\partial t^2 = (Ea/2rw)(\partial^2 P/\partial z^2) \qquad 10a$$

Equation 10a is the characteristic wave equation, which defines

$$V = (Ea/2rw)^{\frac{1}{2}} \qquad 11$$

Equation 11 is the Kortweig equation.

Appendix B

Derivation of Bramwell - Hill Equation (La Bresh (1970))

Define a length of elastic tube of thichness a, radius r, and length dz, with an applied tension per unit length T (Fig 1a). Unroll the tube to define a sheet of height a, width dz, length 1=2 r and cross - sectional area adz. The tension is as shown in Fig. 1b

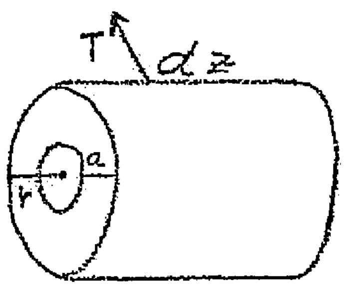

Fig. 1a

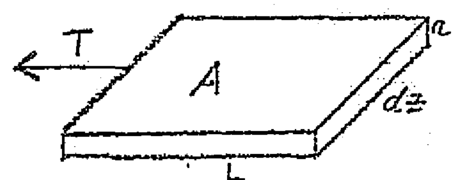

Fig. 1b

The Kortweig equation is:

$$v = (Ea/2wr)^{\frac{1}{2}} \qquad 1$$

Apply Hook's law to the sheet:

$$dl/l = (1/Ea)dTdz \qquad 2$$

As A = adz and l = 2 r:

$$dr/r = (1/Eadz)dTdz = dt/Ea \qquad 2a$$

Laplace's Law for a cylinder states Pr =T; P = pressure;

$$dr/r = (1/Ea)d(pr) = (1/Ea)\ (rdP + Pdr) \qquad 2b$$

Since the amount the wall is extended laterally is assumed to be small, Pdr rdP:

$$dr/r = (1/Ea)(rdP) \qquad 2c$$

$$dP = (Ea/r^2)dr \qquad 2d$$

Introduce volume per unit length:

$$V = \pi r^2 \qquad 3$$

$$\partial v/\partial r = 2\pi r \qquad 3a$$

$$dV/dP = \left(\partial V/\partial R\right)\left(\partial R/\partial P\right) \qquad 4$$

Combine equations 2c, 3a, and 4:

$$dV/dP = 2\pi r(r^2/Ea) = 2\pi r^3/Ea \qquad 5$$

Combine equations 3 and 5:

$$dV/dP = 2Vr/Ea \qquad 6$$

Combine equations 1 and 6:

$$v = (V/wdV/dP))^{\frac{1}{2}} \qquad 7a$$

As w = 1.055:

$$v = 3.57(V/(dV/dP))^{\frac{1}{2}} \qquad 7b$$

$$v = 3.57(dP/(dV/V))^{\frac{1}{2}} \qquad 7c$$

Where:

v = velocity in meters per second

P = pressure in mm Hg

V = Volume in ml

Appendix C

Tables of Experimental Data

The following data were used to construct the curves in Figures 8 through 27. This data includes: 1) P - brachial arterial blood pressure; 2) Δt_1 - the time difference between carotid pulse onset and femoral pulse onset; 3) Δt_2 - the time difference between the first and second heart sounds; 4) Δt_3 - the time difference between ECG and first heart sound; 5) Δt_4 - the time difference between first heart sound and carotid onset; and 6) Δt_5 - the time difference between carotid onset and dicrotic notch.

Induced changes in blood pressure are noted in the final column. Normal indicates no induced change, Amyl Nitrite indicates inhalation of Amyl Nitrite, and Isometric indicates isometric contraction of one arm.

Table I
Transmission Times and Brachial Arterial Blood Pressures from Experiment I

P	Δt_1	Δt_3	Conditions
67	80.0	97.6	Normal
65	82.4	95.2	Normal
66	80.8	84.8	Normal
67	82.4	91.2	Normal
69	80.0	91.2	Normal
69	78.4	89.6	Normal
68	76.8	80.0	Normal
59	74.4	104.0	Amyl Nitrite
51	80.0	93.6	Amyl Nitrite
51	84.0	89.6	Amyl Nitrite
50	94.4	84.0	Amyl Nitrite
50	96.8	80.0	Amyl Nitrite
49	98.4	87.2	Amyl Nitrite
48	93.6	84.0	Amyl Nitrite
46	92.0	83.2	Amyl Nitrite
45	96.0	83.2	Amyl Nitrite
44	95.3	86.4	Amyl Nitrite
43	98.0	80.0	Amyl Nitrite
43	98.0	88.8	Amyl Nitrite
41	98.0	90.0	Amyl Nitrite
40	99.6	89.6	Amyl Nitrite
40	100.4	90.0	Amyl Nitrite
40	96.8	80.0	Amyl Nitrite
40	96.8	90.0	Amyl Nitrite
42	99.6	76.8	Amyl Nitrite
55	84.8	89.6	Amyl Nitrite
64	76.0	90.8	Normal
63	75.2	89.6	Normal
62	77.8	84.0	Normal
78	72.0	88.8	Isometric
79	69.6	95.2	Isometric
79	68.0	84.0	Isometric
80	76.0	88.8	Isometric
81	66.4	76.0	Isometric
80	69.6	95.2	Isometric
80	68.0	84.0	Isometric
82	71.2	91.2	Isometric
83	64.8	91.2	Isometric
85	68.0	87.2	Isometric
98	64.8	77.6	Isometric

Table II

Transmission Times and Brachial Arterial Blood Pressures from Experiment II

P	Δt_1	Δt_2	Δt_3	Δt_4	Conditions
90	62.4	259.2	28.0	49.6	Isometric
90	60.0	259.2	30.4	52.8	Isometric
91	58.4	256.0	39.2	52.0	Isometric
92	61.6	257.6	30.4	51.2	Isometric
91	61.6	262.4	30.4	49.6	Isometric
90	62.4	264.8	33.6	53.6	Isometric
90	57.6	268.0	32.0	49.6	Isometric
86	62.4	257.6	36.0	49.6	Isometric
87	64.0	260.8	24.0	52.0	Isometric
49	90.4	238.4	25.6	49.6	Amyl Nitrite
48	90.4	230.4	28.0	48.8	Amyl Nitrite
47	95.2	229.6	28.0	49.6	Amyl Nitrite
50	92.0	225.6	32.8	40.0	Amyl Nitrite
51	94.4	240.0	32.0	40.0	Amyl Nitrite
49	96.0	236.0	35.2	44.5	Amyl Nitrite
49	95.2	230.0	40.0	40.0	Amyl Nitrite
53	93.6	248.0	30.4	41.6	Amyl Nitrite
56	89.6	254.4	32.0	51.2	Amyl Nitrite
57	90.4	257.6	35.2	46.4	Amyl Nitrite
58	84.0	268.0	30.4	52.8	Amyl Nitrite
60	78.4	261.6	33.6	56.0	Amyl Nitrite
62	76.8	269.6	31.8	63.2	Amyl Nitrite
64	72.8	273.6	28.0	66.4	Amyl Nitrite
65	76.8	274.4	28.8	63.2	Amyl Nitrite
66	64.8	280.0	33.6	59.2	Amyl Nitrite
68	72.8	284.0	40.0	71.2	Normal
70	72.0	290.4	27.4	65.8	Normal
72	67.2	290.4	24.0	69.8	Normal
72	72.0	296.8	35.2	73.6	Normal
65	73.6	284.0	40.0	66.6	Normal
65	72.0	290.4	25.6	71.6	Normal
74	69.8	292.2	31.8	76.8	Normal
80	63.2	324.0	28.0	80.0	Normal
79	64.0	320.0	35.2	80.0	Normal

Table III

Transmission Times and Brachial Arterial Blood Pressures from Experiment III

P	Δt_1	Δt_2	Δt_3	Δt_4	Conditions
60	80.0	290.4	25.6	71.2	Amyl Nitrite
55	93.6	292.0	24.0	88.8	Amyl Nitrite
52	84.8	304.0	27.2	101.6	Amyl Nitrite
50	92.8	304.0	31.2	89.6	Amyl Nitrite
48	97.6	328.0	22.4	56.0	Amyl Nitrite
43	92.8	340.0	27.2	101.6	Amyl Nitrite
47	97.6	296.0	25.6	86.4	Amyl Nitrite
50	90.4	320.0	26.4	70.4	Amyl Nitrite
68	76.8	357.6	12.8	73.6	Normal
69	74.4	357.6	14.4	76.0	Normal
67	76.0	351.2	12.8	85.6	Normal
67	72.8	360.0	14.4	84.0	Normal
68	76.0	354.4	12.8	84.0	Normal
67	79.2	363.2	15.2	75.2	Normal
51	91.2	316.0	25.6	77.6	Amyl Nitrite
51	94.4	314.4	22.4	76.0	Amyl Nitrite
52	93.6	308.8	27.2	74.4	Amyl Nitrite
53	93.6	311.2	26.4	76.0	Amyl Nitrite
52	93.6	306.4	24.0	74.4	Amyl Nitrite
53	92.0	306.4	26.4	74.4	Amyl Nitrite
75	64.0	312.0	31.2	48.0	Isometric
80	66.4	311.2	29.6	44.0	Isometric
81	59.2	300.0	28.0	49.6	Isometric
83	62.4	312.0	27.2	45.6	Isometric
85	64.0	309.6	27.2	40.0	Isometric
90	57.6	290.4	29.6	37.6	Isometric
87	59.2	276.0	33.6	38.4	Isometric
90	94.0	264.0	26.4	76.0	Isometric
91	81.6	262.4	26.4	74.4	Isometric
92	81.6	264.8	26.4	76.0	Isometric
95	71.2	259.2	18.4	70.4	Isometric
99	79.2	260.8	24.0	84.0	Isometric
101	80.0	264.0	20.0	80.0	Isometric
103	78.4	270.4	16.0	93.6	Isometric
101	80.0	264.0	20.0	78.4	Isometric
60	72.0	318.4	18.4	71.2	Amyl Nitrite
64	71.2	330.4	21.6	64.0	Amyl Nitrite
65	72.8	360.0	25.2	62.4	Amyl Nitrite
62	71.2	329.6	24.4	64.0	Amyl Nitrite
61	75.2	328.0	16.8	72.0	Amyl Nitrite

Table IV

Transmission Times and Brachial Arterial Blood Pressures from Experiment IV

P	Δt_1	Δt_2	Δt_3	Δt_4	Conditions
84	64.0	294.4	31.2	54.4	Normal
86	65.6	299.2	27.2	54.4	Normal
86	63.2	309.2	24.8	52.8	Normal
85	60.8	303.2	33.6	49.6	Normal
84	65.6	302.6	29.6	52.0	Normal
82	67.2	304.0	32.8	50.4	Normal
82	65.6	304.8	29.6	57.6	Normal
83	65.6	300.8	30.4	60.0	Normal
91	63.2	307.2	29.6	58.4	Isometric
93	60.0	311.6	28.0	57.6	Isometric
94	59.2	311.6	28.8	55.2	Isometric
96	62.4	313.2	28.0	57.6	Isometric
96	61.6	308.8	25.6	57.6	Isometric
97	62.4	300.0	28.8	56.0	Isometric
99	64.0	294.4	27.2	56.0	Isometric
100	58.4	290.4	28.8	54.4	Isometric
105	54.4	297.6	28.0	57.6	Isometric
106	55.2	303.2	26.4	60.8	Isometric
108	57.6	301.6	27.2	57.6	Isometric
110	61.6	297.6	29.6	55.2	Isometric
107	52.0	300.0	30.4	60.0	Isometric
106	56.0	300.0	30.4	55.2	Isometric
113	60.0	288.0	29.6	51.2	Isometric
116	57.6	284.0	30.4	51.2	Isometric
116	52.4	285.6	32.0	48.0	Isometric
116	52.4	282.4	33.6	49.6	Isometric
76	74.4	276.0	30.4	45.6	Amyl Nitrite
74	68.0	269.6	31.2	49.6	Amyl Nitrite
70	72.8	264.8	30.4	44.0	Amyl Nitrite
67	76.0	259.2	33.6	36.4	Amyl Nitrite
65	73.6	252.0	32.0	40.0	Amyl Nitrite
65	76.0	248.0	32.0	36.0	Amyl Nitrite
63	72.8	249.6	30.4	41.6	Amyl Nitrite
61	76.0	244.8	33.6	37.6	Amyl Nitrite
61	78.4	242.4	32.8	32.8	Amyl Nitrite
60	81.6	236.8	32.8	37.6	Amyl Nitrite
60	82.4	240.8	32.0	38.4	Amyl Nitrite
75	70.4	220.0	30.4	32.0	Amyl Nitrite
75	69.6	214.4	31.2	36.4	Amyl Nitrite
75	68.0	218.4	31.2	37.0	Amyl Nitrite
77	68.0	222.4	28.0	33.6	Amyl Nitrite
80	66.4	217.6	30.4	29.6	Amyl Nitrite

Table V

Transmission Times and Brachial Arterial Blood Pressures from Experiment V

P	Δt_1	Δt_2	Δt_3	Δt_4	Δt_5	Conditions
85	79.2	370.4	13.6	96.8	311.2	Normal
85	80.0	374.4	15.2	102.4	304.0	Normal
87	80.0	368.0	15.2	90.0	306.4	Normal
84	80.0	368.8	13.6	96.8	315.2	Normal
82	80.0	357.2	16.0	95.2	314.4	Normal
86	81.6	367.2	17.6	94.4	306.4	Normal
87	78.4	370.4	12.8	111.2	296.8	Normal
89	77.6	375.2	14.4	104.8	306.4	Normal
86	79.2	373.6	14.4	97.6	313.6	Normal
90	76.8	360.0	16.8	96.8	299.2	Isometric
89	74.4	365.6	14.4	98.4	298.4	Isometric
94	82.4	360.8	12.8	105.6	290.4	Isometric
95	74.4	358.4	13.6	103.2	289.6	Isometric
100	69.6	355.2	12.0	101.6	279.2	Isometric
100	74.4	357.6	15.2	100.8	282.4	Isometric
103	66.4	346.4	16.8	111.0	273.6	Isometric
103	67.2	348.8	15.2	97.6	276.8	Isometric
105	75.2	345.6	12.8	90.4	317.6	Isometric
105	68.0	346.4	10.4	102.4	275.2	Isometric
106	64.8	340.8	12.0	103.2	284.8	Isometric
113	71.2	332.0	12.0	86.4	264.8	Isometric
110	67.2	335.2	10.4	92.8	300.0	Isometric
112	65.6	353.6	8.0	99.2	272.0	Isometric
76	80.8	347.2	16.0	76.0	-----	Amyl Nitrite
74	80.8	349.6	10.4	79.2	-----	Amyl Nitrite
65	89.6	346.4	13.6	71.2	-----	Amyl Nitrite
64	84.8	339.2	13.6	74.4	-----	Amyl Nitrite
63	80.0	339.2	12.8	70.4	-----	Amyl Nitrite
61	83.2	336.8	14.4	66.4	-----	Amyl Nitrite
60	89.6	329.6	16.0	67.2	-----	Amyl Nitrite
56	94.4	330.4	17.6	67.2	-----	Amyl Nitrite
56	96.0	320.8	19.2	63.2	-----	Amyl Nitrite
55	92.0	325.6	19.2	67.2	-----	Amyl Nitrite
54	102.4	316.8	12.0	72.0	-----	Amyl Nitrite
53	106.4	317.6	17.6	61.6	-----	Amyl Nitrite
52	104.0	320.0	16.8	63.2	-----	Amyl Nitrite
53	105.6	316.0	19.2	62.4	-----	Amyl Nitrite
68	83.2	294.4	12.8	76.0	-----	Amyl Nitrite
68	86.4	292.0	14.4	72.0	-----	Amyl Nitrite
70	80.0	296.8	16.8	70.4	-----	Amyl Nitrite
73	84.0	296.0	24.0	64.0	-----	Amyl Nitrite

Bibliography

Bargainer, J. D. (1958) Pulse Wave Velocity in the Main Pulmonary Artery of the Dog. Circ. Res. 20:630

Bayett, H. C. and Dreyer, N. B. (1922) Measurements of Pulse Wave Velocity. Am. J. Physiol. 63:94

Beyerholm, O. (1925) Studies of the Velocity of Transmission of the Pulse Wave in Normal Individuals. A. Med. Scandinav. 67;203

Bramwell, J. C. and Hill, A. V. (1922) The Velocity of the Pulse Wave in Man. Proc. Roy. Soc. Sec. B 93:298

Hafkesbring, R. and Ashman, R. (1943) Pulse Wave Velocities in 90 Subjects. Am. J. Physiol. 100:89

Hallock, P. and Benson, I. (1937) Studies of the Elastic Properties of Human Isolated Aorta. J. Clin. Invest. 16:595

Hamilton, W. F., Remington, J. W., and Dow P. (1945) The Determination of the Propagated Velocity of the Arterial Pulse Wave. Am. J. Physiol. 144:521

Hardung, V. (1962) The Propagation of Pulse Waves in Viscoelastic Tubings. Handbook of Physiology - Circulation Vol. 1, W. F. Hamilton, ed. (American Physiological Society: Washington, D. C.) 107

Haynes, F. W., Ellis, L. B., and Weiss, S. (1936) Pulse Wave Velocity and Arterial Elasticity in Arterial Hypertension, Arteriolsclerosis and Related Conditions. Am. Ht. J. 16:95

Helfant, R. H., Devilla, M. A., and Meister, S. G., (1971) Effect of Sustained Isometric Handgrip Exercises on Left Ventricular Performance. Circulation 44:982

Horeman, H. W. and Noordegraff, A. (1958) Numerical Evaluation of Volume Pulsations in Man. Phys. Med. Biol. 3:51

Hurwitz, C., Parmly W. M., Donoso, R., Marcus, H., Ganz W., Swan, H. C (1971) Effects of Isometric Exercise on Cardiac Performance Circulation. 44:994

La Bresh, K. A. (1970) Pulse Wave Velocity as a Measure of Arterial Blood Pressure. S. B. Thesis, M.I.T.

Lewis, D. H. (1962) Phonocardiography. Handbook of Physiology - Circulation Vol 1 W. F. Hamilton ed. (American Physiological Society: Washington, D. C.) 680

Little, N. C. (1938) Speed of Pulses Along Tubes With Elastic Walls. Am. Phy. Teacher 6:30

McDonald, D. A. (1960) Blood Flow in Arteries Edward Arnold (London)

Nye, E. R. (1964) The Effect of Blood Pressure Alteration on the Pulse Wave Velocity. Brit. Heart J. 26:261

Sands, J. (1924) Studies in Pulse Wave Velocity. Am. J. Physiol. 71:519

Schimmler, W. (1966) Correlation Between the Pulse Wave Velocity in the Aortic Iliac Vessel, and Age, Sex, and Blood Pressure. Angiology 17:314

Steele, J. M. (1937) Interpretation of Arterial Elasticity from Measurements of Pulse Wave Velocities. Am. Heart J. 14:452

Wonnacott R. J. and T. H. Econometrics John Wiley and Sons; New York

TRANSDUCER DEVELOPMENT FOR

BLOOD PRESSURE MEASURING DEVICE

by

Donald Evan Gorelick

S.B., University of Maryland
(1971)

SUBMITTED IN PARTIAL FULFILLMENT OF THE

REQUIREMENTS FOR THE DEGREE OF

MASTER OF SCIENCE

at the

MASSACHUSETTS INSTITUTE OF TECHNOLOGY

June, 1973

Signature of Author Donald E Gorelick
Department of Electrical Engineering, May 11, 1973

Certified by Roger G. Mark, PhD
Thesis Supervisor

Accepted by ______________________________,
Chairman, Departmental Committee on Graduate Students

TRANSDUCER DEVELOPMENT FOR BLOOD PRESSURE MEASURING DEVICE

by

Donald Evan Gorelick

Submitted to the Department of Electrical Engineering on May 11, 1973 in partial fulfillment of the requirements for the Degree of Master of Science.

ABSTRACT

There is a great medical need for new techniques for noninvasively determining blood pressure on a beat to beat basis. Other researchers have proposed that the diastolic blood pressure may be proportional to the aortic pulse wave velocity, the speed the arterial pulse propagates from the heart. To determine pulse wave velocity accurately, sensors are needed to determine the arrival time of the pressure pulse at two points of the arterial system.

In this paper, past methods for monitoring blood pressure and the proposed method are reviewed. Then, the various types of transducers for determining arterial pulse arrival times are considered. The presently available transducers are not ideal for monitoring arterial pulsations on moving patients, since noise and artifacts limit the usefulness of these devices. It was felt that two devices, the doppler ultrasonic blood flow meter and the photoelectric transducer were most promising for long term pulse sensing on uncooperative patients. However, commercially available sensors of these types were not considered to be adequate.

A doppler ultrasonic transducer was built with a beam width greater than commercially available. This device shows improved ease in positioning over the carotid and femoral arteries. However, the device is still not adequate for monitoring of uncooperative patients.

The photoelectric plethysmograph was also tested. A dual channel, differential photoelectric plethysmograph is described. Tests indicate that no great increase in signal to noise ratio is possible from this technique. A single channel plethysmograph was also built and tested. The device was adequate to monitor surface arterial pulsations and blood influx into the skin capillary bed in most regions of the body. For use on ambulatory patients, a system is proposed for monitoring aortic pulse propagation time by sensing arrival times of the blood volume pulse in two regions of the back. Experiments performed indicate, however, that there is little, if any, correlation between aortic pulse propagation times and the difference of pulse arrival times in two regions of the back. A plot of carotid pulse to back time delays for various regions of the back showed that in general, the time delay increased with distance from the top of the shoulder. The origin of the photoelectric pulse signal and some possible applications of the photoelectric transducer are also mentioned.

THESIS SUPERVISOR: Dr. Roger Mark
TITLE: Associate Professor of Electrical Engineering

ACKNOWLEDGEMENT

My most sincere thanks to my thesis advisor, Dr. Roger Mark, for his guidance and encouragement. Also, thanks to Professor Steve Burns, Barry Gaiman, and Joe Walters for help with the equipment used. Of course, all my friends warrant acknowledgements for their support, but I'll just mention those who were patients (and had patience) for my experiments: Lynette Linden, Fran Beaumont, Jerry Bonn, John Myers, Shirez Daya, Tom Lynch, Bruce Anderson, Charles Louy, and Paul Roth. And let us not forget my typists and friends, Diane Horner and Maureen Forte.

TABLE OF CONTENTS

LIST OF TABLES AND FIGURES

INTRODUCTION

In recent years there has been increased interest in continuous monitoring of blood pressure in humans by noninvasive means. This interest is based largely on the need of NASA to monitor life processes during space flight and in various ground-based experiments. Monitoring of both normally active individuals and cooperative subjects is important. Physicians also feel a need for such a device, since many times measurement of a patient's blood pressure in the physician's office gives a poor indication of the blood pressure variations during daily activity. A continuous record of blood pressure of a patient taken for periods of up to a day would be important information for a physician in assessing the actual deviation of blood pressure from normal and the effects of any treatment (such as drug therapy) which might be administered. Another use for such a device would be in hospitalized, critically ill patients whose vital parameters must be constantly monitored. An ideal device for continuous monitoring of subjects would be accurate, comfortable, and relatively insensitive to artifacts induced by patient movement. There is a need, then, for a device which could be used on cooperative, bed-ridden, or ambulatory patients for continuous blood pressure monitoring. Blood pressure measurements might be taken every heartbeat or at short intervals and the results stored for future reference by the physician.

PAST METHODS FOR MONITORING BLOOD PRESSURE

The most reliable way to continually monitor blood pressure is the direct method. This involves inserting either a needle or cannula into an artery. The needle or cannula is then connected to an externally mounted pressure transducer. Another method involves actually inserting a miniaturized pressure transducer at the tip of a catheter into the artery. These methods give reliable, well calibrated continuous pressure readings for long periods. The direct method is the method usually used when continuous records of blood pressure from a bedridden patient such as in the cardiac care ward are desired. Also, Bradfute and Wright [1968] report of using a catheter in the radial artery to monitor pressure in ambulatory patients. The catheter was held in place with tape and an elastic bandage. Most patients noted dull, aching discomfort from the catheter. Arterial spasm occurred in some patients along with severe pain. After the test, the subjects still noted mild to moderate discomfort in the puncture area for up to 48 hours. Also, there was a problem with clotting of blood in the catheter which could only be solved by flushing with heparinized saline every four hours.

To avoid these complications and others such as hemorrhage or infection which can result from introducing a foreign body into an artery, many researchers have developed automatic devices to continually monitor blood pressure indirectly. These methods are usually based on the common auscultatory method used by most physicians to give a quick easy reading of diastolic and systolic pressures. This method was developed largely by Korotkoff [1905]. It involves placing a pressure cuff connected to a manometer around the upper arm. The cuff is in-flated while the brachial artery sounds are monitored below the cuff. When the cuff pressure is below the diastolic (resting) pressure, there will be unimpeded flow of blood in the brachial artery, which is relatively quiet. At pressures above diastolic, characteristic sounds termed Korotkoff sounds are found. These are caused by turbulence due to the interrupted flow of blood past the cuff [Burton, 1965]. When the cuff pressure reaches systolic pressure, the artery remains closed, and no Korotkoff sounds are heard. Normal procedure for a physician is to inflate the cuff to a pressure above the point the Korotkoff sounds disappear, and then slowly release the pressure. The pressure at which the Korotkoff sounds (sharp tapping sounds) first appear is marked as the systolic pressure. As cuff pressure is further reduced, the sounds become louder and extended in time and then diminish. At a cuff pressure slightly before the sound begins to diminish, there is a change in character of the sound known as "muffling," which is usually taken to be the best criterion for diastolic pressure [Burton, 1965].

Many devices have been devised to automate the procedure of determining blood pressure using the auscultatory idea. Gilson et al. [1941] devised an automatic device which records cuff pressure and Korotkoff sounds simultaneously every 30 seconds. The cuff pressure is automatically controlled, and the Korotkoff sounds are picked up by a "suitable device" (a Shure Stethophone) positioned over the brachial artery. The physician is presented with tracings of pressure and sounds and must determine systolic and diastolic pressures from the tracings. Once adjusted for a given patient, Gilson claims the device can be left to run unattended for hours, recording pressure every thirty seconds, with little discomfort to the patient.

Weiss [1941] presented a similar device which has a sinusoidally varying cuff pressure with a period of twenty-five seconds. The Korotkoff sounds are recorded superimposed on the pressure tracing. The physician can then determine systolic and diastolic pressures as the onset and cessation of sounds (the old method for recording diastolic pressure was at the point the Korotkoff sounds disappear [Burton, 1965]).

Another automated device was devised by Rose et al. [1953]. The sounds are detected by a brachial microphone, and diastolic and systolic points are marked on a chart recorder, recording cuff pressure. The device has a cycle speed of 3.5 minutes.

To eliminate the possibility of getting erroneous readings from noisy microphone signals, the Aerospace Medical Labs [1959] developed a computerized blood pressure system in which Korotkoff sounds are accepted only if they correspond to a pulsation in the brachial cuff. Cycle time can be adjusted from one to fifteen minutes. R.A. Johnson [1959] reports that the readouts are reliable and accurate but no comparative data is reported.

The National Aeronautics and Space Administration [1964] report tells of the system used to monitor blood pressure on the first U.S. orbital flight. A special, less cumbersome cuff was devised, so that it could be kept continually in place and not impede critical movements of the astronaut. An oxygen tank and accompanying valves and regulators were devised to fill the cuff. They used a specially damped piezoelectric microphone, filtered to accept only 32 to 40 Hz to pick up Korotkoff sounds. The cuff pressure system, however, proved too difficult to add to a spacecraft, so the system actually employed, was a simple hand pump in conjunction with the microphone.

A similar system is commercially available [Remler Co.]. In this system the patient pumps up the cuff at given times. The cuff pressure and the brachial arterial sounds from a microphone are recorded on a portable magnetic tape recorder carried on the patient's belt. The doctor can later play back the tape and determine the pressures recorded.

Because of the inherent limitations of using a microphone to sense the pulsations of the artery, numerous investigators have devised alternate systems to sense the pulse arrival below or under the cuff. A very novel system was used by Zindema et al. [1955]. They use a water filled plastic balloon directly over the artery and beneath the pressure cuff to sense pulsations of the artery. The balloon is connected to a Statham pressure transducer which indicates the pulse. Jeff Raines [1971] has developed a similar system which extremely accurately measures cuff pressure, so that the pulsations can be seen from the output of the cuff pressure monitor. If this system is accurately calibrated, it can give a good indication of diastolic pressure by noting the amplitude of the pulse excursions. The device must be recalibrated periodically, especially if physiologic changes, such as vasoconstriction, occur

Another device to pick up the pulse was devised by R. Kirby [1969]. He uses a doppler ultrasonic transducer to record the movement of the brachial artery beneath the pressure cuff. He found that the transducer can sense very weak signals which are impossible to obtain with a stethoscope. The system is especially useful for recording pressures from shock patients or infants. Plus or minus 2.2 mm Hg accuracy is claimed.

Electrical Impedance Plethysmography is also used to determine pulse arrival below a pressure cuff. Mann [1937] showed that using a 1000 Hz alternating current bridge in measuring the conductance of a finger, the rhythmical variations disappear as cuff pressure rises above systolic pressure. This method has also been applied to monitor pressure in infants [Schaffer, 1955] where Korotkoff sounds are difficult to detect.

The use of a cuff on the finger has been a useful technique in continuous monitoring of blood pressure, since the cuff is not as uncomfortable as a normal upper arm cuff. Green [1955] used a volume plethysmograph to monitor the pulsation of a finger below a small servo controlled finger pressure cuff.

Traite [1962] devised a similar device which uses a piezoresistive sensor below the finger-cuff to monitor pulsations. The cuff is inflated by a variable speed motor at 5 mm of mercury per second. A narrow bandwidth filter is used to exclude motion artifacts from the signal. Test subjects reported that after ten minutes of use the cycle is largely ignored. Correlation with standard brachial artery pressure measurements is reported to be within five mm of mercury.

The finger cuff also has been used to continually monitor blood pressure by Robinson and Eastwood [1959]. They used a photoelectric plethysmograph to monitor the pulse. This device senses the change in opacity of the tissue caused by the fluctuation of blood within the vascular network.

There are a few systems for blood pressure monitoring which do not use a pressure cuff. A system which relies on a principle very similar to the cuff techniques was developed at the Mayo Clinic [Wood, 1950]. They found that the I.R. Pulse (pulse due to infrared absorption by the blood) can be monitored in the pina of the ear by a suitable light transmission and photoelectric sensing device (photoelectric plethysmograph). When the ear is compressed by a pressure bellows, the I.R. pulse disappears when the bellows reaches systolic pressure. The diastolic point can also be found by noting the pressure at which the pulse reaches maximum amplitude. A system was built which can take pressure readings every ten seconds. NASA further developed this idea [Jones and Simpson, 1966] and found the device is inherently insensitive to motion and noise artifacts. American Heart Association has shown measurements from this device correlate well with those from indwelling catheters. Also, the patient experiences little or no discomfort from the device and may wear it for hours. The device, however, has not been widely accepted by the medical profession, possibly due to the large number of variables which may affect the signal.

Attempts have been made by Corell [1959] to measure blood pressure from the amount of distention of the brachial artery. He sealed a pressure chamber over the artery and measured pressure changes in the chamber caused by the arterial pulsations, by means of a capacitive transducer. He tried to find a linear relationship of this pressure pulse to the blood pressure. Difficulties were encountered with positioning the transducer, motion artifacts, and physiologic changes of the arterial system. These difficulties made it impossible to calibrate the device.

A similar system was developed by Pressman and Newgard [1963], based on a mathematical model of the arterial wall. Their device exerts a pressure on the artery with an arterial rider which partially flattens the artery. They found that the force necessary to maintain the flattened position is linearly related to arterial pressure. They use a strain gauge transducer system to measure the force on the arterial rider. The system showed promise, however, difficulties were encountered with positioning the device accurately over the center of the artery for long periods.

None of these methods for continually monitoring blood pressure have proven to be satisfactory for use on ambulatory patients under the influence of various drugs which have effects on the arterial system. Also, none of the methods give satisfactory blood pressure measurements on a beat to beat basis.

PROPOSED METHOD

For numerous reasons, past attempts for developing a non-invasive blood pressure monitoring system, which can be used continuously for long periods, have proven unsatisfactory. Either the device intruded too much into the patients daily life, for instance by requiring him to pump up a pressure cuff every few minutes, was uncomfortable, or results were just not accurate enough, under various conditions to give a good indication of pressure. Recent work by LaBresh [June, 1970] and Goldberg [January, 1972] has indicated that the pulse wave velocity, the speed with which the pressure pulse travels through the arterial system, gives a fairly good indication of diastolic blood pressure. Since diastolic pressure is usually considered as the more important of the blood pressure parameters, a system which could monitor pulse wave velocity non-invasively on ambulatory patients might prove quite useful as a blood pressure monitoring system.

The contraction of the left ventricle of the heart causes a surge of blood into the aorta, causing a rapid rise in the aortic pressure. This pressure pulse distends the aorta and similarly to a plucked string, the distention travels along the aorta propagating at a velocity which is determined by the distensibility of the arterial wall. The velocity of propagation of the pulse wave is much greater than the actual blood velocity. The "pulse wave velocity" can be found from the Moen's formula:

$$\nu = \sqrt{\frac{Ea}{2\rho r}}$$

where

ν = pulse wave velocity

E = modulus of elasticity for lateral expansion of the artery

a = thickness of the arterial wall

ρ = density of blood (1.055)

r = radius of the artery

More practically, this may be expressed in the form $\nu(\text{m/sec}) = 3.57/D^{1/2}$ [Burton, 1965 and LaBresh, June 1970] where D is the "distensibility", defined as the percentage of change in arterial volume (V) per 1 mm Hg rise of pressure. This is the Bramwell-Hill equation more frequently written: $\nu = 3.57(dP/(dV/V))^{1/2}$. From experimentally determined pressure-volume curves it is possible to derive a relationship between pulse wave velocity and pressure (P). LaBresh [June, 1970] shows that $dP/(dV/V)$ has approximately the form of a parabola for some experimental data. This leads to the approximate relationship $\nu = k_1 \, x(P - k_2)$ where k_1 and k_2 are constants that vary with age and bodily conditions. For measurements over periods of a few days or weeks, the changes in these constants for one individual are due mainly to the degree of contraction of the smooth muscle in the arterial wall. Chang [1971] shows for instance, that smoking a cigarette can cause a 50% increase in pulse velocity between the hand and the elbow, due to the constriction of the arterial smooth muscle. Changes of this magnitude in pulse wave velocity would make any correlation with pressure impossible in this region of the body.

Despite this, a system using the pulse wave velocity in the arm to measure pressure was developed by Wichmann and Salisbury [1964]. They would measure the propagation speed of a 10 to 60 Hz signal applied with a noninvasive arterial tapper to the proximal part of the artery. The signal was superimposed on various portions of the arterial pressure signal, so that both diastolic and systolic pulse wave velocities could be determined and related to pressure.

McDonald [1968] indicates that the aorta has comparatively very little smooth muscle in its wall, so that a change in pulse wave velocity in the aorta is a more reliable indication of a pressure change, than pulse wave velocity in the more peripheral arteries. LaBresh [June, 1970] shows that in dogs there is good linearity between the pulse wave velocity, measured between the arch of the aorta and the femoral artery, and the diastolic blood pressure. This relationship holds under varying conditions such as vasoconstriction, vasodilation and hypovolumia. Pulse wave velocity measured from the carotid to femoral arteries shows greater deviation from linearity, but there is still good correlation between the diastolic pressure and the pulse wave velocity. Nielson et al. [1968] indicates that the pulse wave velocity determined from the carotid to femoral region using piezoelectric microphone transducers agrees very well with the pulse wave velocity determined in the aorta with indwelling catheter pressure transducers. In experiments on resting, healthy human subjects, Goldberg [1972] shows that the pulse wave velocity between the carotid and femoral arteries gives a fairly good indication ($\pm$ 8 mm Hg or better) of diastolic blood pressure measured by a catheter, connected to a pressure transducer, inserted in the brachial artery. For each patient, plots of pressure versus $1/\Delta t$ were made. Each patient's data could be fit by a straight line, although slope and intercept were different for each patient. Therefore, indications are that a device for measuring blood pressure from pulse wave velocity could be calibrated for each patient by measuring pulse wave velocity at two widely different pressures.

Both LaBresh and Goldberg measured the onset of the pressure pulse in the two regions with mechanical transducers which sensed the expansion of the artery due to the pressure pulse. Δt, the time difference between the "foot" (point of rapid uprise due to ventricular contraction) of the pulses was then determined from a chart recording at high speed. The delay of the pulse foot was used to determine the pulse wave velocity, since it corresponds to the lowest point of the pressure wave form which "sees" the diastolic pressure. Therefore, the foot of the wave propagates with a velocity determined by the diastolic (resting) blood pressure level. Other points of the pressure pulse waveform propagate at a greater speed due to the higher pressures "seen" by these points [Burton, 1965].

The results of LaBresh and Goldberg are questioned by results from other experimenters. Eliakim et al. [1971] measured pulse wave velocity from the femoral to dorsalis pedis (foot) artery on patients and found that the blood pressure level had no effect on the pulse wave velocity. Large beat-to-beat variations in diastolic pressure in cases of atrial fibrillation and premature ventricular beats, as well as large blood pressure changes caused by cardiac pacing at increased rates had no effect on pulse wave velocity as measured between the two peripheral sites. Malindzak and Meredith [1970] in dog experiments similar to La-Bresh's [June, 1970] found conflicting results. In Malindzak's experiments pulse wave velocity was found to increase with blood pressure, as was shown by LaBresh, for blood pressure increases caused by administering Norepinephrine. While a decrease in blood pressure due to a dose of acetylcholine also caused an increase in pulse wave velocity. Malindzak explains these contradictions by surmising that the reflection from the unmatched peripheral vascular bed influences the position of the pulse foot. Changing peripheral resistance to alter blood pressure, therefore, may cause a rise or fall in pulse wave velocity depending on the extent of the pressure change in relation to the peripheral resistance change.

So the problem of correlating pulse wave velocity and blood pressure under various conditions remains. What is needed for studies of this type and for completion of the long range goal of developing a system to monitor blood pressure on ambulatory patients, is a convenient, noninvasive, reliable, transducer to monitor the pulse at two locations (probably the carotid and femoral regions) of the body. Such a device would also be useful for monitoring bed-ridden as well as cooperative subjects. An easy way to measure pulse wave velocity might also prove useful in screening of patients for artereosclerosis, since this condition may cause a variation from normal values for an age group in pulse wave velocity as reported by Eliakim et al. [1971].

ASPECTS OF A GOOD TRANSDUCER

In searching for the ideal transducer to monitor pulse wave arrival, it is useful to form a set of criteria for evaluating the device. As with any physiological transducer, the primary consideration is that it does not drastically affect the event it is measuring. In this case, it is important that the transducer system affect neither the pulse wave velocity nor the blood pressure. Other criteria for evaluating the transducer, include:

1. POSITIONING: The transducers must pick up signals from two regions which correspond to the linear pressure versus velocity region in the arterial system. It is hoped signals from the carotid and femoral arteries will show a linear pressure versus velocity relationship under most physiologic conditions.

2. ACCURACY: The arrival of the arterial pulse wave is the target variable. The transducer must accurately sense this arrival or a closely correlated parameter (perhaps skin color, for instance).

3. RELIABILITY: For use on ambulatory patients, the sensor must be capable of giving reliable signals as a patient goes about his daily routine. Environmental factors such as temperature, humidity and gravity should have little effect on the device. Also, artifacts from patient movements such as breathing and speech should be small.

4. SENSITIVITY: There should be a la.ge response from the small arterial signal so that an accurate and sharp wave foot can be located. Also, the signal to noise ratio should be large even in somewhat poor electrical environment, for instance, near a car with a poor ignition system. The frequency response must allow a sharp systolic upswing, yet should not accept 60 cycle noise.

5. BASELINE STABILITY: For accurately determining the foot of the pulse wave, baseline drift should be at a minimum.

6. CURRENT REQUIREMENTS: The device must be battery operated, therefore, small current drain is an important requirement. It may be possible to have the device turn on and off at regular intervals thereby lowering battery drain.

7. RUGGEDNESS: The transducer system must be able to withstand a certain degree of mistreatment such as being accidentally dropped. It must be able to withstand the many knocks it will encounter during a day on the job.

8. EASE OF OPERATION: The transducer system should be quickly attachable to the exact locations required. If possible, this could be done by a non-technical person, possibly the patient himself. Controls, if any, should be simple in operation.

9. COMFORT: The device must be comfortable to use for long periods. It shouldn't interfere with normal patient activity or make him overly

aware he is being monitored. The transducer and electronics, therefore, should be relatively small and light in weight.

10. SAFETY: The transducer should have no adverse effects on the skin or underlying tissue. Also, voltage levels should not be so high that they present a shock hazard.

11. COST: The initial cost and the cost of maintenance and repair should be at a reasonable level. The reasonable cost will of course depend on the market. Use by a patient in his home would require a device less costly than one to be used by an astronaut in a space ship. Cost trade-offs are always possible.

METHODS USED FOR PULSE MONITORING

There are many devices which can adequately sense the arrival of the arterial pulse wave. Most of these have been used in systems similar to the ones previously described for indicating the pulse below a pressure cuff, in systems for automated monitoring of blood pressure. Many of these devices sense the mechanical movement of the artery. Different methods have been devised to transduce the mechanical movement of an artery to an electrical signal. Clamann, [1951] used a special subminiature triac radio tube (RCA-5734) with a projecting pin connected to the plate. Movement of the pin by the artery produces a change in distance between the plate and cathode, causing a change in the circuit gain. A modern day version of this [Gorelick and Kim, 1971] uses a Pitran, pressure sensitive transistor, mounted in a water chamber which is placed over the artery. The water coupling to the skin helps alleviate placement difficulties as was shown by Davis, Gilmore, and Freis [1963]. The Davis device uses a strain gauge transducer system to monitor pressure changes in the water chamber. Pressman and Newgard [1963] also used a strain gauge transducer in monitoring pulsations of a small button riding on the artery. A differential transformer has also been used [Jones and Simpson, 1966] to measure pulsations of an arterial rider.

Benjamin et al. [1962] used a device similar in principle to Corell's [1959] blood pressure measuring device for picking up arterial pulsations. A chamber is sealed over the artery, and pressure fluctuations are picked up by a moving coil which acts as the inductive part of a transistorized 100 KHz Colpitts oscillator. A stationary coil is part of the input circuit to a transitorized clipper amplifier. Varying the distance between the coils causes a change in coupling which changes the amplitude of the 100 KHz signal (amplitude modulation).

The piezoelectric microphone is frequently used for picking up pulses. Geddes and Hoff [1960] used a high efficiency crystal from a phonograph cartridge to pick up pulsations from the radial and brachial arteries. They used a .02 uf capacitor to eliminate high frequency muscle tremors which were causing interference in the signal. This microphone has proven to be useful in studies of pulse wave velocity by G.L. Woolam et al. [1962] and other researchers. For use on uncooperative patients, all these electromechanical transducers have basically the same problems. They are all very prone to noise from movement of the patient and from slight changes in the position of the device relative to the skin. Also, speech and swallowing have extremely adverse effects on traces from the carotid artery, making the pulse waveform almost impossible to recognize. For use on cooperative patients in a controlled environment, the electromechanical transducers are probably quite adequate. Possibly the best sensitivity and frequency response may be obtained from the device devised by Gorelick and Kim [1971], however, in its present form this device would be difficult to mount for long periods over an artery. Slight modifications in the housing design would probably make it easier to attach over the artery.

Another technique used to monitor the pulse arrival is volume plethysmography. A part of the body such as the finger is placed in a rigid air tight container, and the pressure variations caused by the blood volume pulse are monitored [M.H. Lader, 1967]. Difficulties with this method is that it is very sensitive to muscular contraction and movement. There also is difficulty in using such a device in the vicinity of the femoral and carotid artery, although a system similar to Jeff Raines [1971] where pressure variations in a cuff are monitored can be used in these regions. The cuff would still be sensitive to muscular contractions and movement, however.

Electrical impedance plethysmography can also be used to sense the pulse wave [J. Nyboer, 1970]. This method monitors changes in the blood content. The technique can be localized to pick up the pulse from an artery. Again, however, this technique suffers from noise introduced by muscle movement [LaBresh, Sept. 1970]. Even an EKG gated filter cannot reduce the unwanted noise component of the signal.

Another technique for monitoring pulse arrival is the photoelectric plethysmograph. The changes in the blood content of the surface tissue causes changes in the light absorption coefficient of the tissue. The light absorption changes can be measured by using a photocell to monitor reflected light in the 8000 to 9000 A spectrum [Weinman, 1967] from a miniature bulb. Hertzman [1938] found that the pulsation of an artery can be monitored by this technique, because the movement of the skin surface affects the optical characteristics of the light-skin-photocell system. In this system, however, movement of the instrument with respect to the skin from muscular contraction also occurs, which results in sensing errors. A similar system was used to measure pulse time differentials between regions of the facial tissue by Behrendt and Shawaluk [1968]. They didn't sense arterial movement, but rather the influx of blood into the capillary bed of the tissue. They assumed that the time for the pulse to move from the major arteries to the capillary bed is essentially constant at all locations at which they were measuring, so that their measurements represent, to some degree at least, the arterial pulse wave time differential between the two points of measurement. One advantage of this method is that by its nature it is relatively insensitive to noise. However, Strong [1970] indicates that there may be trouble with movement artifacts on ambulatory patients.

A relatively new technique for sensing the arrival of the pulse wave uses a transcutaneous doppler ultrasonic blood flow meter to measure the arterial blood velocity. The blood flow pattern has a waveshape similar to the pressure pulse waveform, with the initial rise of the pulses corresponding in time, as can be seen in a report by Freis et al. [1966]. The blood velocity is measured from the doppler shift in a backscattered ultrasonic (2-10 MHz) sound wave. Stegall et al. [1966] found that they could easily monitor blood flow in the carotid and femoral artery. LaBresh [Sept. 1970] found that good signals can be recorded even when the subject is undergoing normal activities. He, however, indicates that placement over the artery is difficult because of the narrow beam width of the transducer used. Doppler transducers have been used successfully by Nippa et al. [1971] to measure pulse wave velocity in human veins, however, the measurements were only for short time periods. An added advantage of the doppler ultrasonic probe is that it can monitor the pulse in very deep arteries, even the aorta [L.H. Light, 1969] which should exhibit a higher degree of linearity between pulse wave velocity and blood pressure than the more superficial arteries [LaBresh, June 1970]. Another possible use of the doppler ultrasonic transducer is in measuring the actual motion of the artery as it expands with each pressure pulse. The movements of the wall cause a doppler shift in the frequency of the ultrasonic beam reflected from the artery. Baker and Simmons [1968] and Hokanson et al. [1972] indicate that phase-lock techniques can be used successfully for measuring arterial diameter changes ultrasonically. Placement over the artery in this technique is extremely critical, however, so it would probably not prove useful on ambulatory patients. There are questions about the safety of ultrasonic beams, but there is a large volume of reports which indicate that clinical use of low intensity ultrasound has no harmful effects. So there seem to be very great indications that at the intensities (10-100 mw/cm^2) of the doppler flow meter, there should be no adverse affects. According to Alt [1966], "sufficient experiments have been run to warrant the statement that sound levels below 1 W/cm^2 are non-destructive as far as biological tissues are concerned." Also, Lele [1972] states that, "from all evidence available it is conceded that current diagnostic practices (ultrasonic) pose no short term or long term hazard to patients."

Another device which measures flow velocity from doppler shift is the laser doppler velocity meter [Morikawa, et al., 1971]. There have been proposals for using such a device for transcutaneous blood flow measurements [Fine and Klein, Nov. 1969], however, the extreme attenuation of the laser light through the skin, and the opacity of the arterial wall makes it highly unlikely that a satisfactory device can be developed for measuring flow in the major arteries, at least at presently available wavelengths [Fine and Klein, July 1969]. Therefore, development of a satisfactory transcutaneous laser doppler flow meter seems to be unlikely in the near future.

Researchers frequently use the events in the heart as a reference to determine pulse wave velocity. Demonchy et al. [1970] used the second heart sound as a reference, and then measured delay times to the carotid and femoral arteries. The second heart sound, however, is very difficult to sense accurately in the presence of patient movements such as breathing, speech, and muscular contraction. Also, Goldberg [1972] indicates that the onset of left ventricular ejection to second heart sound delay time is too variable to serve as a reference for ejection. Therefore, this technique would probably not prove useful on an ambulatory patient.

Another reference which is used, is the R wave of the EKG. M. Monnier [1967] obtained variations of 3.4% in pulse wave velocity determined from the R wave and the sharp rise in the pulse wave of the dorsalis pedis (foot) artery. However, K. LaBresh [June 1970] indicates that under the effects of various drugs, the variability in the EKG to aortic pressure onset delay time is too large to make it useful as an indication of the aortic pressure rise. Goldberg [1972] further substantiates these findings.

VIEW OF DEVICE SUITABILITY FOR
AMBULATORY PATIENT MONITORING
BASED ON LIBRARY STUDY

S - Satisfactory
U - Unsatisfactory
? - Questionable

	Mech Trans	Volume Plethy	Elec. Imp	Photo Elec	Doppler Ultra
1. Positioning	S	U	S	S	?
2. Accuracy	S	U	S	?	S
3. Reliability	U	U	U	S	S
4. Sensitivity	S	U	S	S	S
5. Baseline Stability	S	S	S	S	S
6. Current Requirement	S	S	S	S	S
7. Ruggedness	S	S	S	S	?
8. Ease of Operation	?	U	S	S	?
9. Comfort	S	U	S	S	S
10. Safety	S	S	S	S	S
11. Cost	S	S	S	S	S

It can be seen that the most promising devices are the Doppler Ultrasonic and the Photoelectric Plethysmograph. These are further investigated.

DOPPLER ULTRASONIC TRANSDUCER

The doppler ultrasonic blood flow transducer is fairly simple in principle. A piezoelectric crystal (see Figure 1) is excited at its resonant frequency by a high frequency (1-10 MHz) electric signal. The crystal vibrates at this frequency, and emits sound waves into the surroundings. An acoustic coupling gell (Aquasonic) is used to acoustically couple the transducer to the skin surface. The incident beam is transmitted into the skin and reflected back by any interfaces or inhomogeneities in the medium. The receiving crystal picks up the "echoes" and converts the acoustic signal back to an electric signal which can then be amplified. The received signal consists of the reflected signal from the skin inhomogeneities, the non-moving interfaces, the moving arterial wall, and the moving blood particles. Reid et al. [1969] indicates that the red blood cells contribute by far the greatest amount to the reflection from the arterial blood. The reflected waves from the moving objects such as red cells will be doppler shifted in frequency. The frequency shift is related to the blood velocity, the angle of incidence and reflectance and the ultrasonic frequency used, by the following equation [Stegal et al. 1966]:

$$\Delta f = f - [f(c - \nu \cos \alpha)/(c + \nu \cos \beta)]$$

this reduces to

$$\Delta f = [(2f \cos(\frac{\alpha+\beta}{2})c]\nu \quad \text{for } \nu << c,$$

where c is the speed of sound in the medium (about 1500 m/sec).

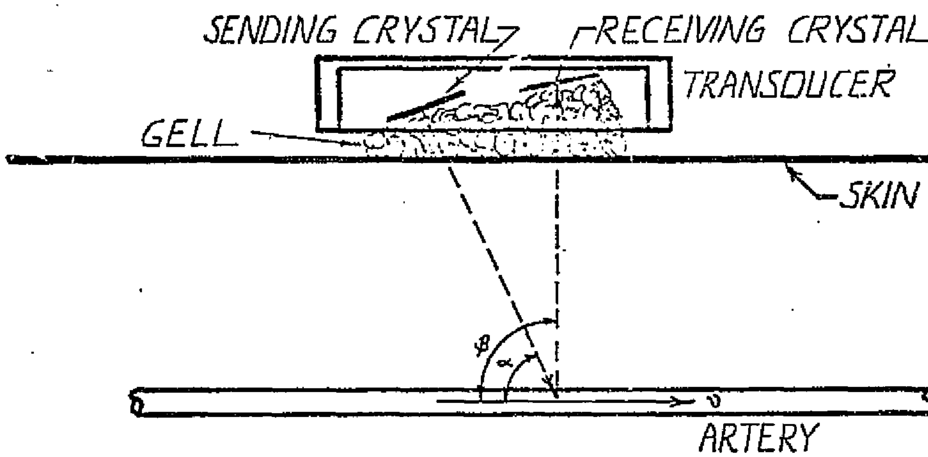

Figure 1

Movement away from the crystals causes a decrease in frequency, while movement towards the crystals causes an increase in frequency. The received signal of f + Δf is electronically detected to yield the difference frequency Δf. As the velocity of blood changes with each heart beat, Δf will vary accordingly. For no flow, Δf will be 0 and vary linearly to about 6.7 KHz for a flow of 100 cm/sec (which is near the maximum in the aorta) for flow directly away from the crystals at an incident frequency of 5 MHz. The change in Δf can be electronically converted to a change in output voltage with a zero-crossing detector, see Figure 2. The output signal then, represents the velocity of blood in the artery and the velocity of the arterial wall which can be filtered out since it is only at a velocity of about 2.5 cm/sec [Stegal et al. 1966], which is below the normal slowest blood velocity. Since the initial rise of arterial pressure and the blood velocity correspond in time, the

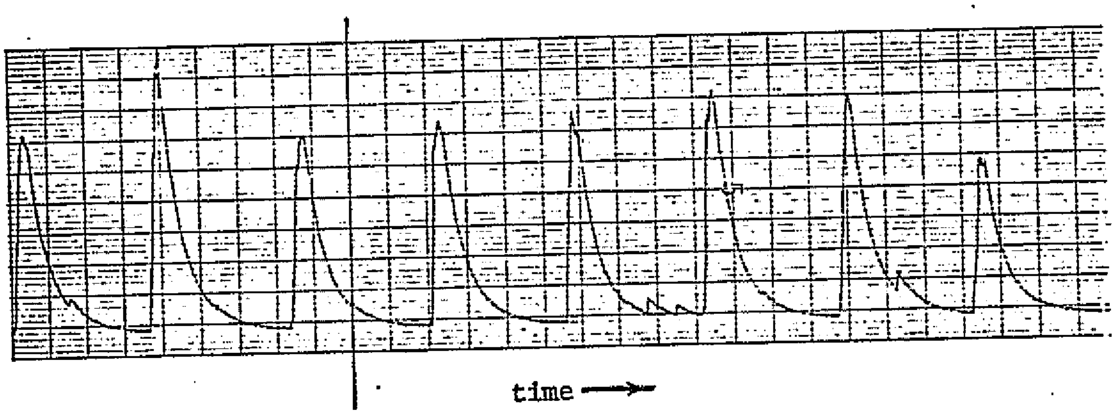

FIGURE 2

Femoral Pulse Recorded With Doppler Ultrasonic Transducer foot of the blood velocity signal from the doppler ultrasonic transducer can be used to determine the foot of the pressure pulse.

There are still many problems involved with the use of the ultrasonic doppler transducer. Presently available probes have very narrow beam widths which make them difficult to position accurately over the artery. The Parks Electronics model 802 Doppler instrument used in the preliminary tests for instance, comes equipped with a probe having crystals approximately 2 x 1 mm on a side with a 10 MHz resonant frequency. Positioning of the probe over the artery is quite critical and even if the transducer can be firmly attached to the skin, any movement of the artery with respect to the skin as with turning the head in the case of the carotid artery causes loss of the signal.

To broaden the beam width, probes with crystals (PTZ-5) of 5 x 10 mm were constructed [LaBresh, Sept. 1970]. These probes were much easier to position accurately over an artery, but did not retain an adequate signal when the artery was moved due to body motion.

Another variable which was changed to broaden the beam width was the resonant frequency of the transducer. Lower frequency crystals inherently have a broader beam width [Wells, 1969], however, the doppler shift decreases linearly with the frequency. This is partially offset by a decrease in the absorption at the lower frequency. Ultrasonic waves are absorbed by tissue due to a phase lag in the tissue of the translational motion of the sound wave with respect to the stress. This effect increases almost linearly with frequency. Normal values for the absorption coefficient of soft tissue is between .5 and 3.5 db cm^{-1} MHz^{-1} [Alt, 1966 and Wells, 1969]. Results with a lower frequency (5 MHz) transducer were comparable to the previous results, indicating that a change in frequency would not be a great improvement in performance.

To broaden the beam, convex crystals may also be used [Wells, 1969]. A convex crystal or a flat crystal with a convex lens should have less directional sensitivity than a flat crystal. In fact, a transducer constructed from convex 5 x 10 mm crystals was tested and proved to be just not sensitive enough to pick up good signals except when positioned extremely accurately.

The effect of the angle of incidence and reflection of the beam was investigated using a specially constructed jig illustrated in Figure 3. A pulsatile flow pump consisting of a motor driven syringe with a gravity feed reservoir serving as a capacitance vessel so that flow would never reach zero, was used in a closed loop system. The circulating fluid used was milk, which has reflectance properties similar to that of blood [Flax et al. 1969]. The milk flowed through a plastic tube (1/4" O.D.) in a water bath which provided a good acoustic coupling to the transducer also placed in the water bath. The transducer angle jig was placed so that there was 8 mm from the center of the tubing to the center of the crystals. Table 1 shows the results of changing the separation of the crystals with constant crystal angles, while Table 2 shows the optimum angles determined for various crystal separations. It can be seen that the variation in output was fairly minimal over a wide range of angles and separations. Therefore, it is believed that the actual angle and separation of the crystals used in the transducer is not critical. This agrees well with results found by LaBresh [Sept. 1970].

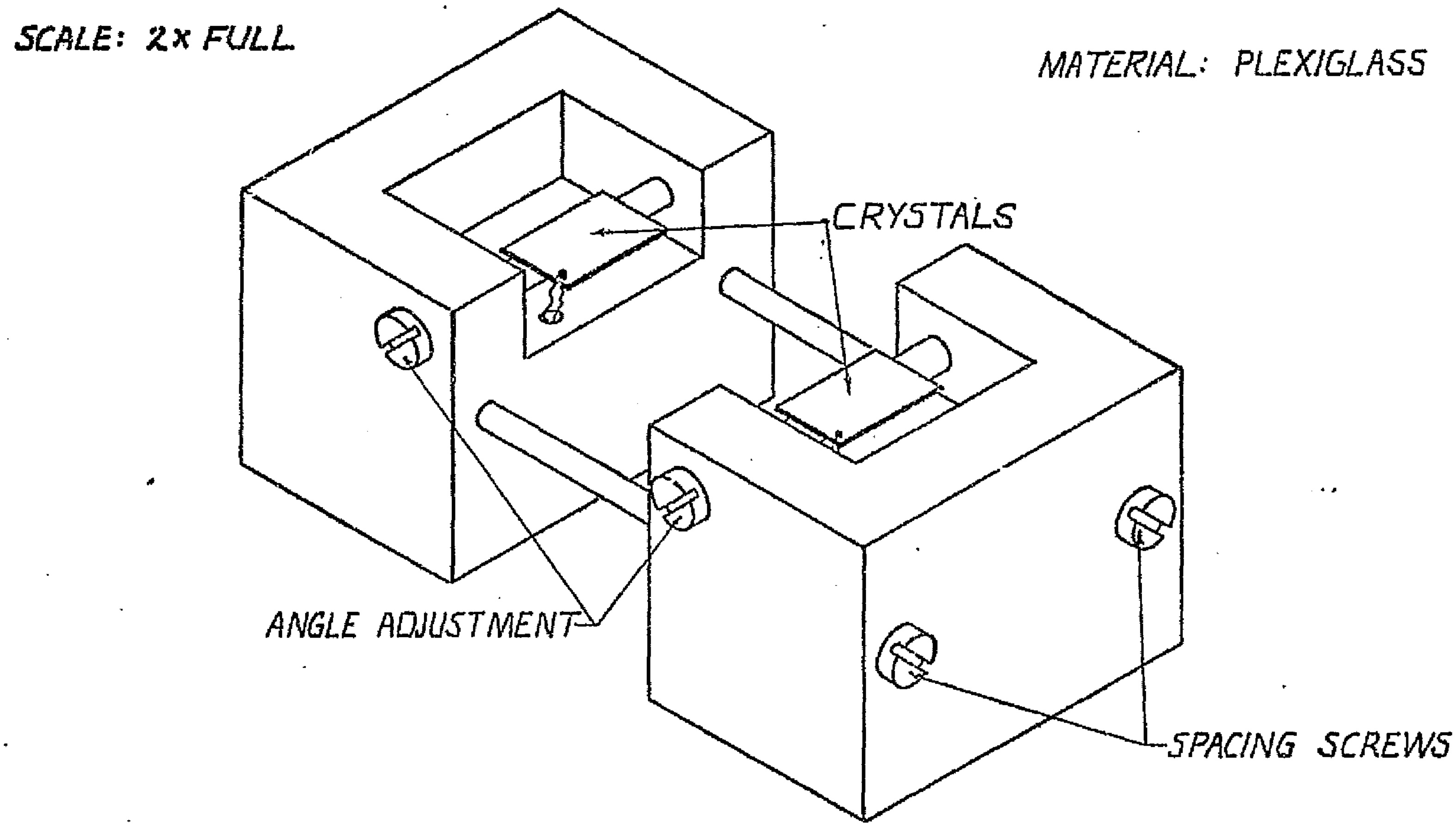

ANGLE JIG

FIGURE 3

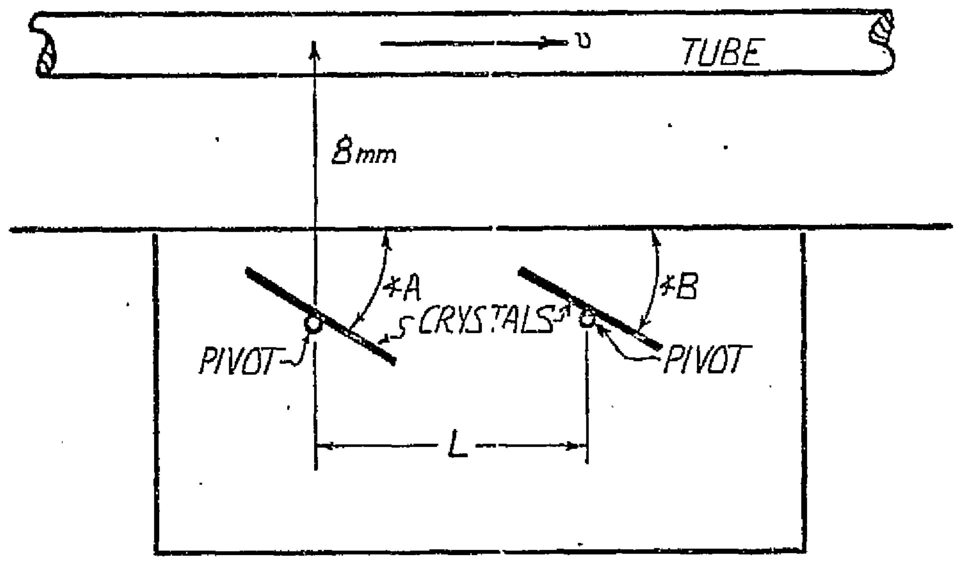

TABLE 1

ANGLE A = 39°, ANGLE B = 28°

CRYSTALS 5 x 10 mm @5MHz

SEPARATION, L, mm	OUTPUT, VOLTS
12.0	1.9
11.0	1.9
10.0	1.8
9.0	1.9
8.0	2.0
7.5	2.1
7.0	2.3
6.5	2.1
6.0	2.1
5.5	2.1

TABLE 2

SEPARATION, L, mm	OPTIMUM ANGLES A	OPTIMUM ANGLES B	OUTPUT, VOLTS
12.0	39	28	1.9
11.0	39	28	1.9
10.0	49	25	2.3
9.0	49	25	3.0
8.5	49	25	2.5
7.5	50	23	2.9
7.0	50	23	3.0
6.0	45	25	3.0
5.5	45	25	3.0

Another transducer was constructed containing two 5 x 10 mm crystals resting at fixed angles of 45° and 25° with about 6 mm separating the centers of the crystals resting on a candle wax backing, within a metal hemispherical shell. Performance over the carotid and femoral artery was comparable to the performance of the adjustable transducer set at optimum angles. This transducer had a rubber rim to increase friction between the skin and the transducer to make positioning easier. Also, this serves to keep acoustic coupling jell which is very slippery from getting under the transducer-skin interface. Furthermore a special two sided adhesive ring used for positioning EKG electrodes was placed between the rubber and skin interface. Also, an elastic band was used to help hold the transducer in a stable position. Difficulty was encountered in using a plain elastic band to hold the transducer over the femoral artery, because the position of the artery is such that an elastic band around the leg is too low to cover it. To circumvent this, a sock garter was used inverted so that it could be attached to the subjects shirt, pulling it high enough on the hip to cover the femoral region. Experiments over the carotid and femoral artery again showed that the signal disappeared quite easily when any motion in the region occured. It is felt that the movement of the skin relative to the artery is the reason for this.

Loren Parks [July 1972] manufacturer of doppler probes and flow meters indicated that there has never been a transducer devised for continuous monitoring. He recommended that the crystal length be further increased. However, he cautioned that signal-to-noise ratio becomes a problem for such large transducers. Two such transducers were constructed. Both had crystals 20 mm x 5 mm imbedded in wax. One transducer was at 5 MHz while the other at 10 MHz. Both transducers were slightly easier to position than the 10 mm long crystal transducers, however, there was a great deal of noise, some due to the flow of the venous blood which runs near the artery. It was felt that a more complex instrument, a directional doppler such as Parks model 806 which distinguishes between, and can be set to measure only, flow towards or away from the transducer could be used to help reduce the venous noise. Since this instrument was not immediately available at MIT, one was borrowed [Raines, 1972] from Mass. General Hospital. Indeed, the device did reduce the venous noise when used with the large transducers. However, noise was still great, and positioning was still fairly critical since the transducer only picked up good signals when the middle was positioned over the artery. An auxillary oscillator was used to boost the voltage reaching the sending crystal, but the only noticeable effect this had was to actually heat the skin in the area. This was judged to be unacceptable and not pursued further because of the possible hazards of ultrasound at high intensities [Alt, 1966]. The larger 20 x 5 mm crystals were judged therefore not to be as effective as the 10 x 5 mm crystals.

Different probe designs such as two concentric washers were considered. However, Wells [1970] indicates that the other popular probe designs would have little to recommend them over the design used, where the crystal angles can be changed so that the convergence of the two beams can be set.

Signals can be detected from blood flow in the aorta, however, the distance from the aorta to the body's surface makes this signal extremely difficult to detect. Light [1969] found he could measure flow in the aorta by positioning his probe between two ribs, while Baker and Cole [1971] found that the suprasternal notch (below the neck) was a good location to measure flow in the aorta. Signals, indeed, could be detected in both regions, but it was found that positioning was an extreme problem. In fact, signals were at times difficult to find at all. Because of the great difficulties in positioning doppler ultrasonic probes, it was felt that other methods might be more useful in pulse detection on ambulatory subjects. The photoplethysmograph is considered in the next section.

PHOTOPLETHYSMOGRAPH

The use of a photosensitive device to monitor flow of blood into a region of the body is not a new idea. Hertzman [1938] showed that the light reflected from the skin varied with the pulsations of blood with each heartbeat. This change in reflected light, the "opacity pulse", is fairly easily monitored with a suitable photosensitive device. The photoplethysmograph is non-invasive and can be used over almost any region of the body, and therefore has proven useful in pulse wave velocity studies. Behrendt and Shawaluk [1968] measured pulse wave velocity between regions of the face using photoplethysmographs to sense the influx of blood into the capillary bed. While Weinman et al. [1971] used them to measure pulse wave velocity between the femoral and dorsalis-pedis artery.

The origin of the opacity pulse phenomenon is not completely understood. What does seem clear is that the pulse represents the flow of blood into the tissue, since there seems to be great correlation between the volume plethysmogram and the photoplethysmogram measured in the same region [Montagna, 1960 and Westenholme, 1954]. Ikegami [1958] did a comparitive study of the photoplethysmogram with other plethysmographic techniques. He found no discrepancy between the photoplethysmogram and the other methods in relation to time courses and in magnitude of spontaneous or vasomotor fluctuations. He concludes, therefore, that the reflection photoplethysmograph represents chiefly features of capillary vessels in superficial layers of skin. With each heartbeat there is a sudden increase in blood influx into the capillary bed due to the arterial pressure increase during systole. The outflow at first is not as great as the inflow, so there is a net increase in volume during systole. However, when the arterial pressure drops in diastole, the rate of outflow is greater than inflow so that by the beginning of the next heartbeat, the net increase in volume is zero. The amount of change in blood volume between the diastolic minimum and the systolic peak is termed the "blood volume pulse."

The origin of the reflected opacity pulse can be more easily understood if one looks at light transmitted through the skin, for instance, the cheek or finger web. The influx of blood into the vascular bed causes a decrease in light transmitted through the tissue. This is easily explained by the fact that blood absorbs light, so the more blood in the tissue, the less light transmitted. Weinman [1965] indicates that a layer of whole normal human blood 1.3 mm thick would transmit only .7% of the incident light at 8050 Å, while a layer of tissue of the same thickness would transmit nearly 50% of the incident radiation. This big difference in transparency makes the photoplethysmographic technique possible.

The "reflectance mode" of photoplethysmography shows a similar phenomenon: more blood present in the tissue causes a decrease in light reflected back to the photocell. To explain these findings it is necessary to look at the mechanisms influencing the reflection of the light. Longini and Zdrojkowski [1968] use a photodiffusion theory to help explain the multiple scattering processes found in biological heterogeneous media. The light incident on the skin is scattered and absorbed by the skin itself and the flesh behind it. Some of the light reemerges (is reflected) after multiple scattering while the rest is eventually absorbed or transmitted. If the skin is considered to be finely grained and divided by planes into many thin elementary sheets parallel to the surface, they deduce the following equations for reflection and absorption of incident Lambertian light:

Transmittance $T(a) = [\cosh(qa) + (k+w)/q \sinh(qa)]^{-1}$

Reflectance $R(a) = k/q\, T(a) \sinh(qa)$

where $k = \sum k_i V_i$ $\quad k_i$ = scattering coefficient of component i.

V_i = volume fraction of component i.

$w = \sum w_i V_i$ $\quad w_i$ = absorption coefficient of component i.

$q = [w(w + 2k)]^{1/2}$

a = the sample thickness

for $qa >> 1$ as for thick samples where almost no light will be transmitted, $\cosh(qa) = \sinh(qa) = 1/2 \exp(qa)$, so the reflectance reduces to:

$$R(a) = k/(q + w + k) \qquad (1)$$

The meaning of k and w can be more easily seen for $a = \varepsilon$, a very small thickness. $T(\varepsilon) = 1 - k\varepsilon - w\varepsilon$ and $R(\varepsilon) = k$ to the first order. So k is the coefficient for the fraction of light backscattered from the elemental sheet, while w is the coefficient for the fraction absorbed. Zdrojkowski and Pisharoty [1970], show that results computed from this theory agree well with experimental findings. For the analysis of the blood volume pulse, it is useful to consider:

$$k = k_T(1 - V_b(t)) + k_b V_b(t) \tag{2}$$

$$w = w_T(1 - V_b(t)) + w_b V_b(t) \tag{3}$$

where:

$V_b(t)$ = time varying volume fraction occupied by the blood.

k_T = scattering coefficient for nonperfused tissue.

k_b = scattering coefficient for blood.

w_T = absorption coefficient for nonperfused tissue.

w_b = absorption coefficient for blood.

The red cells in the blood account for most of the scattering in the blood. This equation considers that there is no difference in coefficients for oxygenated and reduced blood. This only is true at 8050 Å wavelength. For other wavelengths the equation must be further modified to consider the amount of oxygenated and reduced blood. This lends little to the analysis so that it suffices to consider the coefficients for blood to be the weighted average for oxygenated and reduced blood. These coefficients have been determined by Cohen and Longini [1971] to be the following at a wavelength of 8050 Å.

$k_b = 16\ cm^{-1}$

$w_b = 5.1\ cm^{-1}$ for a hematocrit of .40

$k_T = 30$

$w_T = .3$

Calculations for the reflectance change due to a blood volume fraction change from .05 to .15 at 8050 Å in Equations 1, 2, and 3 show the reflectance will vary from .825 at .05 to .765 at .15. Showing that reflectance decreases with increasing blood volumes. A change of from .05 to .15 as might occur under drastic vasodilation is quite large compared to the actual change due to the blood volume pulse. Weinman [1967] indicates that a typical blood volume pulse in a finger may be from 2.17% to 2.24% of tissue volume. Calculations from equations 1, 2, and 3 show that reflectance will vary from .84806 at 2.17% to .84746 at 2.24%. The reflectance also will vary with light wavelength, geometry of the transducer-skin interface, hematocrit and oxygen saturation of the blood. 8050 Å, the near infrared region, however, is the isobestic wavelength for blood, where both oxygenated and reduced blood have the same optical coefficients.

Although this theory seems to adequately explain the opacity pulse, there is some contradictory evidence presented by Heck [1972]. He indicates that when erythrocyte suspensions of fixed volume are made to flow, the amount of light transmitted changes, probably because of the streaming orientation of the red blood cells. This red cell reorientation leads to a change in reflectance. Also, he considers the fact that flowing blood particles tend to move centrally into an axial core. This widens the relatively cell free peripheral plasma zone which may partially account for the change in transparency of the tissue. This indicates that the photoplethysmograph would be influenced very strongly by the velocity of the flowing blood particles. D'Agrossa and Hertzman [1967] in microscopic studies of opacity pulses from individual minute arteries, capillaries, and venous vessels of the frog mesentery, found that indeed the opacity pulse is correlated with the flow velocity rather than the flow volume. A decrease in blood flow with no change in arterial diameter, they found, is accompanied by a decrease in opacity pulse amplitude and a less opaque field. In vitro experiments using a perfusion pump exhibited similar results. Increasing the stroke volume causes an increase in the opacity pulse. To rule out the possibility that the observed effect is due to an unobservable volume pulsation of the vessel, the outflow resistance was increased so that the arterial diameter increased. This diameter increase causes an increase in the opacity (DC) level, however, the preparation showed a decrease in opacity pulse amplitude probably due to the decreased flow velocity. Also of interest, is the fact that no opacity pulses were noted in capillary or venous vessels. There is irregular variation of opacity level in these vessels, probably caused by the random conglomeration and orientation of blood cells. They conclude, therefore, that the opacity pulse is due primarily to the change in orientation of erythrocytes which occurs with change in blood velocity. Heck [1972] agrees stating, "the data available correlating opacity change to direct observations of microvascular activity suggests that amplitude of the opacity pulse wave is related more closely to changes in flow velocity than necessarily to changes in volume flow." For observations over larger non-microscopic areas, the integrative effect of all the vessels and the effect noted by D'Agrossa and Hertzman of the increase in opacity DC level caused by increased vessel diameter must be taken into account. Whether the photoplethysmogram is best described by particle velocity or by the percent volume of blood in the skin is a conjecture at this time. In any event, the use of the opacity pulse to determine the arrival of the pressure pulse in the tissue seems to be valid.

The reflection of light from the tissue, then, shows changes due to the inflow of blood with each heartbeat as well as changes occurring over a longer time course caused by various effects. Factors which may influence the pulse with each heartbeat include; increased blood volume in systole, changing distribution of the blood volume from a single heartbeat, changes in blood velocity through the microvessels and possibly changes in the refractile properties of the wall itself with change in transmural pressure gradient and vessel wall thickness [Heck, 1972]. Changes occurring at a rate independent of heart rate include; changes in volume and velocity of flow caused by pressure gradients due to the respiratory cycle or vasomotor activity, changes in concentrations of oxygenated and reduced hemoglobin, changes in hematocrit, contraction of underlying muscle in the region being monitored as well as other effects such as the gravitational force on the blood column, and changes in arterial pressure. Control of vasoconstriction is at both local and central levels. Changes in local temperature and core temperature cause changes in blood flow to the extremities. Also, circulating hormones affect vasoconstriction as well as signals from the sympathetic nervous system.

So far consideration has been given only to the opacity pulse monitored in the microcirculation. It is also possible to use the photoplethysmograph to monitor volume pulses in the major surface arteries. This was first noticed by Hertzman [1938]. He found that the movement of the skin in the vicinity of pulsating arteries, such as the radial artery, could be monitored by a light and photocell located strategically over the artery. Weinman [1965] claims that the actual pulsatile change in arterial diameter can be monitored although it is not clear that this effect is not due to movement of the transducer caused by pulsations of the artery, since he says that "one has to be careful to use the minimum pressure sufficient to hold the transducer in place, otherwise a distortion in the shape of the blood volume pulse will occur." Further experiments [Weinman, 1972] show that while monitoring pulses from larger peripheral arteries an inverse plethysmogram may be obtained. That is, instead of recording the normal "more blood = less light" it was found that in certain locations near major arteries the inverse relation, "more blood = more light", was found. Investigations of pulses from agar blocks with imbedded blood-filled rubber tubings showed that the photosensor output contained three components: "A) due to the absorption of back-scattered light by the blood-filled tube; B) due to reflection from the background (blocks were placed on both white and black surfaces); C) due to reflection from the tube surface. The relative intensity of these three components sometimes creates conditions which are responsible for the appearance of the inverted plethysmograms." Although this idea seems reasonable, it is also possible to explain these findings by the fact that the skin in the vicinity of the pulsating artery moves in two directions. The skin directly over the artery, moving upwards, while the skin displaced from the center of the artery moves slightly down and laterally. Also, if the transducer were not firmly enough attached to the skin, the pulsations of the artery could have various effects on the transducer-skin interface. Another factor which must not be overlooked is that the flow into the vascular bed over the artery could be influenced by the pulsations of the underlying artery, with the result that in certain regions the pressure of the artery pressing the skin against the transducer could actually cause a decrease in skin perfusion near the artery during systole. Other experiments by Weinman [1972] with simultaneous recordings of intra-arterial pressure and arterial plethysmograms led to the conclusion that the plethysmogram does actually reflect blood volume changes in the artery and consequently variations in arterial diameter. Indeed it seems as though quite good tracings can be recorded from the carotid artery (see Figure 13), however, this may be the result of movement of the transducer over the artery. The photoplethysmograph seemed to be a promising method to monitor blood pulsations at various points on the body. It was felt that if the signal from the major arteries could not be used successfully, it might be possible to monitor blood flow into the vascular bed of the skin on the back, which might give a good indication of pulse wave velocity in the aorta.

PHOTOELECTRIC TRANSDUCER

Development of an adequate photoelectric transducer, which will be highly sensitive and relatively free from movement artifacts is an important consideration. It was initially thought that a differential technique could be used to reduce noise due to ambient light and movement artifacts caused by slight changes in the geometry of the transducer-skin interface. This technique has been used by Bracale et al. [1969] and Fuller [1972]. They consider the principle of operation to be that the blood absorbs light more strongly in the red region of the spectrum than in the blue and green regions. Therefore, if two photosensitive devices are used side by side as shown in Figure 4, the red filtered cell will receive a stronger pulse signal than the green filtered one. However, noise artifacts caused by ambient light and movement of the transducer should affect both cells relatively equally. Considering Sr and Sg the pulse signals from the red and green channels and Nr and Ng the noise signals from the red and green channels, it is seen that the signal to noise ratio will be different for the two channels:

$$\frac{Sr}{Nr} \neq \frac{Sg}{Ng}$$

When the gain of the green channel is adjusted so that the artifacts on both channels will have equal amplitude, that is, Nr = Ng, the pulse signal will still be greater in the red channel. The subtraction of the two signals, in a differential amplifier should cause cancellation of the noise signals, while the pulse signal will still remain.

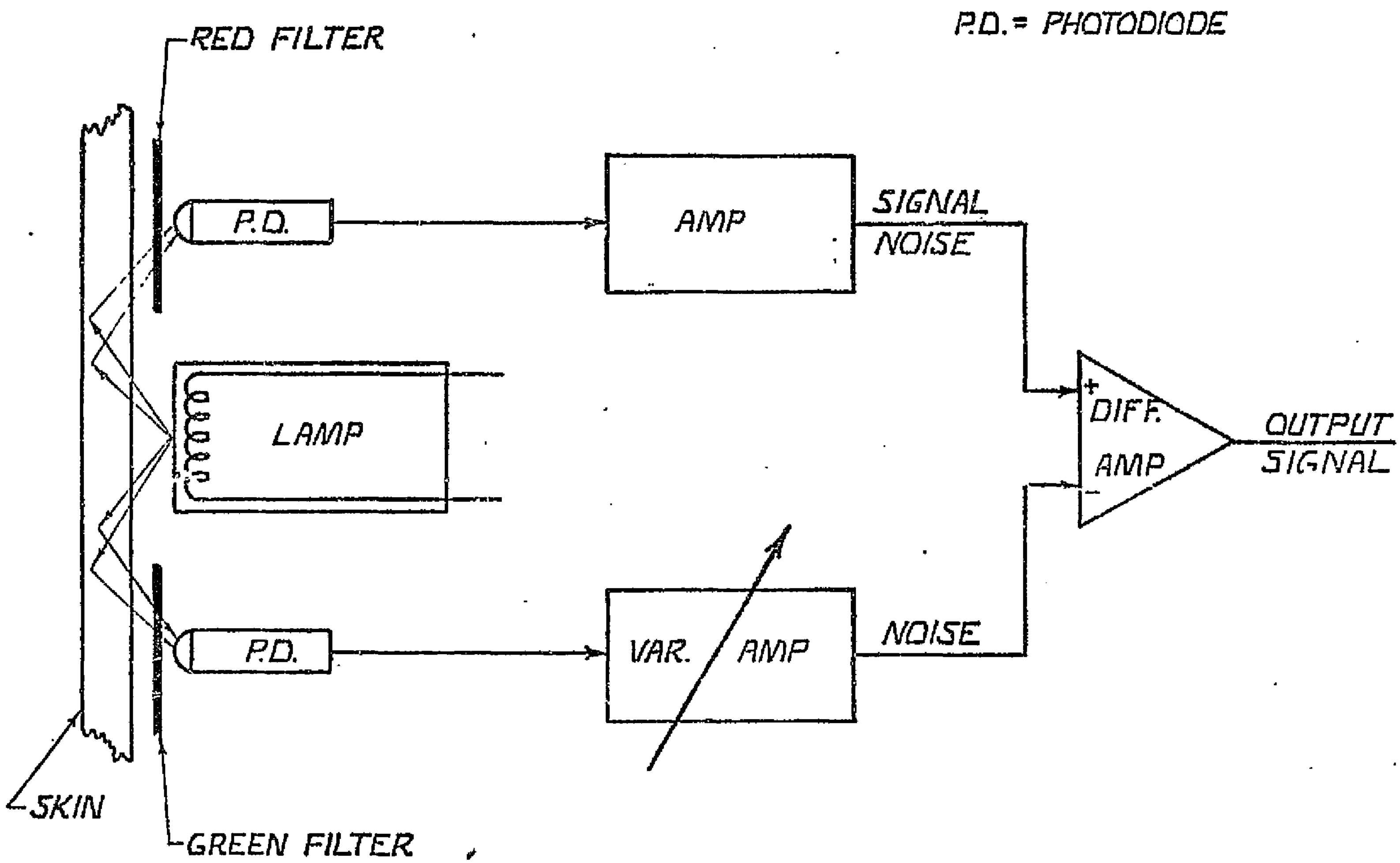

DIFFERENTIAL DEVICE

FIGURE 4

Bracale et al. [1969] describes experiments in which a differential phototransducer is used in vitro to reduce noise from a clear rotating disk filled with blood. The disk contained blood at two concentrations and a semitransparent strip on the disk is used to produce the noise signal. Indeed, using the differential technique reduced the noise amplitude for this in vitro experiment. However, results from in vivo experiments were not shown. Whether this technique is useful for patient monitoring must still be decided.

More recently, Fuller [1972] has built and tested a differential phototransducer. It is difficult to judge from his report what type of noise is actually eliminate by his device, but it seems as though 60 cycle noise from room lighting can be greatly reduced, along with other noise which may be due to movement although he doesn't say this. The device was physically too large to be used conveniently over most areas of the body. It seemed that Fuller's device was not really adequate, even for testing purposes, because of its large size, inadequate shielding from ambient light, and the large distance between the photosensors. Therefore, a smaller device was designed and constructed from an indicator lamp socket as shown in Figure 5. Type 1N2175 photodiodes with sensitivity of 22.3 $uA/mw/cm^2$ and a broad spectral response were used as the photosensors. The first stage of amplification (see Figure 6) was mounted directly on the lamp socket to help reduce noise. An infrared filter (Kodak 89-B wratten gelatin filter) or a red filter were used for the "signal" channel, while a green filter with peak transmittance at 5000 A (Kodak 64) or a blue filter with peak transmittance at 4200 A (Kodak 47-B) were used to monitor the "noise." The gains of the amplifiers were adjusted

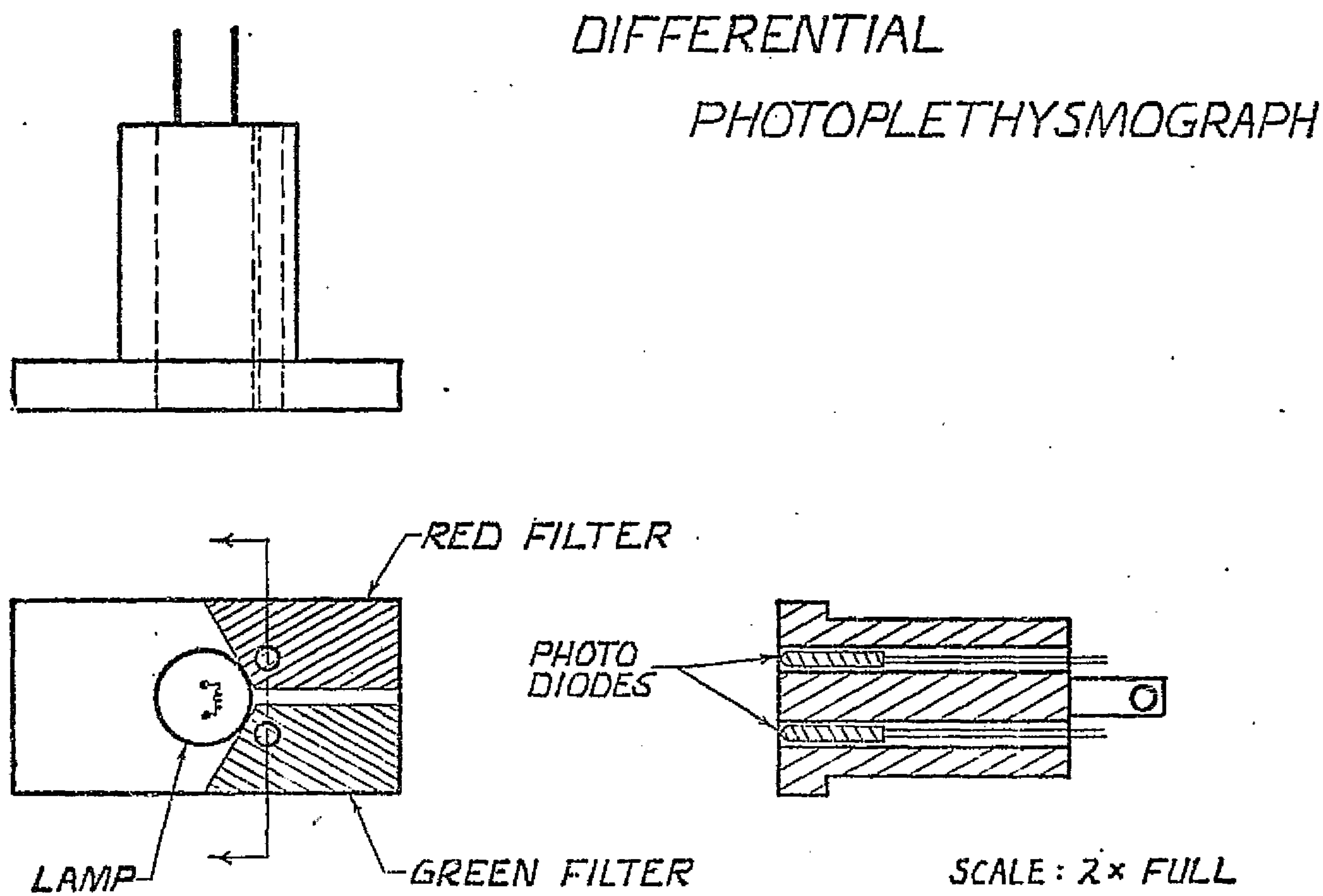
DIFFERENTIAL
PHOTOPLETHYSMOGRAPH
RED FILTER
PHOTO DIODES
LAMP
GREEN FILTER
SCALE: 2× FULL

FIGURE 5

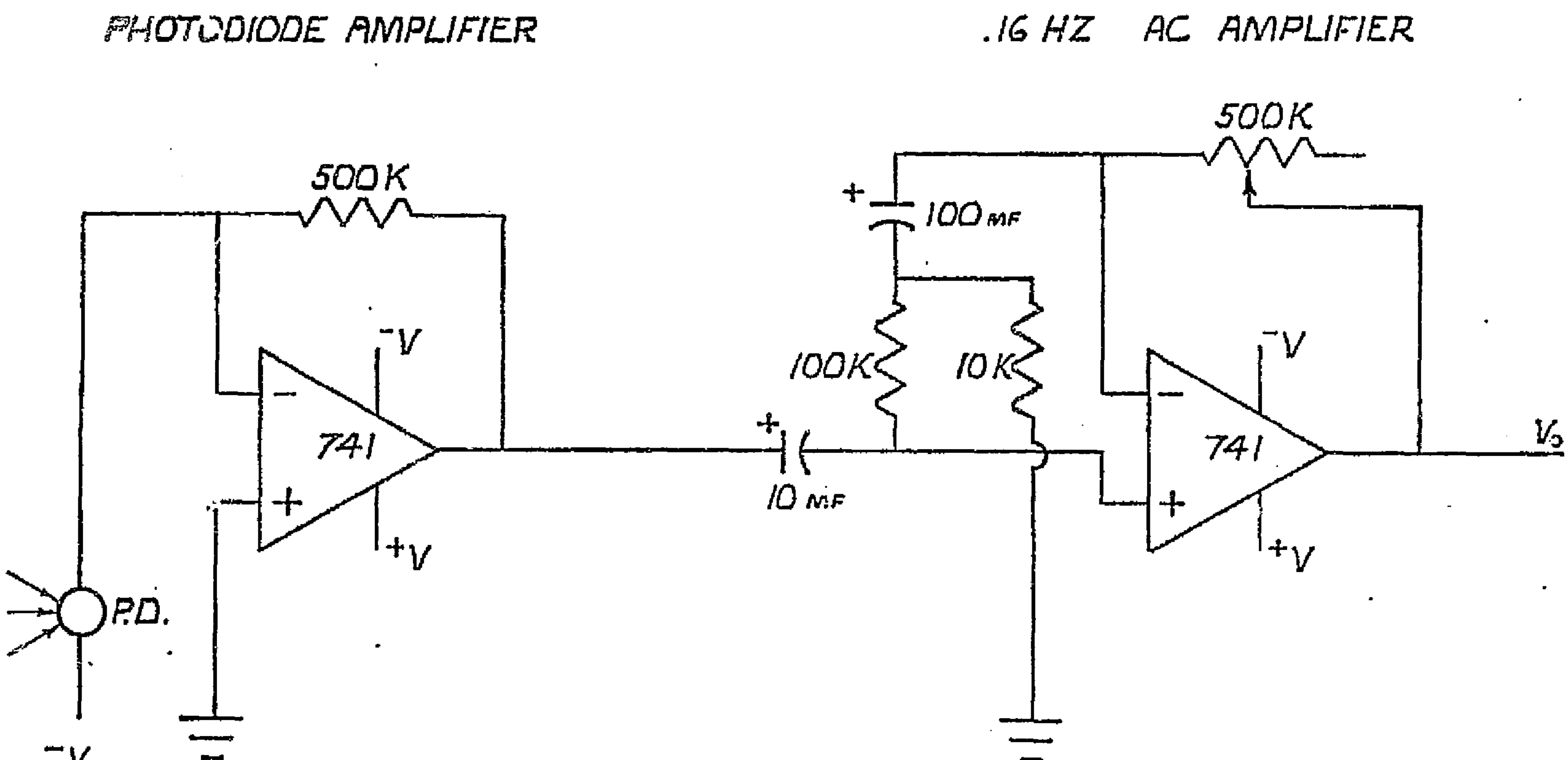

PHOTODIODE CIRCUIT

FIGURE 6

so that the noise caused by slight movements of the transducer on each channel was of equal magnitude. The signals were subtracted and displayed using the oscilloscope. As can be seen from Figure 7, the outputs from both channels were nearly equal in magnitude. Thus, subtracting the signals resulted in not only reducing the noise, but reducing the signal to a large extent, as well. For large magnitude signals as obtained from highly perfused skin areas such as the finger tips, it is possible to juggle the gain so that a good signal results and the noise level may be slightly reduced. However, the gain needed seems to vary over long periods of time and with slight change in position of the transducer, possibly due to changes in skin color and geometry of the skin-transducer interface. It can be also seen from Figure 7 that the signal from each channel is relatively free of noise compared to signals obtained by Fuller's [1972] device. Also, in contrast to Fuller's findings, it was possible to obtain relatively good signals from regions such as the stomach and back, from each channel individually. However, when the channels were subtracted the signal level was too close to the noise level of the amplifiers and photodiodes to be useful. Figures 8 and 9 show signals obtained from the stomach and back respectively, for a single channel and the two channels added to increase the gain. Results were similar for all combinations of filters. Because of the poor functioning of the differential device, it was decided to analyze more carefully the function of the device using a very simple model. If one considers two wavelengths of light, λ_1 and λ_2; S, the reflectance of the skin; $V_b(t)$ the volume of blood varying with time; A, the absorption coefficient

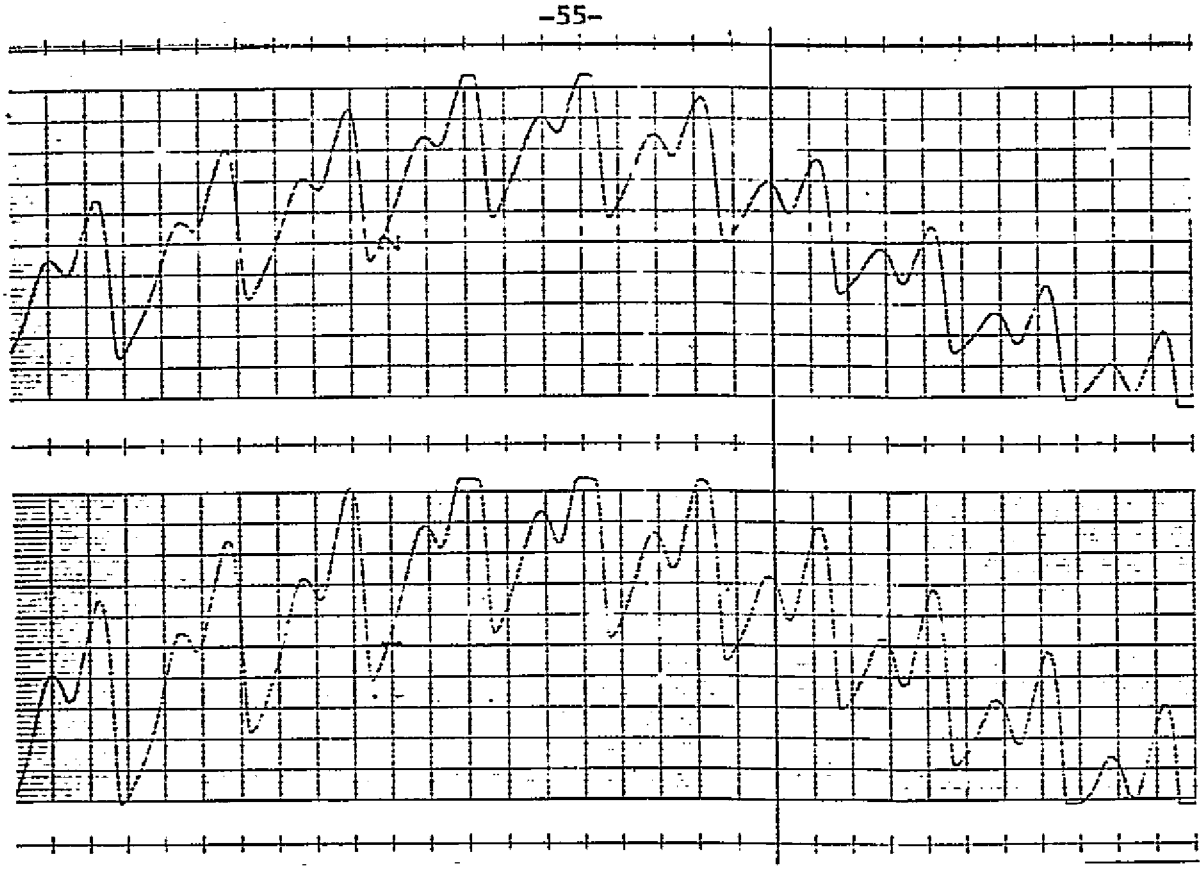

FIGURE 7

Top: Green Filtered Finger Pulse

Bottom: Red Filtered Finger Pulse

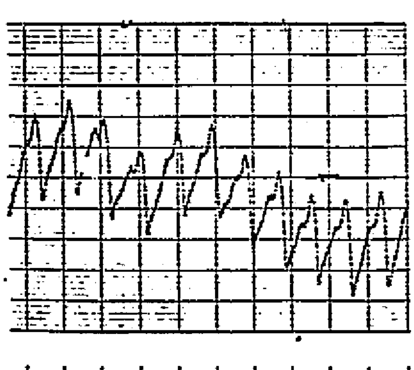

FIGURE 8

Stomach Pulse, Red Channel

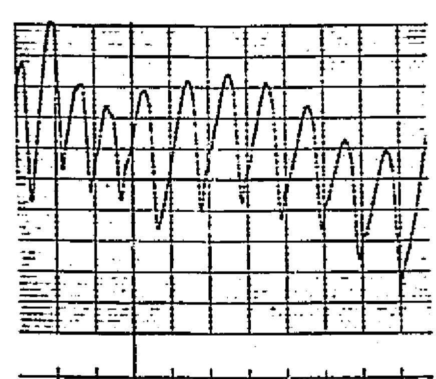

FIGURE 9

Back Pulse, Channels Added

C. 3

of the blood; $G(t)$, the geometric factor for the skin-photocell interface; and L_i, light incident. Then the output X for the λ_1 channel can be found approximately from:

$$X(\lambda_1) = L_i G(t)[S(\lambda_1) - V_b(t)A(\lambda_1)]$$

The output from the λ_2 channel can be found approximately from:

$$X(\lambda_2) = L_i G(t)[S(\lambda_2) - V_b(t)A(\lambda_2)$$

If $X(\lambda_2)$ is scaled by Y and subtracted from $X(\lambda_1)$ the differential output can be found.

$$X = X(\lambda_1) - YX(\lambda_2) = L_i G(t)[(S(\lambda_1) - YS(\lambda_2)) - V_b(t)(A(\lambda_1) - YA(\lambda_2))]$$

If Y is chosen to cancel the effects of transducer movement with respect to the skin:

$$S(\lambda_1) - YS(\lambda_2) = 0$$

so that,

$$X = L_i G(t)[-V_b(t)(A(\lambda_1) - YA(\lambda_2))]$$

It is seen that the variance of the geometric factor will still affect the pulse signal, so that from this analysis the differential technique cannot completely reduce the noise. Furthermore, an approximation of the signal to noise ratio can be made for the single channel and the difference of the channels signals. For the single channel at frequency λ_1, the pulse signal will have magnitude of approximately $L_i V_b(t)A(\lambda_1)$ if the geometric factor, $G(t)$ is considered equal to one in the normal position. When movement of the transducer occurs, $G(t)$ will vary, so a noise signal of approximately $L_i G(t)S(\lambda_1)$ will result since the factor

$-L_iG(t)V_b(t)A(\lambda_1)$ is negative and will tend to reduce the noise level to a degree. Then, in the worst case, the signal to noise ratio for the λ_1 channel is approximately:

$$\frac{V_b(t)A(\lambda_1)}{G(t)S(\lambda_1)}$$

For the difference equation the pulse signal amplitude is similarly $L_iV_b(t)[A(\lambda_1) - YA(\lambda_2)]$, and the noise will be $L_iG(t)[A(\lambda_1) - YA(\lambda_2)]$. So the signal to noise ratio is then:

$$\frac{V_b(t)}{G(t)}$$

Since $S(\lambda_1) > A(\lambda_1)$, it is seen that the differential signal will generally have a greater signal to noise ratio than the single channel signal as long as $L_iV_b[A(\lambda_1) - YA(\lambda_2)]$ is sufficiently large to keep the signal level much greater than the differential mode noise in the system. For low level signals, as obtained from the back, the differential technique unfortunately does not give good results because of the low signal levels.

It was decided to concentrate on construction of a small, single channel, extremely sensitive photoplethysmograph. A transducer was built from a 14 pin IC socket. Holes were drilled for a pinhead sized LS600 phototransistor and a 715 miniature light. The device worked well, but the sensitivity was not great enough to record signals from the back or stomach. In a personal communications, Weinman [1972] indicated that a photoconductive cell might perform better for this application, since its detectivity is nearly the same as a photodiode's and it is more immune to environmental noise because of its greater output signal. The photoconductive cell has certain disadvantages, in that its output is temperature and light history dependent, and the rise time is slow compared with a phototransistor. However, for the purpose of pulse monitoring the output may be AC coupled so that drift caused by temperature or light history dependence should not be a problem. Also, Weinman and Yaakov [1965] indicate that the response time of CdSe photoconductive cells is only 8 to 10 msec. to reach 63% of their final value. This is equivalent to an upper 3 db point of 16 to 20 cycles per second. This is probably quite adequate for reproducing the high frequency components of the systolic upslope without great attenuation. The CdSe photoconductive cell has advantages, in that it is readily available, rugged, low in cost, and easily instrumented. A CdSe cell photoplethysmograph was therefore built as shown in Figure 10. This was modeled after a transducer described by Weinman [1967]. Two miniature, 715, 5 volt lamps are used to illuminate the tissue. A Clairex CL903 photocell .21 inches in diameter and .15 inches high is used to monitor reflected light. Both the bulbs and the photocell are force fit into cutouts in an one-eighth inch thick, black rubber mount. Shielded twin lead phonopickup cable is attached to the bulbs and the photocell. The leads are anchored to the rubber by means of heavy black thread sewn to the rubber. Another, thinner black rubber piece is used to cover the wiring and back of the components. The front and back are held together by means of narrow bands of Scotch "magic" tape. The tape also covers the bulbs to help diffuse the light and slightly insulate the skin from the hot bulbs. To help reduce noise from ambient lighting, an infrared filter, type Kodak 89B, is taped over the photocell. This filter has almost no effect on .

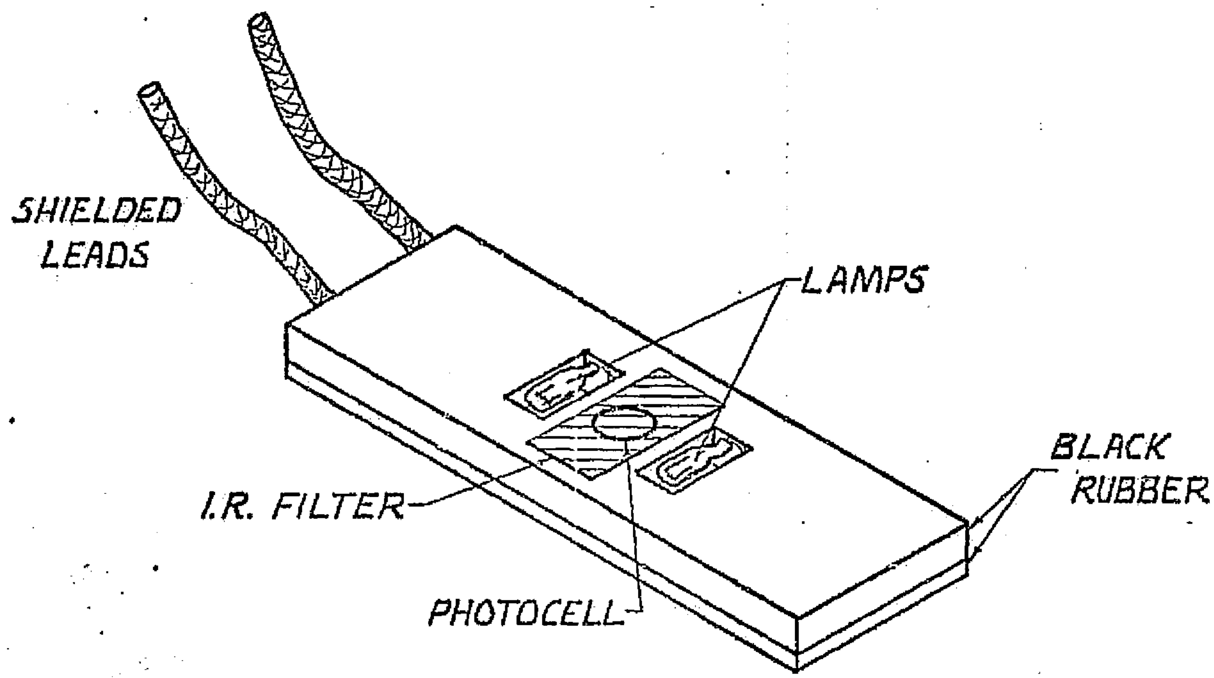

SCALE: 2 × FULL.

PHOTOPLETHYSMOGRAPH

FIGURE 10

the signal from the blood volume pulse, while greatly reducing noise from room lights. The complete device is light in weight, compact, and rugged. Also, it is easily mounted by tape or straps to almost any part of the body since the rubber mounting surface allows the transducer to fit body contours, while still providing a fairly good seal for preventing stray light from reaching the photocell or skin surface under the transducer.

Instrumentation for the photoplethysmograph is shown in Figure 11. Changes in light level with the blood volume pulse cause corresponding changes in the conductance of the photocell. More blood causes a reduction in light reaching the cell which causes a decrease in conductance of the cell. This decreases the current through the cell, which appears as a decrease in voltage across the potentiometer. This level is amplified by an AC amplifier with a cutoff frequency of .16 Hz. This cutoff frequency according to Weinman and Yaakov [1965] is adequate for good reproduction of the pulse waveform, while still retaining a fairly good baseline stability. For certain experiments, the DC level of the signal was needed. This was obtained by placing a DC amplifier with offset voltage adjustment in parallel with the AC amplifier. By waiting a few minutes for temperature stabilization of the cell, DC level changes over short periods can be recorded. The lamp intensity is controlled by a potentiometer, and should be set at the highest intensity which will not cause pain from the heat of the bulbs, if maximum signal levels are required.

Results with this device are quite good. Large signals are easily obtained from the fingers. Signals from other regions, such as

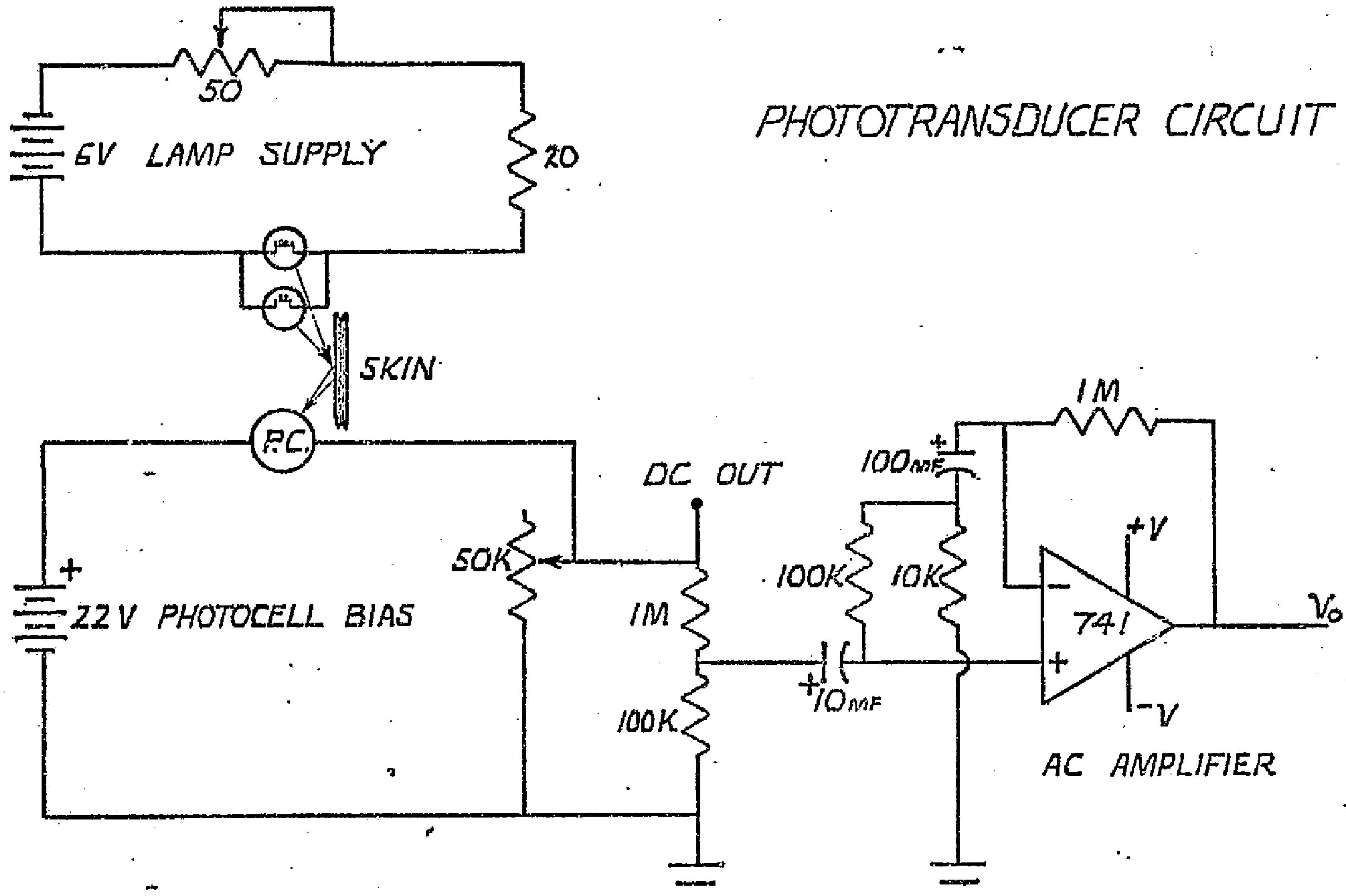
PHOTOTRANSDUCER CIRCUIT
50
6V LAMP SUPPLY
20
SKIN
P.C.
DC OUT
+
22V PHOTOCELL BIAS
50K
1M
100K
100MF
+
100K
10K
1M
+V
741
-V
V_o
+10MF
AC AMPLIFIER

FIGURE 11

the back and stomach are of smaller amplitude because of smaller tissue perfusion in these regions, however, after a minute or so, the heating effect of the lamps causes an increase in skin blood flow which then gives good pulse signals. Typical output waveforms are shown in Figure 12. Since this photoplethysmograph, although possibly not the best possible gives adequate signals for further physiologic experiments, two identical photoplethysmographs with dry cell battery supply were mounted in a 5" x 6" x 9" aluminum box for clinical use.

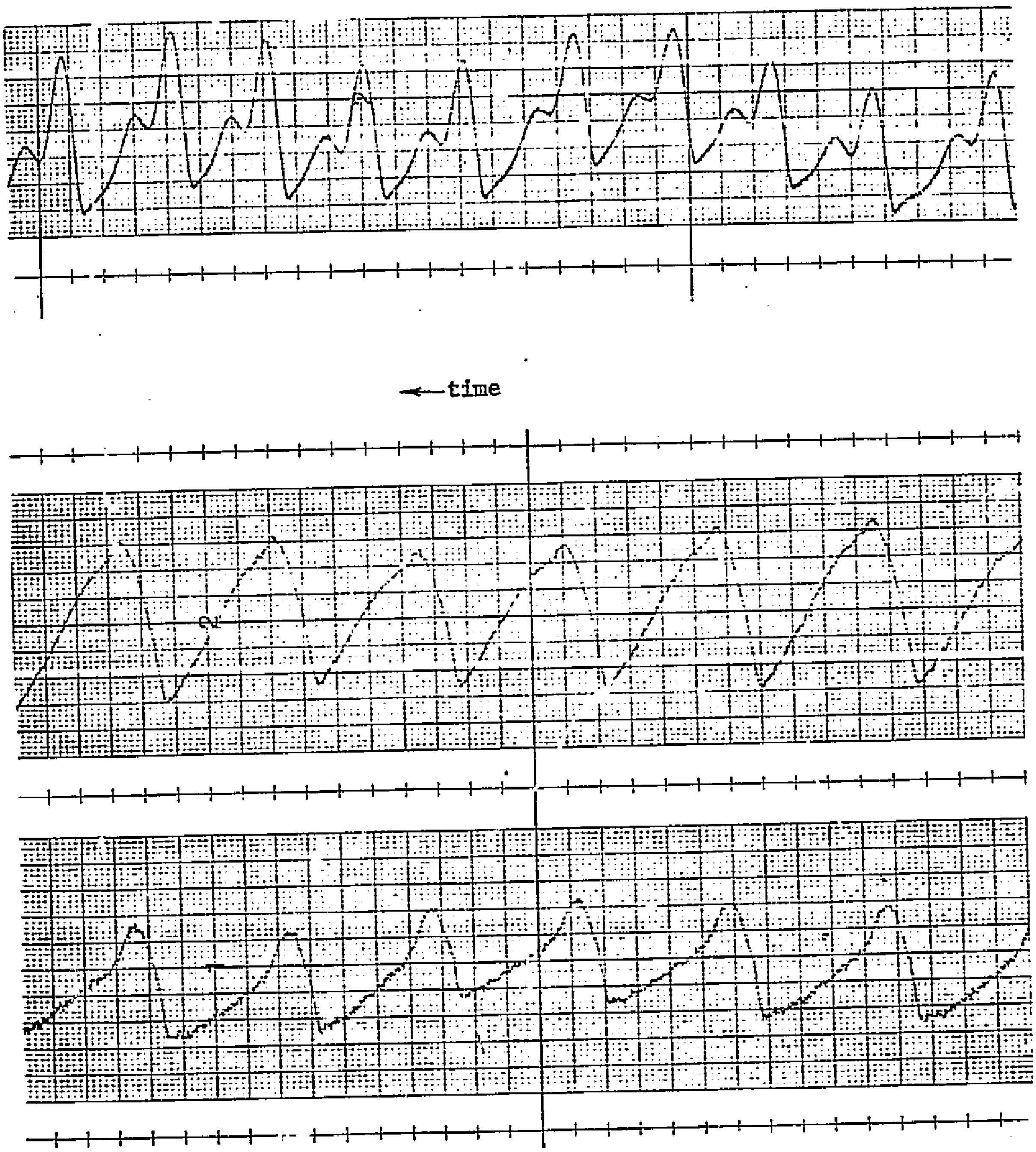

FIGURE 12

Top: Finger Pulse

Middle: Upper Back Pulse

Bottom: Lower Back Pulse

EXPERIMENTS

1. Pulse Sensing in Major Arteries

The photoplethysmogram can be used in two modes to pick up pulses from the major arteries as previously mentioned. It was found that in most normal patients the device can pick up quite good carotid pulse signals if the transducer is held lightly over the carotid artery directly under the chin with an elastic strap. In this case it , that the transducer is actually moved by the pulsation of the y so that the geometric factor of the light-skin interface changes. s gives tracings that very closely resemble the normal carotid pulse (see Figure 13). The signal is easy to locate, but since the transducer is not firmly attached to the skin, patient movements cause artifacts and may shift the transducer out of position. Depending on positioning and strength of the mechanical pulsation, this mode of operation produces signals two to ten times greater in amplitude than the other mode, in which the transducer is held quite firmly over the carotid artery in the mid-neck region (see Figure 14). In this case, it seems possible that the signal is caused by the change in skin reflectivity in the region when the artery changes diameter. However, other factors such as blood flow to the skin under the transducer and slight movements of the transducer may also be influencing the signal. This method seems quite immune to movement artifacts as can be seen in Figure 15b. This figure shows the pulse signal from the carotid artery in the mid-neck region when the head is turned. A second channel in this figure shows for comparison the output from a doppler ultrasonic

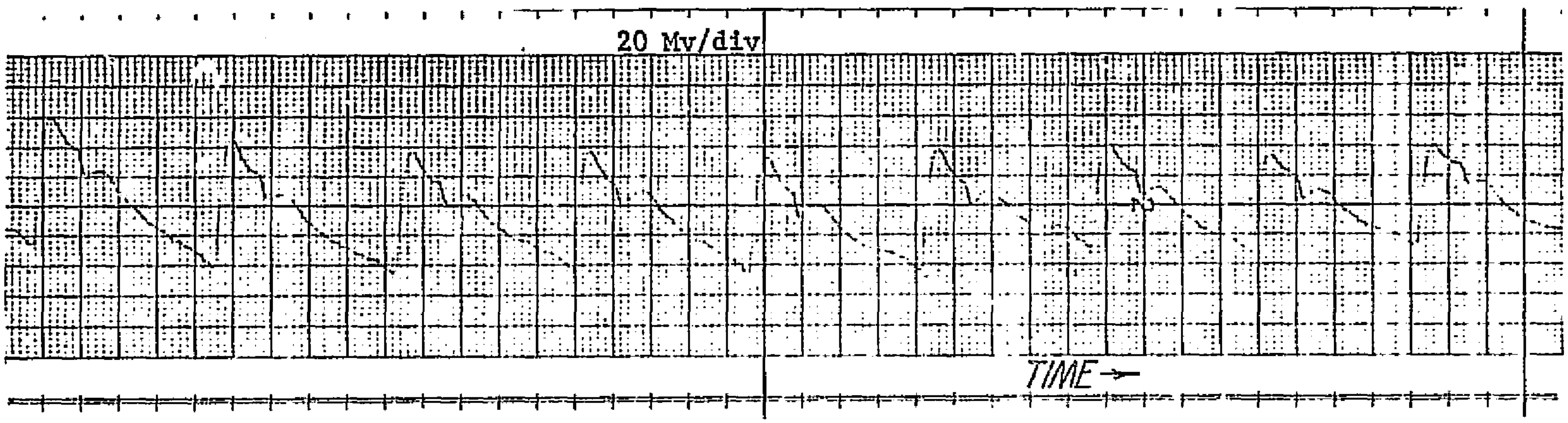

FIGURE 13

Photoplethysmogram of Carotid Pulse with Transducer Loosely Attached

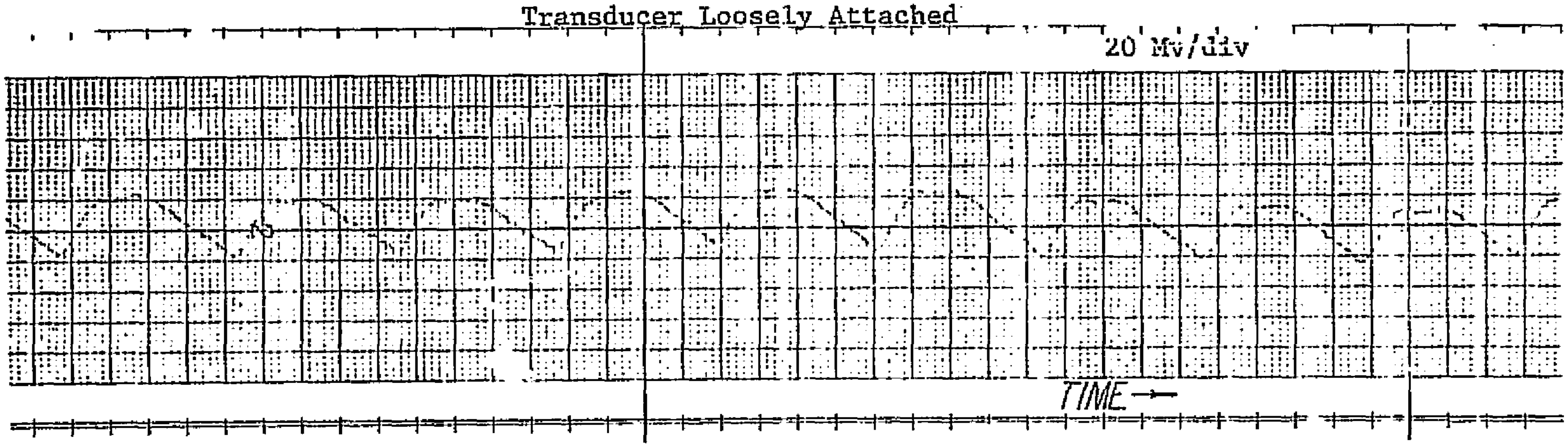

FIGURE 14

Photoplethysmogram of Carotid Pulse in Midneck Region

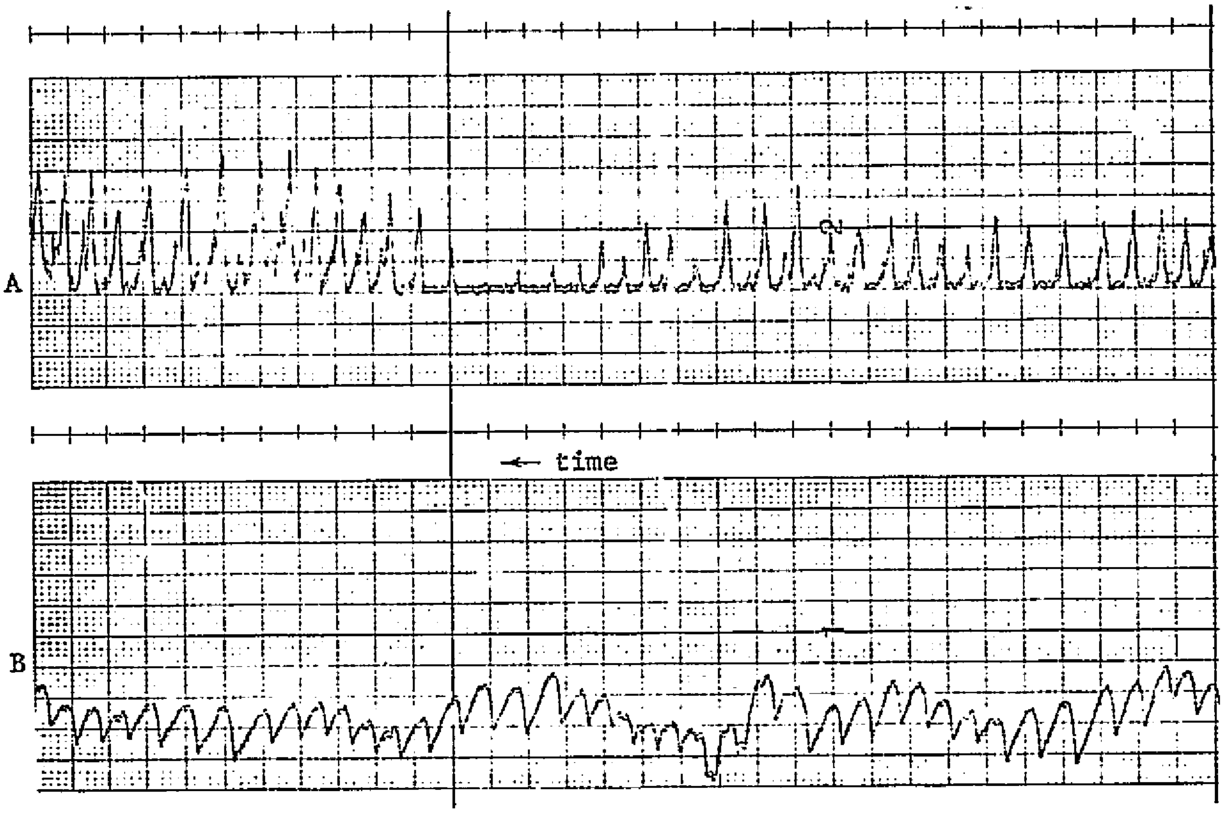

FIGURE 15

A) Doppler Ultrasonic Transducer Neck Pulse

B) Photoelectric Transducer Neck Pulse as Head Turns

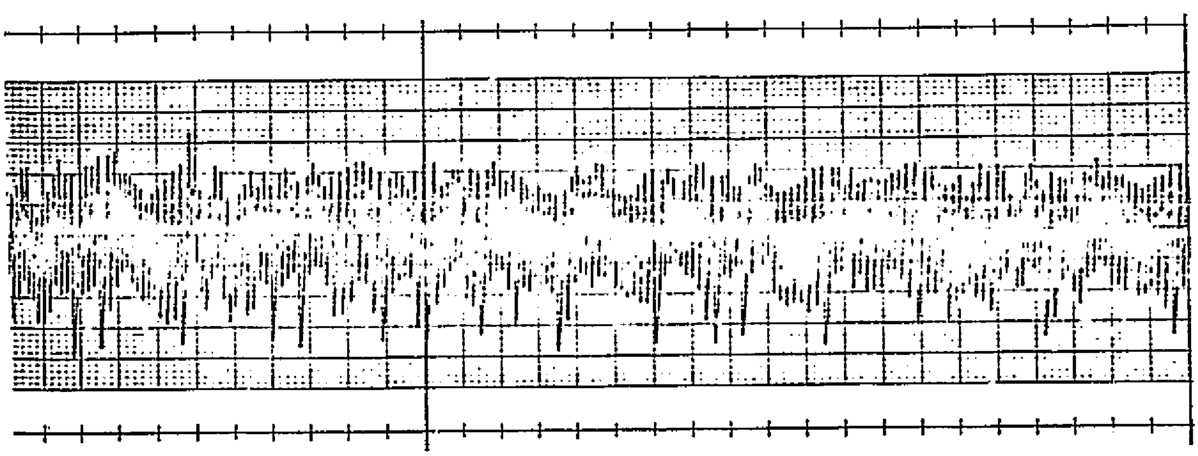

FIGURE 16

Back Pulse on Walking Subject

transducer mounted over the other carotid artery. It is seen that the photoelectric transducer in this mode of operation is less sensitive to movement than the doppler ultrasonic device. Although the carotid pulse is easy to find, more difficulty is experienced in monitoring the femoral pulse. On cooperative subjects, it is possible to monitor the femoral pulse by lightly strapping the photoelectric transducer directly over the artery. However, any patient movement gives rise to noise, and often causes loss of the signal. This same problem of course occurs with the doppler ultrasonic probe as well. For use on cooperative subjects, a mechanical type transducer as already described probably functions as well as the photoelectric or doppler ultrasonic transducers. In cases where the patient is apt to move frequently, there is presently no good way to monitor the arterial pulsations. For this reason a new approach to the problem of measuring pulse wave velocity was tried.

2. Experiments on the Back

When there is adequate blood flow to the skin of the back, very good pulse waveforms may be recorded using the photoplethysmogram. Furthermore, if the transducer is firmly attached to the skin, for example by an adhesive tape such as Elastoplast, the signal is relatively insensitive to artifacts. Figure 16 illustrates the output from the photoplethysmogram, mounted with Elastoplast directly under the scapula about 4 cm from the spine. This tracing was taken as the patient was walking normally. It is seen that the signal is relatively noise free. Other movements, such as arm movements don't greatly affect the signal either. Therefore, it seemed advantageous to monitor the pulse on two regions of the back. Although this method doesn't directly measure the pulse wave velocity in the aorta, it may be possible to correlate the signals from the back with the aortic pulse wave velocity. It can be seen from Figures 17 and 18 that the arteries which vascularize the skin regions in the back come directly from the aorta at various levels [Sabotta, 1957]. This can be schematically represented as shown in Figure 19. It may be possible to find two arterial paths from the aorta to the skin which exhibit similar pulse propagation times. Or it may be possible to find two paths which show a specific difference in delay times under varying physiologic conditions. If so, the aortic pulse propagation time between the origin of these two branches may be determined. For example, if t_2 equals t_7, then the time delay of the pulse from A to B is equal to $T_7 - T_2$. Difficulties, of course, arise in finding the regions of the skin C and D where the time delays from the aorta will be equal or always differ by a given amount.

The idea of measuring pulse propagation times from the skin of the back, therefore, seemed quite interesting and unique, since it seemingly has never been done before. So, experiments were performed to determine if the propagation times to regions of the back in any way reflect the aortic pulse wave velocity. Time delays from the carotid pulse (measured also with a photoplethysmograph) to regions of the back were measured on a number of normal subjects, age 21 to 25 years. The results are shown in Table 3 and the graph in Figure 20. The time delays were measured from a high speed (125 mm/sec) chart recording as shown in Figure 21. The average time delay for a few beats is computed.

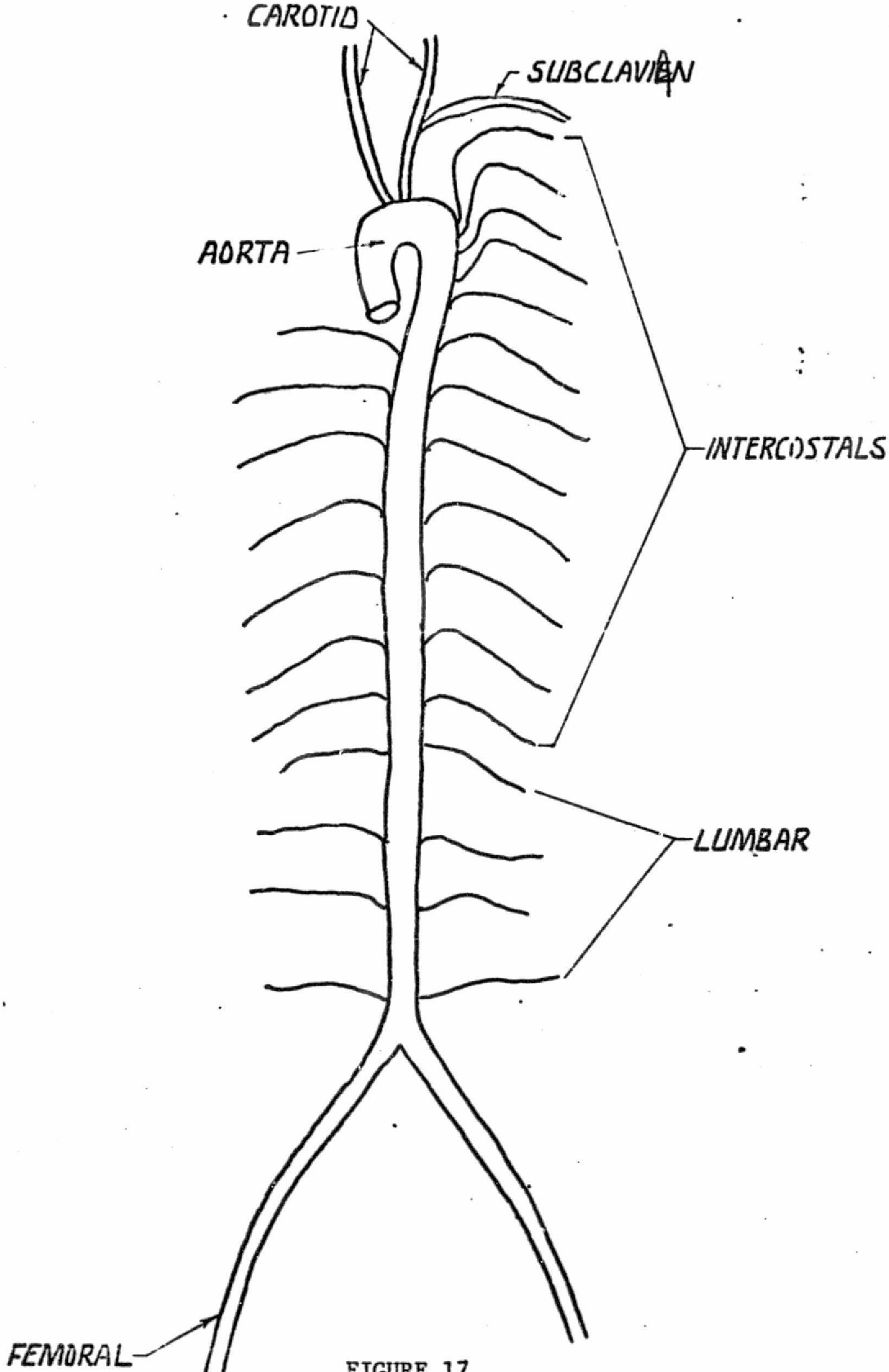

FIGURE 17
Arterial Tree

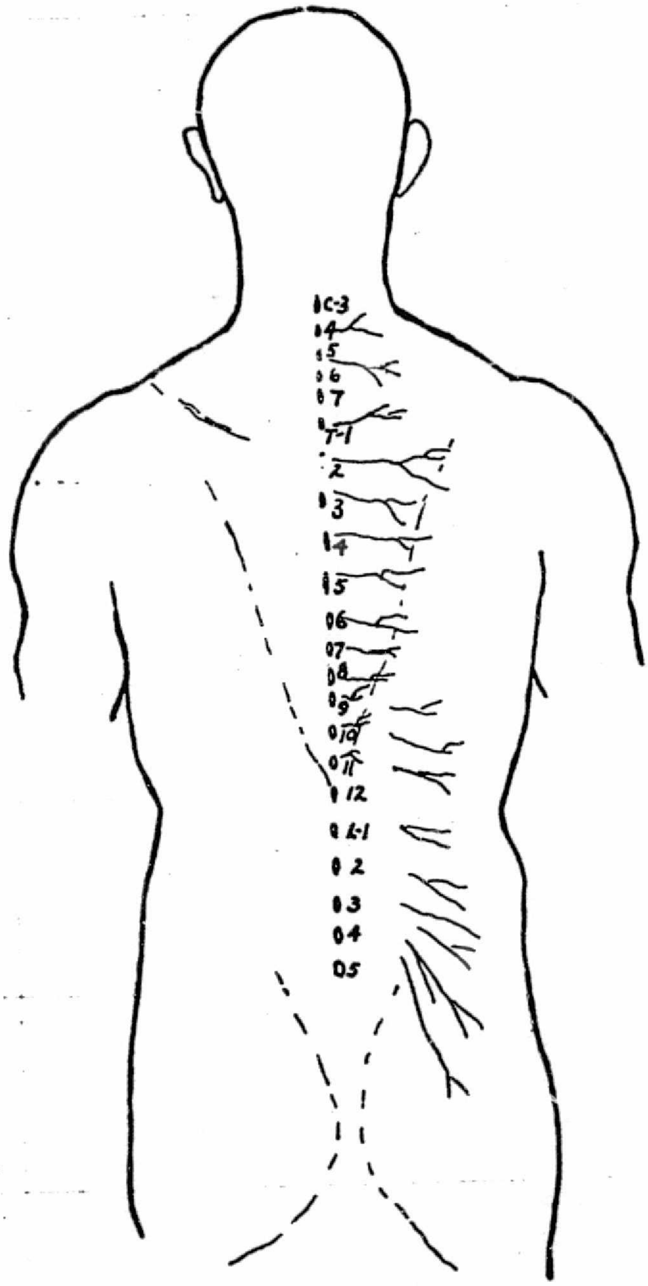

FIGURE 18
Arteries to the Skin of Back

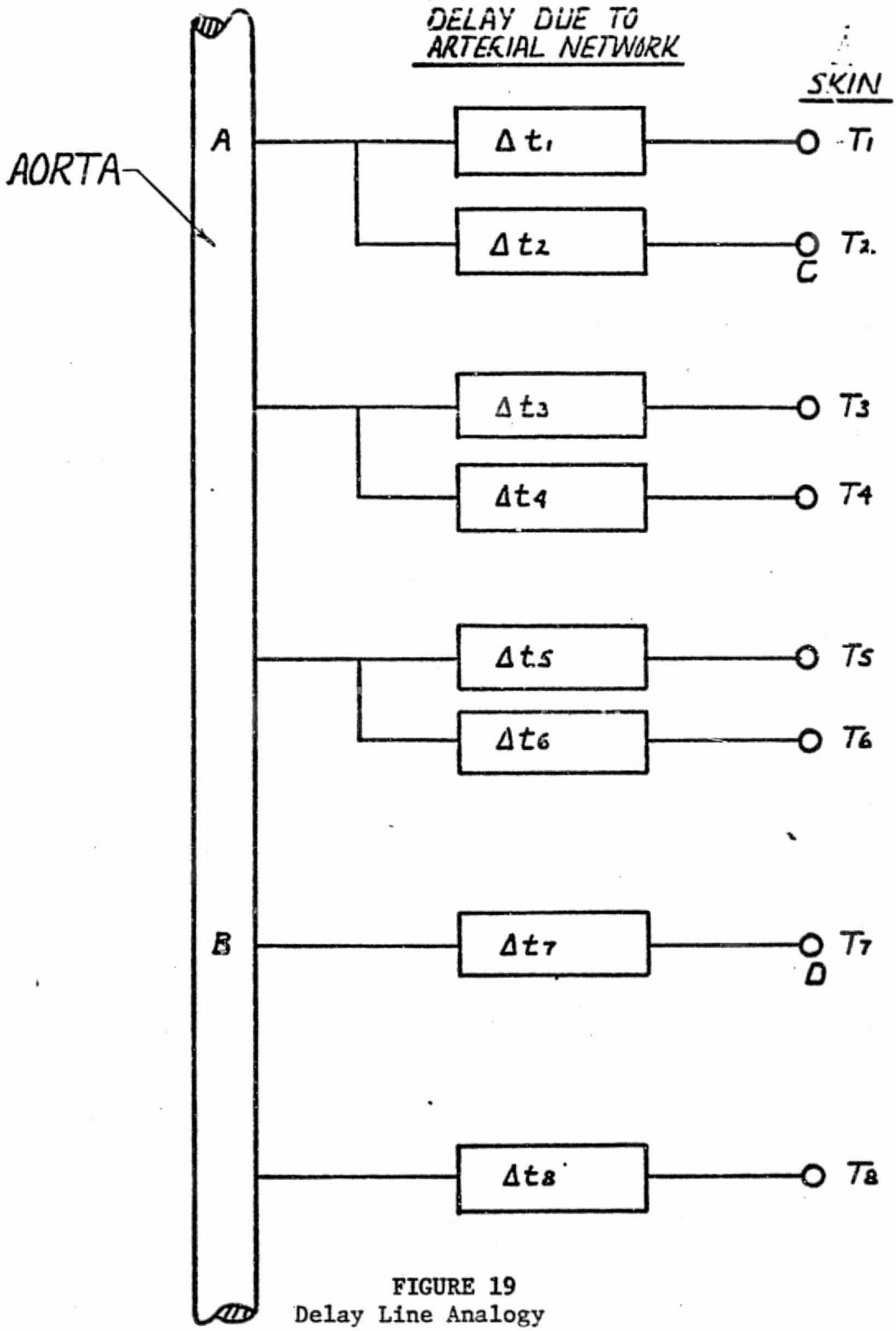

FIGURE 19
Delay Line Analogy

TABLE 3

SUBJECT	DISTANCE FROM TOP OF THE SHOULDER IN CM IN A VERTICAL LINE 7CM FROM SPINE	CAROTID TO BACK TIME DELAY IN MSEC	α
1	0	24	4.8
	6	28	5.1
	12	30	5.0
	18	30	4.8
	24	44	4.8
	30	64	9.0
	36	72	6.0
	42	80	3.6
	48	88	4.0
2	0	28	4.0
	6	32	6.0
	12	36	3.0
	18	40	5.0
	24	48	5.0
	30	64	4.0
	36	72	6.0
	42	84	4.0
	48	96	5.0
3	0	12	4.8
	6	16	5.1
	12	20	2.1
	18	16	6.1
	24	38	5.8
	30	44	4.0
	36	52	5.2
	42	62	2.1
	48	84	4.0
4	0	28	5.0
	6	24	3.0
	12	24	5.0
	18	28	3.0
	24	36	7.0
	30	52	6.0
	36	64	4.0
	42	70	5.2
	48	80	2.5
5	0	24	5.0
	6	28	4.0
	12	28	3.0
	18	28	4.0
	24	44	5.0
	30	68	6.0
	36	92	5.0
	42	98	3.0

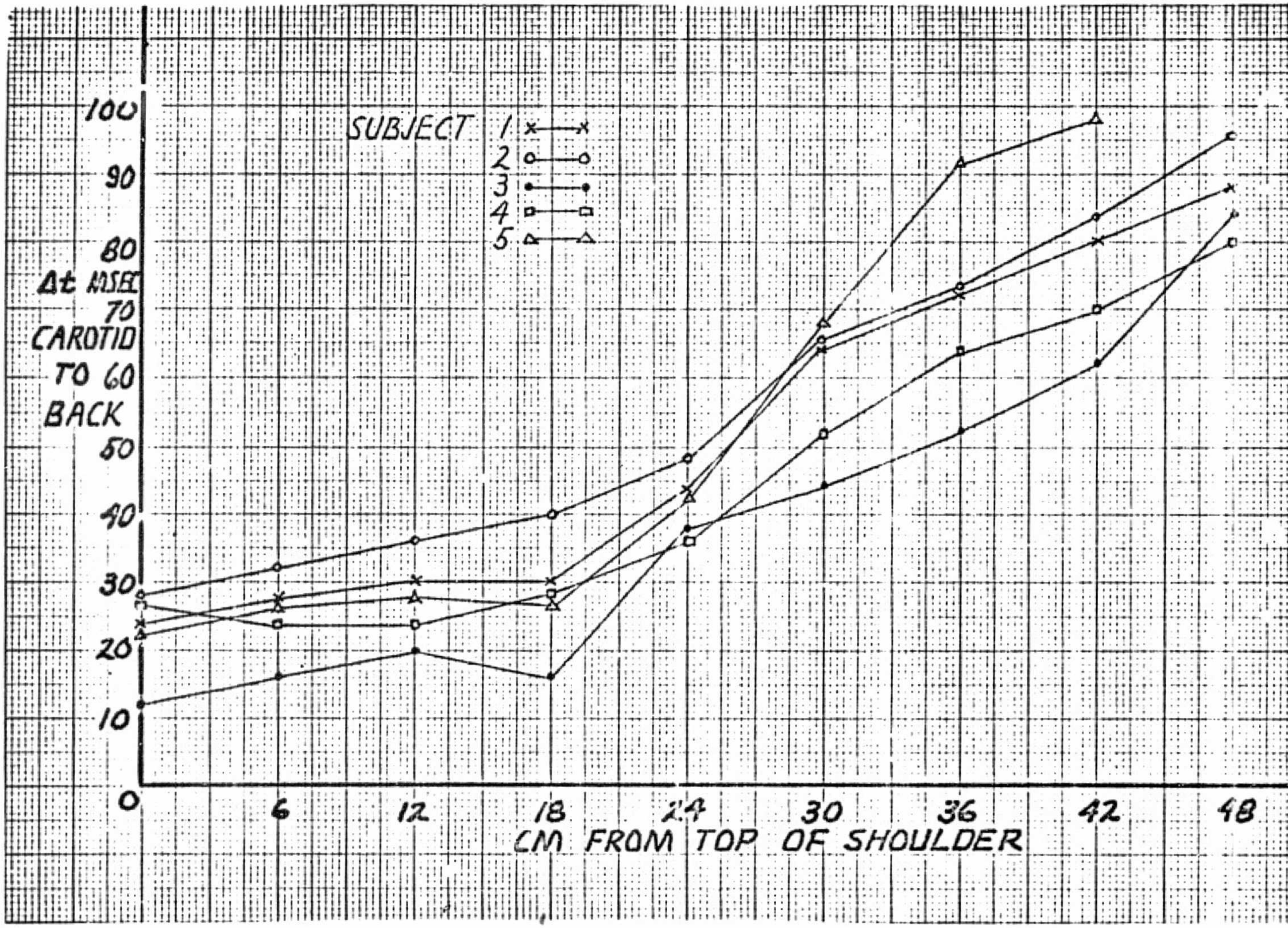
100
90
80
Δt MSEC
70
CAROTID
TO 60
BACK
50
40
30
20
10
0
SUBJECT 1
2
3
4
5
6
12
18
24
30
36
42
48
CM FROM TOP OF SHOULDER

FIGURE 20

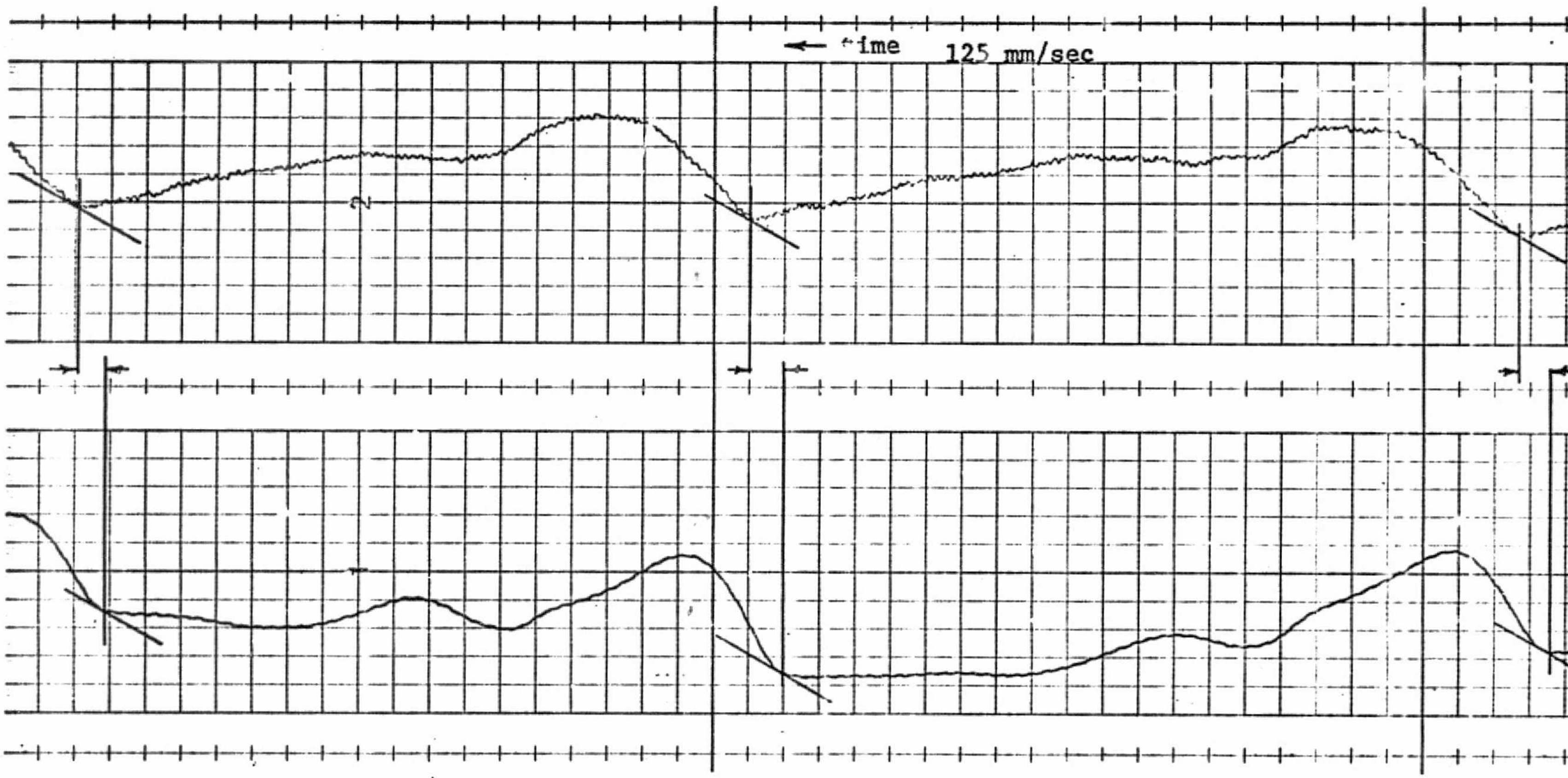

FIGURE 21

Measurement of Delay Times
Top: Back Pulse
Bottom: Carotid Pulse

It is seen that the time delay increases with distance in most regions. However, the upper back regions exhibit a different slope of distance versus time delay. This can be explained from the way this region is vascularized. The blood supply to the upper back is from the first, second and third intercostal arteries and the subclavian (shoulder) artery. These intercostals originate close together in the descending aorta and travel upwards to the intercostal spaces. Therefore, their paths to the skin are longer than the paths from the lower intercostal arteries to the skin.

The pulse wave velocities computed from this data are well within the range of normals for this age group determined by Nielsen et al. [1968]. It was felt therefore, that this technique deserved further attention. A more detailed map of the propagation times to various regions of the back was made on two subjects. To facilitate processing of the recorded data, the signals from the transducers are filtered by a linear phase-shift low pass filter and then differentiated by the networks shown in Figure 22. This is similar to methods used by Brown [1972] and Weinman [1971]. Typical output from the 10 Hz filter and the differentiator are shown in Figure 23. A counter-timer is set to trigger on the upslope of the differentiated signals. The trigger pulses from the counter-timer are also used to start and stop a millisecond clock attached to the analog input of a NOVA mini-computer. An oscilloscope is used to set the trigger levels and monitor the recorded signal. For each heart beat, the delay time between the two signals may be read from the counter-timer and stored simultaneously in the computer. A plotter routine for the computer is used to plot the

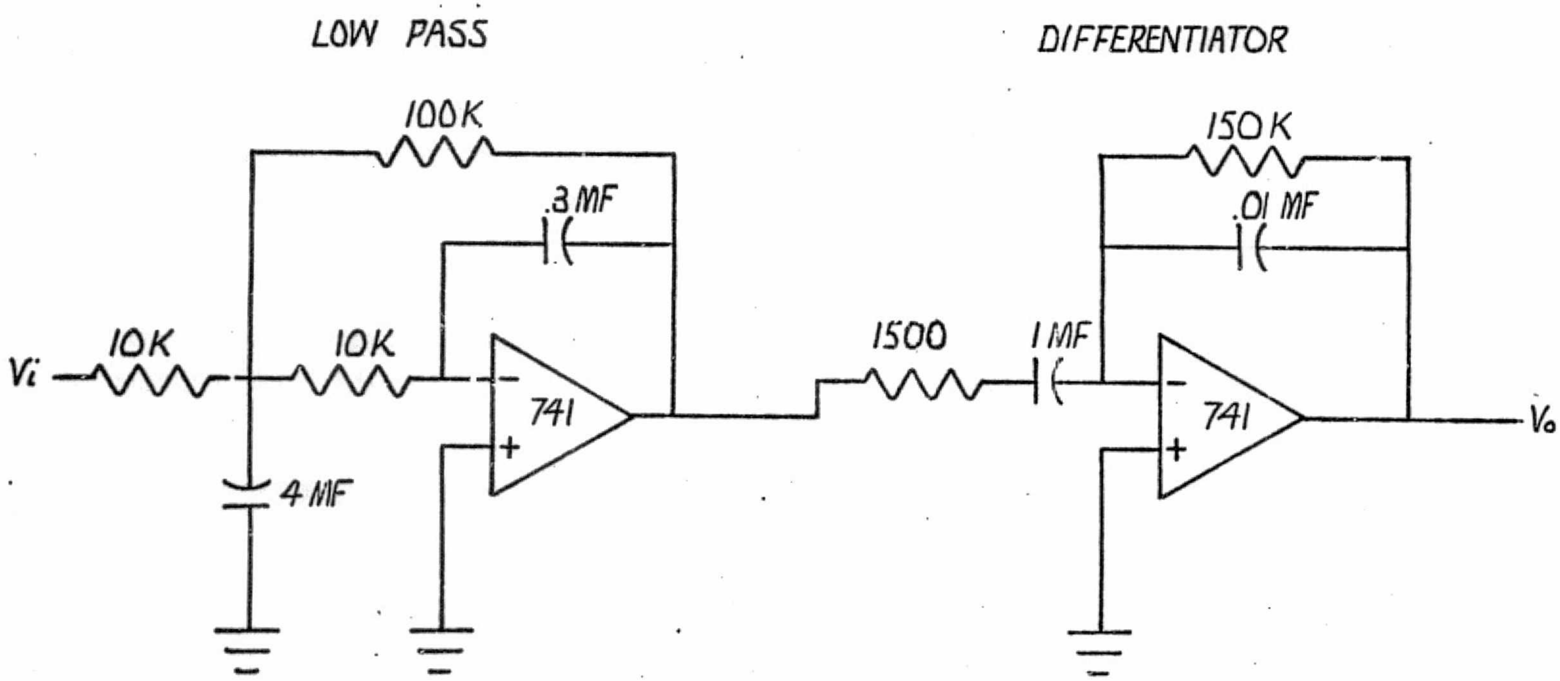

FIGURE 22

Filter and Differentiator

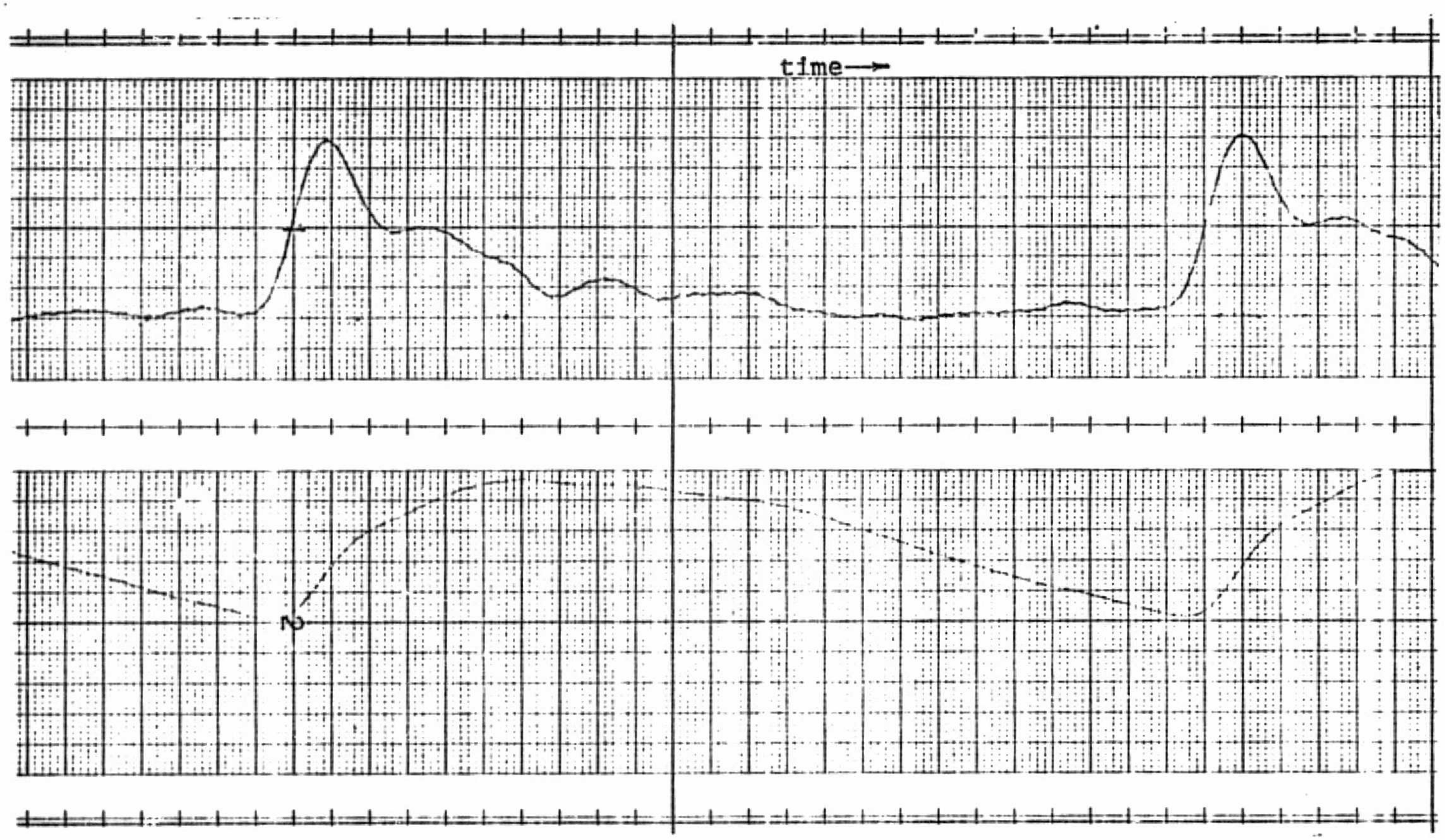

FIGURE 23

Top: Differentiation of Filtered Signal
Bottom: 10 Hz Lowpass Filtered Signal

time delay in milliseconds for each heartbeat. The average time delay for the entire interval of the plotted data is also computed. Values due to mistriggering or noisy signals are ignored. Typical data plots are shown in the following figures. It is seen that there is great beat to beat variability in the delay time. The time delays appear cyclical in nature with a period of about five heartbeats. However, the average values, even over fairly long intervals (10 minutes) seem to remain constant within a few milliseconds. The averages of carotid to back time delays are shown for different regions in Figures 24 and 25. The absolute values shown, of course, reflect to some degree the effects of triggering; however, the relative delays for the different regions are fairly accurate and are similar to those found when the same data is spot-checked by measuring delays on a strip chart recording. The strip chart recordings also show a similar variability in delay times. The two back plots indicate that the delay times, in general, increase with increasing distance from the heart. However, inconsistencies do appear.

The beat to beat variability in delay times shown in the computer plots is quite large. This may be due to blood pressure changes during respiration as well as other spontaneous pressure changes influencing the pulse wave velocity. The rhythmic variations in diastolic pressure due to respiration may be as great as 10 mm Hg [Selkurt, 1971]. The pressure usually decreases with inspiration and increases during expiration. Tursky et al. [1972] report that the total magnitude of the natural variation of systolic and diastolic pressure due to sinus arrhythmia and other beat to beat fluctuations may be

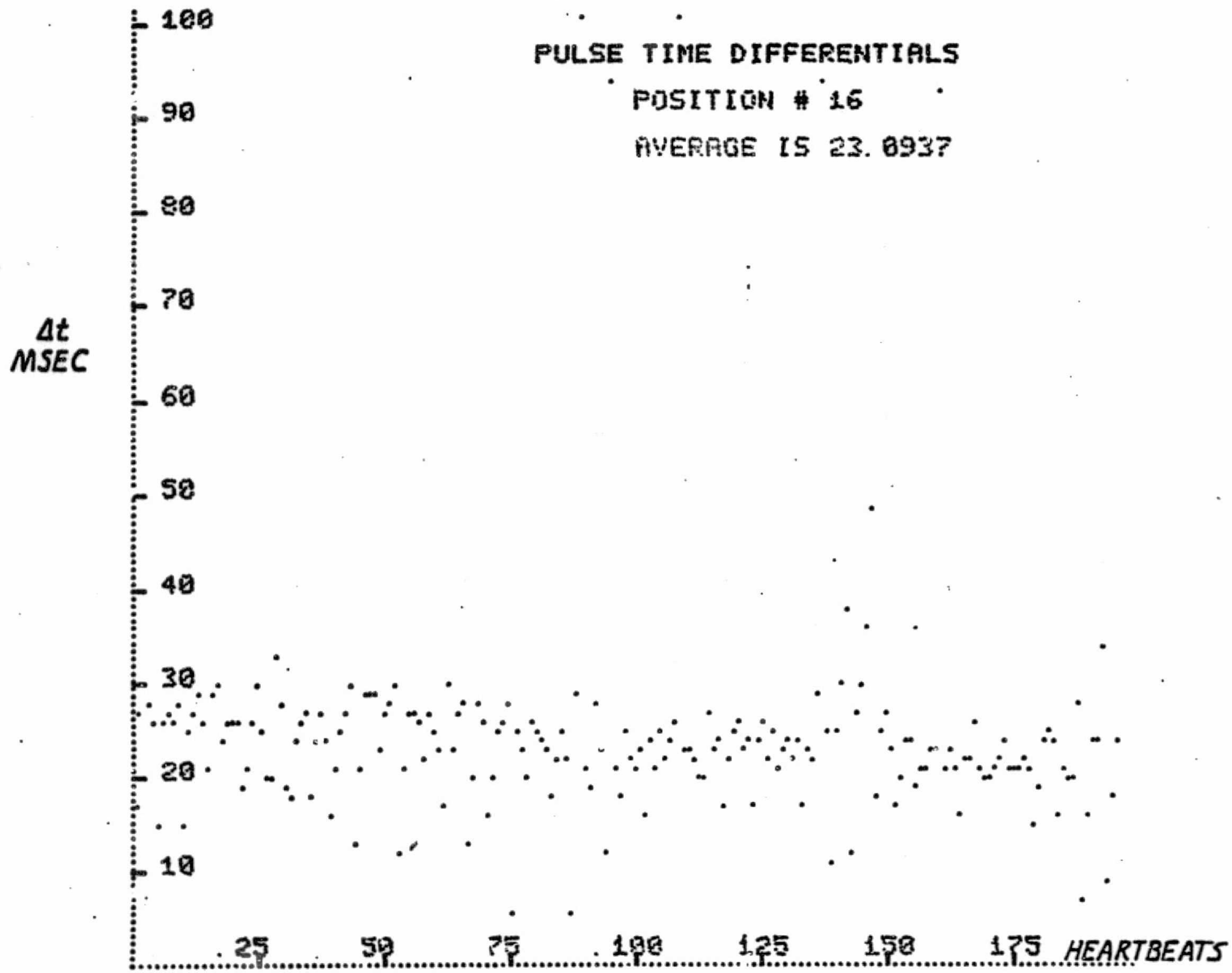
PULSE TIME DIFFERENTIALS
POSITION # 16
AVERAGE IS 23.0937
Δt
MSEC
100
90
80
70
60
50
40
30
20
10
25
50
75
100
125
150
175
HEARTBEATS

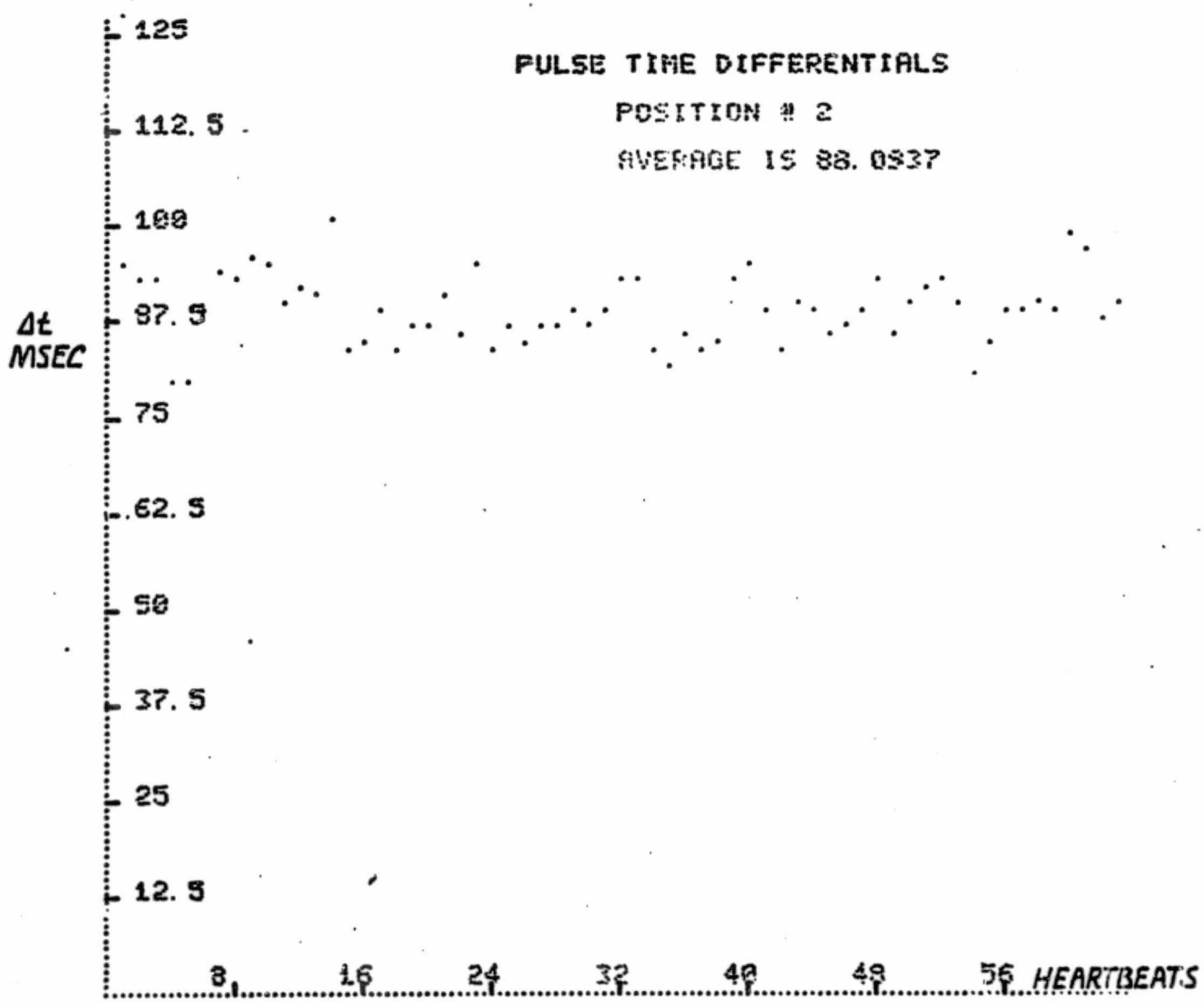
PULSE TIME DIFFERENTIALS
POSITION # 2
AVERAGE IS 88.0937
Δt MSEC
125
112.5
100
87.5
75
62.5
50
37.5
25
12.5
8
16
24
32
40
48
56
HEARTBEATS

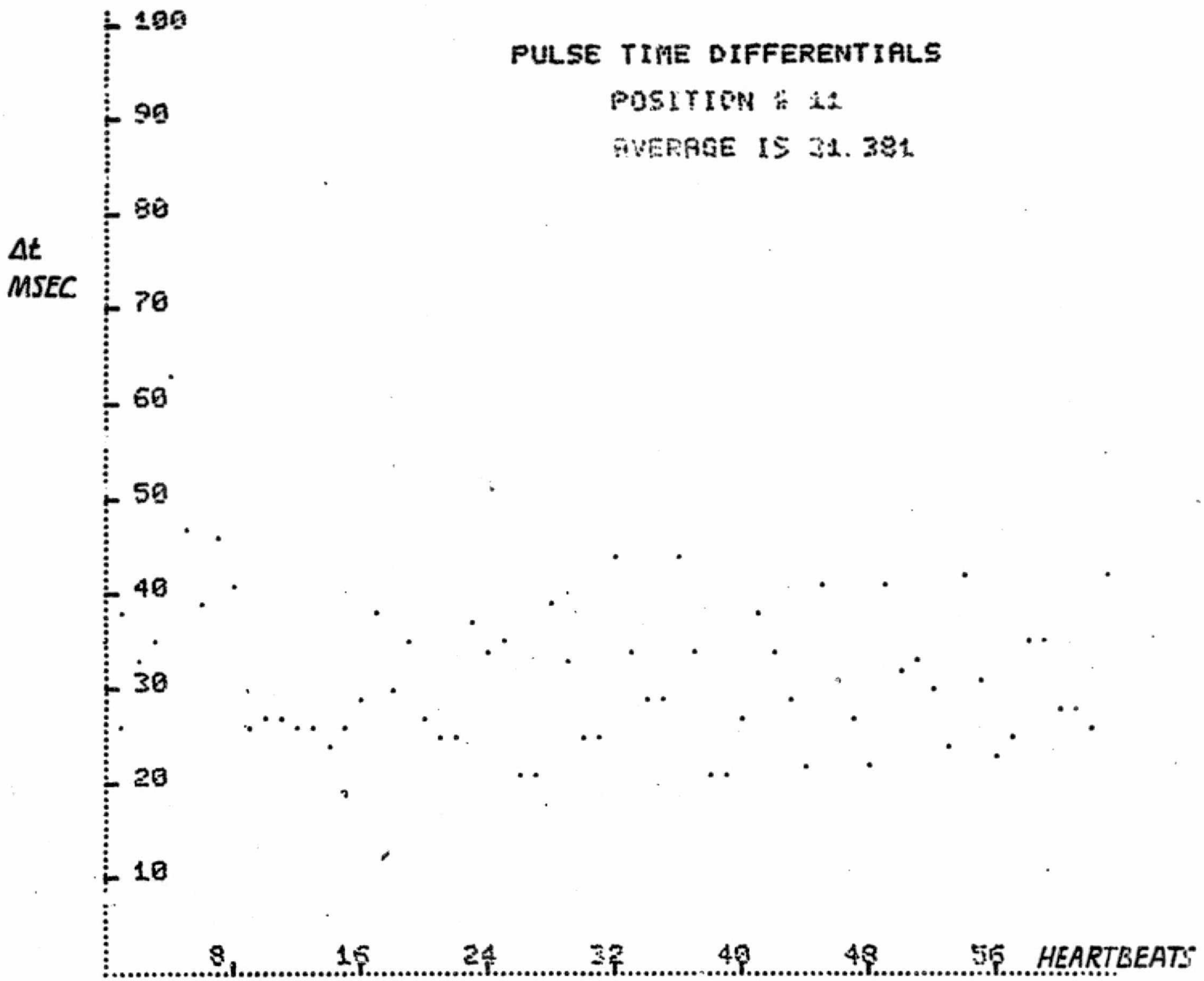
PULSE TIME DIFFERENTIALS
POSITION # 11
AVERAGE IS 31.381
Δt
MSEC
100
90
80
70
60
50
40
30
20
10
8
16
24
32
40
48
56
HEARTBEATS

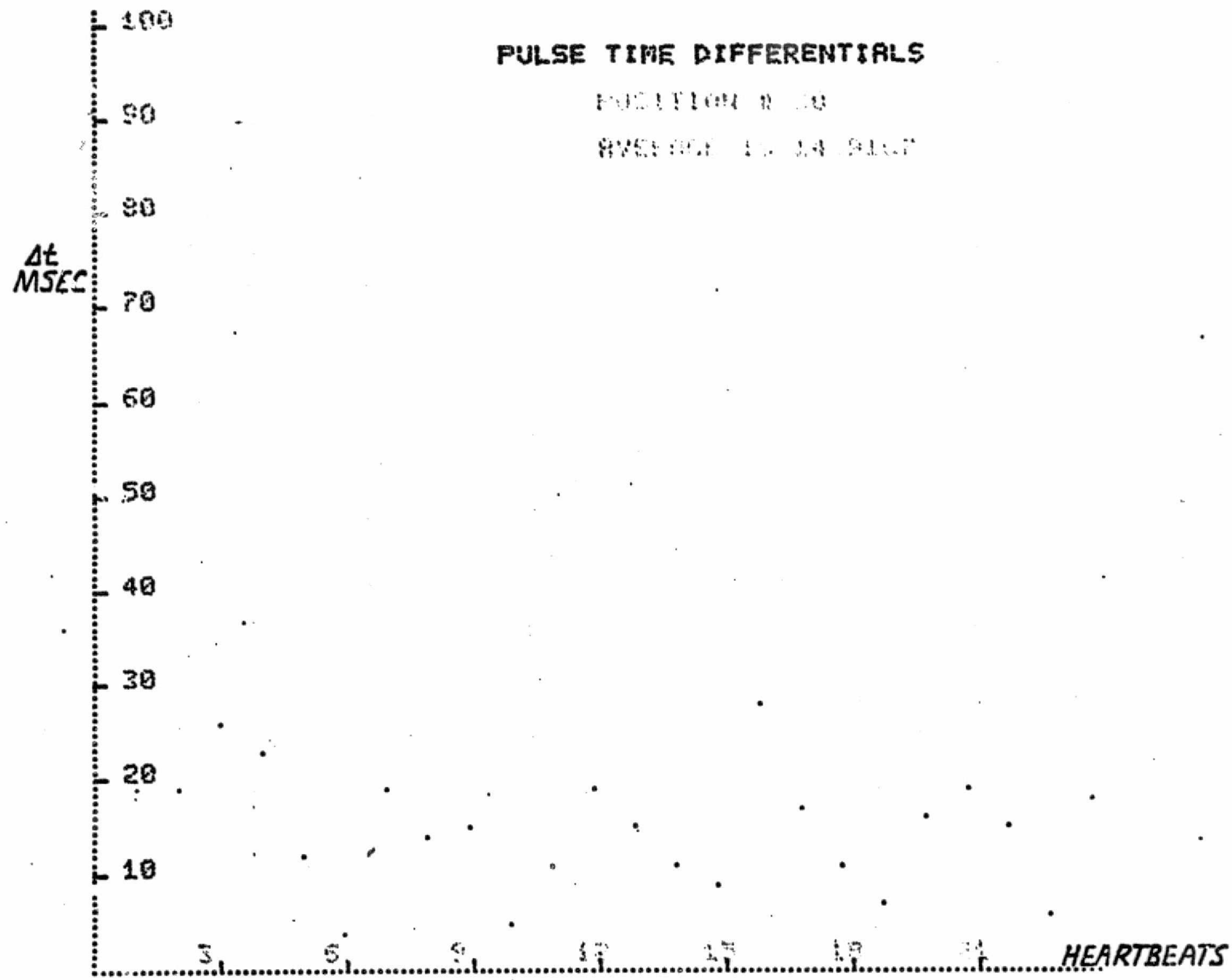
PULSE TIME DIFFERENTIALS
Δt MSEC
100
90
80
70
60
50
40
30
20
10
3
6
9
HEARTBEATS

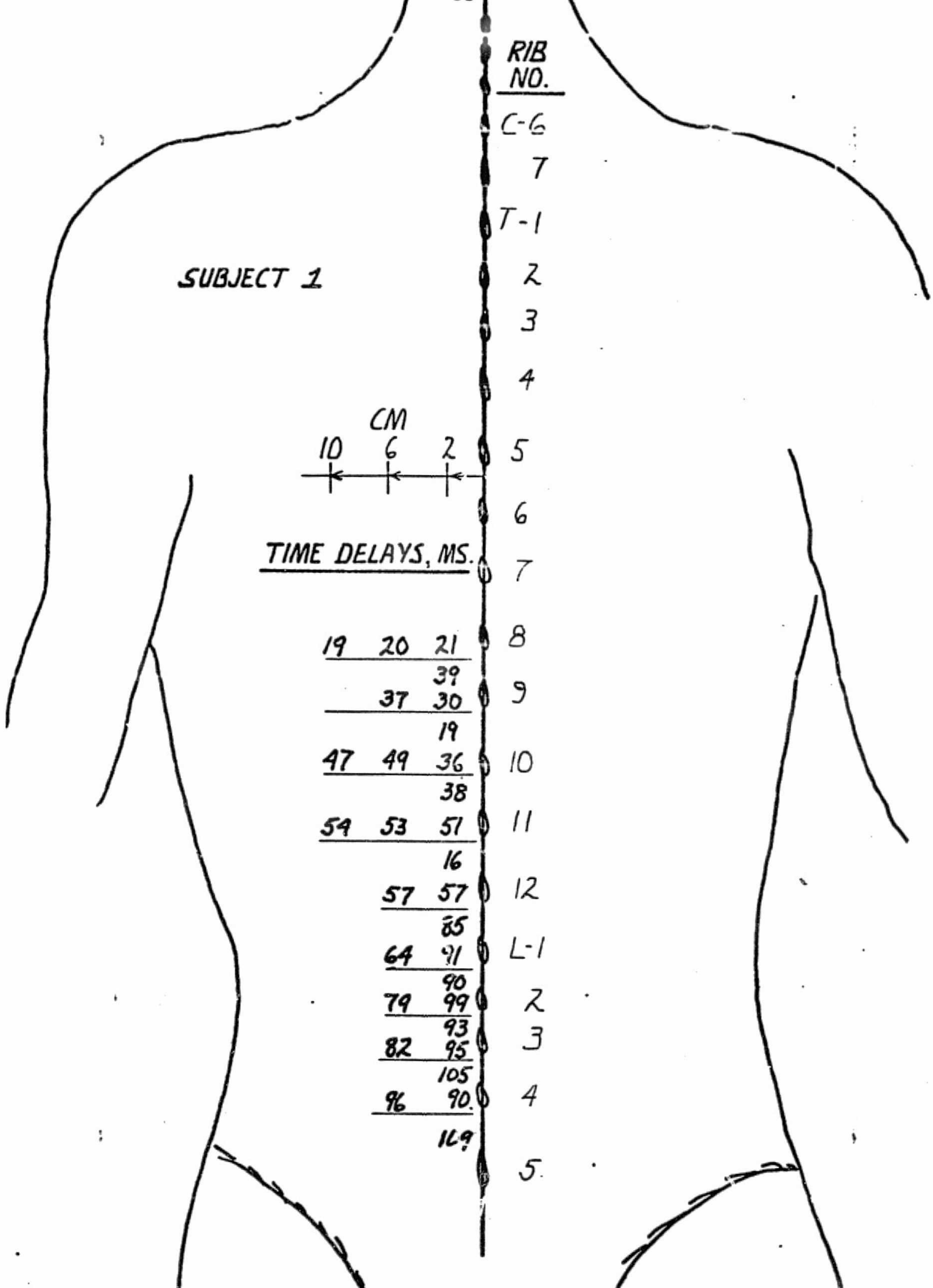
RIB NO.
C-6
7
T-1
2
3
4
5
6
7
8
9
10
11
12
L-1
2
3
4
5
SUBJECT 1
CM
10 6 2
TIME DELAYS, MS.
19 20 21
39
37 30
19
47 49 36
38
54 53 51
16
57 57
65
64 91
90
79 99
93
82 95
105
96 90
109

FIGURE 24

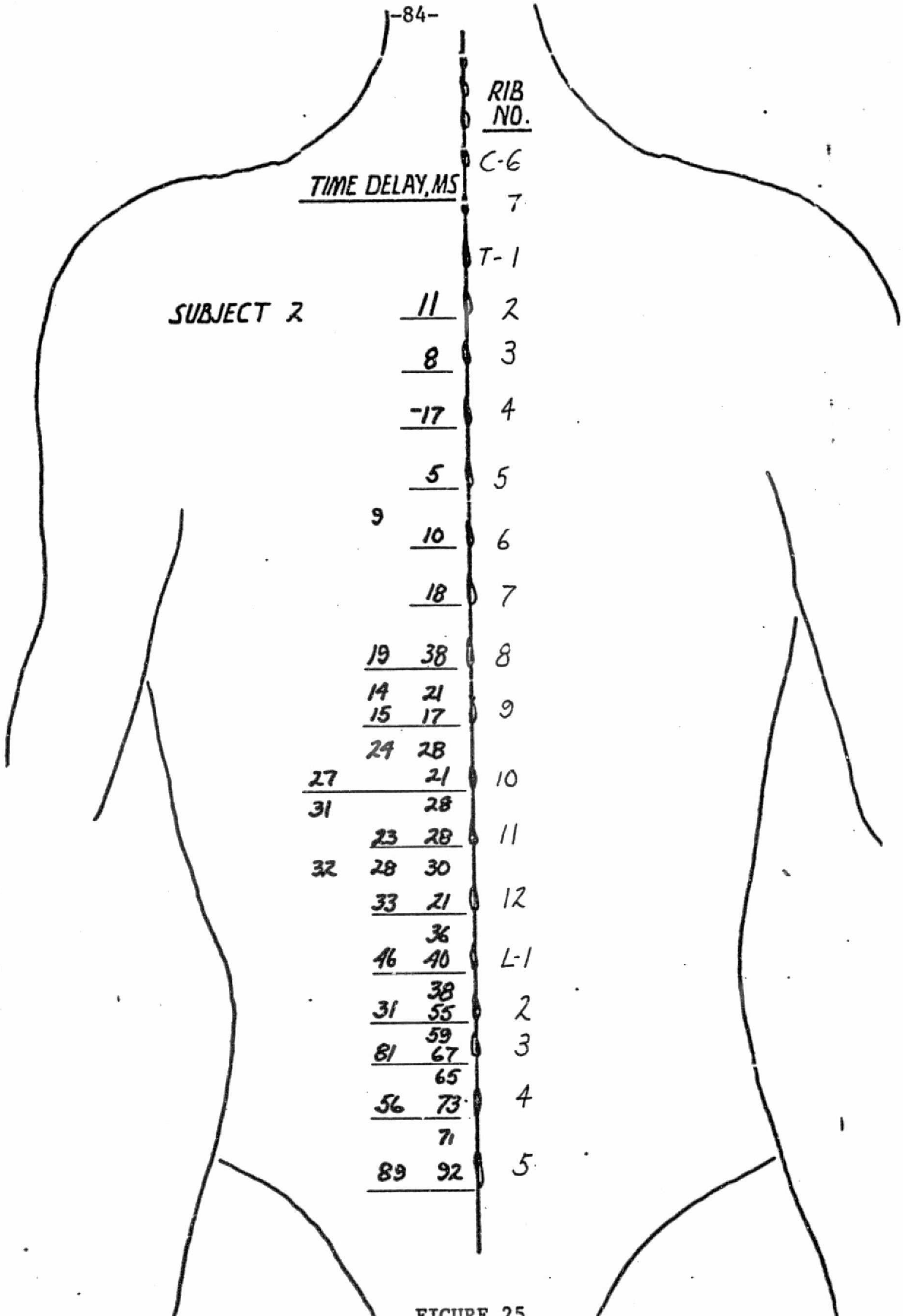
RIB NO.
TIME DELAY, MS
SUBJECT 2
C-6
7
T-1
11 2
8 3
-17 4
5 5
9
10 6
18 7
19 38 8
14 21
15 17 9
24 28
27 21 10
31 28
23 28 11
32 28 30
33 21 12
36
46 40 L-1
38
31 55 2
59
81 67 3
65
56 73 4
71
89 92 5

FIGURE 25

much larger. They found variations of blood pressure in five subjects over a period of fifty heartbeats ranged from 10 to 34 mm Hg. These large variations, of course, should greatly alter the time delays.

It was decided to further investigate the effect of the respiratory cycle on the time delays, as well as the effect on the blood volume pulse signal. To this end, a simple, yet reliable, respiration monitor was constructed. The device consists of a 10 K potentiometer with levers attached to the body and the wiper shaft. The device is strapped onto the chest by two alligator clip leads around the torso attached to the lever arms. The lever arms are held together by a rubber band. As the chest expands during inhalation, the lever arms are pulled apart, thereby moving the wiper arm and changing the resistance of the potentiometer. This change can be measured by biasing the potentiometer with a fixed voltage and measuring the voltage of the wiper arm with respect to ground. Using this device to monitor respiration, time differentials were measured on a subject (see Figure 26). It is seen that indeed, the cyclical variability of the delay times corresponds to the respiratory cycle. During inspiration, there is an increase in the time delay, which would correspond to a decrease in pulse wave velocity. This finding is consistent with the fact that inspiration causes a decrease in blood pressure. However, the large changes in time delays seem to be in disagreement with results of Goldberg [1972] who found that for a pressure change of 10 mm Hg the changes in delay time should be in the range of 10 to 20 percent of the average time delay. Therefore, further effects of respiration were investigated. The photoplethysmograph responds to the blood volume level as well as the blood .

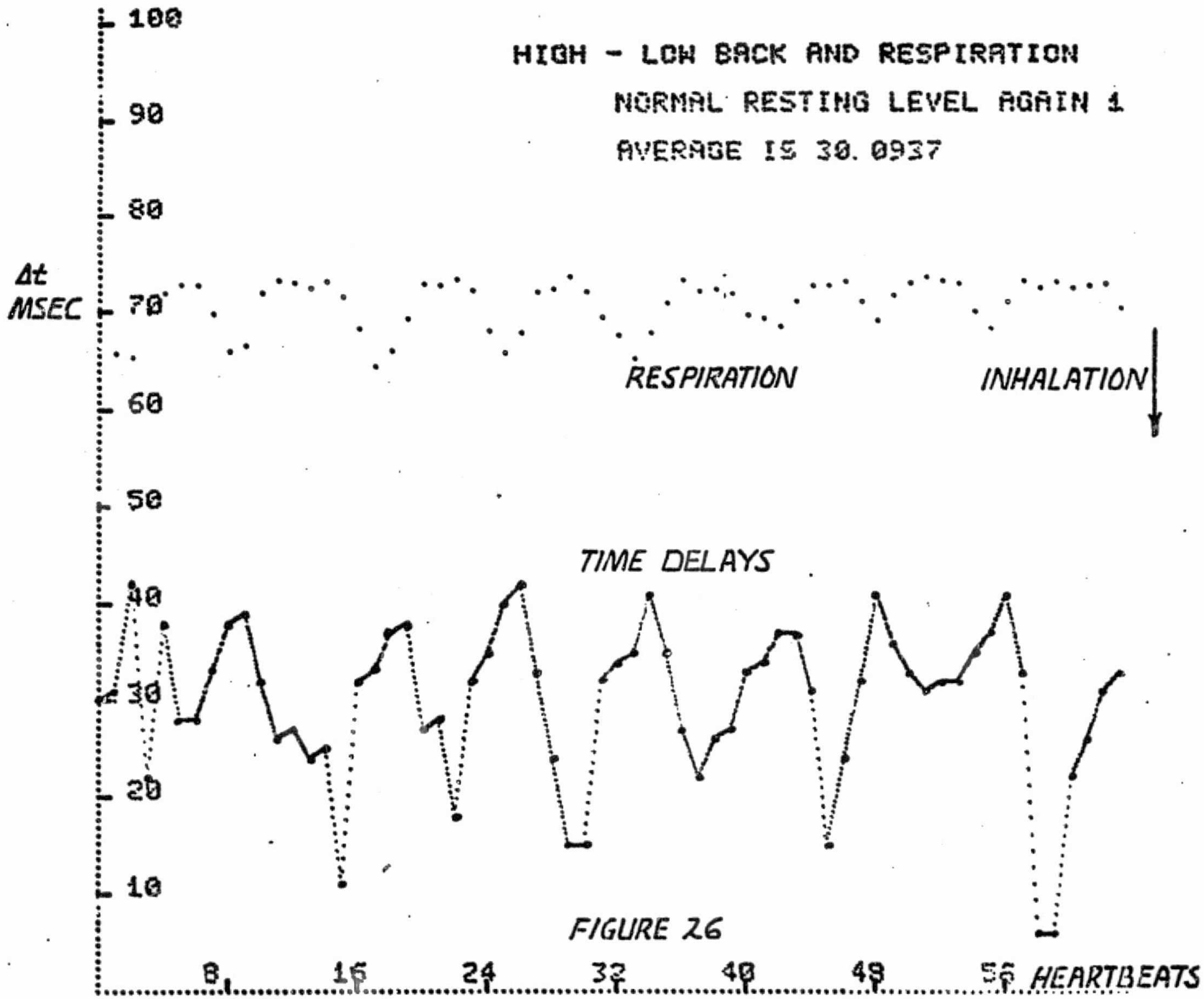

HIGH - LOW BACK AND RESPIRATION
NORMAL RESTING LEVEL AGAIN 1
AVERAGE IS 30.0937
100
90
80
Δt
MSEC
70
60
RESPIRATION
INHALATION
50
TIME DELAYS
40
30
20
10
8
16
24
32
40
48
56
HEARTBEATS

FIGURE 26

volume pulse. Changes in blood volume level were also noticed to correspond to respiration. Figure 27 shows the baseline variation with respiration of a signal from the upper back region. It is seen that during inspiration the baseline of the pulse signal shifts in the direction of "more blood." Since inspiration decreases the intrathoracic pressure, one would expect an increased venous return during inspiration and therefore, less rather than more blood in the skin. Heck [1972] in fact did find that inspiration caused a decrease of blood in the skin. To try to further understand these discrepancies, other experiments were undertaken. It was thought that possibly the AC coupling used introduced a large phase shift in the baseline variations. However, Figure 28 shows that the phase shift between the AC coupled and the DC signal is quite small. To alleviate the possibility that the baseline shift was caused by transducer movement during respiration, the finger pulse was monitored. Experiments on the finger pulse indicate that the baseline variation of the signal depends on the depth and rate of respiration. Figure 29 shows that for rapid respiration, inhalation causes an increase in blood in the skin. Slower breathing as shown in Figure 30 causes a decrease in blood with inspiration. These findings indicate that the system has a varying phase response, possibly due to the RC nature of venous drainage. Other findings of interest are shown in Figures 31 and 32. Here the venous return is blocked by constricting the veins or raising the intrathoracic pressure by a valsalva maneuver (forced expiratory effort against a closed glotis). The photoplethysmogram shows the expected increase in blood level due to reduction in venous return.

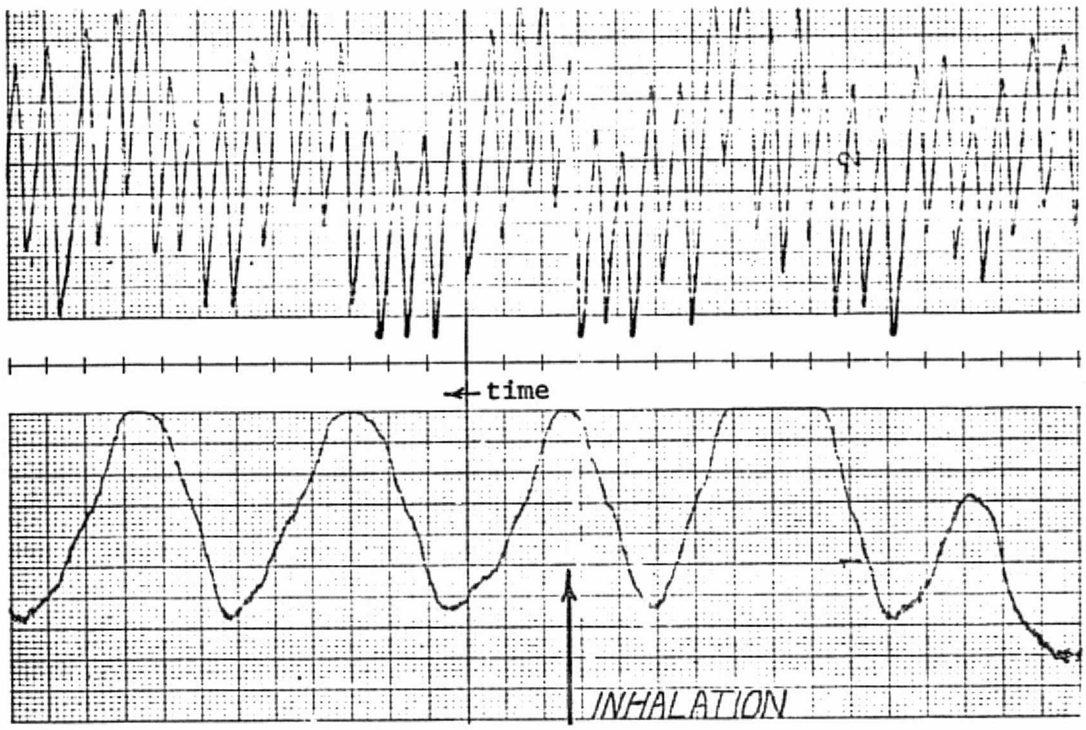

FIGURE 27

Top: Upper Back Signal, Up Denotes More Blood
Bottom: Respiration

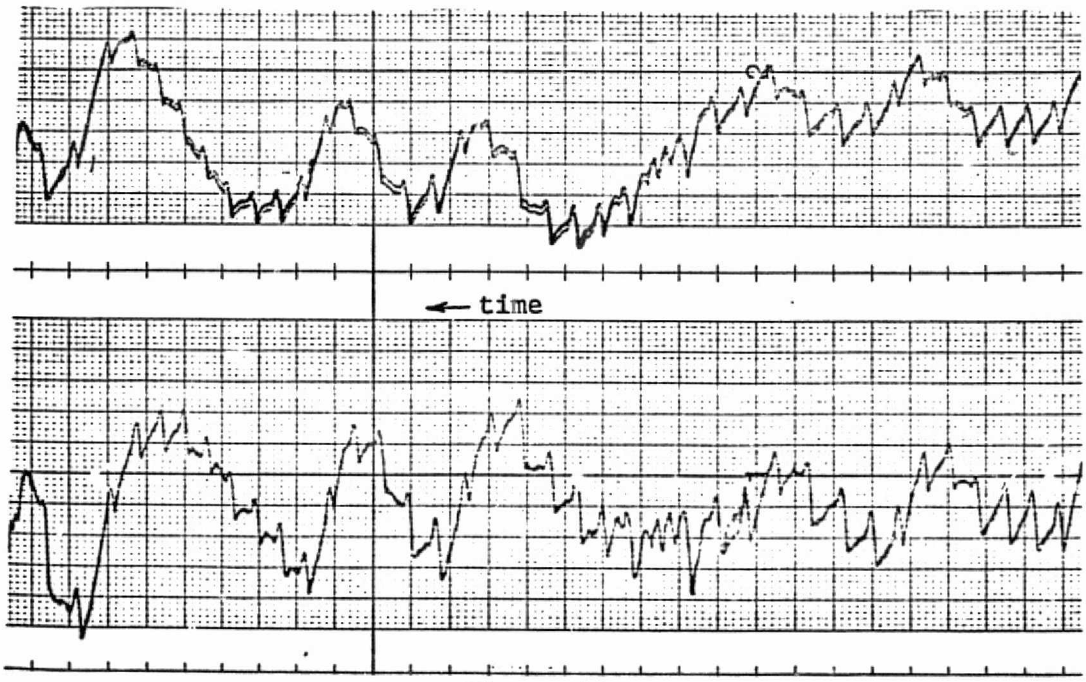

Figure 28
Top: DC Coupled Back Pulse
Bottom: AC Coupled Back Pulse

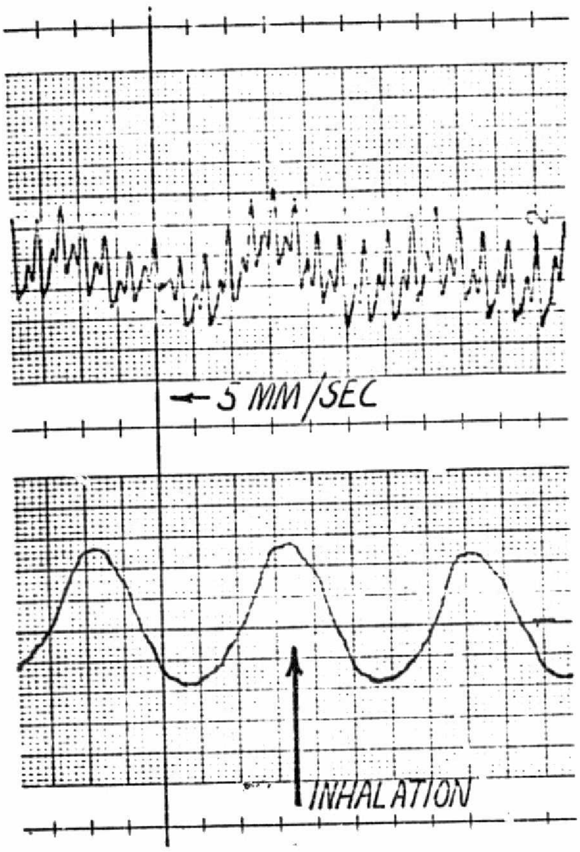

FIGURE 29

Finger Pulse and Respiration

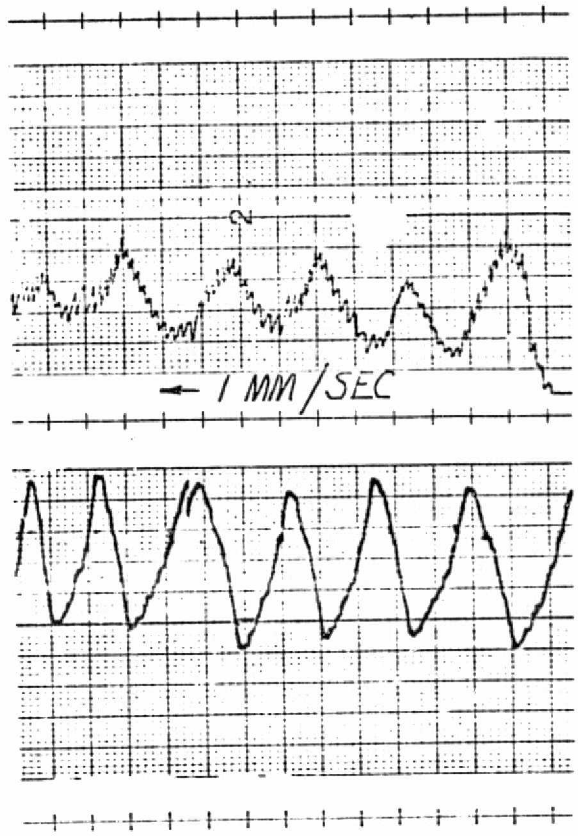

FIGURE 30

Finger Pulse and Respiration

UP SIGNIFIES MORE BLOOD

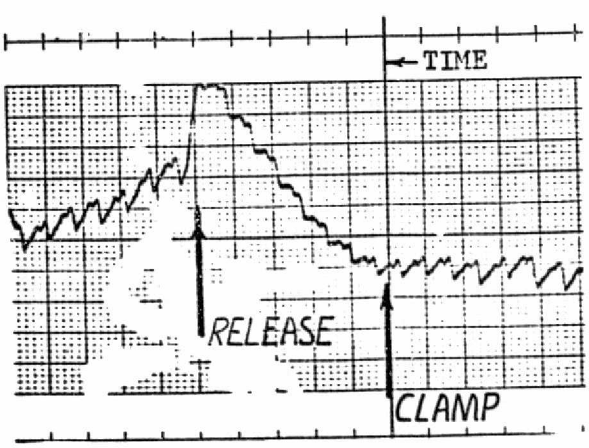

FIGURE 31

Effect on Finger Pulse of Clamping Upper Arm Veins

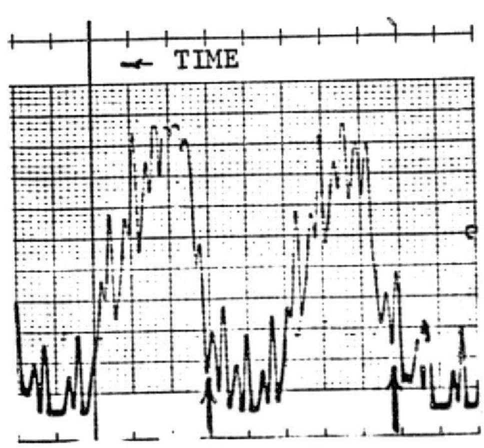

FIGURE 32

Valsalva Maneuver Begins at Arrows

An analysis was made by Weinman [1971] to determine the effect of a rising or falling baseline on the position of the arterial pulse wave foot. He derives a formula for the shift of the pulse foot based on a sine wave approximation to the pulse shape:

$$t = -n/w^2 \text{ in seconds}$$

where:

n = the number of pulse wave amplitudes the baseline rises or falls in one second

w = 2π times the sine wave frequency which best approximates the foot of the pulse wave.

In the worst cases, n was approximately equal to 1 and w approximately 12.5 giving a delay of about 7 msec. Since the baseline of both tracings from the back rise or fall together, the effects will tend to cancel when the time difference is computed. Therefore, the rising and falling baseline should have little effect on the delay times measured.

The question, then, of the large variability in delay time remains unanswered. It is noted however, that other investigators using a photoplethysmograph to measure delay times have also found large beat to beat variability in their measurements. Weinman et al [1971] found beat to beat variations of up to 25 msec. in pulse wave velocity studies of the human lower extremities. Also, Heck and Hawthorne [1969] found similar variability in propagation time of the pulse to the conjunctiva of dogs. This variability also appeared largely syncronous with the respiratory cycle. It seems likely, then, that the blood pressure variability with respiration and spontaneous changes in blood pressure has an exaggerated effect on pulse propagation times through the smaller non-major arteries leading to the skin.

Measuring pulse wave velocity on the back, therefore, presents two major difficulties. The first is the large beat to beat variation in time delays. This may be partially surmounted by averaging over a number of beats. The second problem is to find regions on the back where the delay from the aorta to the skin will be relatively the same. However, there presently seems to be no way to noninvasively determine the delay from the aorta to the skin surface. To test the basic validity of the idea of measuring pulse wave velocity on the back, experiments were performed with one transducer mounted at a point under the scapula about 4 cm to the left of the spine. The second transducer was placed vertically below this level with the top of the pelvis. The distance between the transducers was approximately 30 cm as compared with 37 cm which was found by Nielson et al. [1968] to be the average distance used when computing pulse wave velocity from the carotid to the femoral artery. Isometric contraction of one hand was used to raise blood pressure above the normal resting level. Goldberg [1972] found that this type of contraction could raise diastolic pressure up to 40 mm Hg. In some cases the isometric contraction was followed by a decrease in pulse propagation delay times. This can be seen in the following plot labeled "Isometric." Here the average time delay decreased slowly until it reached a value about 15 msec shorter than the normal resting level of 80 msec. However, in tests on most subjects isometric contraction seemed to have no consistent effect on the pulse propagation times. In a similar experiment, time delays from the upper to lower back were measured on a patient while his brachial arterial pressure was monitored by sphygmomanometric technique. Results are shown in Table 4. The time intervals shown represent the

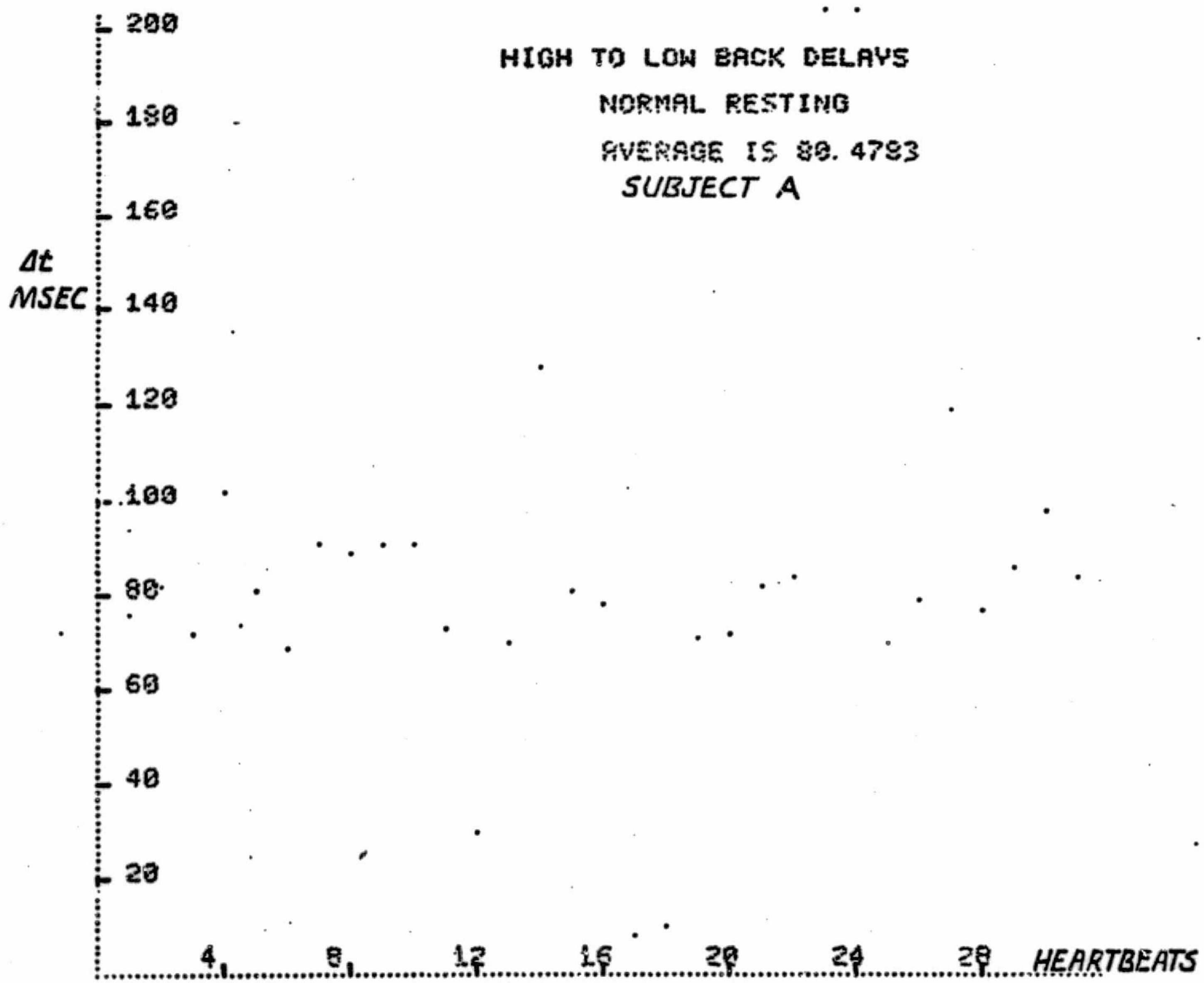
HIGH TO LOW BACK DELAYS
NORMAL RESTING
AVERAGE IS 80.4783
SUBJECT A
Δt MSEC
200
180
160
140
120
100
80
60
40
20
4
8
12
16
20
24
28
HEARTBEATS

-92-

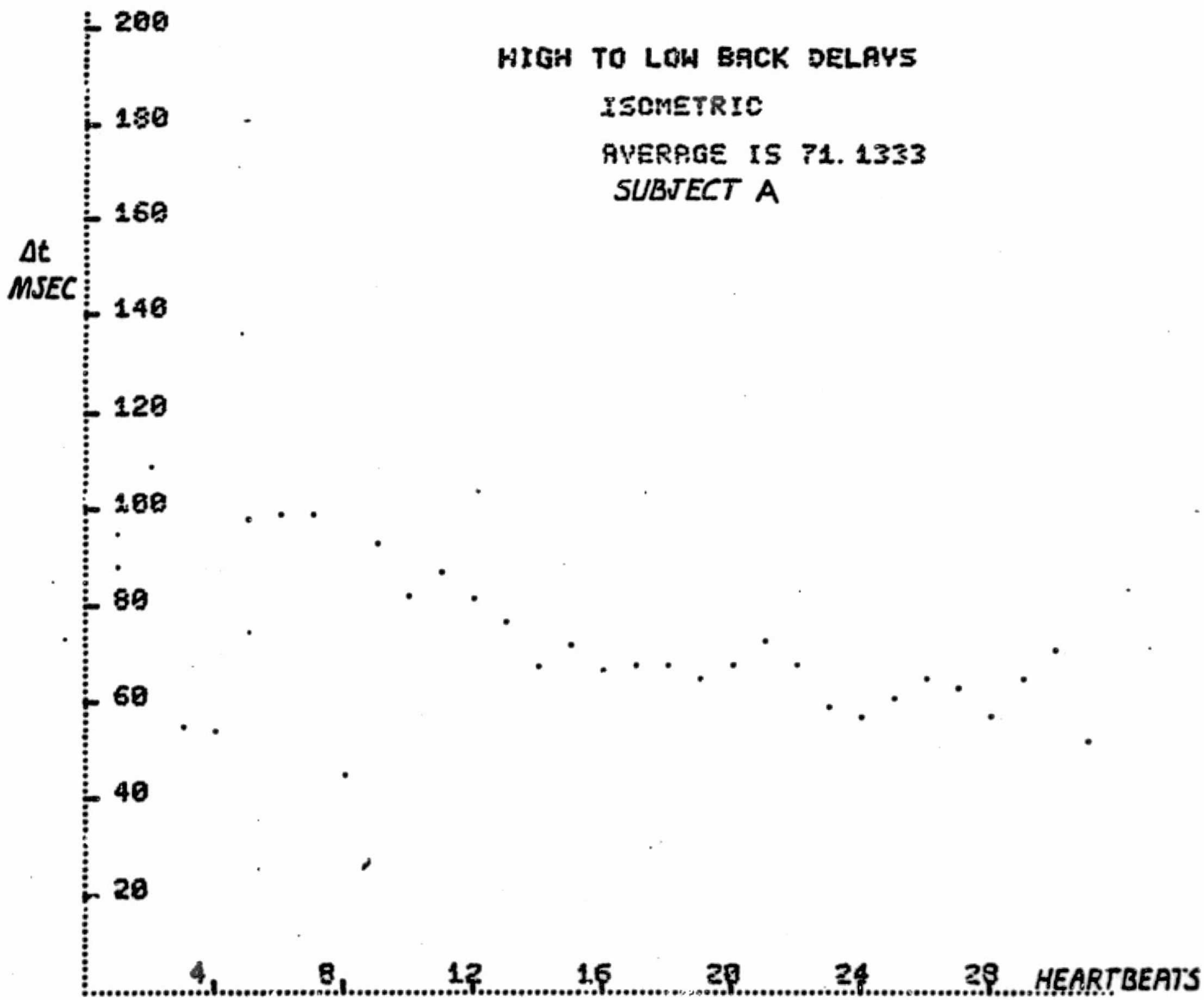
HIGH TO LOW BACK DELAYS
ISOMETRIC
AVERAGE IS 71.1333
SUBJECT A
Δt
MSEC
200
180
160
140
120
100
80
60
40
20
4
8
12
16
20
24
28
HEARTBEATS

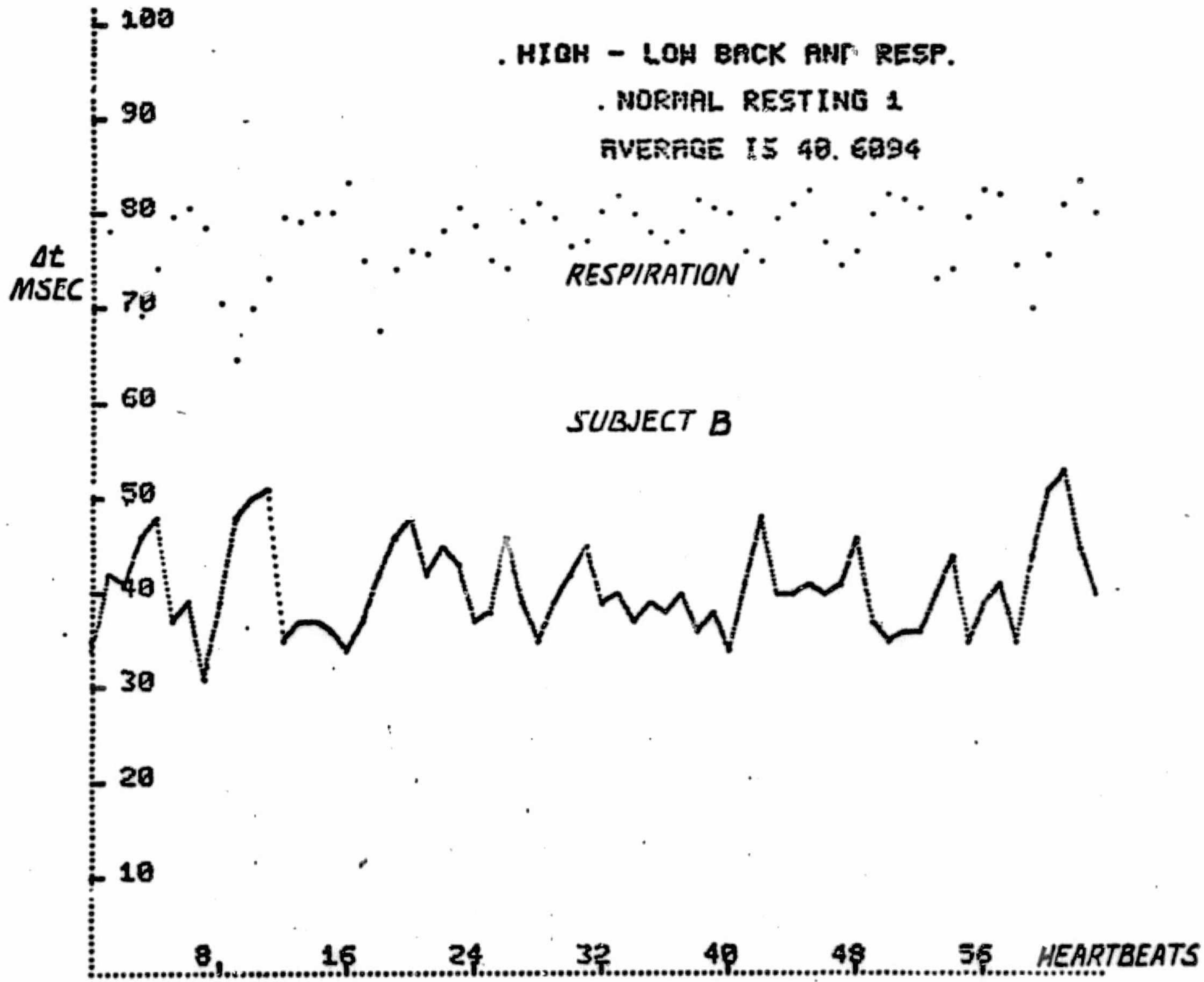
. HIGH - LOW BACK AND RESP.
. NORMAL RESTING 1
AVERAGE IS 40.6094
RESPIRATION
SUBJECT B
Δt
MSEC
100
90
80
70
60
50
40
30
20
10
8
16
24
32
40
48
56
HEARTBEATS

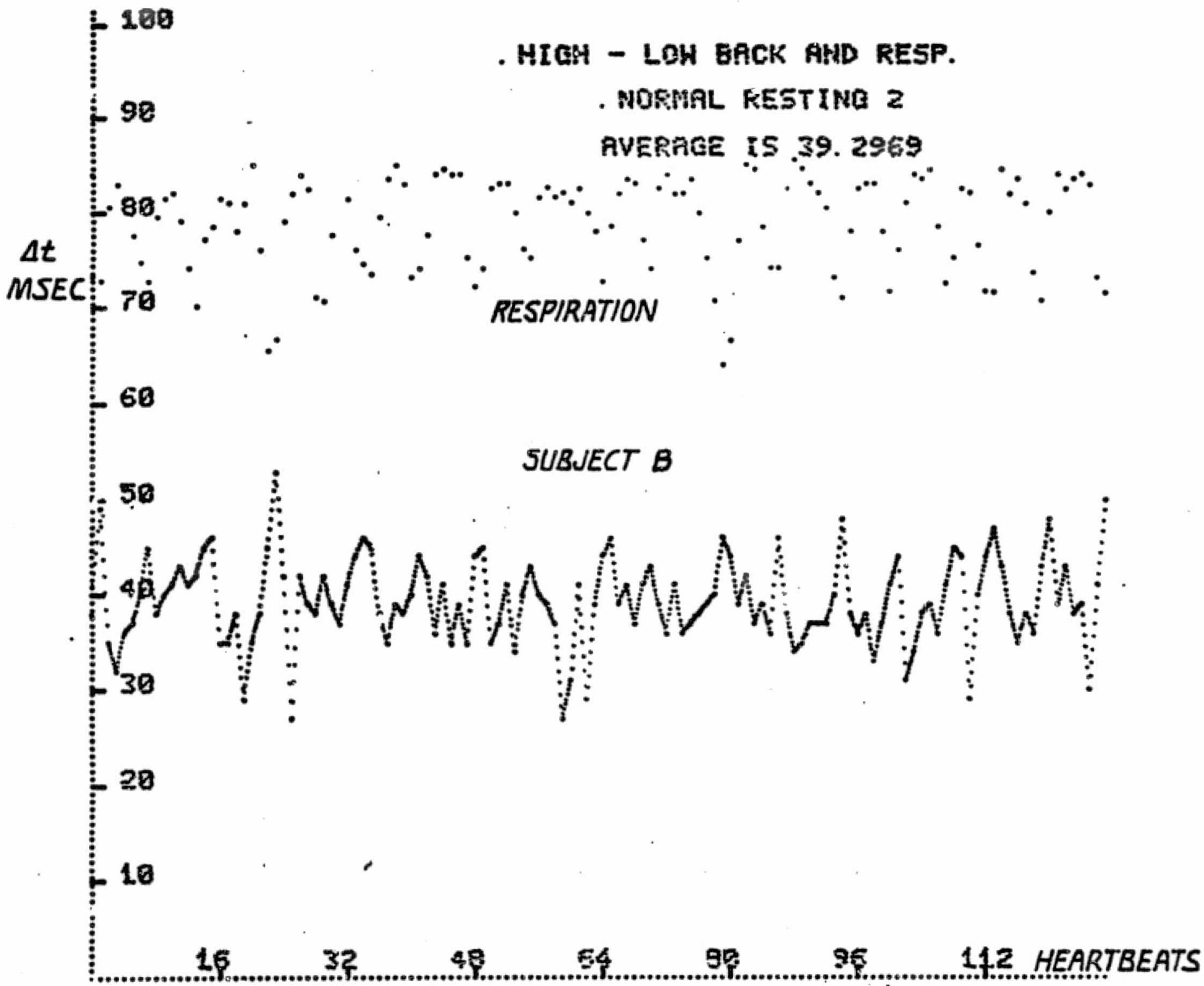
. HIGH - LOW BACK AND RESP.
. NORMAL RESTING 2
AVERAGE IS 39.2969
RESPIRATION
SUBJECT B
Δt MSEC
100
90
80
70
60
50
40
30
20
10
16
32
48
64
80
96
112
HEARTBEATS

TABLE 4

CONDITIONS	PRESSURE	TIME DELAY MSEC
Normal	107/68	40
Normal	107/68	39
Normal		39
Normal		38
Normal		39
Normal		39
Normal	107/68	39
Isometric		37
Isometric	115/68	37
Isometric		37
Isometric	125/75	33
Isometric	135/94	27
Isometric	140/98	27
Isometric		28
Normal	110/70	30
Normal		29
Normal	110/70	29
Normal		31
Isometric	125/80	28
Isometric	140/100	28

SUBJECT B

average values determined by the computer for approximately a one minute interval. It is seen that the time interval does indeed fall as the pressure rises. However, as the pressure returns to normal, the time delay does not return to normal. This was checked to be sure it was not due to a triggering error by using a strip chart recording. This result implies that there are some other factors besides pressure which help determine the propagation times. As a final check of this, time delays were measured simultaneously on a subject between the high and low back, and the carotid and femoral arteries. Mechanical transducers were used to record the carotid and femoral pulsations as was done by Goldberg [1972]. Figure 33 shows a typical strip chart recording from which the time delays were measured. Time delays for many beats were measured. Some typical data points are plotted in Figure 34. Results fairly conclusively show that the carotid to femoral time delays definitely follow to some extent changes in blood pressure caused by isometric hand contraction or a valsalva maneuver. However, it seemed that in most cases the high back to low back time delays varied independently of the carotid to femoral delay times and therefore showed almost no dependence on pressure. Also, the variability of the back delays was greater than that seen in the carotid to femoral propagation times.

It appears, therefore, that pulse propagation through the smaller arteries leading from the aorta is highly variable. Heck and Hawthorne [1969] noted that the pulse propagation time to the conjunctiva vascular bed was dependent on any vascular changes. In one experiment on dogs, for instance, they noted that an arterial dilatation of 30% as noted in the vascular bed gave rise to an increase of 7.13% in the time delay

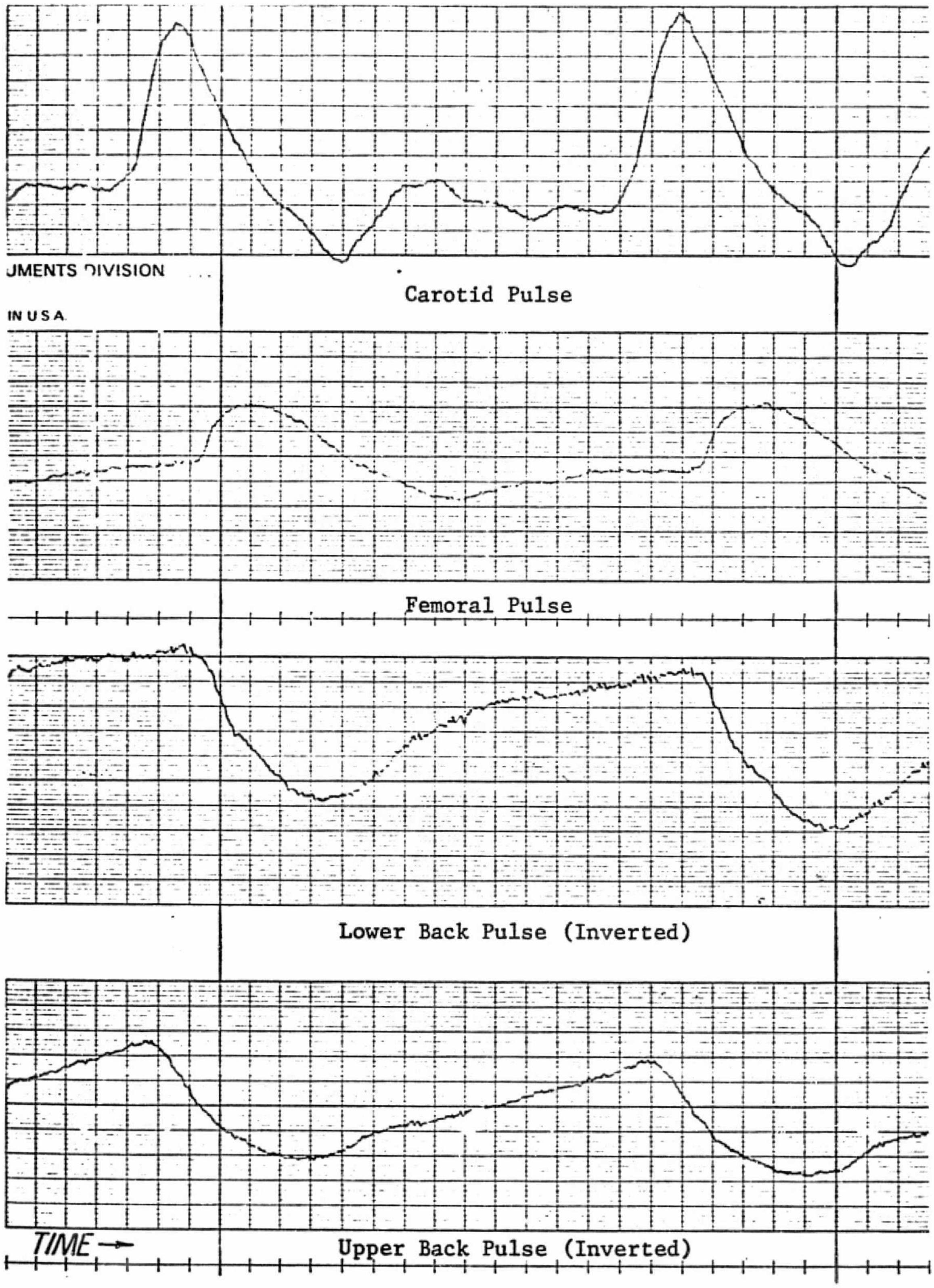
Carotid Pulse
Femoral Pulse
Lower Back Pulse (Inverted)
TIME →
Upper Back Pulse (Inverted)

FIGURE 33

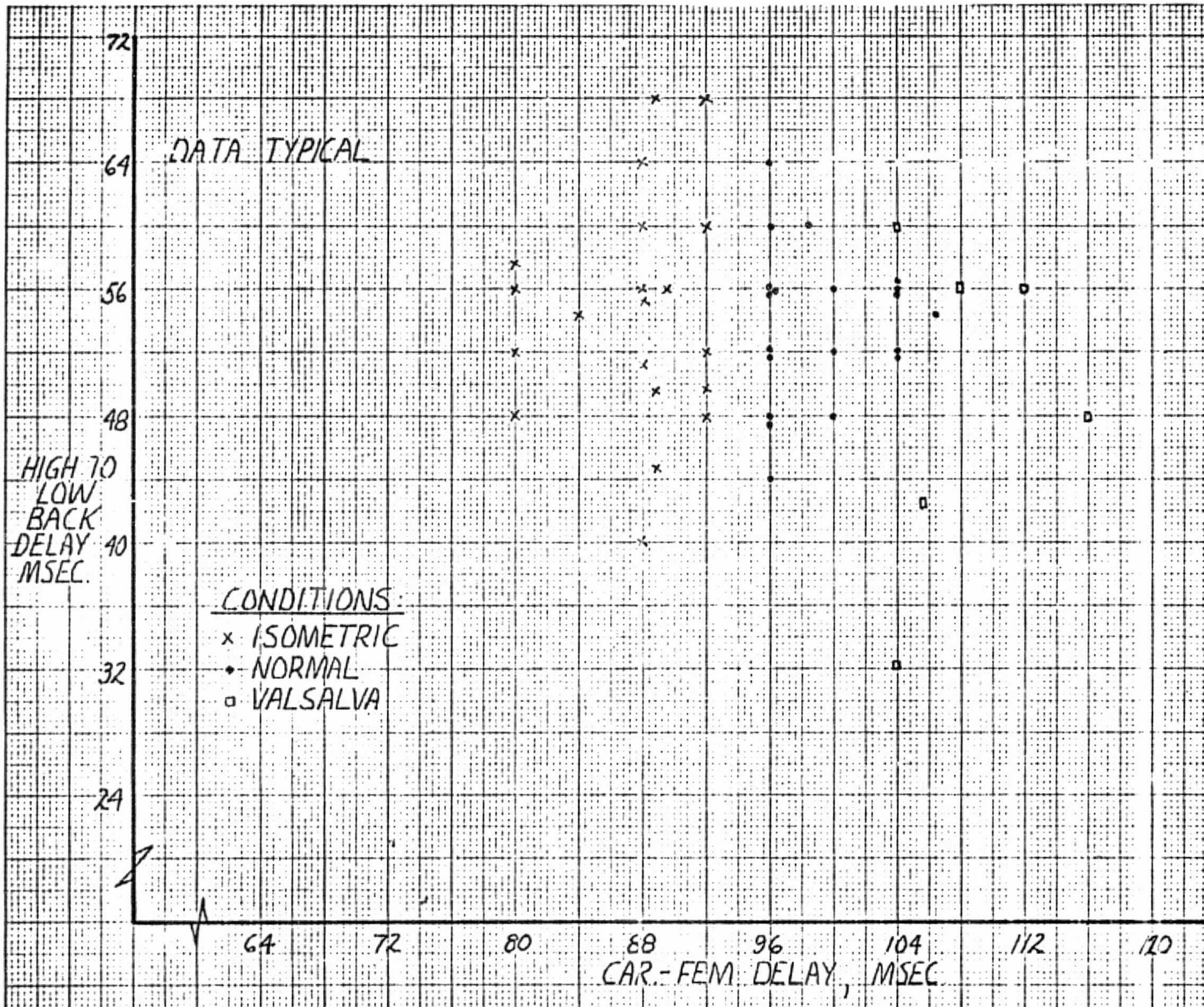

DATA TYPICAL
HIGH TO LOW BACK DELAY MSEC.
72
64
56
48
40
32
24
CONDITIONS:
× ISOMETRIC
• NORMAL
▫ VALSALVA
64
72
80
88
96
104
112
120
CAR.-FEM. DELAY, MSEC

FIGURE 34

between the R wave of the EKG and the pulse arrival at the eye. Constriction of the arteries is associated with a decrease in the time delay. These changes were found to occur spontaneously. Spontaneous rhythmic fluctuations in blood flow not associated with respiration are also noted by Tatai et al [1962] in photoplethysmographic studies of many body regions. The fluctuations in symmetric areas on opposite sides of the body, for instance the right and left ear lobes, were found to be independent. The mechanism for these changes is thought to be contraction and relaxation of the vascular smooth muscle of arterial walls as well as the precapillary and venous sphincters. Another factor which influences propagation time has been noted by Heck [1970]. He found that digital compression of the carotid artery caused a marked increase in the time delay from the R wave to the appearance of the pulse at the ear lobe. He is further investigating the possibility of determining partial one sided occlusion of the carotid arteries by comparing pulse propagation times to various regions of the face. His initial results look promising.

The possibility of monitoring aortic pulse wave velocity from the pulse arrivals in the skin of the back, therefore, seems quite remote. The pulse propagation times through the diffuse arterial bed leading to the skin is too variable to give consistent results.

DIRECTIONS FOR FURTHER RESEARCH

While experimenting with the photoplethysmograph many paths for further research have been opened. Some of these are included in this section.

1. Patency of Veins

From Figures 31 and 32 it is seen that the DC signal level of the photoplethysmogram is highly dependent on the venous return. Since the veins are basically capacitance vessels, changing conditions such as release of a clamped vein as in Figure 31 gives rise to an exponential type curve. Preliminary results indicate that by placing a photoplethysmograph on each leg or toe it is possible to compare the exponential curves for venous drainage from each leg during changes in posture or a valsalva maneuver. Figure 35 shows tracings from the right and left leg of an individual as he changes his posture from sitting with legs extended horizontally to lying. Both legs exhibit similar curves for the drainage of blood from the veins. However, when the veins of the left leg are blocked by a tourniquet, the discharge curve for the left leg shows a change. This change would be greatly inhanced if a tilt table were used to change posture more drastically. Further research in this area should be done to determine normal curves and the practicality of this technique for diagnosing venous occlusive disease. Other information about the inflow outflow characteristics of the circulatory system may also be gained from these experiments.

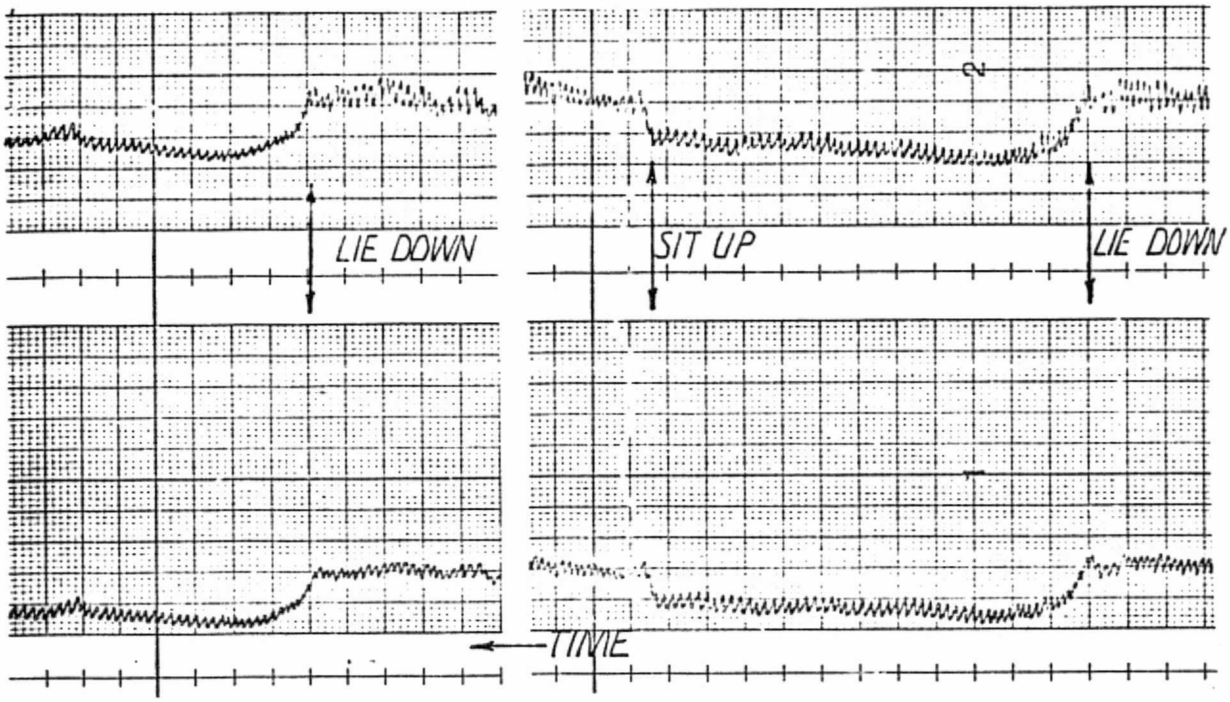

FIGURE 35

Venous Drainage Experiment
Top: Right Toe
Bottom: Left Toe

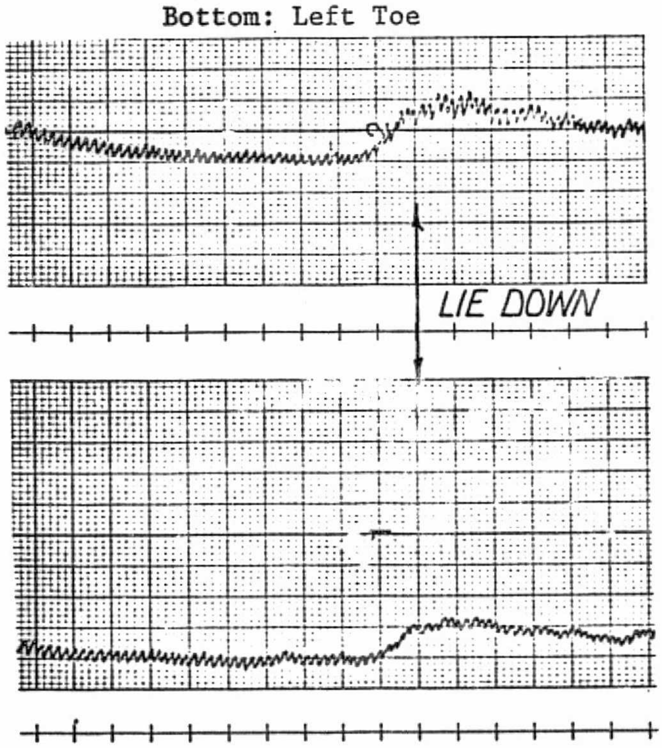

FIGURE 36
Top: Right Toe
Bottom: Left Toe, Band on Leg

2. Circulatory Magnitude and Phase Response

It is possible to monitor the baseline shift of the blood volume in the skin during the respiratory cycle. Controlled experiments with varying depth and rate of respiration might yield interesting magnitude and phase plots of the system. Modeling as a resistance and capacitance network may be possible.

3. Plot of Pulse Arrival Times on the Back

Careful plotting of the pulse arrival times in different regions of the back may be possible. If enough points are plotted a map of these arrival times may be useful in exploring flow patterns to the skin. Comparison of the map with the pattern of vascularization of the back shown in Figure 18 may prove interesting. It may be possible to locate the exact regions where the deeper arteries come through the muscular body layers and reach the skin. Limitations, of course, will be great due to the large spontaneous variability of the time delays.

4. Nature of the Photoplethysmographic Signal

To intelligently use the photoplethysmogram it is necessary to better understand the phenomenon involved in producing the signal. A few theories of the operation have already been mentioned, however there is still no total agreement on what actually accounts for the photoplethysmographic signal. Further experiments on animals, with attention to the microscopic circulation and formulation of new theories are necessary.

CONCLUSION

A technique for measuring pulse wave velocity through monitoring the blood volume pulse at two locations on the skin of the back has been explored. It seems this technique does not give good results probably due to the complex mechanisms affecting the pulse propagation from the aorta to the skin at various locations.

Different types of transducers including the differential photoplethysmograph, the photoplethysmograph, and the doppler ultrasonic transducers have been built and tested to see if they might offer alternatives to mechanical transducers which are highly subject to movement artifacts when used on ambulatory subjects to monitor carotid and femoral pulses. At present, it appears that none of these devices are adequate for monitoring ambulatory patients. For use on cooperative subjects, the photoelectric and doppler ultrasonic probes are good, but not significantly better than mechanical transducers. It is felt that in time, with the onset of new methods and new techniques, it may be possible to monitor arterial pulsations on ambulatory subjects. Then the relationship of blood pressure to pulse wave velocity may be more fully explored.

BIBLIOGRAPHY

Alt, F., "Advances in Bioengineering and Instrumentation," Plenum Press, New York, 1966.

American Medical Association, "The Wonderful Human Machine," 1961.

Anson, B , "An Atlas of Human Anatomy," Saunders Co., Philadelphia, 1963.

Appleton, A., Hamilton, J., "Surface and Radiological Anatomy," Heffer and Sons Limited, Cambridge, 1958.

Arndt, J., Klauske, J., Mersch, F., "The Diameter of the Intact Carotid Artery in Man and Its Change with Pulse Pressure," Pflugers Archiv 301: 230-240, 1968.

Baker, D., and Simmons, V., "Phase Track Techniques for Detecting Arterial Blood Vessel Wall Motion," 21st ACEMB, Houston, 1968.

Baker, D., and Cole, J., "Transcutaneous Measurement of Blood Flow Acceleration and Peak Velocity in the Aortic Arch of Man," 24th ACEMB, Las Vegas, 1971.

Behrendt, T., and Shawaluk, P., "Clinical Measurement of Pulse Time Differentials," Canad. J. Ophthal., 3:138-142, 1968.

Belincourt, Don, Kikuchi, Y., and Meitzler, A., "Ultrasonic Transducer Materials," Plenum Press, New York, 1971.

Benjamin, F.B., Mastrogiovanni, F., and Helvey, W., "Bloodless Method for Continuous Recording of Pulse Pressure in Man," J. Appl. Physiol., 17:844, 1962.

Blaquier, P., and Hoobler, S.W., "A New Blood Pressure Cuff for Self-Determination of the Blood Pressure," Univ. Mich. Med. Bull., 23:356-365, October 1957.

Bracale, M., DeFilippis, P., and Marcato, M., "A Differential Photo-Plethysmographic System," 8th ICMBE, Chicago, 1969.

Bradfute, G., Wright, J., "System for Beat-to-Beat Blood Pressure Telemetry in Ambulatory Humans," Bio. Med. Sci. Instr., 4:7-20, 1968.

Brown, L., "Instrumentation for Computing Pulse Propagation Velocity in Human Subjects," Bachelors Thesis, MIT, June 1972.

Burton, A.C., "Physiology and Biophysics of the Circulation," Year Book Medical Pub. Inc., Chicago, 1965.

Chang, Po-Cheng, "Immediate Smoking Effects as Observed from the Dispersive Nature of Pulse Wave Velocity," 24th ACEMB, Las Vegas, 1971.

Clamann, H.G., Prof. Soc. Exptl. Biol. Med., 78:50-52, 1951.

Cohen, A., Longini, R., "Theoretical Determination of the Blood's Relative Oxygen Saturation in Vivo," Med. and Biol. Engng., 9:61-69, 1971.

Corell, R.W., "Theoretical Analysis and Preliminary Development of an Indirect Blood Pressure Recording System," Masters Thesis, MIT, June 1959.

Couch, N.P., "Noninvasive Measurement of Peripheral Arterial Flow," Arch. of Surg., 102:435-439, May 1971.

D'Agrossa, L., Hertzman, A., "A Photometric Study of Vasomotion in the Bat Wing," Fed. Proc., 24:459, 1965.

D'Agrossa, L., Hertzman, A., "Opacity Pulse of Individual Minute Arteries," J. of Appl. Physiol., 23:613-620, 1967.

Davis, M., Gilmore, B., and Freis, E., "Improved Transducer for External Recording of Arterial Pulse Waves," IEEE Biomed., BME-10:73-81, April 1963.

DeMonchy, "Determination of Central and Peripheral Pulse Wave Velocity in Children from 2 to 12 Years," Pflugers Arch., 314:174, 1970.

Eliakim, M., Sapoznikov, D., Weinman, J., "Pulse Wave Velocity in Healthy Subjects and in Patients with Various Disease States," American Heart Journal, 82:448-457, 1971.

Fine, S., and Klein, E., "Lasers in Biology and Medicine," Laser Focus Magazine, July 1969.

Fine, S., and Klein, E., "Lasers in Biology and Medicine," Developments in Laser Technology Seminar Proceedings, Univ. of Rochester, Vol. 20, November 17-18, 1969.

Flax, S., Webster, J., and Updike, S., "Theoretical and Experimental Evaluation of Doppler Blood Flow Information," 8th ICMBE, Chicago, 1969.

Fraser, M.P., "Transcutaneous Spectral Blood-Flowmeter," MIT, Lincoln Laboratory, Technical Note, 1970-7, 1970.

Freis, E.D., Heath, Luchsinger, and Snell, "Changes in Carotid Pulse with Age and Hypertension," American Heart Journal, June 1966, page 757.

Fuller, M , "An Optical Differential Plethysmograph," B.S. Thesis, MIT, June 1972.

Geddes, L.A., Hoff, H.E., "Graphic Recording of the Pressure-Pulse Wave," J. Appl. Physiol., 15:959-960, 1960.

Gilson, W.E., Goldberg, H., and Slocum, "An Automatic Device for Periodically Determining Both Systolic and Diastolic Pressure in Man," Science, 94:194, 1941.

Goldberg, Harvey, Bachelors Thesis, to be completed at MIT, 1972.

Goldman, Richard, "Ultrasonic Technology," Reinhold Publishing Co., New York, 1962

Gorelick, D.E., and Kim, C., "Improved Instrumentation for External Recording of Arterial Pulse Waves," NASA, Goddard Space Flight Center, Greenbelt, Md., unpublished report, Technology Utilization Office, August 1971.

Green, J.H., "Blood Pressure Follower for Continuous Blood Pressure Recording in Man," J. Physiol. (London), 130:37P-38P, 1955.

Heck, A., "Opacity Pulse Propagation in Internal and External Carotid Vascular Beds of Experimental Animals," Stroke, 1:401-410, 1970.

Heck, A., "Photoelectric Measurements: Comments on the Origin of Opacity Phenomena in Tissue and Applications in Assessment of Cardiovascular Function," in "Physiological Applications of Impedance Plethysmography," by Allison, Instrument Soc. Am., 1972.

Heck, A., and Hall, V., "A Technique for Differential Photoelectric Plethysmography of Brain and Ear," Appl. Physiol. 19:1236-1239, 1964.

Heck, A., Hawthorne, I., "Opacity Pulse and Pulse Propagation in the Microcirculation," 5th Europ. Conf. Microcirc., Bibl.,Anat.,10:579-591, 1969.

Heck, A., Hawthorne, B., "Opacity Pulse Recordings from the Microcirculatory Bed of the Conjunctiva," Angiology, 21:89-102, 1970.

Heck, A., Price, T., "Opacity Pulse Propagation Measurements in Humans," Stroke, 1:411-418, 1970.

Heck, A., Price, T., "Atraumatic Detection of Occlusive Vascular Disease in Carotid and Subclavian Arteries by Opacity Pulse Propagation Techniques," Angiology, 22:153-164, 1971.

Hertzman, A.B., "Blood Supply of Various Skin Areas as Estimated by the Photoelectric Plethysmograph," Amer. J. of Physiol., 124:328-340, 1938.

Herzfeld, Karl, and Litovitz, "Absorption and Dispersion of Ultrasonic Waves," Academic Press, New York, 1959.

Hokanson, E., Mogersky, Sumner, Strandness, "A Phase-Locked Echo Tracking System for Recording Arterial Diameter Changes in Vivo," Journal of Applied Physiology, 32:728-733, 1972.

Ikegami, "Critical Studies on Various Plethysmographic Methods with Special Reference to the Reflexion Photoelectric Plethysmograph," Resp. Circ., 6:881-890, 1958.

Johnson, C., "Optical Transmission in Blood, " 21st ACEMB, Houston, 1968.

Johnson, C., "Optical Diffusion in Blood," IEEE Bio-Med. Eng., 17:129-133, 1970.

Johnson, C., Moaveni, M., "An Optical Multiple Scattering Theory for Blood," 23rd ACEMB, Washington, 1970.

Johnson, R.A., "Model 16 Automatic Blood Pressure Measuring Instrument," WADC Technical Report, 59-429, U.S. Govt. Dept. of Commerce, Wash. D.C., 1959.

Johnston, A., Cyprus, J., "Spectral Analysis of Doppler Ultrasonic Flowmeter Signals," 21st ACEMB, Houston, 1968.

Jones, W., Simpson, W., "NASA Contributions to Cardiovascular Monitoring," NASA -Sp-5041, 1966.

Kirby, R.R., Anesthesiology, 31:86-89, 1969.

Korotkoff, N.S., Izv. Voenno-Med. Akad., 11:365, 1905.

Krasilnikov, V.A., "Sound & Ultrasound Waves," National Science Foundation, Washington, D.C., 1963.

LaBresh, L.A., "Pulse Wave Velocity as a Measure of Arterial Blood Pressure," Bachelors Thesis, MIT, June 1970.

LaBresh, L.A., "Pulse Detection on Ambulatory Patients," unpublished paper, September 18, 1970.

Lader, M.H., "A Manuel of Psychophysiological Methods," Ed. P.H. Venables, North-Holland Publ. Co., Amsterdam, 1967.

Lele, P., "Application of Ultrasound in Medicine," New England Journal of Medicine, June 15, 1972.

Lees, V., Barber, F., Aaronson, C., "Ultrasonic Determination of the Cross Section of a Simulated Blood Vessel," 8th ICMBE, Chicago, 1969.

Light, L.H., "Non Injurious Ultrasonic Technique for Observing Flow in the Human Aorta," Nature, 224:1119-1121, 1969.

Longini, R., Zdrojkowski, R., "A Note on the Theory of Backscattering of Light by Living Tissue," IEEE Bio. Med. Eng., 15:4-10, 1968.

Malindzak, G., Meredith, J., "Comparative Study of Arterial Transmission Velocity," Bio. Mechanics, 3:337-350, 1970.

Mann, H., "Study of Peripheral Circulation by Means of an Alternating Current Bridge," Proc. Soc. Biol. Med., 36:670, 1937.

McDonald, D.A., "Regional Pulse-Wave Velocity in the Arterial Tree," Journal of Applied Physiology, 24:73-78, 1968.

McLeod, F.D., "Directional Doppler Demodulation," 20th ACEMB, Boston, 1967.

Monnier, M., "Changes in Pulse Wave Velocity with Age," Gerontologia Clinica, 9:81-86, 1967.

Montagna, W., Ellis, R., Advances in Biology of Skin, Volume 2, Pergamon Press, New York, 1961.

Morikawa, S., Lany, O., and Johnson, C., "Laser Doppler Measurement of Localized Pulsatile Fluid Velocity," IEEE Bio. Med., BME-18:416, November 1971.

Myers, George, Parsonnet, V., "Engineering in the Heart and Blood Vessels," Wiley-Interscience, New York, 1969.

Nielson, L., Fabricius, J., "Pressure Wave Velocity in the Human Aorta," J. of Am. Ger. Soc., 16:647-657, 1968.

Nielson, L., Roin, J., Fabricius, J., "Carotid-Femoral Pulse Wave Velocity," J. of Am. Ger. Soc., 16:658-665, 1968.

Nippa, J.H., Alexander, R., Folse, R., "Pulse Wave Velocity in Human Veins," Journal of Applied Physiology, 30:558-563, 1971.

Nyboer, J., "Electrical Impedance Plethysmography," Charles C. Thomas Publisher, Springfield, Ill., 1970.

Olson, R., Shelton, D., "Ultrasonic Measurement of Aortic Diameter vs. Time, Position, and Pressure," 24th ACEMB, Las Vegas, 1971.

Parks, L., "Transcutaneous Doppler Manual," Parks Electronics Lab, Beaverton, Ore.

Parks, L., "Personal Communications," July, 1972.

Raines, J., Personal Communications, December 8, 1971, Thesis to be published at MIT.

Raines, Jeff, Loan of Model 806 Doppler Instrument, July, 1972.

Reid, J., Sigelman, Nassar, Baker, "The Scattering of Ultrasound by Human Blood," 8th ICMBE, Chicago, 1969.

Remler Company, 2101 Bryant Street, San Francisco, California.

Robinson, R.E., Eastwood, D.W., "Use of Photo-Sphygmometer in Indirect Blood Pressure Measurements," Anesthesiology, 704:Sept. - Oct., 1959.

Rose, R.C., Gilford, S.R., Broida, H.P., and Freis, E.D., "Clinical and Investigative Applications of a New Instrument for Continuous Recording of Blood Pressure and Heart Rate," New Engl. J. Med., 249:515, 1953.

Sabotta, J., Atlas of Descriptive Human Anatomy, Volume III, Hafner Publishing Co., New York, 1957.

Sawada, "Regional Characteristic of Fluctuation of the Level in Cutaneous Volume Pulse," Resp. Circ., 6:417-424, 1958.

Schade, C., Duff, W., "In Vitro Model for Ultrasonic Flow Measurement," 24th ACEMB, Las Vegas, 1971.

Schaeffer, A.I., "Neonatal Blood Pressure Studies," Amer. J. Dis. Child., 89:204-209, 1955.

Selkurt, E., Physiology, Little, Brown and Company, Boston, p. 360, 1971.

Smith, C.R., Bickley, W.H., "The Measurement of Blood Pressure in the Human Body," NASA SP-5006, April 1964.

Stegall, H.F., Rushmer, R.F., Baker, D.W., "Transcutaneous Ultrasonic Blood-Velocity Meter," J. of Appl. Physiol., 21:707-711, 1966.

Strong, P., "Biophysical Measurements," Tektronix Inc., Oregon, 1970.

Tatai, Asano, Yoshida, Osada, Tatai, "Rhythmic Circulatory Changes in the Peripheral Vasculature," Ann. N.Y. Acad. Sci., 98:1069-1082, 1962.

Technical Resources Inc., "Technical Bulletin," Waltham, Mass.

Traite, M., Germain, L.M., Pratt, A.W., "Systolic and Diastolic Blood Pressure on a Finger," 15th Annual Conf. on Eng. in Med. and Bio., November 1962.

Transducer Products, 95 Walcott Ave., Torrington, Conn.

Tursky, B., Shapiro, D., Schwartz, G., "Automated Constant Cuff-Pressure System to Measure Average Systolic and Diastolic Pressure in Man," IEEE Bio. Med. Trans., July 1972.

Weinman, J., "Photoplethysmography," in A Manuel of Psychophysiological Methods, Ed. P.H. Venables, North-Holland Publ. Co., Amsterdam, 1967.

Weinman, J., Personal Communications, August, 1972.

Weinman, J., Ben-Yaakov, S., "The Physical and Physiological Basis of Photoplethysmography," 6th ICMEBE, Tokyo, p. 54, 1965.

Weinman, J., Sapoznikov, D., "Reliability of Photoplethysmography in Cardiovascular Studies," 8th ICMBE, Chicago, 1969.

Weinman, J., Sapoznikov, D., "Equipment for Continuous Measurements of Pulse Wave Velocities," Med. and Biol. Engng., 9:125-138, 1971.

Weinman, J., and Sapoznikov, D., "The Shift of the Arterial Pulse-Wave Foot on Recordings with Rising or Falling Baseline," IEEE Trans. Bio-Med, p. 56, 1971.

Weinman, J., Sapoznikov, D., Eliakim, M., "Arterial Pulse Wave Velocity and Left Ventricular Tension Period in Cardiac Arrhythmias," Cardio Research, 5:513, 1971.

Weiss, H., "An Automatic Blood Pressure Recording Apparatus," J. Lab. Clin. Med., 26:1351-1358, 1941.

Wells, P.N.T., "Physical Principles of Ultrasonic Diagnosis," Academic Press, New York, 1969.

Wells, P.N.T., "The Directivities of Some Ultrasonic Doppler Probes," Med, and Biol. Engng., 8:241-256, 1970.

Wichmann, T., Salisbury, P., "Indirect Blood Pressure Monitoring," Bio. Med. Sci. Instr., Volume 2, William Murray Editor, Plenum Press, New York, pp 185-194, 1964.

Womersley, H.R., "An Elastic Tube Theory of Pulse Transmission and Oscillating Flow in Mammalian Arteries," WADC Tech. Report, TR 56-614, January 1957.

Wood, E.H., Proc. of Staff Meetings of Mayo Clinic, July 5, 1950, 25:14:377-405, 1950.

Woolam, G.L., Schnur, P.L., Hoff, H.E., "The Pulse Wave Velocity as an Early Indicator of Athereosclerosis in Diabetic Patients," Circulation, 25:533, 1962.

Wostenholme, G., Freeman, J., Peripheral Circulation in Man, Little, Brown and Co., Boston; 1954.

Yamada, "Volume Pulse in Human Skin Recorded by Direct Coupled Reflexion Photoelectric Plethysmograph with Special Reference to Spontaneous Fluctuations of Its Base Line," Resp. Circ., 7:283-289, 1959.

Zdrojkowski, R., Longini, R., "Further Studies on the Optics of Blood," 21st ACEMB, Houston, 1968.

Zdrojkowski, R., Pisharoty, N., "Optical Transmission and Reflexion by Blood," IEEE Bio-Med. Eng. 17:122-127, 1970.

Zuidema, G.D., Edelberg, Saltzman, E., "A Device for Indirect Recording of Blood Pressure," WADC Tech note, 55-427, September 1955.

CARDIOVASCULAR MONITORING SYSTEM

VOLUME I

USERS' MANUAL

Prepared by:

Biomedical Engineering Division
Thorndike Memorial Laboratory
Boston City Hospital
Boston, Massachusetts

June 1974

TABLE OF CONTENTS

THE CARDIOVASCULAR MONITORING SYSTEM

I. General Description

The Cardiovascular Monitoring System (CMS) is intended to monitor diastolic blood pressure (BP) and heart rate (HR) in a non-invasive manner on a beat-by-beat basis. It is suitable for use in assessing cardiovascular conditioning in cooperative subjects at rest, and is particularly well-suited for lower-body negative pressure experiments.

The propogation velocity of pulse waves in the aorta is a function of diastolic blood pressure. Furthermore, pulse wave propogation velocity is approximately proportional to $\frac{1}{\Delta T}$, where ΔT is the time between onsets of the carotid and femoral pulse waves. (See Appendices A and B). The CMS detects both pulse waves and measures the difference between their onset times (ΔT). Diastolic blood pressure is then calculated according to the linear equation:

$$BP = \frac{M}{50}\left[\frac{1}{\Delta T} - \frac{1}{T_o}\right] + \frac{P_o}{4}$$

where M, $\frac{1}{T_o}$ and P_o are constants. The CMS also calculates instantaneous heart rate, which is computed from the pulse wave signals or the EKG.

The pulse waves are detected using contact microphone transducers which are positioned firmly against the skin over the carotid and femoral arteries. The resultant signals are amplified, differentiated and then filtered to reduce the amplitude of baseline shifts, movement artifacts and other noise which might obscure the pulse wave. Further noise reduction is obtained by correlating the pulse signals with the EKG. Using the QRS complex, a time interval (or window) is established during which the carotid pulse must occur. The instrument is sensitive to inputs from the carotid transducer only during this window, and thereby rejects improperly timed noise.

The EKG is amplified and filtered to attentuate baseline shifts, muscle noise and most of the T-Wave. A QRS complex is detected whenever the filtered signal exceeds 50% of its previous peak amplitude. The carotid window is opened 60 msec. after the QRS and closed after a carotid pulse is detected, or 200 msec. after the QRS, whichever comes first.

An analogous procedure is applied to obtain a femoral window. The femoral pulse is predicted by a carotid pulse. Therefore, the window is opened at the onset of a carotid pulse and closed after detection of a femoral pulse or after 280 msec., whichever comes first.

The principal task of the CMS is to determine the onset times of the carotid and femoral pulses. However, this is not easy. As one can see by looking at a strip chart tracing, the upward slope of a pulse wave is not very steep (Figure 1).

By defining different points along the upward slope to be the onset, one could easily obtain answers differing by up to 20 msec. Since the nominal delay time between carotid

Figure 1

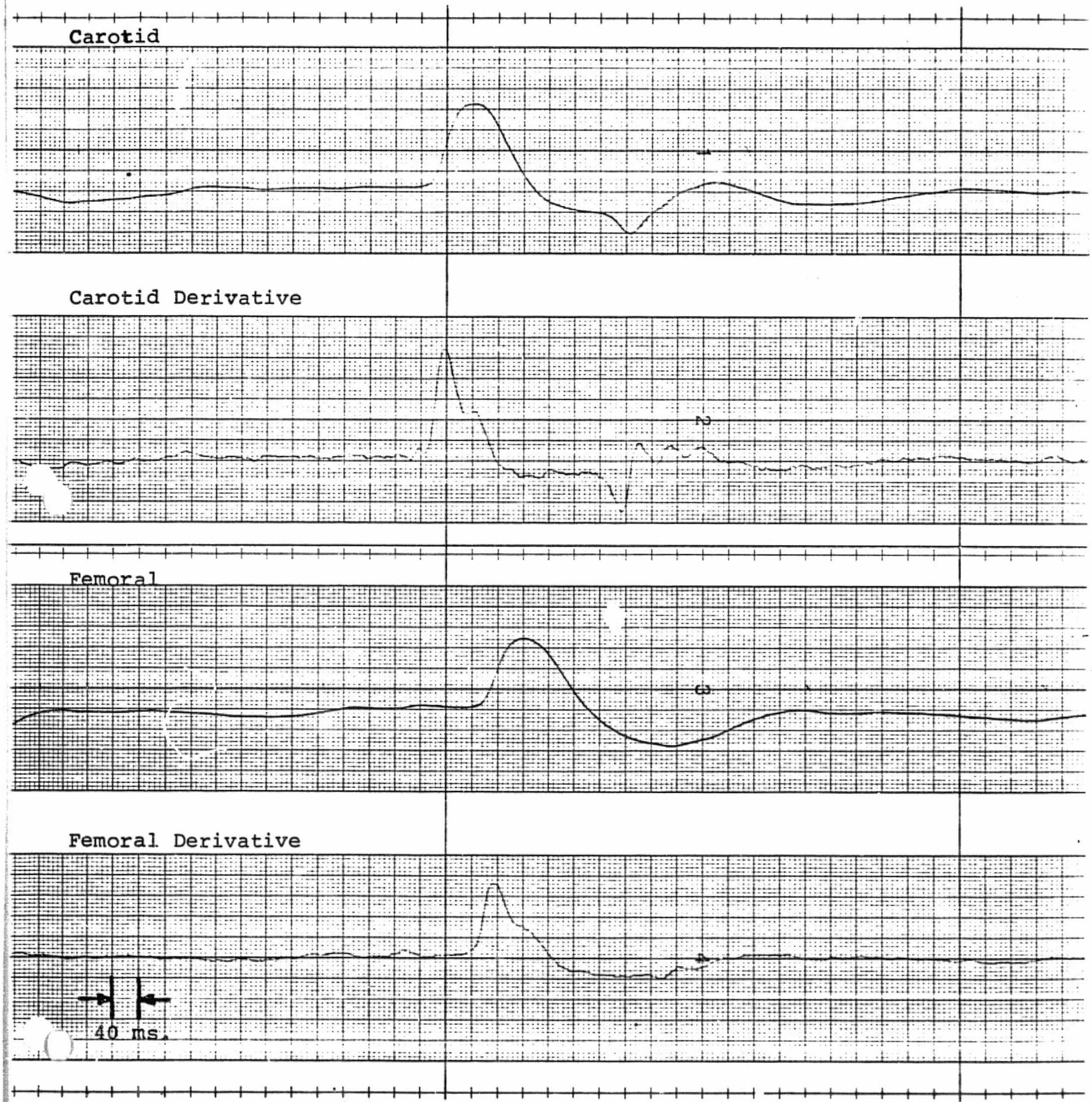
Carotid
Carotid Derivative
Femoral
Femoral Derivative
40 ms.

and femoral onset times is about 70 msec., such a variation could cause significant error if inconsistent. The derivative of the pulse wave signal has a much steeper upward slope, but is also much noiser.

Fortunately, the pulse wave signal and its derivative are highly correlated. This has been exploited to combine the best features of both in defining the onset. The derivative is used to pinpoint the onset, while the pulse-wave signal is used to verify that the peak in the derivative signal belongs to a pulse wave and not to some noise pulse.

The algorithm for defining the onset times for both carotid and femoral pulses is depicted in Figure 2. The time at which the derivative crosses an operator-selected threshold defines a possible pulse wave onset and starts a timer. If the pulse-wave signal crosses a preset threshold (60% of its average peak level) before the derivative crosses zero, the algorithm is satisfied that a pulse wave has occurred and outputs a marker 160msec. after the timer was started. If the algorithm is not fulfilled, no output marker will occur and the timer will be reset.

The interval between carotid and femoral onsets is measured by counting pulses from a crystal controlled clock and storing the resultant binary number, ΔT. The clock is turned on by the output marker from the carotid onset detector, and is turned off by the femoral marker. The propoagation time ΔT is then both reciprocated $(\frac{1}{\Delta T})$ and

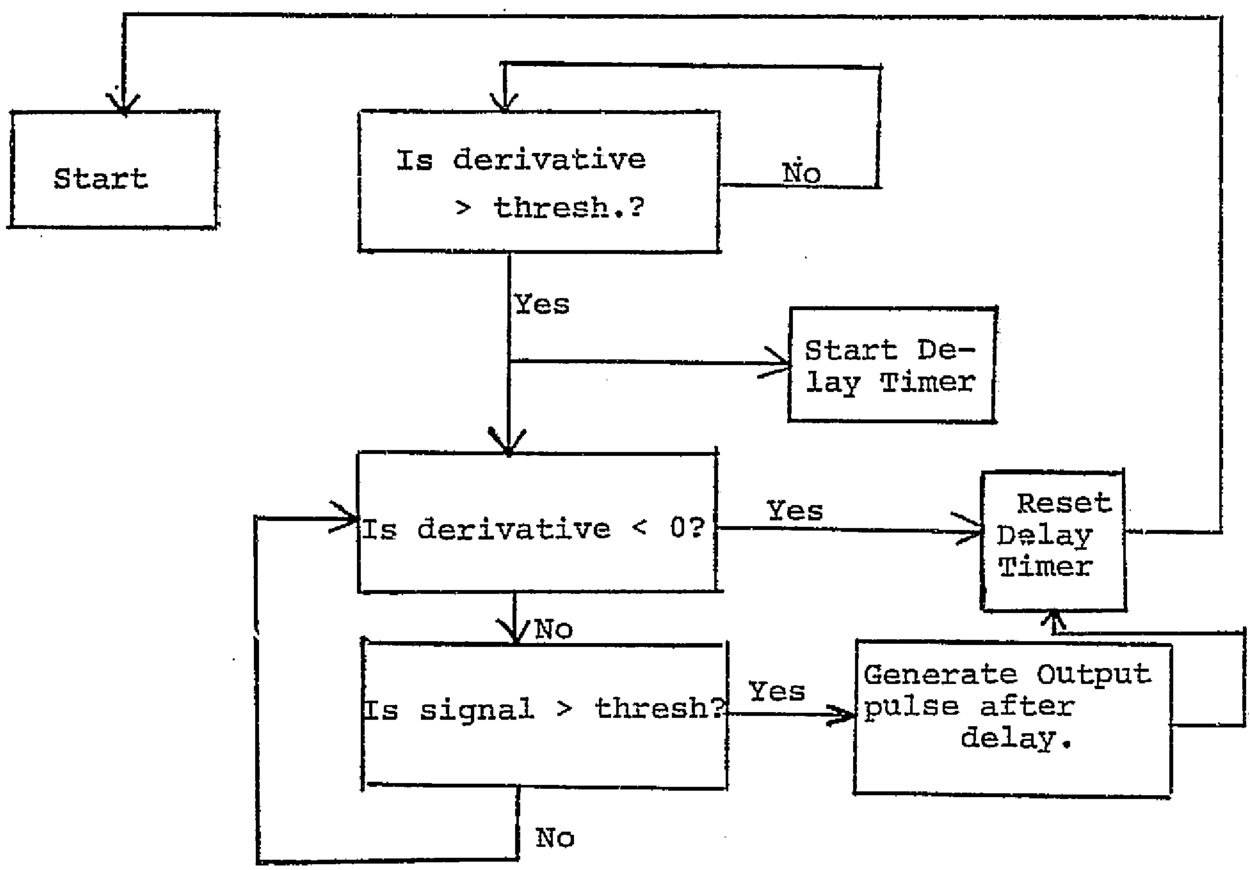

Figure 2

converted to an analog voltage by a special D to A converter. Finally, constants M, $\frac{1}{T_o}$, and P_o are introduced according to the equation at the beginning of this section to provide a calibrated output.

Heart rate is computed by determining the time, T, between successive carotid and femoral pulse pairs. A second reciprocating D/A converter produces an analog output voltage proportional to heart rate ($\frac{1}{T}$) on a beat-by-beat basis. When the EKG is used, the R-wave is used for HR.

A block diagram of the instrument is shown in Figures 3A and 3B. A more detailed description of the blocks is presented in Section IV.

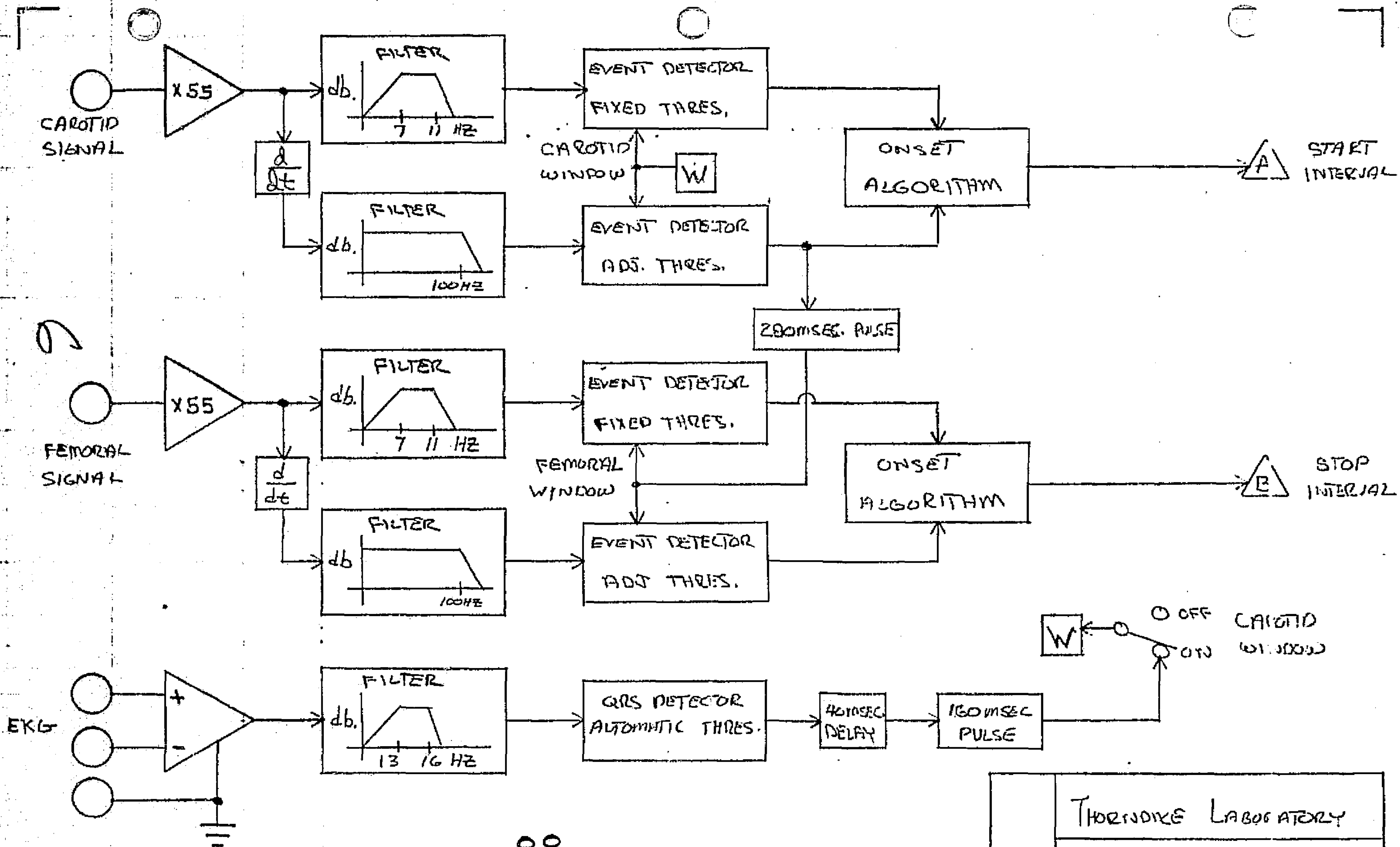

Thorndike Laboratory	
Blood Pressure Machine	
Block Diagram	
6-12-74	Fig. 3A

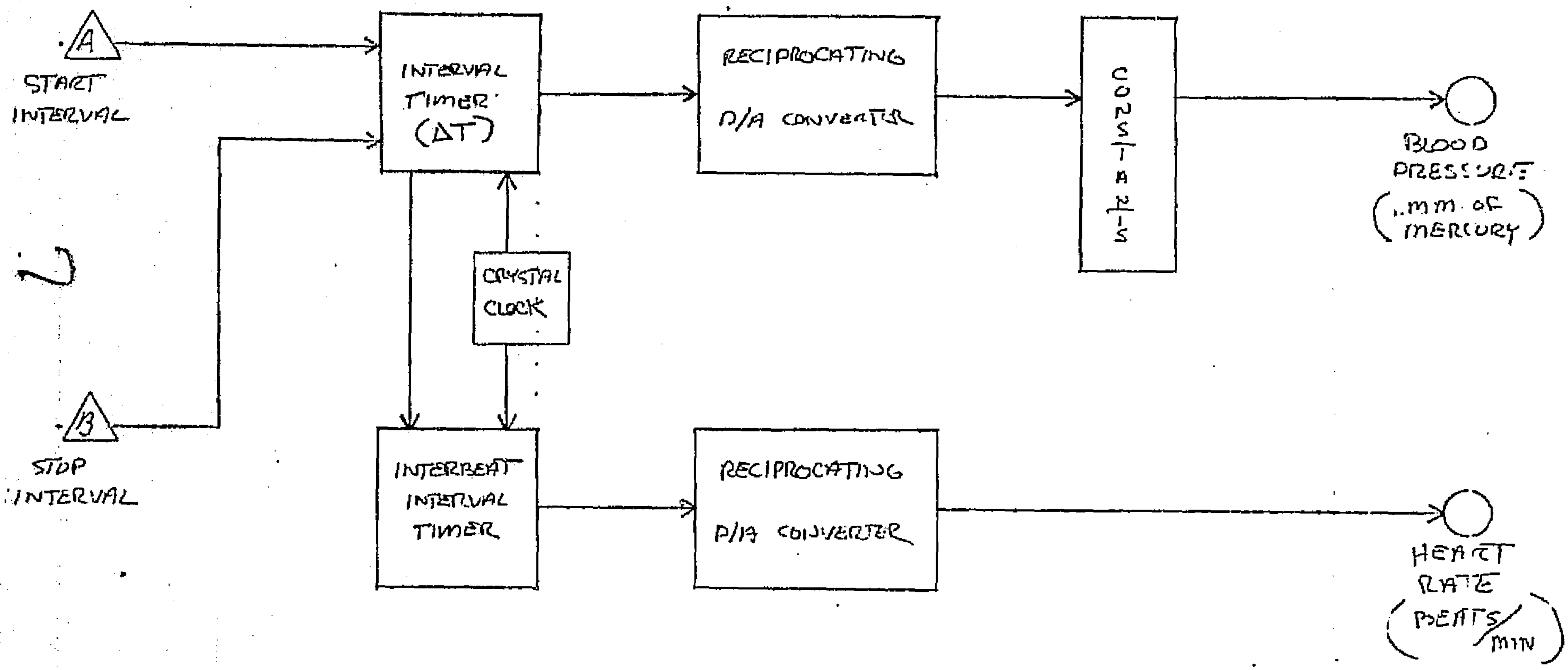

Thorndike Laboratory	
Blood Pressure Machine	
Block Diagram	
6-12-74	Fig 3B

II. Description of Front Panel Controls

(See Figure 4.)

A. EKG INPUT JACK and GATE INDICATOR LAMP.

This jack accepts the three-electrode EKG cable, which is used whenever EKG synchronization is desired. The EKG-triggered gate is indicated by the lamp, which should blink once for each heart beat.

B. CAROTID PULSE SECTION

1. The Input jack accepts the carotid pulse transducer.

2. Signal Output. The filtered carotid pulse signal is provided at this connector for display on an external chart recorder or oscilloscope. With proper transducer placement, the signal amplitude should be on the order of one volt.

3. Derivative Output. The differentiated carotid pulse signal is provided at this connector. In addition, the threshold level may be multiplexed onto the same output if desired. The threshold multiplex feature is convenient if an oscilloscope display is used, but cannot be used with a chart recorder. The multiplex option may be switched off using a behind-the-panel switch located on the output board. (See paragraph H below.)

4. Level Control. This potentiometer controls the threshold level for triggering on the carotid derivative.

C. FEMORAL PULSE SECTION

The controls here are exactly analogous to the carotid section.

D. INDICATOR LAMP SECTION

The five indicator lamps are provided to permit the operator to correctly set the carotid and femoral trigger levels without using an oscilloscopic display. Their function is described below in Section III, paragraph C.

E. CALIBRATION SECTION

This section contains three potentiometers which provide an adjustable linear calibration of the output voltage. Thus, the output voltage may be set to be a linear function of the pulse wave velocity, $\frac{1}{\Delta T}$, according to the equation indicated:

$$V_{out} = BP = \frac{M}{50}\left(\frac{1}{\Delta T} - \frac{1}{T_o}\right) + \frac{P_o}{4}.$$

The procedure for calibration is described in Section III.

F. OUTPUT SECTION

This section contains a digital voltmeter which will display instantaneous heart rate or diastolic blood pressure, as selected by a switch located just to the right of the meter.

The HOLD-RUN push-button switch permits the operator to hold a given value of HR and BP in order to perform the calibration process. In the "HOLD" position the instrument will not accept any new data, but will continue to display the held value for HR or BP.

Analog output voltages corresponding to HR and BP are provided via the two BNC connectors. The multiple pin connector provides the BCD output of the DVM, for computer use.

G. POWER SECTION

The power on-off switch and indicator lamp are included in this section, as well as a line fuse (1 ampere slow blow).

H. BEHIND-THE-PANEL SWITCHES. (See Figure 5.)

1. EKG board - This switch disables the EKG-triggered carotid window, and must be "OFF" (down) when the EKG is not used.

2. Output Board - This switch controls the chopping multiplexer. It must be "OFF" (down) when using a chart recorder, or when the threshold level multiplexing is not desired.

Figure 4

PRECEDING PAGE BLANK NOT FILMED

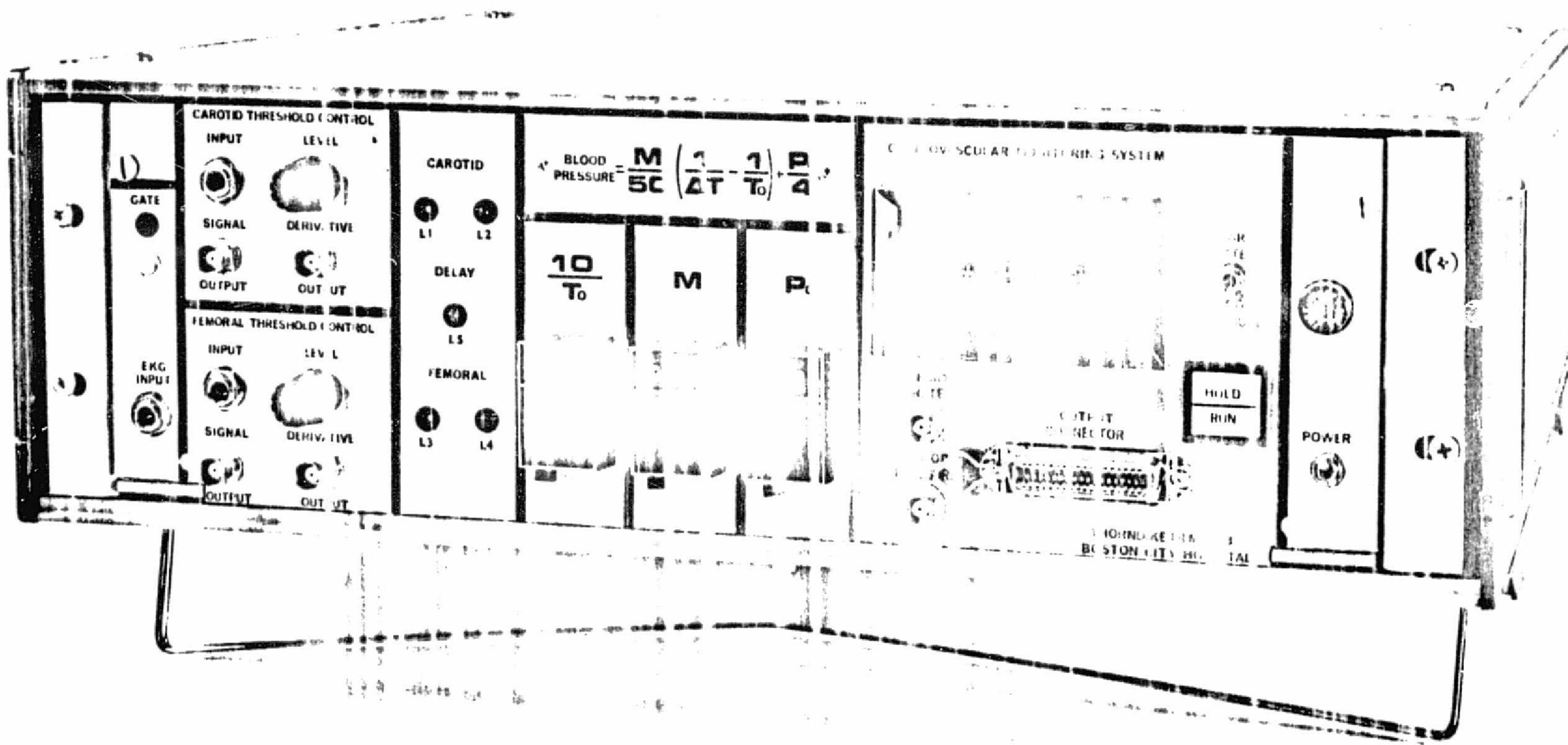
CAROTID THRESHOLD CONTROL
INPUT
LEVEL
SIGNAL
OUTPUT
GATE
EKG INPUT
FEMORAL THRESHOLD CONTROL
INPUT
SIGNAL
OUTPUT
CAROTID
L1
L2
DELAY
L5
FEMORAL
L3
L4
BLOOD PRESSURE $= \frac{M}{5C}\left(\frac{1}{\Delta T} - \frac{1}{T_0}\right) + \frac{P}{4}$
$\frac{10}{T_0}$
M
HOLD
RUN
POWER
BOSTON CITY

Figure 5

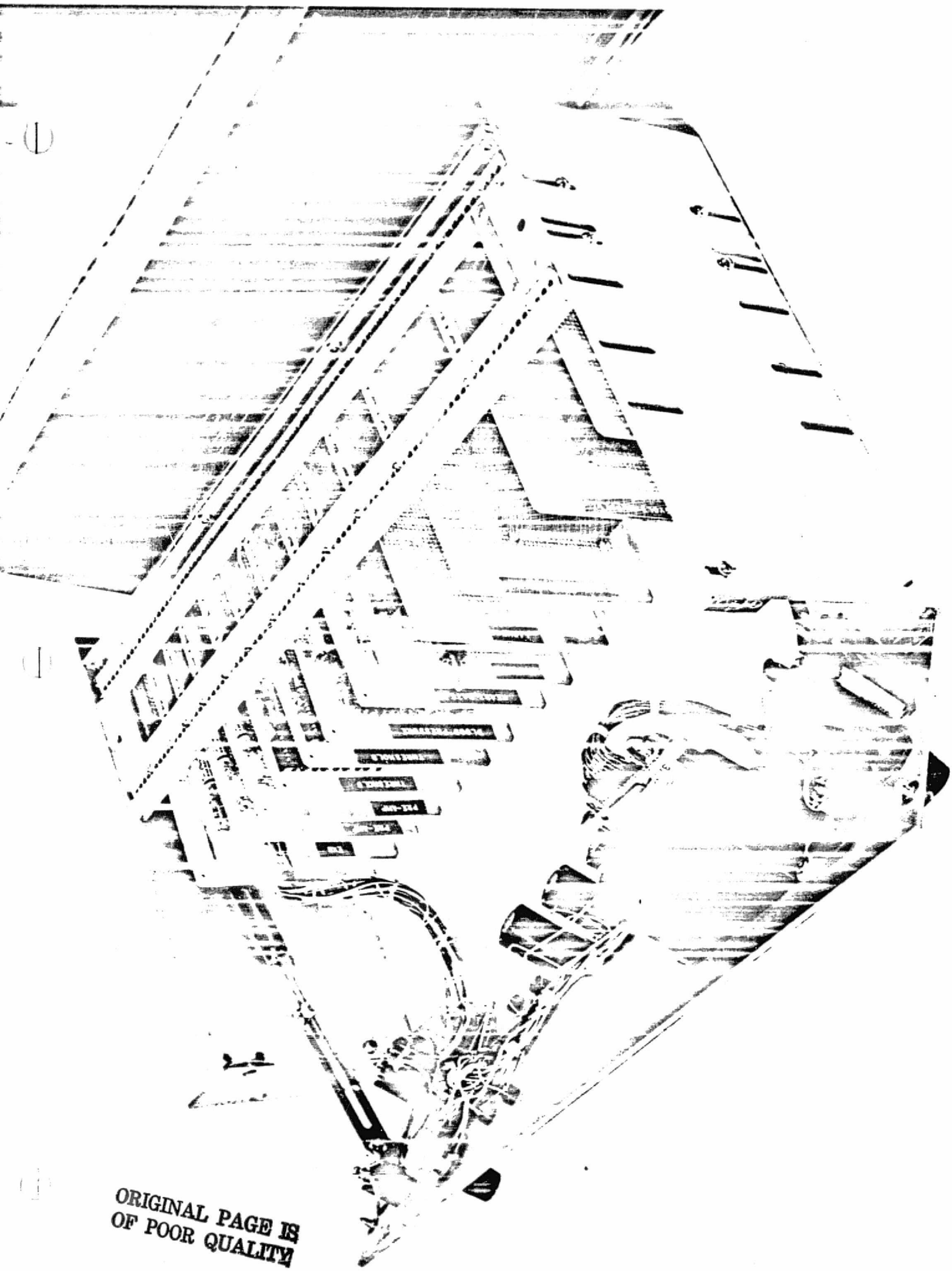

III. Operating Instructions

A. EKG LEADS

The EKG leads are placed as illustrated in Figure 6. The skin should be cleaned with alcohol and the cups filled with conductive paste before they are applied. The light above the EKG input connector should flash once per heart beat. Uninterrupted operation of the light indicates excessive 60 cycle noise, which is usually caused by one or more poorly conducting leads.

Note: If the EKG is not used, the disabling switch on the EKG Board must be moved to the "OFF" position (down). Otherwise the carotid and femoral detectors will not operate.

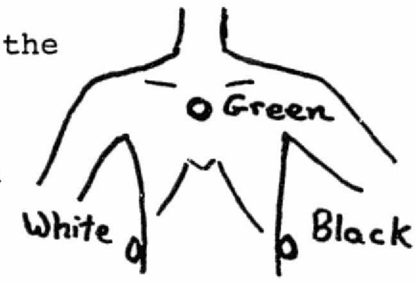

Figure 6

B. CAROTID AND FEMORAL TRANSDUCER PLACEMENT

The transducers should be positioned over the carotid and femoral arteries with the harnesses supplied (see figures 7,8, and 9). For best results, they should be tightly held, consistent with patient comfort. Note that two tips are supplied with each transducer. Over fleshy areas best results are obtained with the wide tip. However, with thin-necked people, the thin tip is preferable.

Figure 7

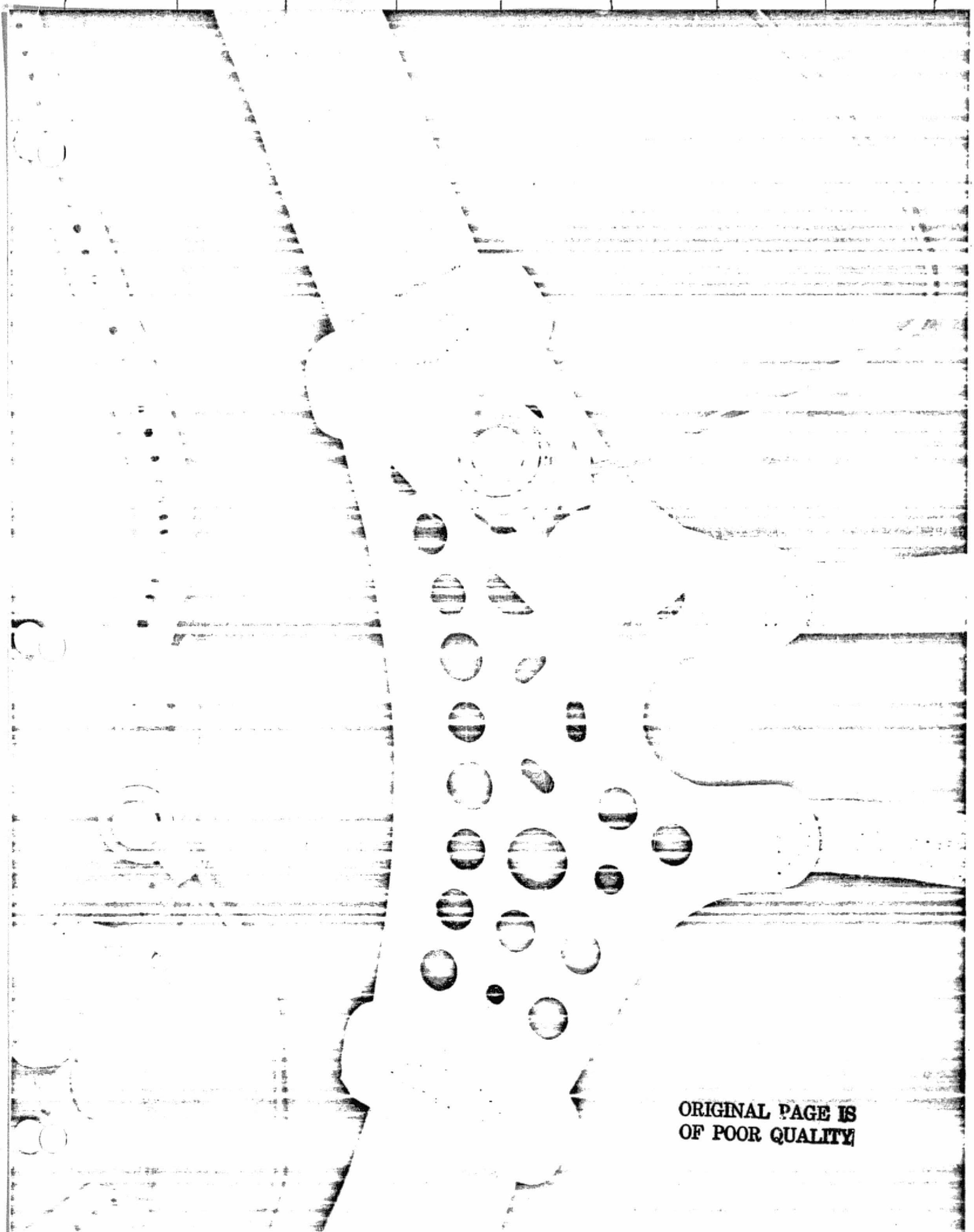

Figure 8

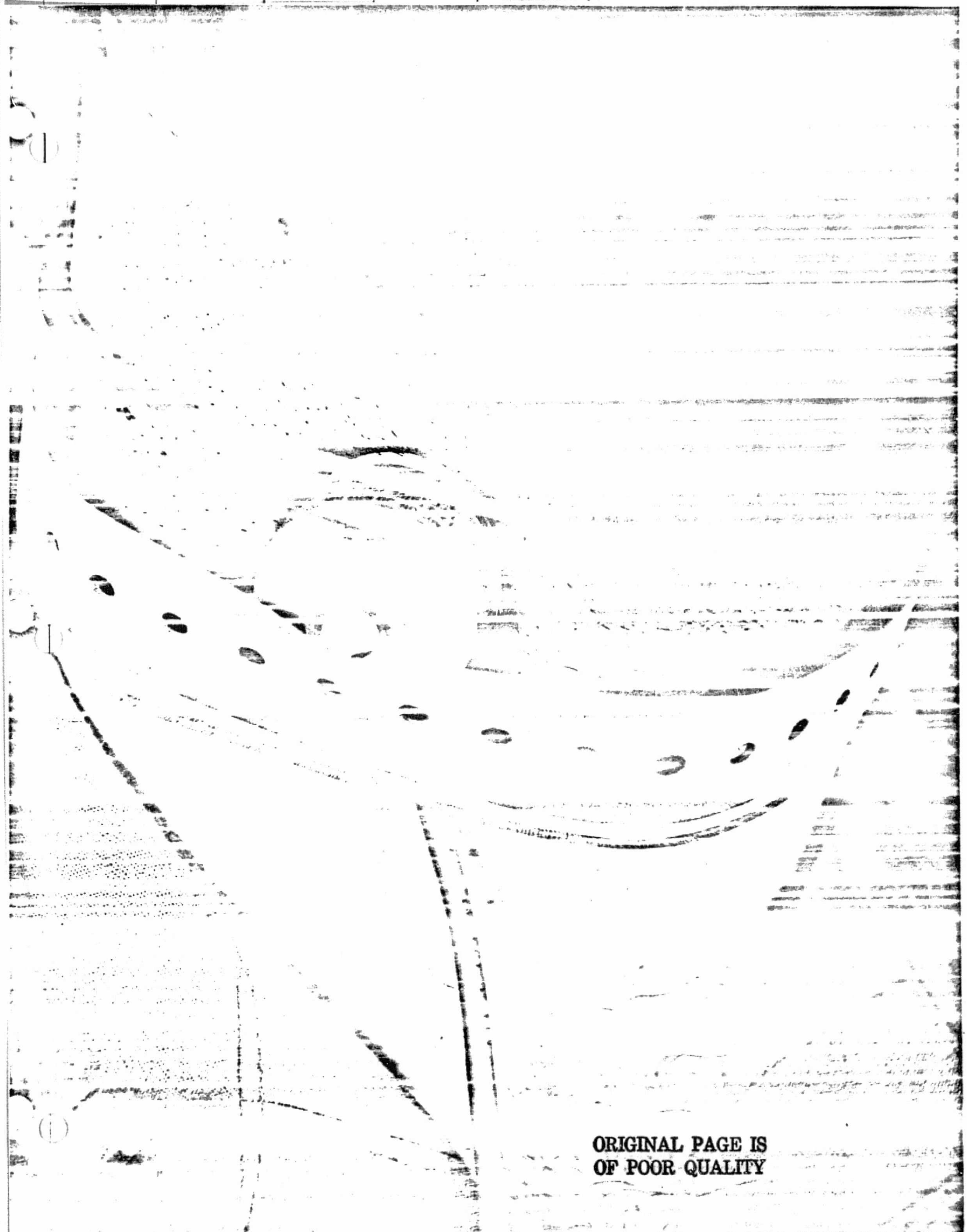

Figure 9

C. THRESHOLD ADJUSTMENTS

Threshold adjustments may be made most conveniently with the help of an oscilloscope. The pulse signal derivative and the threshold level are multiplexed and provided for oscilloscopic viewing at the "derivative output" connector. The threshold level should be adjusted to give unambiguous triggering.

If an oscilloscope is not available, lights L_1 - L_5 may be used to adjust threshold levels properly. L_1 and L_2 relate to the carotid signal, while L_3 and L_4 relate to femoral pulse signals. L_1 (or L_3) changes state each time the derivative signal crosses threshold. L_2 (or L_4) flashes whenever the instrument identifies a pulse according to its algorithm. Normal operation will lead to one change in state of L_1 and one flash of L_2 per heart-beat. In cases where a large dicrotic notch is present, the derivative may cross threshold more than once, causing double triggering of L_1 (or L_3). Under these conditions the threshold should be adjusted to obtain one flash of L_2 (or L_4) per beat.

Note: The carotid lights will not operate unless an EKG is present or the carotid window is disabled. Also, the femoral lights will not operate correctly until the carotid threshold is adjusted correctly.

D. CALIBRATION

The heart rate channel is calibrated internally and should not require further adjustment. Calibration of the blood pressure channel requires an independent measure of blood pressure, such as a standard sphygmomanometer, or intra-arterial measurement. Initially the controls in the calibration section should be set approximately as follows:

$$M = 500$$
$$\frac{1}{T_o} = 0$$
$$P_o = 0$$

With the CMS operating, obtain an independent BP reading and push the HOLD button. The CMS will hold the most recent values for BP and HR. With the meter switch in the BP position, adjust the $\frac{1}{T_o}$ control until the meter reads zero. Next adjust the P_o control until the meter reading agrees with the subject's diastolic BP. Next, a significant change in the subject's BP must be induced. (Isometric muscle exercise, inhalation of amyl nitrite, LBNP, etc. are some potential methods.) Document the new BP with the standard technique, and immediately push "HOLD" again. Adjust only the M control until the meter reading indicates the the observed new BP. Lock all controls. Additional calibration points may be checked if desired.

An example of the analog BP output channel as displayed on a slowly moving strip chart recorder is shown in Figure 10. The subject was in this case, a dog, and simultaneous records of intra-arterial BP and the CMS BP output are shown. (The periodic oscillations in BP are due to respiration.) The BP was manipulated using levophed.

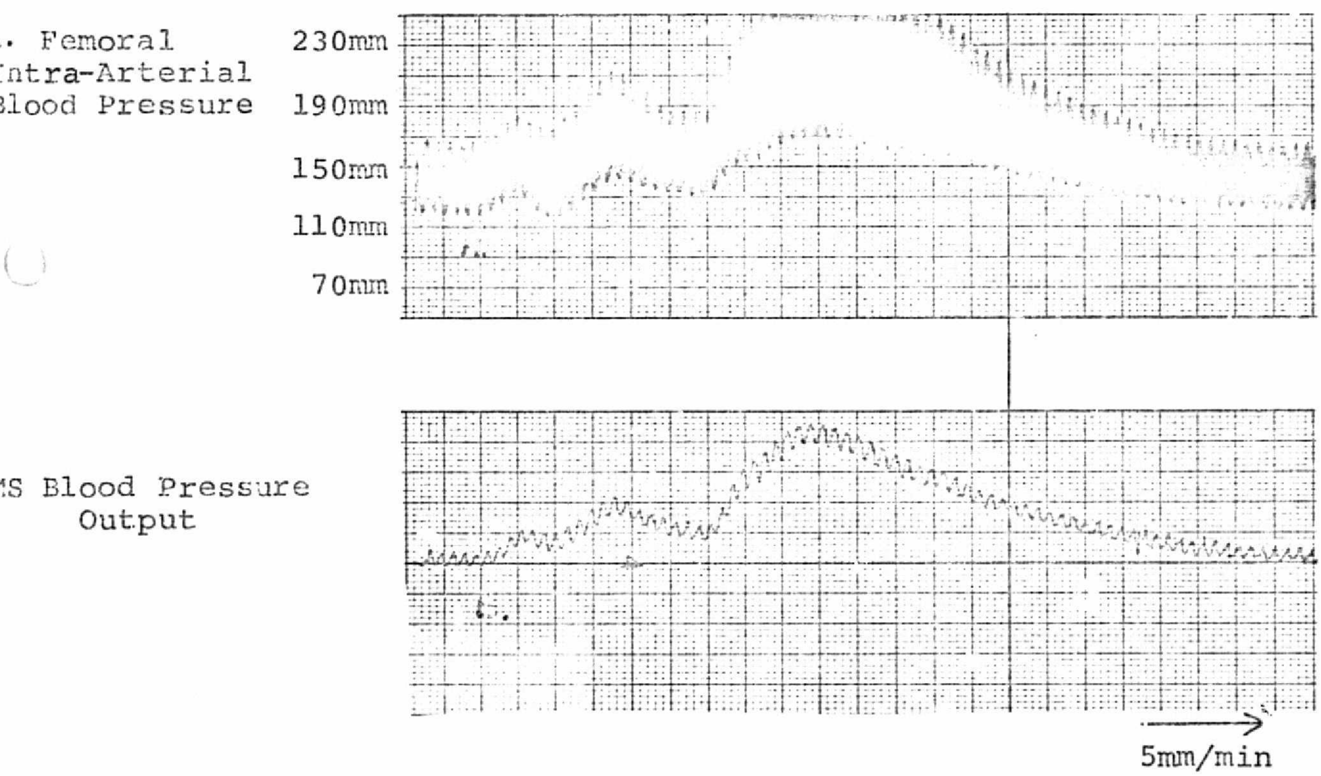

Administration of Levophed

Figure 10

A. Intra-arterial BP in a dog.
B. Output from the CMS BP Channel. (See Text.)

IV. Circuit Descriptions

Section V contains the relevant circuit diagrams and part layouts.

A. PRE-AMPLIFIER BOARD (Figures 11 A,B)

The input signal from each pulse wave transducer is buffered and amplified (x55) by an FET-input op-amp, Q_1. It is then processed to yield three output signals (V_1,V_2 and V_3). V_1 corresponds most closely to the pulse wave signal with baseline shifts and high frequency noise attenuated. V_2 and V_3 correspond to the first and second derivatives of V_1, respectively, but have been filtered to reduce noise above 100 Hz. In addition, they have been amplified to restore their signal to the 1 volt level. Refer to the block diagram (Figure 3) for approximate filter characteristics.

B. EKG AND WINDOW BOARD (Figures 12 A,B,C)

The EKG is buffered and amplified by a three op-amp differential amplifier (Q_1,Q_2 and Q_4) with a gain of 100. It is then high pass filtered at 13 Hz to reduce baseline shifts and remove most of the T wave, amplified by 68 (Q_5), and low pass filtered at 16 Hz to reduce muscle noise. Peaks in the EKG are detected by half-wave rectifier Q_7 and averaged and buffered by Q_6 to create a threshold level for comparator Q_3. Every time a QRS complex occurs, the comparator's output goes low and triggers both a 200 msec. pulse for lamp L_6, and a 60 msec. pulse. The end of the 60 msec. pulse opens the carotid window, which is closed 40 msec. after the detection of a carotid pulse or automatically after 160 msec. The femoral window is opened by the carotid derivative and closed 40 msec. after a femoral pulse or automatically after 280 msec.

C. THRESHOLD BOARD (Figures 13 A,B,C,D)

Events in pulse signal V_1 and derivative V_2 are detected by an amplitude criterion and then processed according to the algorithm described in Section I. The circuitry in Figure 13A computes threshold levels by averaging previous peak values and compares them to the current signal amplitudes. Peaks are detected by the half-wave rectifiers, Q_1 and Q_4. During the appropriate window, (see paragraph B, above) the signal peaks are transferred through the CMOS switches and stored on the capacitors. The resultant waveforms are smoothed by additional RC's and buffered by Q_2 and Q_5 to provide threshold levels for comparators, Q_3 and Q_6.

Each time a signal exceeds threshold its comparator output goes low and triggers a 1 msec. pulse at point A or B (See Figure 13 B) denoting the occurence of an event. In addition, the pulse causes the CMOS switches to reset the capacitor voltage to zero, enabling it to charge to a new peak value which may be lower than the last one.

The circuitry used to realize the onset determination algorithm is straight-forward. (See Figure 13 C.) A pulse at point B sets the left flip-flop, which disables the reset and starts the CD4024 counter. If point A is pulsed before C, the right flip-flop is set and the count continues. When the counter reaches 160 msec., it stops and an output pulse occurs at point D. However, if point C is pulsed before A, the right flip-flop does not get set; the left flip-flop and the counter are both reset and no output pulse occurs.

D. BLOOD PRESSURE BOARD (Figures 14A,B,C)

The delay time(ΔT) between carotid and femoral onsets is measured by counting pulses from a crystal controlled clock in the CD 4020, 14-bit counter. The count begins when the carotid onset pulse (from the Threshold Board) sets a flip-flop (Figure 14 A) which enables the clock input. It stops when a femoral onset pulse resets the flip-flop or when the count reaches 280 msec. Resetting the flip-flop triggers a series of pulses which first transfer the count to the latches and then reset the counter. The count is stored in the latches until the next sequence. (Engaging the "HOLD" button prevents transfer of new data.) The latches control switches (SSS4416), which control a binary weighted resistor ladder such that the total series resistance, R_T, is proportional to the count, ΔT.

In turn, the ladder is part of an op-amp circuit in which:

$$V_4 \propto \frac{V_{REF}}{R_T}$$

Therefore, V_4 is proportional to the reciprocal of the delay time $(\frac{1}{\Delta T})$. The reference (V_{REF}) is provided by a LM723 precision voltage regulator.

E. HEART RATE BOARD (Figures 15 A,B)

This circuitry is similar to the Blood Pressure Board. It counts pulses from a crystal clock and stores the number in a group of latches, which control switches that modify a resistor ladder. The timing sequence is initiated by the Blood Pressure Board Transfer, which transfers the interbeat interval to the latches and then the counter. The reciprocating D/A ladder is analogous to its counterpart on the Blood Pressure Board. The timing sequence may also be initiated by the EKG.

F. OUTPUT BOARD (Figures 16 A,B,C)

The voltage from the Blood Pressure Board (V_4) is added to $(-\frac{1}{T_o})$ by op-amp Q_3 and the sum is multiplied by (-M). P_o is added by Q_4 and the result is inverted to yield a positive output.

The output multiplex circuitry (Figure 16B) switches between the derivative signals and their thresholds at 770 Hz, such that when viewed with an oscilliscope, the two signals will appear superimposed. The multiplexing is disabled by a switch mounted on the board.

G. LIGHT BOARD (Figures 17 A,B)

The Light Board supplies buffered signals to the various indicator lights on the front panel. The carotid and femoral signals (B) are used to clock J-K flip-flops. Their outputs are buffered to drive lights L_1 and L_3, which turn on with one pulse and off with the next. Carotid and femoral signals at D indicate that the onset algorithm has been satisfied, and they drive lights L_2 and L_4. Pulse E and light L_5 are on for the duration of the carotid-femoral delay time (ΔT). Convert H indicates successful transfer of data and computation of the new BP and HR. It is intended for computer use and appears only on pin 14 of the multiple-pin output connector. Finally, EKG G drives the light above the EKG input on the front pannel, which indicates that a QRS complex has been detected. The light remains on for 200 msec.

H. GENERAL CONSIDERATIONS

1. All op-amps operate from $\pm$15V.
2. All CMOS, except on the Light Board, operate from +15V and ground.

V. Circuit Diagrams and Wiring Lists

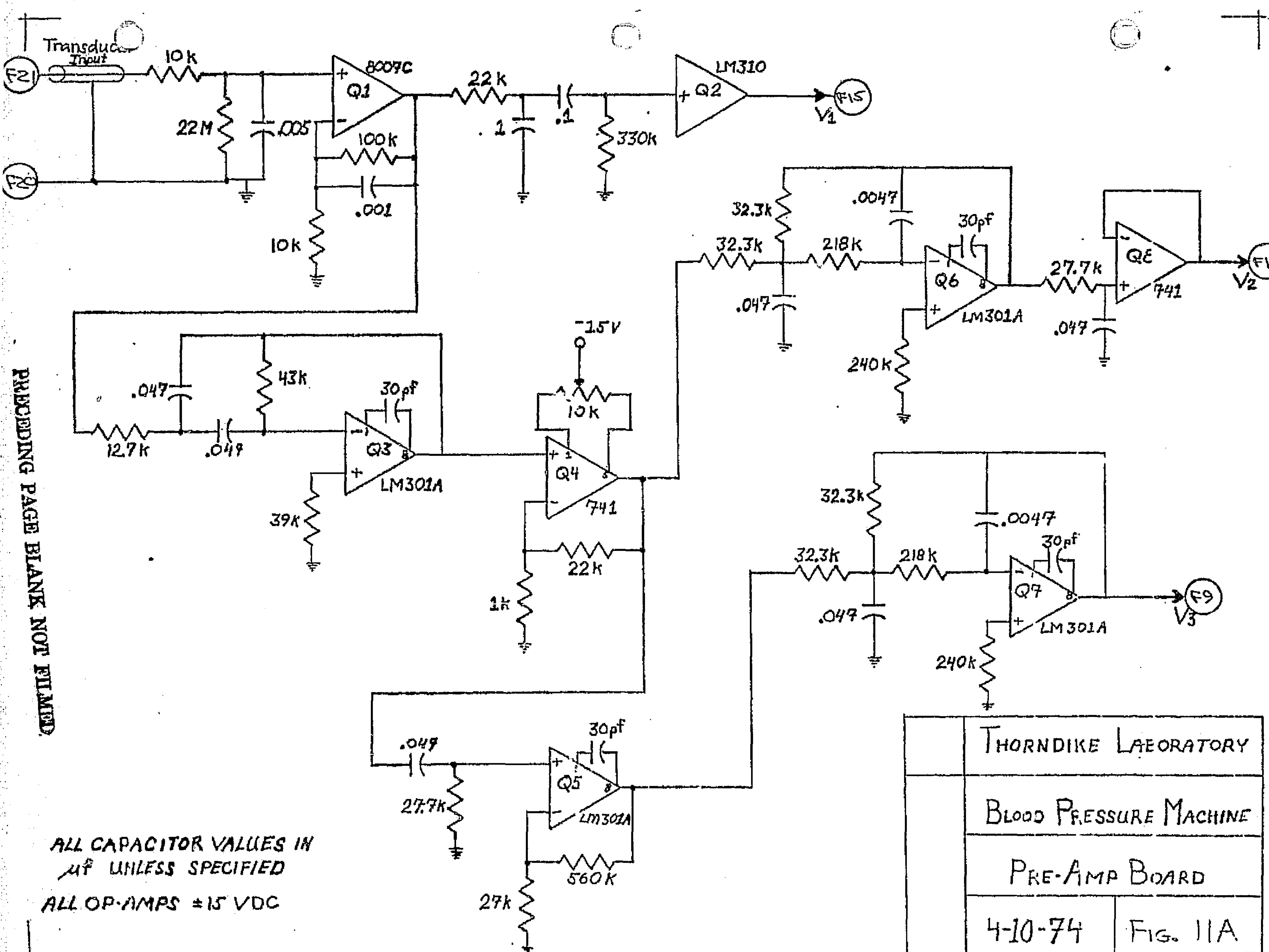

ALL CAPACITOR VALUES IN μf UNLESS SPECIFIED

ALL OP-AMPS ±15 VDC

	THORNDIKE LABORATORY
	BLOOD PRESSURE MACHINE
	PRE-AMP BOARD
4-10-74	FIG. 11A

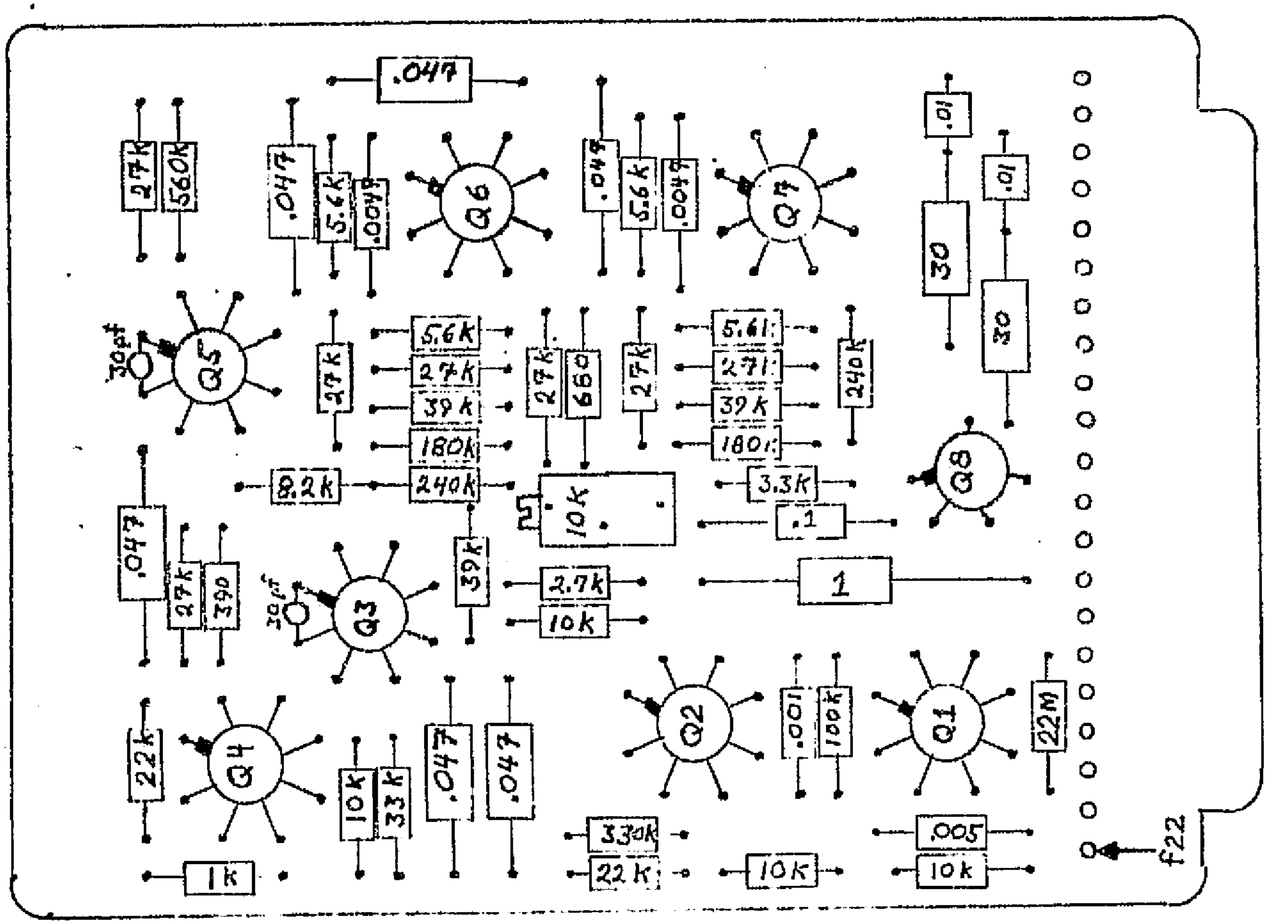

	THORNDIKE LABORATORY
	BLOOD PRESSURE MACHINE
	PRE-AMP CARD
	4-10-74 — FIG. 11B

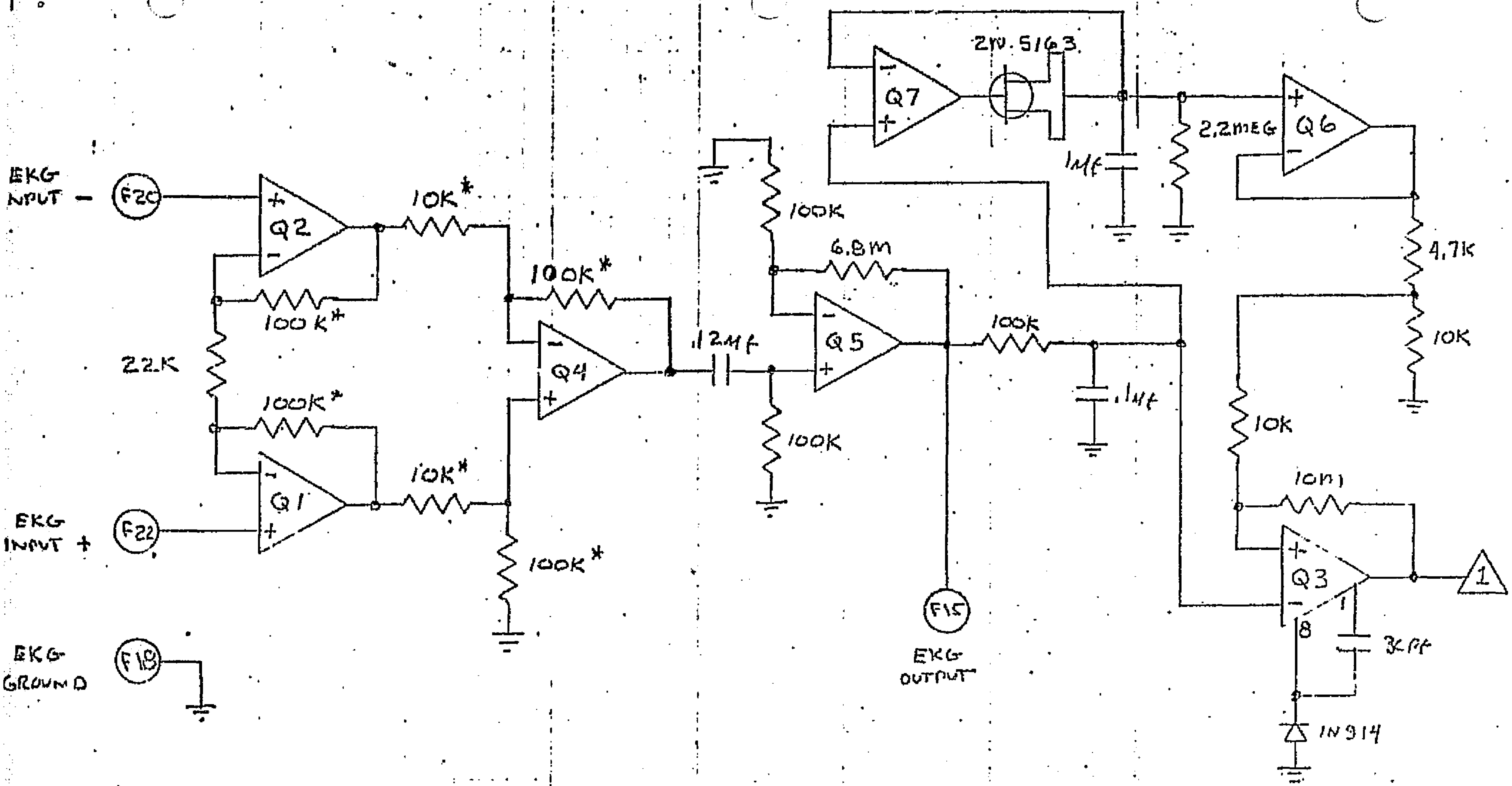

* NOTES

1. STARED RESISTORS ARE 1%
2. Q 3 IS A LM 301A
3. ALL OTHERS ARE μ741
4. Q1 & Q2 ARE LM 301A

Thornoike Laboratory
Blood Pressure Machine
EKG Board
5-7-74 / Fig. 12A

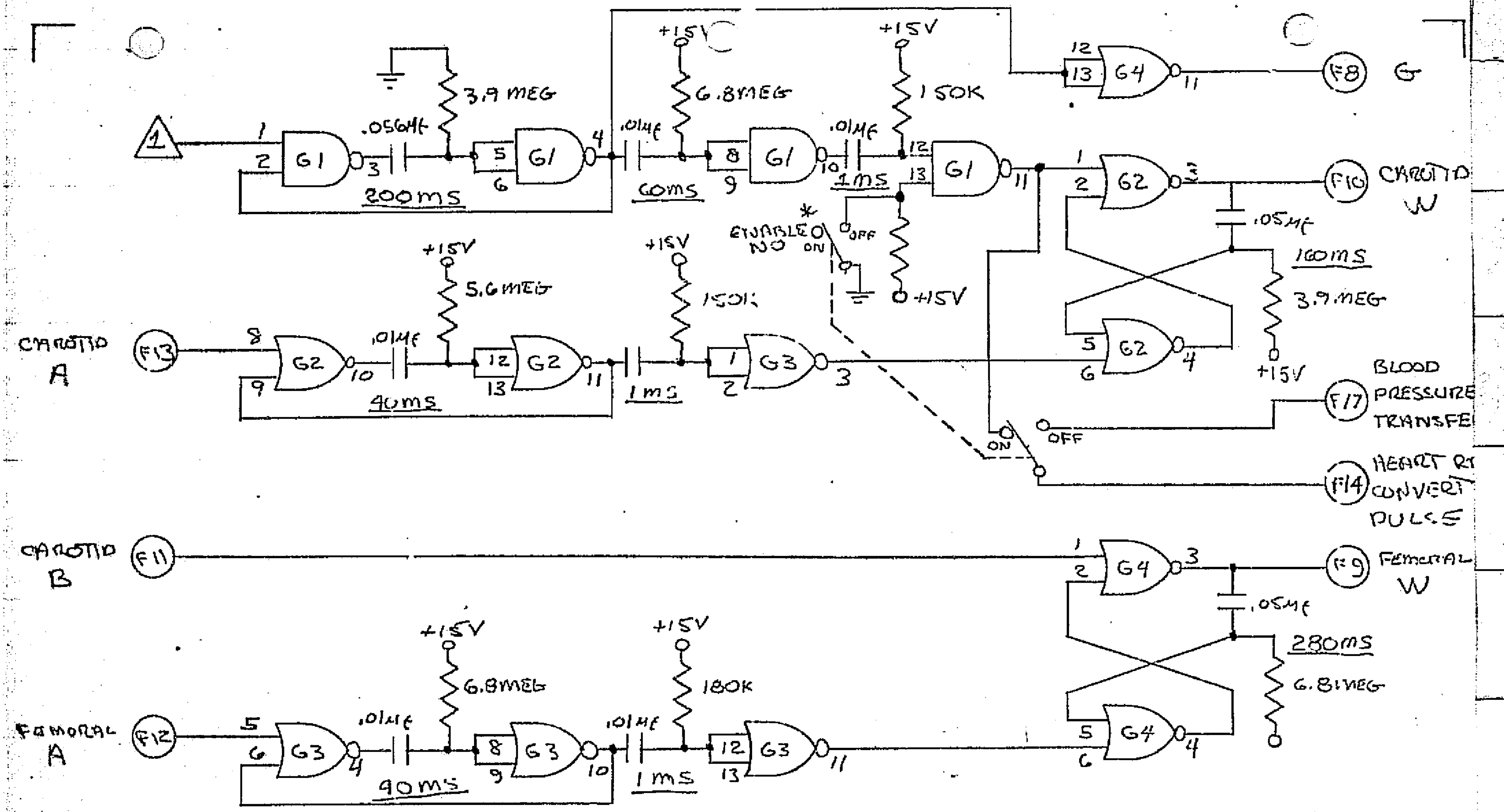

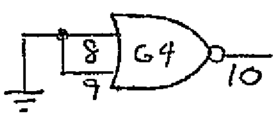

*NOTES

SWITCH AT G1 LOCATED AT REAR OF BOARD

THORNDIKE LABORATORY	
BLOOD PRESSURE MACHINE	
EKG BOARD	
5-7-74	FIG. 12B

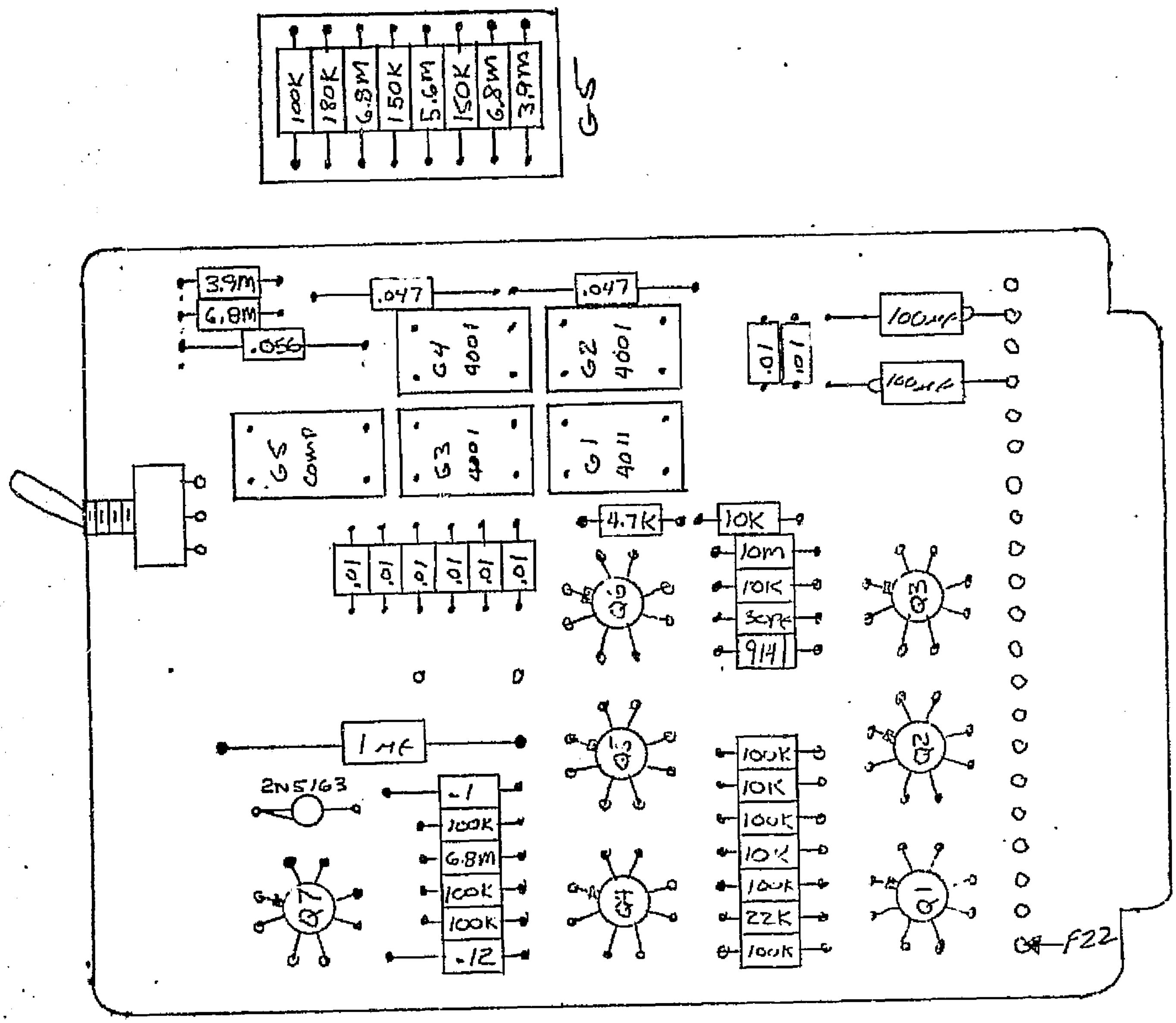

Thorndike Laboratory	
Blood Pressure Machine	
EKS Board	
5-15-74	Fig. 12C

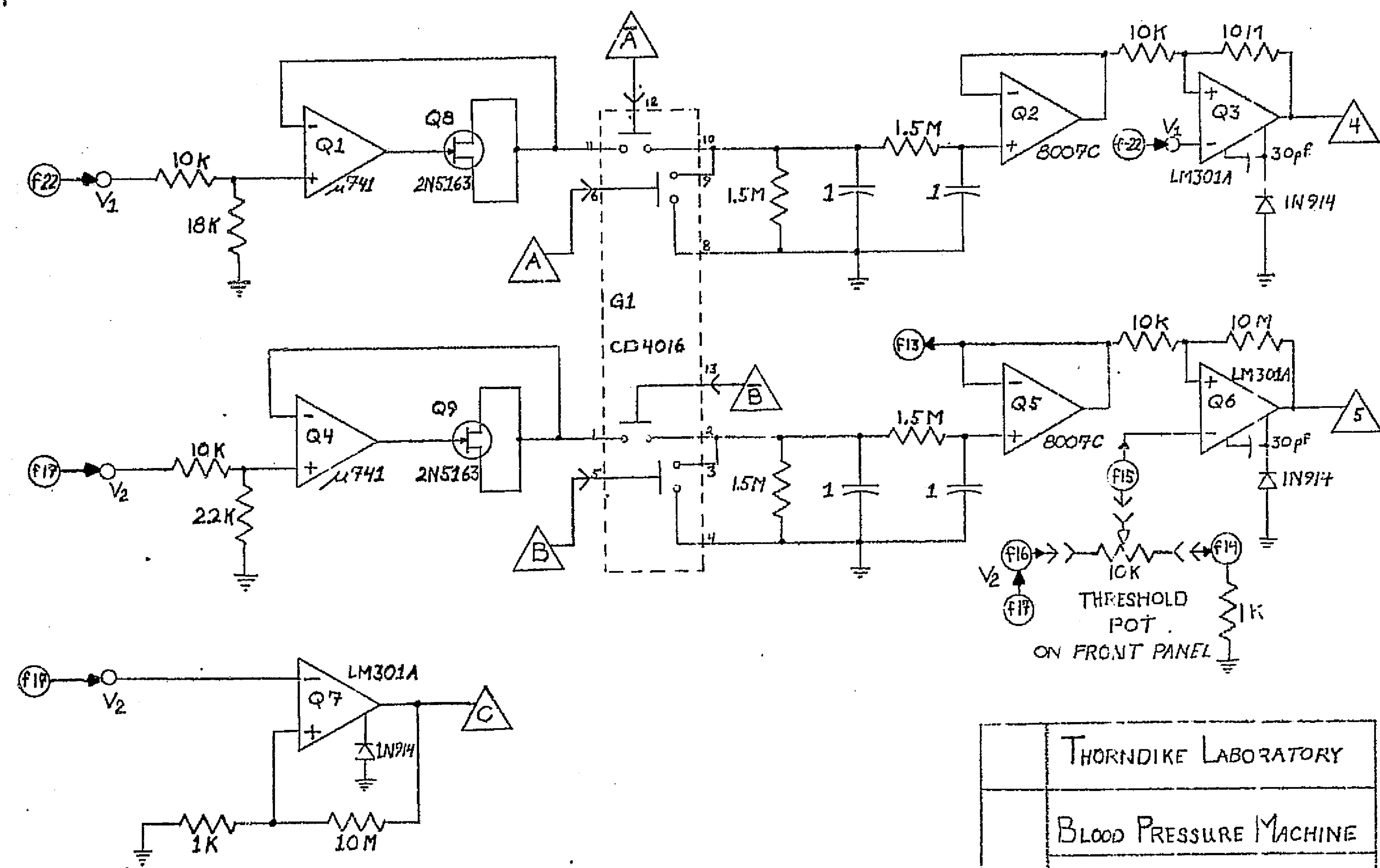

THORNDIKE LABORATORY

BLOOD PRESSURE MACHINE

THRESHOLD BOARDS

4-11-74

FIG. 13A

ALL CAPACITORS IN µf UNLESS SPECIFIED
ALL OP-AMPS ±15VDC

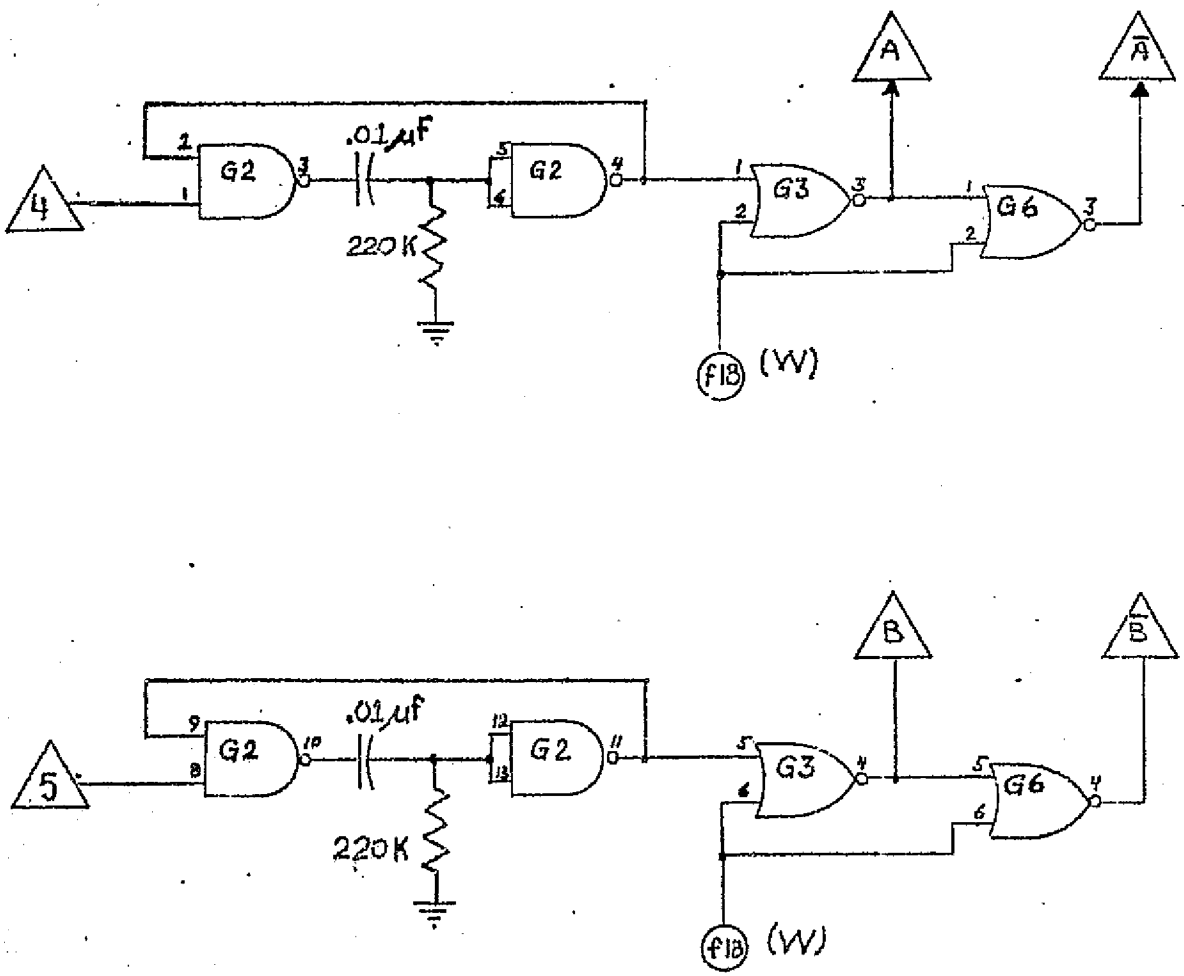

THORNDIKE LABORATORY

BLOOD PRESSURE MACHINE

THRESHOLD BOARDS

4-11-74

FIG. 13B

C-4

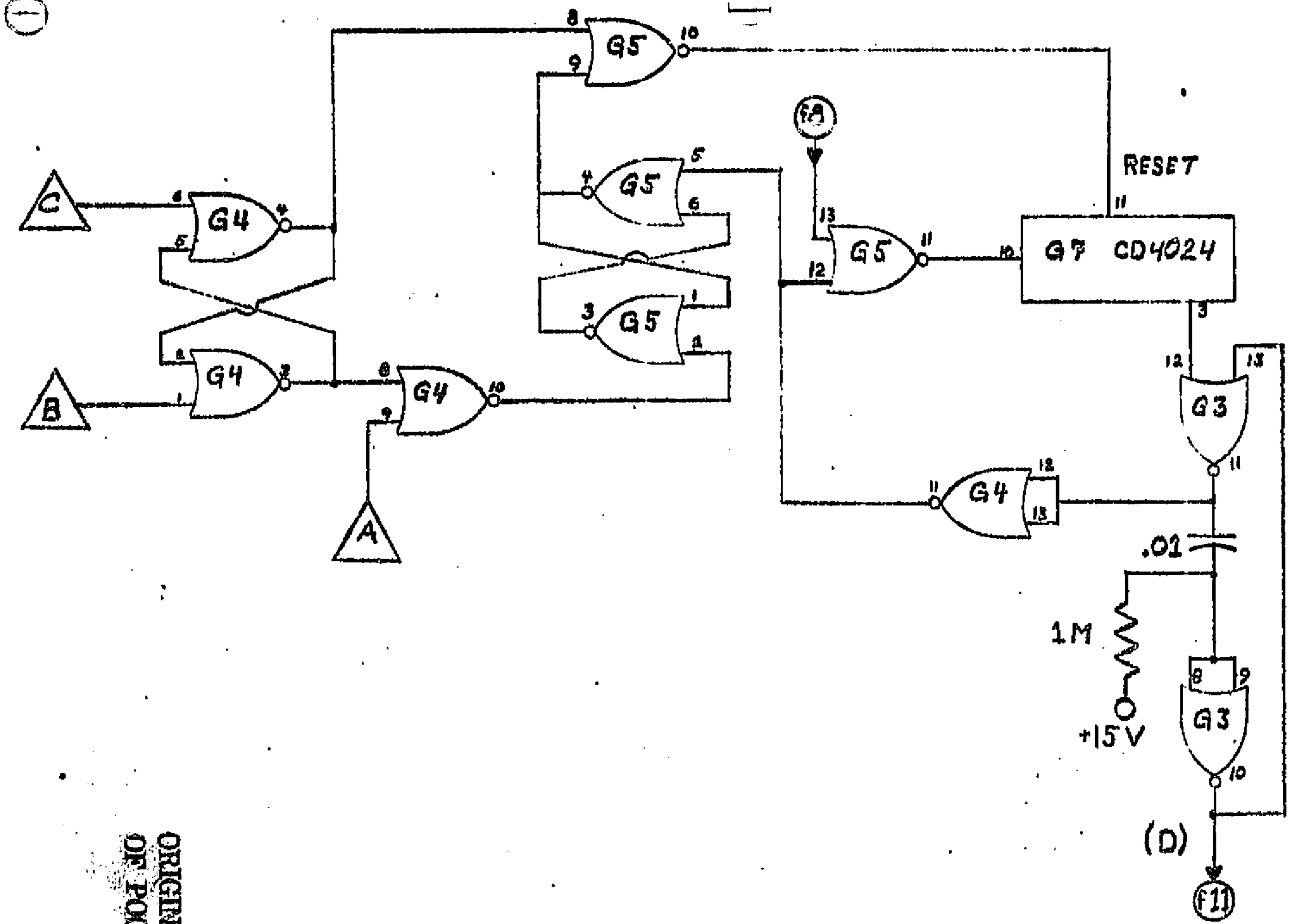

THORNDIKE LABERATORY

BLOOD PRESSURE MACHINE

THRESHOLD BCARDS

4-11-74 | FIG. 13C

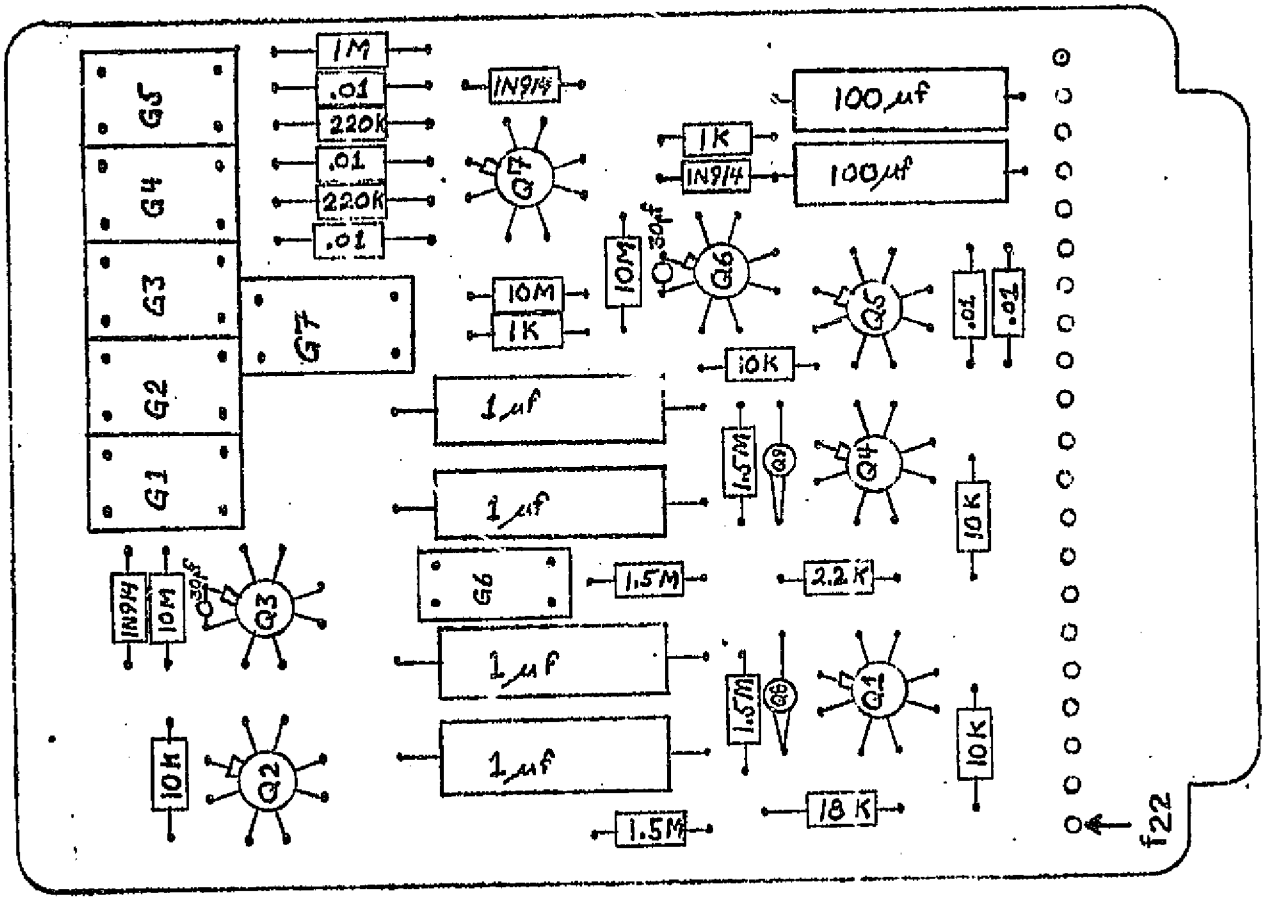

LOCATION OF G6 IS DIFFERENT ON EACH BOARD

2N5163 

TOP VIEW

	THORNDIKE LABORATORY
	BLOOD PRESSURE MACHINE
	THESHOLD BOARDS
	4-11-74 — FIG. 13.D

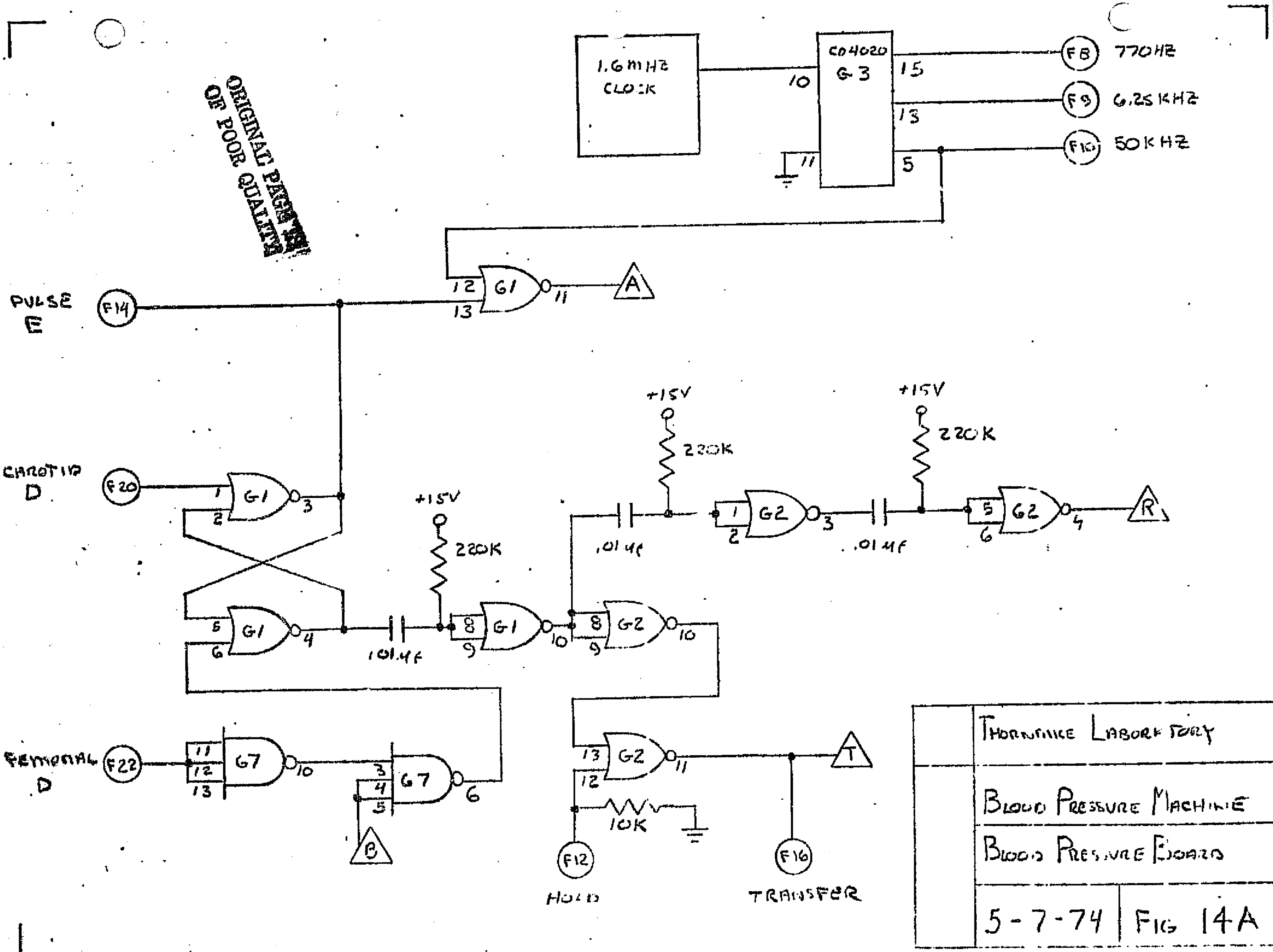

Thorndike Laboratory

Blood Pressure Machine

Blood Pressure Board

5-7-74

Fig 14A

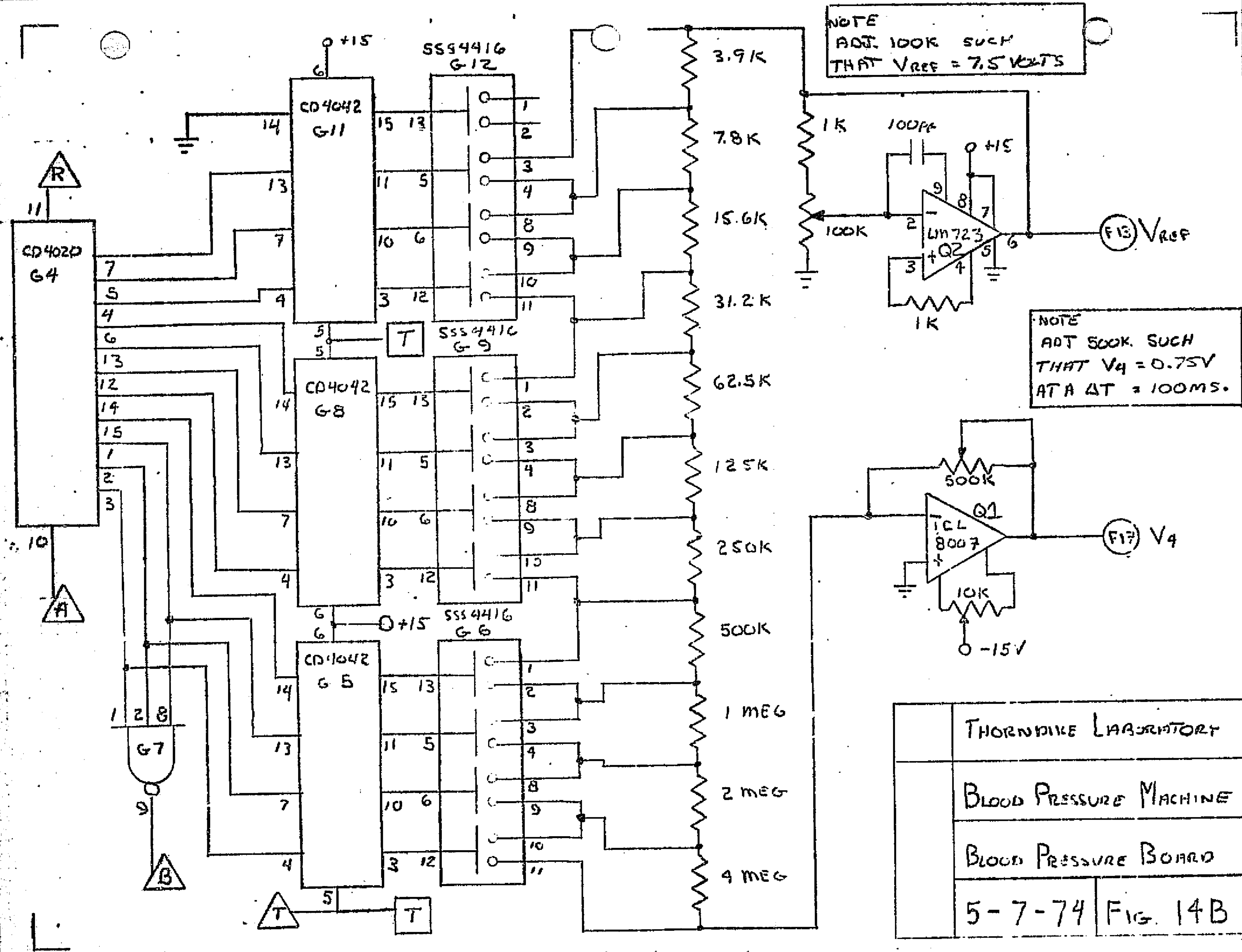

Thorndike Laboratory

Blood Pressure Machine

Blood Pressure Board

5-7-74

Fig. 14B

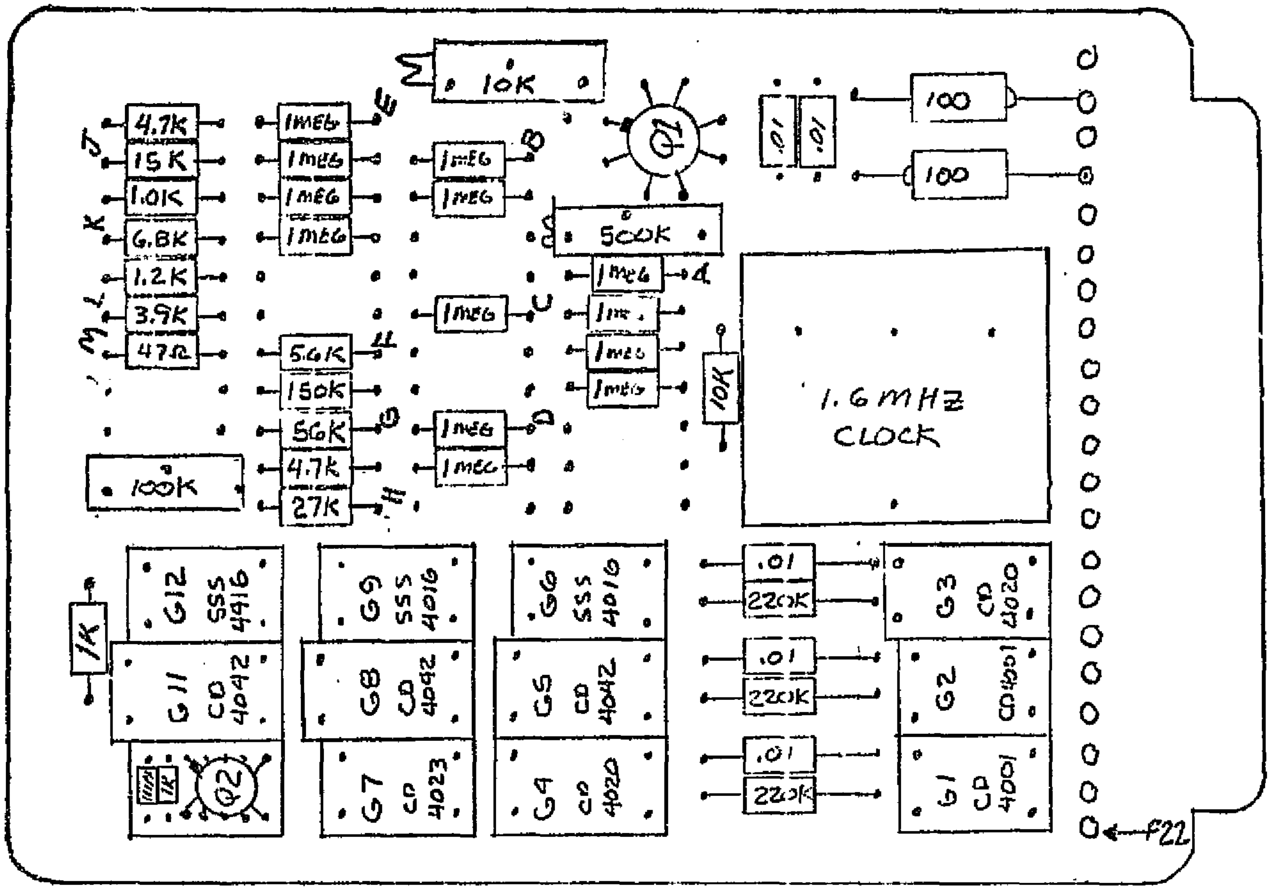

THORNDIKE LABORATORY	
BLOOD PRESSURE MACHINE	
BLOOD PRESSURE BOARD	
5-14-74	FIG. 14C

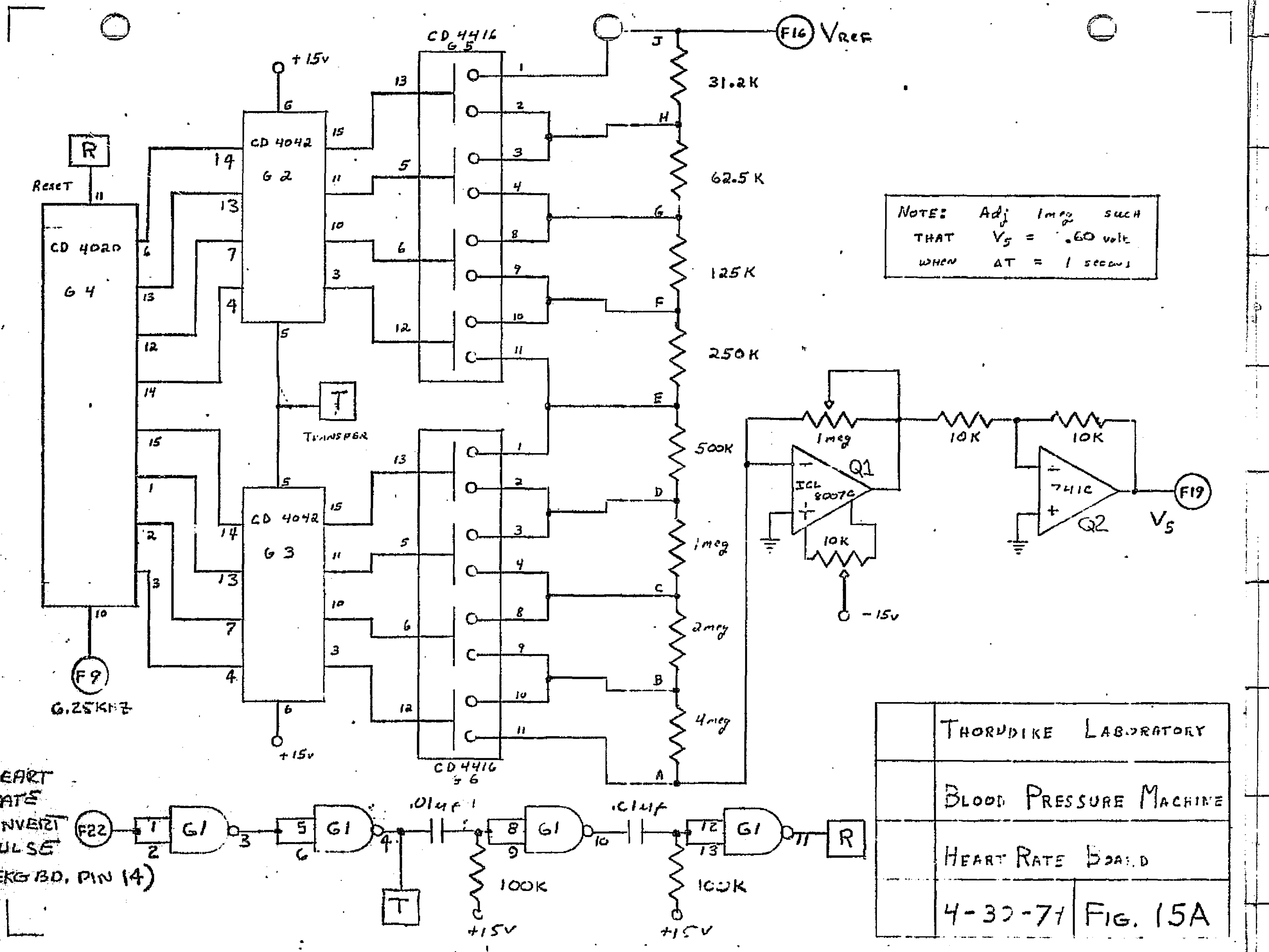

VREF
F16
CD 4416
G 5
+15v
CD 4042
G 2
R
RESET
CD 4020
G 4
T
TRANSFER
31.2K
62.5K
125K
250K
500K
1meg
2meg
4meg
NOTE: Adj 1meg such that V_5 = .60 volt when ΔT = 1 second
1meg
10K
10K
Q1
ICL 8007C
741C
Q2
F19
V_5
10K
-15v
CD 4042
G 3
CD 4416
G 6
F9
6.25KHZ
HEART RATE CONVERT PULSE (EKG BD. PIN 14)
F22
G1
.01uf
.01uf
100K
100K
+15V
+15V
THORNDIKE LABORATORY
BLOOD PRESSURE MACHINE
HEART RATE BOARD
4-30-71
FIG. 15A

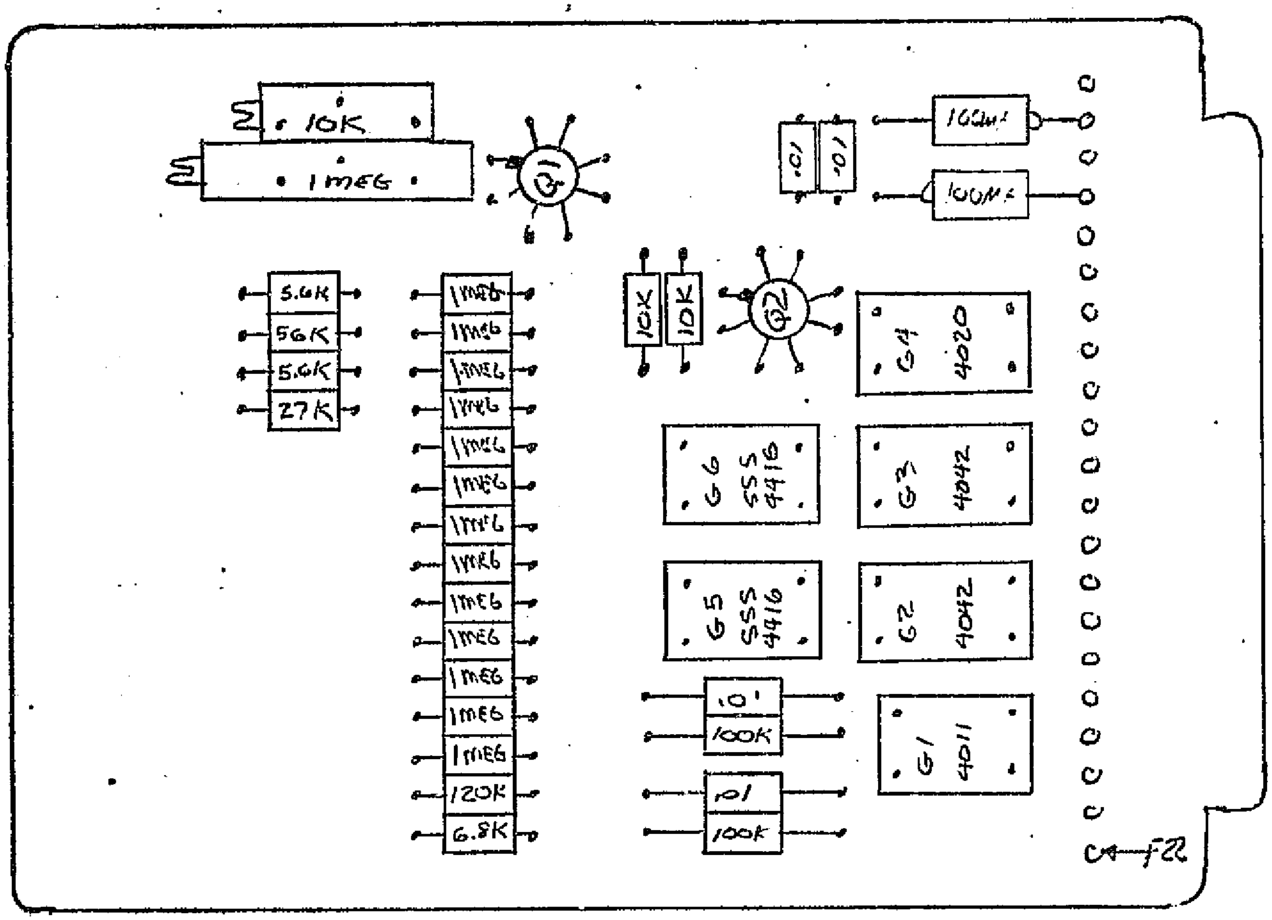

THORNDIKE LABORATORY	
BLOOD PRESSURE MACHINE	
HEART RATE BOARD	
5-15-74	FIG. 15B

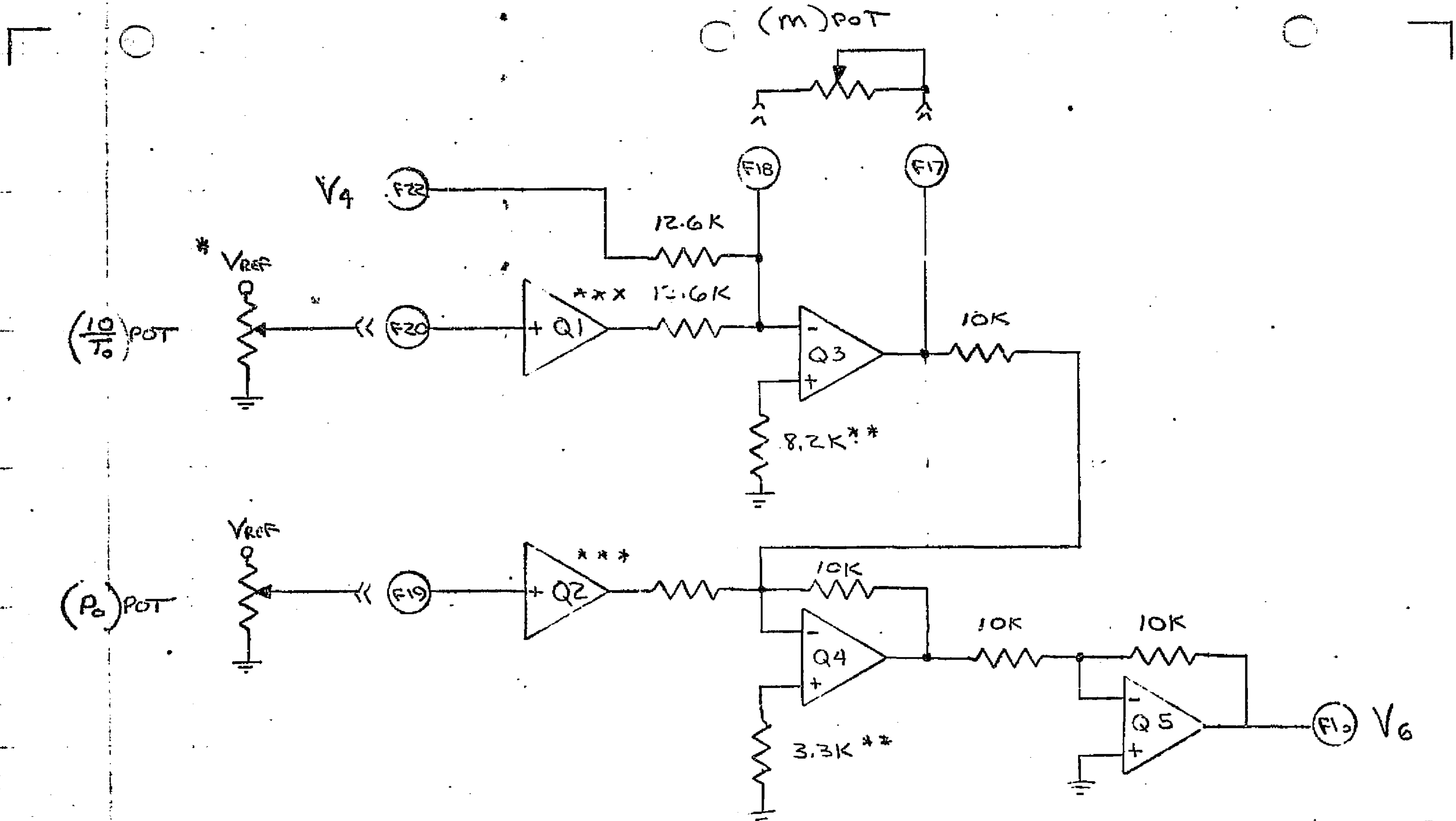

* NOTES

* ALL CONTROL POTS ARE ON FRONT PANEL AND ARE ALL 100KΩ TEN TURN

** RESISTOR ARE 5% ALL OTHERS 1%

*** Q1 & Q2 - LM310 ALL OTHERS ARE μ741

Thorndike Laboratory	
Blood Pressure Machine	
Output Board	
5-8-74	Fig. 16A

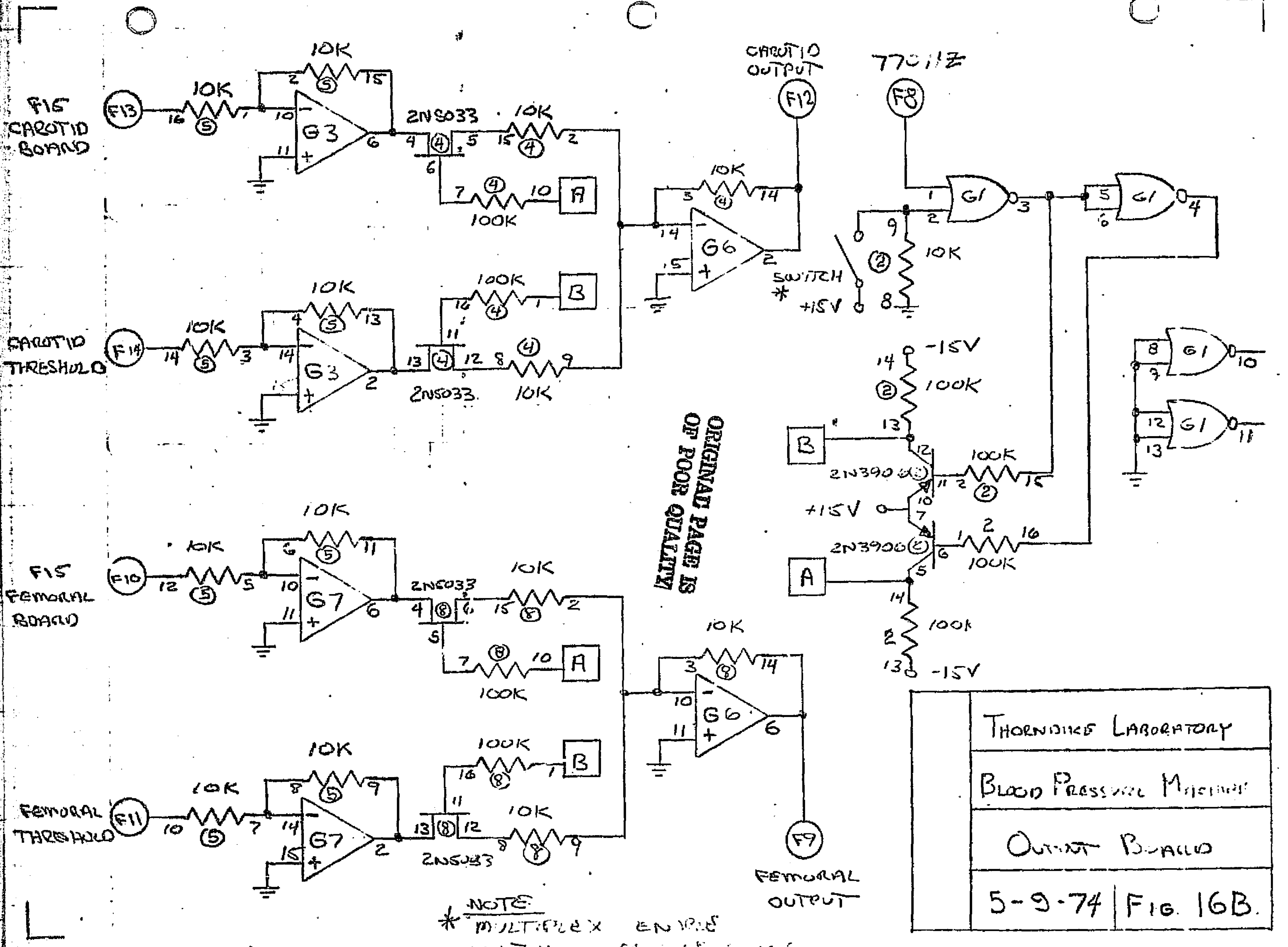

ORIGINAL PAGE IS OF POOR QUALITY

THORNDIKE LABORATORY	
BLOOD PRESSURE MACHINE	
OUTPUT BOARD	
5-9-74	FIG. 16B.

* NOTE
MULTIPLEX ENABLE

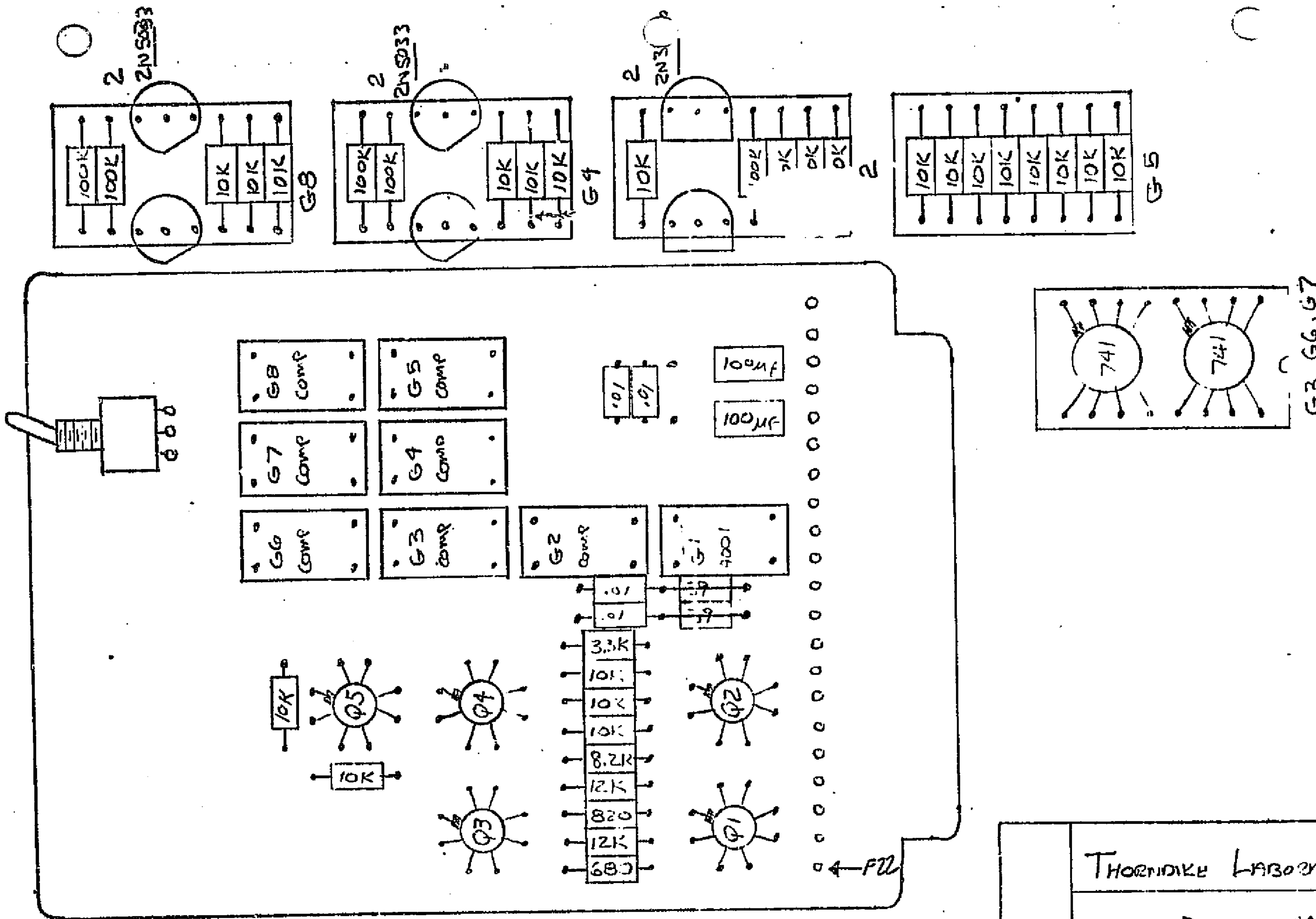

Thorndike Laboratory	
Blood Pressure Machine	
Output Board	
5-15-74	Fig. 16C

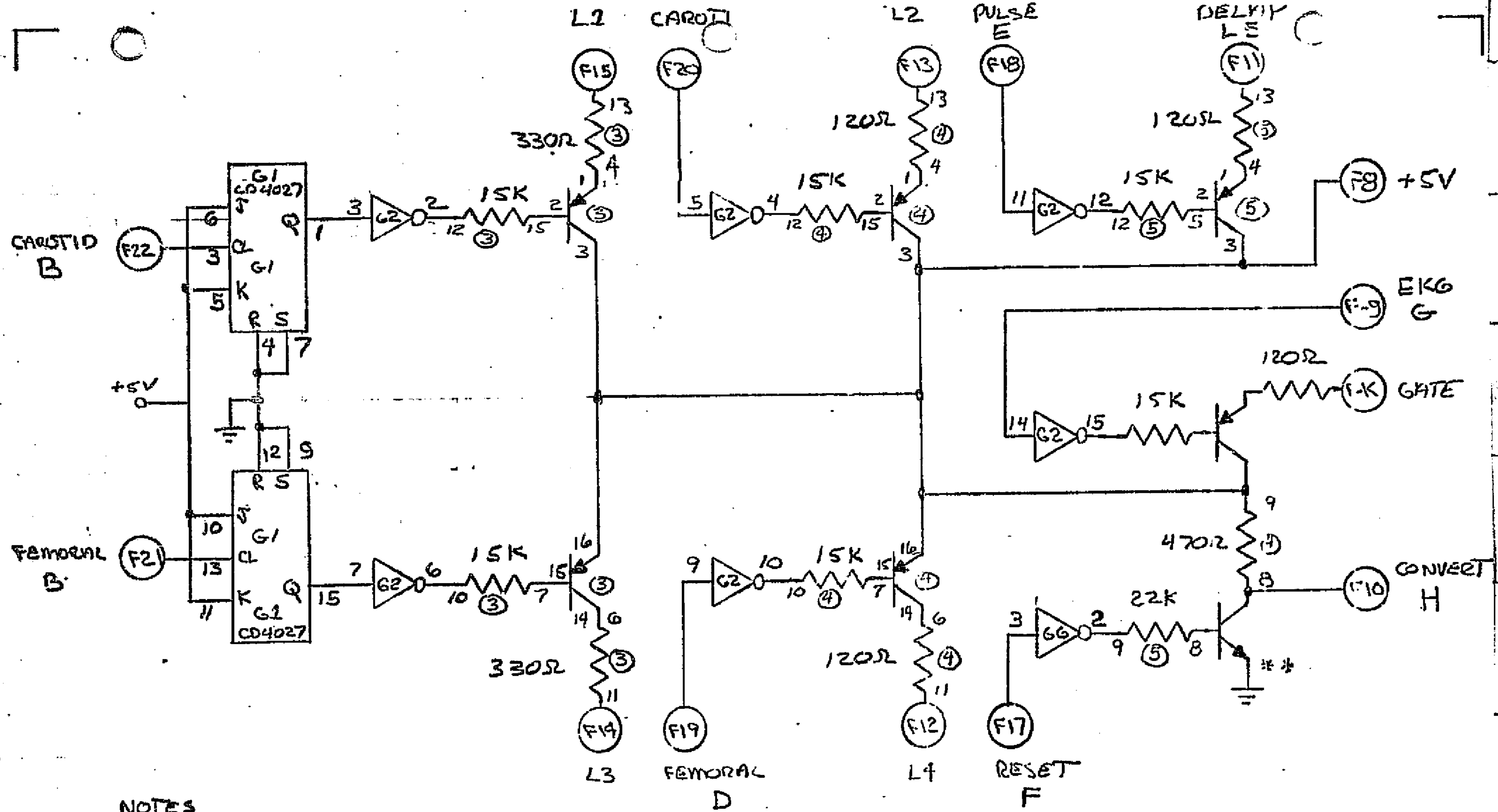

NOTES

* ATTACH +5V TO PIN 1 OF G2 AND G6

** 2N3904 ALL OTHERS ARE 2N3906

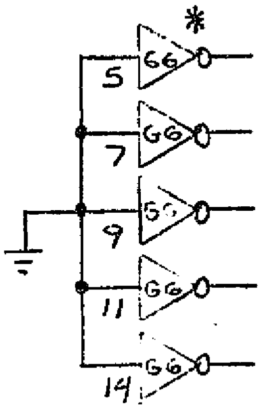

	THORNDIKE LABORATORY
	BLOOD PRESSURE MACHINE
	LIGHT BOARD
5-9-74	FIG. 17A

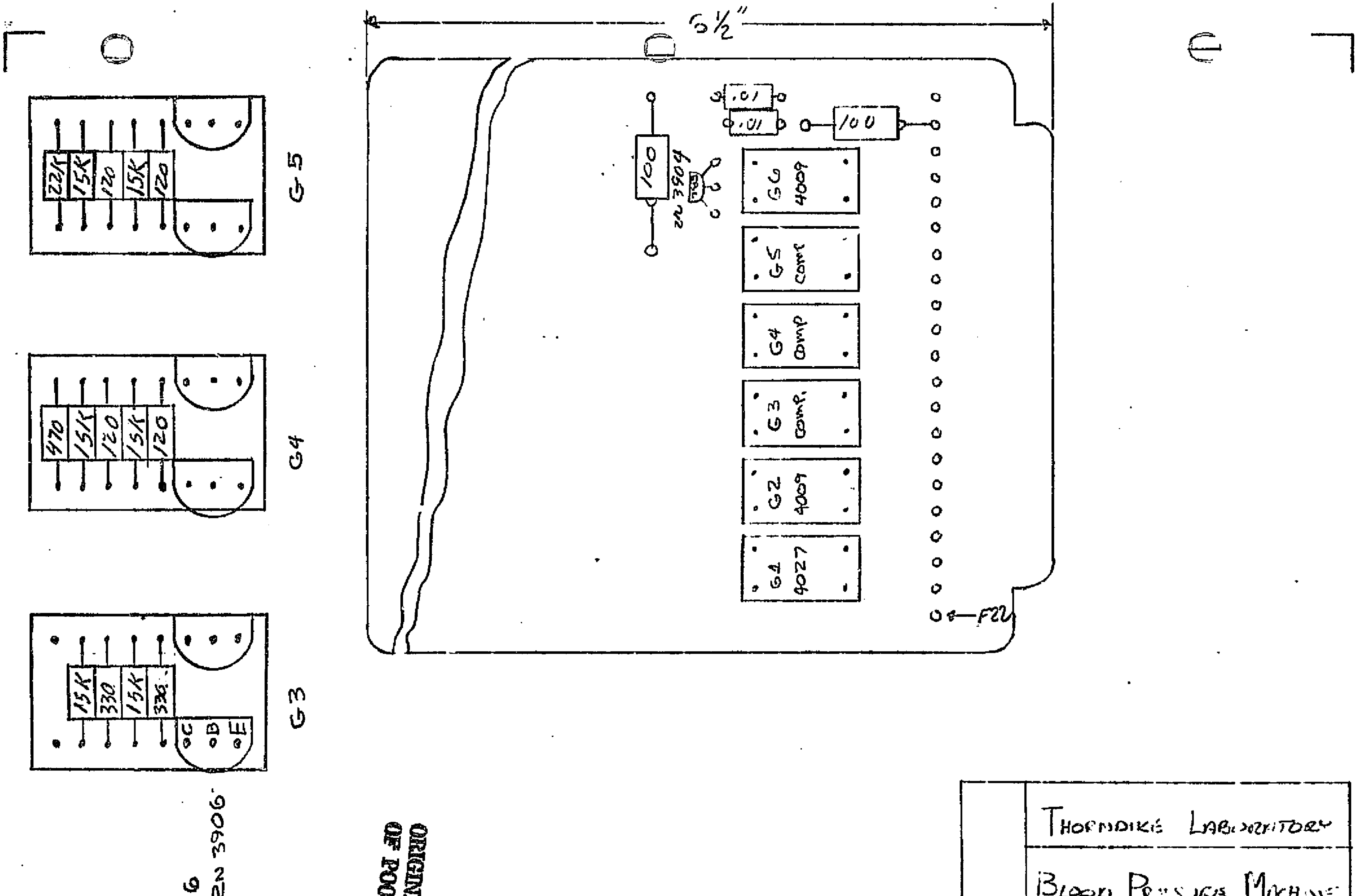

THORNDIKE LABORATORY	
BLOOD PRESSURE MACHINE	
LIGHT BOARD	
5-13-74	FIG. 17B

DATEL SYSTEMS, INC.

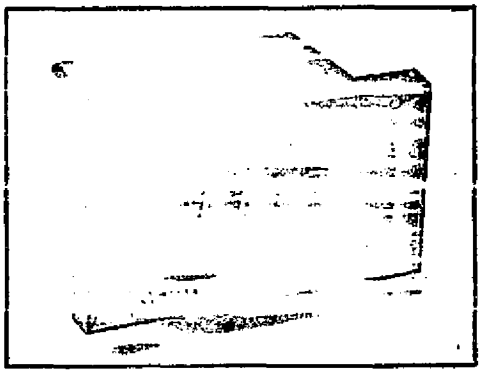

DIGITAL PANEL METER

MODEL

DM-2000 SERIES

DESCRIPTION

The Datel Datamite DM-2000 is the first LED 3½ digit panel meter to sell for below $100.00 in single quantities. This has been made possible by the wide acceptance of Datel Systems line of Datamite Digital Panel Meters which have a proven record of performance and reliability.

The DM-2000 combines the ease and accuracy of digital readout with high input impedance and noise rejection to provide an inexpensive digital panel meter (digital voltmeter) that will enhance the operation, performance and appearance of any instrumentation system.

The DM-2000 is ideal for new equipment design or may be utilized in updating existing instruments or systems that require a stable, accurate digital readout for voltage. Simple to install, the DM-2000 is supplied complete and ready to operate, requiring only a connection of an input signal and power cable. Applications include measuring or any parameter for which a suitable output voltage is available. These include absorption, acceleration, current, displacement, distortion, emission, flow, frequency, Ph, pressure, strain, torque, and many others.

The DM-2000 provides a differential input with a 100 MegOhms input impedance and a common mode rejection of 70 db at 60 Hz. The input range is ±1.999 volts or ±199.9 millivolts. The display is 3½ digits including automatic polarity and overflow indication. In addition the output is presented to the I/O connector as BCD/TTL information.

High quality computer grade components, superior workmanship and wide-safety-margin designs combine to make Datamite DM-2000 a must in your present equipment or future generation designs.

WORLD'S FIRST LED 3-1/2 DIGIT DPM FOR UNDER $100 IN SINGLE QUANTITY

FEATURES

- ☐ ±199.9mV or ±1.999V Full Scale Inputs
- ☐ True Floating Bipolar Differential Input
- ☐ Automatic Polarity and Overflow Display
- ☐ Up to 200 Readings per Second
- ☐ Operates From Single +5VDC Supply
- ☐ Solid State Led Display
- ☐ Adjustable Zero Control Compensating For External Offset Voltages

ORIGINAL PAGE IS OF POOR QUALITY

MOUNTING DETAILS

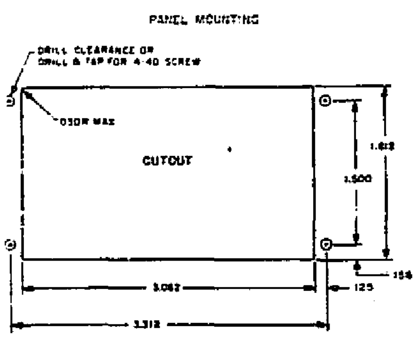

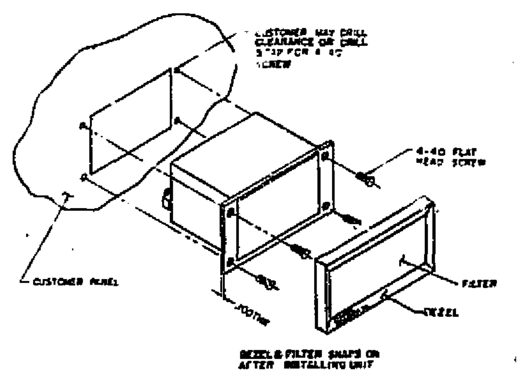

Calibration Procedure (Using Trimpots Shown At Right)

The following adjustment procedure is recommended after allowing for a five minute warm-up.

Balance Control

1) Short the analog input terminals to analog common. (See I/O chart for proper pin connection.)
2) Rotate the balance control until the display is flickering between (+) zero and (–) zero.

Zero Control

1) Connect a precision voltage reference source to the analog input terminals.
2) Adjust the voltage output from the reference source to .3LSD (30µV Model A, 300µV Model B). Rotate the zero control until the LSD (Least significant digit) flickers between zero and one.

Full Scale Control

1) Adjust the output from the reference source to 1.990 volts. Rotate the full scale control of the panel meter until the meter displays 1.990 volts.

MECHANICAL DIMENSIONS (INCHES)

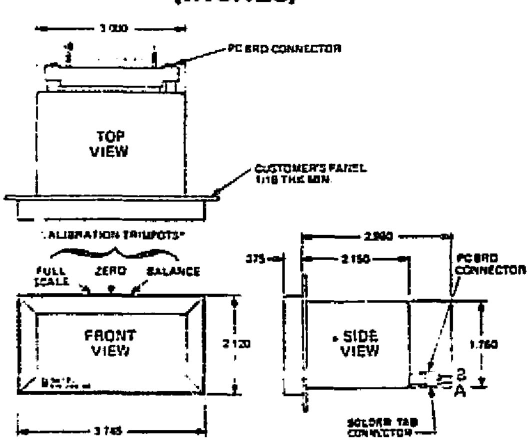

*Calibration trimpots are behind pop-off front panel bezel and filter

INPUT/OUTPUT CONNECTIONS

	PC BRD CONNECTOR BOTTOM A	PC BRD CONNECTOR TOP B	
ANALOG INPUT (LO)	1	1	ANALOG INPUT (HI)
SHIELD GROUND	2	2	SHIELD GROUND
NOT USED	3	3	NOT USED
NOT USED	4	4	LOGIC GROUND
DECIMAL POINT 100	5	5	BIT 1 OUT
DECIMAL POINT 10	6	6	BIT 2 OUT
DECIMAL POINT 1	7	7	BIT 4 OUT
E.O.C. (STATUS)	8	8	BIT 8 OUT
OVERLOAD SCALE OUT	9	9	BIT 10 OUT
INT START GATE	10	10	BIT 20 OUT
INT START ADJ	11	11	BIT 40 OUT
INT START OUT	12	12	BIT 80 OUT
START INPUT	13	13	BIT 100 OUT
LAMP TEST	14	14	BIT 200 OUT
1000 OUT	15	15	BIT 400 OUT
SIGN OUT	16	16	BIT 800 OUT
NOT USED	17	17	NOT USED
POWER INPUT, +5VDC RETURN	18	18	POWER INPUT, +5VDC +

24

SPECIFICATIONS Typical @ 25°C 5 minute warm up, +5VDC ± .25V unless noted

Input

Input Voltage Range	±199.9mV DM-2000A ±1.999V DM-2000B
Input Impedance	>100 MEGOHMS
Input Bias Current	20 nA
Input Configuration	Differential
Input Polarity	Bipolar — Automatic
Common Mode Rejection	70dB @ 60Hz
Common Mode Voltage	±2V max. to digital output common
Accuracy @ 25°C	±0.05% of Reading ±1 Count
Resolution	100μVolts (DM-2000-A), 1mVolt (DM-2000-B)
Temperature Coefficient	50ppm/°C
Conversion Speed	*0 to 200 Conversions/Second. See Diagrams below*
Input Settling Time	50 μsec for a F.S. Change
Operating Temperature Range	0°C to +60°C
Storage Temperature Range	−20°C to +85°C
Warm Up Time	5 Minutes to Specified Accuracy
Adjustments	Zero, Balance, Full Scale Located Behind Snap On Front Bezel
Input Power	5VDC ±0.25VDC @ 750mA

Display Output

Display Type	Solid State LED for Data Digits, 100% Overrange, Overflow, Decimal point and Polarity — Character Height .3 in.
Overflow	Indicated by the Letters "OF"
Decimal Points	Selectable at rear Connector
BCD Outputs	12 Parallel Lines, BCD (8–4–2–1) Positive Logic Loading: 2TTL loads
Overrange (Connection A15)	>1000 counts indicated with a HIGH. Loading: 2TTL loads

Polarity	Input signal polarity indicated with a HIGH-positive, LOW-negative. Loading: 2TTL loads
Overflow (OF) ≥±0.2V (MODEL A) ≥±2V (MODEL B)	HIGH-input signal within range. LOW-input signal outside range. Loading: 2TTL loads
End of Conversion (EOC) (Connection A8)	HIGH During the conversion period LOW — Conversion complete. Loading: 2TTL loads
External Start Conversion Command (Connection A13)	Positive pulse 100 nsec min. Transition from "LOW" to "HIGH" resets output register and blanks readout. The conversion process is initiated upon return from "HIGH" to "LOW". Loading: 1TTL load. Max. Input 5.5V
Internal Start Gate (Connection A10)	Controls internal start clock "HIGH" — Run "LOW" — Stop loading: 1TTL load
Internal Start Adjust (Connection A11)	Controls Rate of Internal Start Clock — see Applications Section.
Internal Start Out (Connection A12)	Positive Pulse Output of Internal Start Clock— see Applications Section.
Lamp Test Input (Connection A14)	Grounding this input displays + 1888 for testing all display segments. Loading: Sink 35mA
Decimal Point Inputs (DP1, DP10, DP100)	Grounding inputs illuminates corresponding decimal points on the display. Loading. Sink 15mA
Case Size	3"W x 1.75"H x 2.25"D
Case Material	Black LEXAN
Weight	6 oz. Approx.
Mounting	Through a 1.75" x 3.00" Cut-Out and Secured with Four 4-40 Tapped Holes

Notes:
Module is fully repairable and features snap-together PC Boards.

Digital Inputs: "0" ≤ +0.8V, "1" ≥ +2.0V

Digital Outputs: "0" ≤ +0.4V, "1" ≥ +2.4V

APPLICATIONS

SINGLE ENDED INPUT

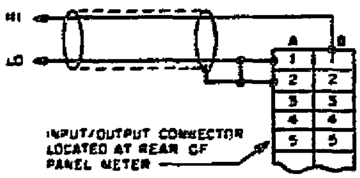

FOR SINGLE ENDED INPUT, CONNECT "LO" AND "SHIELD" TOGETHER AT THE CONNECTOR (A1 TO A2)

DIFFERENTIAL INPUT

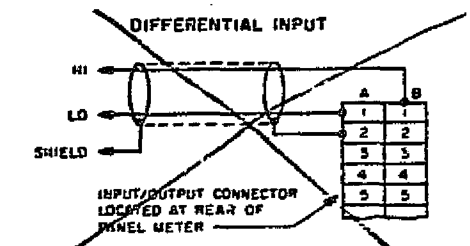

FOR DIFFERENTIAL INPUT THE COMMON MODE VOLTAGE BETWEEN "LO" AND "SHIELD" MUST NOT EXCEED THE MAXIMUM SPECIFIED COMMON MODE VOLTAGE

USING THE METER WITH THE INTERNAL "START" CLOCK

NOTE 1 — Use timing capacitor shown for units without -A serial number suffix. For -A suffix units, substitute a 0.1μF, 50V capacitor and reverse polarity. Disconnect capacitor lead from B4 and reconnect to jumper A12/A13.

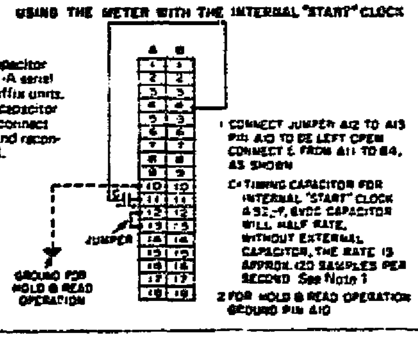

USING THE METER WITH AN EXTERNAL "START"

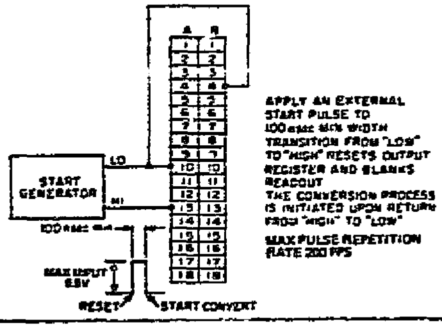

ORDERING INFORMATION

DM-2000 —

INPUT RANGE
A = ±199.9mV INPUT
B = ±1.999V INPUT

PRICE —	MODEL DM-2000—A	$99.00 ea.
	MODEL DM-2000—B	$99.00 ea.
(SOLDER TAB)	I/O CONNECTOR #3VH18/1JN-5	$ 3.95 ea.
(WIRE WRAP)	I/O CONNECTOR #3VH18/1JHD-5	$ 3.95 ea.

DATEL

PRICES AND SPECIFICATIONS SUBJECT TO CHANGE WITHOUT NOTICE

BOARD NAME FRONT PANEL CONNECTOR

BOARD NUMBER 1 (2 SHEETS)

FINGER NUMBER OR LETTER	SIGNAL NAME	SIGNAL ORIGIN	SIGNAL DESTINATION
1	GND		
2	GND		
3	+15 V		
4	+15 V		
5	+5 V	(10-8)	
6	L1	(8-15)	
7	L2	(8-13)	
8	L5	(8-11)	
9	BLOOD PRESSURE	(7-16)	
10	HOLD		(5-12)
11	M		(7-17)
12			(7-18)
13	CAROTID DERIVATIVE	(7-12)	
14	CAROTID V1	(3A-15)	
15	CAROTID LEVEL POT — LOW		(4A-14)
16	CT		(4A-15)
17	HIGH		(4A-16)
18	GATE	(8-K)	
19	EKG SHIELD		(2-18)
20	EKG −		(2-20)
21	EKG +		(2-22)
22	LOCATING SLOT		

BOARD NAME FRONT PANEL CONNECTOR

BOARD NUMBER 1 (2 SHEETS)

FINGER NUMBER OR LETTER	SIGNAL NAME	SIGNAL ORIGIN	SIGNAL DESTINATION
A	GND		
B	GND		
C	+15V		
D	+15V		
E	+5 VOLTS	(10-8)	
F	L3	(8-14)	
H	L4	(8-12)	
J	CONVERT H	(8-10)	
K	HEART RATE	(6-19)	
L	VREFERENCE	(5-13)	
M	1/To POT CT		(7-18)
N	Po POT CT		(7-19)
P	FEMORAL DERIVATIVE	(7-9)	
R	FEMORAL V1	(3B-15)	
S	FEMORAL LEVEL POT V2F — LOW		(4B-14)
T	CT		(4B-15)
U	HIGH		(4B-16)
V	FEMORAL SIGNAL — SHIELD		(3B-20)
W	+		(3B-21)
X	CAROTID SIGNAL — SHIELD		(3A-20)
Y	+		(3A-21)
Z	LOCATING SLOT		

BOARD NAME EKG

BOARD NUMBER 2

FINGER NUMBER LETTER	SIGNAL NAME	SIGNAL ORIGIN	SIGNAL DESTINATION
1	GND		
2	GND.		
3	+15V		
4	+15V		
5	−15V		
6	−15V		
7	LOCATING SLOT		
8	G		(8-9)
9	FEMORAL W		(4B-18)
10	CAROTID W		(4A-18)
11	CAROTID B	(4A-10)	
12	FEMORAL A	(4B-9)	
13	CAROTID A	(4A-9)	
14	TRANSFER	(5-16)	
15	EKG OUTPUT		
16			
17	HEART RATE CONVERT PULSE		(6-22)
18	SHIELD	(1-19)	
19			
20	− LEAD	(1-20)	
21			
22	+ LEAD	(1-21)	

BOARD NAME CAROTID PREAMP

BOARD NUMBER 3A

F GER N BER OR LETTER	SIGNAL NAME	SIGNAL ORIGIN	SIGNAL DESTINATION
1	GND		
2	GND		
3	+15V		
4	+15V		
5	−15V		
6	−15V		
7			
8			
9	CAROTD V3		
10	LOCATING SLOT		
11			
12	CAROTID V2		(4A−17), (1−17), (7-13)
13			
14			
15	CAROTID V1		(4A-22), (1−14)
16			
17			
18			
19			
20	SHIELD	(1 − X)	
21	CAROTID INPUT	(1 − Y)	
22			

BOARD NAME FEMORAL PREAMP

BOARD NUMBER 3B

FINGER NUMBER OR LETTER	SIGNAL NAME	SIGNAL ORIGIN	SIGNAL DESTINATION
1	GND		
2	GND		
3	+15V		
4	+15V		
5	−15V		
6	−15V		
7			
8			
9	FEMORAL V3		
10	LOCATING SLOT		
11			
12	FEMORAL V2		(4B-17), (1-U), (7-10)
13			
14			
15	FEMORAL V1		(4B-22), (1-R)
16			
17			
18			
19			
20	SHIELD	(1-W)	
21	FEMORAL INPUT	(1-X)	
22			

BOARD NAME CAROTID THRESHOLD

BOARD NUMBER 4A

FINGER NUMBER LETTER	SIGNAL NAME		SIGNAL ORIGIN	SIGNAL DESTINATION
1	GND			
2	GND			
3	+15V			
4	+15V			
5	-15V			
6	-15V			
7				
8	50 KHZ		(5-10)	
9	CAROTID A			(2-13)
10	CAROTID B			(8-20), (2-11)
11	CAROTID D			(5-20), (8-20)
12	RESET			
13	THRES. C			(7-14)
14	CAROTID LEVEL POT	LOW	(1-15)	
15		CT	(1-16)	
16		HIGH	(1-17)	
17	CAROTID V2		(3A-12)	
18	CAROTID W		(2-10)	
19	LOCATING SLOT			
20				
21				
22	CAROTID V1		(3A-15)	

BOARD NAME FEMORAL THRESHOLD

BOARD NUMBER 4B

FINGER NUMBER OR LETTER	SIGNAL NAME	SIGNAL ORIGIN	SIGNAL DESTINATION
1	GND		
2	GND		
3	+15V		
4	+15V		
5	−15V		
6	−15V		
7			
8	50KHZ	(5-10)	
9	FEMORAL A		(2-12)
10	FEMORAL B		(8-21)
11	FEMORAL D		(5-22), (8-19)
12	RESET		
13	THRES F		(7-11)
14	FEMORAL LEVEL POT LOW	(1-5)	
15	FEMORAL LEVEL POT CT	(1-T)	
16	FEMORAL LEVEL POT HIGH	(1-V)	
17	FEMORAL V2	(3B-12)	
18	FEMORAL W	(2-9)	
19	LOCATING SLOT		
20			
21			
22	CAROTID V1	(3A-15)	

BOARD NAME BLOOD PRESSURE

BOARD NUMBER 5

FINGER NUMBER LETTER	SIGNAL NAME	SIGNAL ORIGIN	SIGNAL DESTINATION
1	GND		
2	GND		
3	+15V		
4	+15V		
5	-15V		
6	-15V		
7			
8	770HZ		(7-8)
9	6.25KHZ		(6-9)
10	50KHZ		(4A-8), (4B-8)
11	LOCATING SLOT		
12	HOLD	(1-10)	
13	V REFERENCE		(1-2), (6-16)
14	PULSE E		(8-18)
15	PULSE F		(8-17)
16	TRANSFER		(1-21)
17	V4		(7-22)
18			
19			
20	CAROTID D	(4A-11)	
21			
22	FEMORAL D	(4B-11)	

BOARD NAME HEART RATE

BOARD NUMBER 6

FINGER NUMBER OR LETTER	SIGNAL NAME	SIGNAL ORIGIN	SIGNAL DESTINATION
1	GND		
2	GND		
3	+15V		
4	+15V		
5	−15V		
6	−15V		
7			
8			
9	6.25 KHZ	(5-9)	
10			
11			
12	LOCATING SLOT		
13			
14			
15			
16	$V_{REFERENCE}$	(5-13)	
17			
18			
19	V5		(1-K)
20			
21			
22	HEART RATE CONVERT PULSE	(2-17)	

BOARD NAME OUTPUT

BOARD NUMBER 7

F GER N BER OR LETTER	SIGNAL NAME	SIGNAL ORIGIN	SIGNAL DESTINATION
1	GND		
2	GND		
3	+15V		
4	+15V		
5	−15V		
6	−15V		
7			
8	770 HZ	(5−8)	
9	FEMORAL OUTPUT		(1−P)
10	FEMORAL V2	(3B−12)	
11	THRES. F	(4B−13)	
12	CAROTID OUTPUT	(1−13)	
13	CAROTID V2	(3A−12)	
14	THRES C	(4A−13)	
15	LOCATING SLOT		
16	V6		(1−9)
17	M	(1−11)	
18		(1−12)	
19	P_0 POT CT	(1−N)	
20	$1/T_0$ POT CT	(1−M)	
21			
22	V4	(5−17)	

BOARD NAME LIGHT ISOLATED

BOARD NUMBER 8

FINGER NUMBER OR LETTER	SIGNAL NAME	SIGNAL ORIGIN	SIGNAL DESTINATION
1	GND		
2	GND		
3	+15V		
4	+15V		
5	-15V		
6	-15V		
7	LOCATING SLOT		
8	+5 VOLTS	(10-8)	
9	EKG G	(2-8)	
K	GATE		(1-18)
10	CONVERT H		(1-J)
11	L5		(1-8)
12	L4		(1-H)
13	L2		(1-7)
14	L3		(1-F)
15	L1		(1-6)
16	LOCATING SLOT		
17	PULSE F	(5-15)	
18	PULSE E	(5-14)	
19	FEMORAL D	(4B-11)	
20	CAROTID D	(4A-11)	
21	FEMORAL B	(4B-10)	
22	CAROTID B	(4A-11)	

BOARD NAME ±15 VOLT SUPPLY

BOARD NUMBER 9

FINGER NUMBER OR LETTER	SIGNAL NAME	SIGNAL ORIGIN	SIGNAL DESTINATION
1	GND		BOARDS 1-8
2	GND		"
3	+15V		"
4	+15V		BOARDS 1-8
5	-15V		BOARDS 2-8
6	-15V		BOARDS 2-8
7			
8			
9			
10			
11			
12			
13			
14		LOCATING SLOT	
15			
16			
17			
18	AC GND	(11-16)	
19			
20	AC NET.	(11-18)	
21			
22	AC HOT	(11-20)	

BOARD NAME +5 VOLT SUPPLY

BOARD NUMBER 10

FINGER NUMBER OR LETTER	SIGNAL NAME	SIGNAL ORIGIN	SIGNAL DESTINATION
1			
2			
3			
4			
5			
6			
7			
8	+5 VOLTS		(8-8), (1-5)
9			
10			
11			
12			
13			
14			
15			
16			
17			
18	AC. GND	(11-16)	
19			
20	AC. NEUT.	(11-18)	
21			
22	AC. HOT	(11-20)	

BOARD NAME OUTPUT CONNECTOR

BOARD NUMBER FRONT PANEL

FINGER NUMBER OR LETTER	SIGNAL NAME	SIGNAL ORIGIN	SIGNAL DESTINATION
1	BIT 1		
2	2		
3	4		
4	8		
5	10		
6	20	FROM DATEL	
7	40	DIGITAL PANEL	
8	80	METER	
9	100	* ONLY CAN	
10	200	DECODE WHATEVER SIGNAL IS ON	
11	400	THE METER AT	
12	800	TIME OF CONVERT PULSE.	
13	BIT 1000		
14	CONVERT H	(1-J)	
15			
16	ANALOG BLOOD PRESSURE	(1-9)	
17	ANALOG HEARTRATE	(1-K)	
18	GROUND	(1-1)	
19-36	OPEN		